

University of Windsor

Scholarship at UWindor

Electronic Theses and Dissertations

Theses, Dissertations, and Major Papers

1-1-2006

New interlocked molecular machines.

Sarah J. Vella

University of Windsor

Follow this and additional works at: <https://scholar.uwindsor.ca/etd>

Recommended Citation

Vella, Sarah J., "New interlocked molecular machines." (2006). *Electronic Theses and Dissertations*. 7226. <https://scholar.uwindsor.ca/etd/7226>

This online database contains the full-text of PhD dissertations and Masters' theses of University of Windsor students from 1954 forward. These documents are made available for personal study and research purposes only, in accordance with the Canadian Copyright Act and the Creative Commons license—CC BY-NC-ND (Attribution, Non-Commercial, No Derivative Works). Under this license, works must always be attributed to the copyright holder (original author), cannot be used for any commercial purposes, and may not be altered. Any other use would require the permission of the copyright holder. Students may inquire about withdrawing their dissertation and/or thesis from this database. For additional inquiries, please contact the repository administrator via email (scholarship@uwindsor.ca) or by telephone at 519-253-3000ext. 3208.

New Interlocked Molecular Machines

By

Sarah J. Vella

A Dissertation
submitted to the Faculty of Graduate Studies and Research
through Chemistry and Biochemistry
in Partial Fulfilment of the Requirements for
the Degree of Doctor of Philosophy at the
University of Windsor

Windsor, Ontario, Canada

2006



Library and
Archives Canada

Published Heritage
Branch

395 Wellington Street
Ottawa ON K1A 0N4
Canada

Bibliothèque et
Archives Canada

Direction du
Patrimoine de l'édition

395, rue Wellington
Ottawa ON K1A 0N4
Canada

Your file *Votre référence*
ISBN: 978-0-494-42387-5
Our file *Notre référence*
ISBN: 978-0-494-42387-5

NOTICE:

The author has granted a non-exclusive license allowing Library and Archives Canada to reproduce, publish, archive, preserve, conserve, communicate to the public by telecommunication or on the Internet, loan, distribute and sell theses worldwide, for commercial or non-commercial purposes, in microform, paper, electronic and/or any other formats.

The author retains copyright ownership and moral rights in this thesis. Neither the thesis nor substantial extracts from it may be printed or otherwise reproduced without the author's permission.

AVIS:

L'auteur a accordé une licence non exclusive permettant à la Bibliothèque et Archives Canada de reproduire, publier, archiver, sauvegarder, conserver, transmettre au public par télécommunication ou par l'Internet, prêter, distribuer et vendre des thèses partout dans le monde, à des fins commerciales ou autres, sur support microforme, papier, électronique et/ou autres formats.

L'auteur conserve la propriété du droit d'auteur et des droits moraux qui protègent cette thèse. Ni la thèse ni des extraits substantiels de celle-ci ne doivent être imprimés ou autrement reproduits sans son autorisation.

In compliance with the Canadian Privacy Act some supporting forms may have been removed from this thesis.

While these forms may be included in the document page count, their removal does not represent any loss of content from the thesis.

Conformément à la loi canadienne sur la protection de la vie privée, quelques formulaires secondaires ont été enlevés de cette thèse.

Bien que ces formulaires aient inclus dans la pagination, il n'y aura aucun contenu manquant.


Canada

© Sarah J. Vella

All Rights Reserved

ABSTRACT

This thesis presents the design, synthesis and characterization of a range of new interlocked molecular machines based on bis(pyridinium)ethane and benzylanilinium/24-crown-8 macrocycle recognition motifs. Chapter 1 introduces the concept of molecular machines with definitions and representative examples of existing systems found throughout the literature.

In Chapter 2, a new type of molecular machine coined a mechanical “Flip-Switch” is described. These compounds consist of a single recognition site where the two ends of the molecule are different. The chapter begins by providing evidence for the existence of two different states, continues with the presentation of a method for determining the preferred co-conformation in an unsymmetric scenario and ends by showing the manner in which the ratio can be biased using solvents of various polarities. Solid state and solution data show that the preferred co-conformation of the flip-switches is that which has the naphtho ring of the crown ether over the dipyridinium ring of the thread.

Chapter 3 presents an electronically controlled molecular switch involving a 1,2-bis[(*N,N*-dimethylaminophenyl)pyridinium]ethane thread and dibenzo-24-crown-8 ether macrocycle. The threading and unthreading (*ON/OFF*) of the pseudorotaxane complex is controlled by pH through an intramolecular charge transfer. A five-fold increase in association constant (K_{assoc}) is observed from the *ON* to the *OFF* scenario.

Chapter 4 describes a new recognition site for 24-crown-8 macrocycle, *N*-benzylanilinium, which is an amalgamation of two well-established recognition sites: 1,2-bis(pyridinium)ethane and dibenzylammonium. Solution, solid state and gas phase evidence is presented that demonstrates the hybrid nature of this new motif.

Chapter 5 describes incorporation of 1,2-bis(pyridinium)ethane and *N*-benzylanilinium recognition sites into two different [2]rotaxane molecular shuttles. Results indicate that the crown ether resides exclusively on the bis(pyridinium)ethane site when the thread is unprotonated, regardless of the solvent. Protonation of the [2]rotaxanes in acetonitrile (a polar solvent) results in shuttling of the crown ether between the two sites in ratios of 3:1 (for the first rotaxane) and 9:1 (for the second rotaxane). In dichloromethane (a non-polar solvent), both [2]rotaxanes show complete bistability.

Synthetic modification and incorporation of the two recognition sites, 1,2-bis(pyridinium)ethane and *N*-benzylanilinium, into a [2]catenane circumrotational shuttle is discussed in Chapter 6.

Chapter 7 illustrates the concept of integrating molecular shuttles comprised of the bis(pyridinium)ethane and *N*-benzylanilinium recognition sites with 24-crown-8 macrocycles into functional materials. Rotaxanes synthesized to this end are presented and characterized.

DEDICATION

*This work is dedicated to my mom, my dad, Jeff, Josh
and to my husband and best friend, Jason.*

ACKNOWLEDGEMENTS

First and foremost, I would like to thank my advisor, Steve Loeb, for his guidance and support throughout the years, and for believing that this day would really come! As the last one of this generation of students, I can only imagine the patience it required to keep me as long as he did.

I would also like to thank my second advisor, Tricia Carmichael, for giving me the opportunity to work with her at the IBM T. J. Watson research center. What started as a summer internship, turned into a long-term collaboration, which I was very fortunate to be a part of. (I am also grateful for all the dinners that we have been invited to over the years and look forward to those in the future.)

I have learned so much from both of my advisors and I truly appreciate all of their efforts to help make this thesis a success.

Another person to whom I owe a great deal thanks is Jorge Tiburcio. Jorge helped me get the ball rolling on much of my chemistry. He was a constant source of information and patience. Muchos Gracias, Jorge!!

A special thank you to Dave Tramontozzi and Nicolle Habermehl for proof reading my thesis. I still can't believe how many mistakes I made that you caught.

In my long residence on the third floor of Essex Hall, I have had the great fortune of working with and befriending many people. My years here have definitely been the most fun in my life. (Yes, even though it represents almost one fourth of my life).

Lastly, I would like to thank my family for standing by me through all these years of school. They have always been a source of encouragement. Thank you to my husband,

Jason, for his patience, understanding and love. I also want to thank Oliver for knowing exactly when I needed a break. I love you all...

TABLE OF CONTENTS

ABSTRACT	iv
DEDICATION	vi
ACKNOWLEDGEMENTS.....	vii
TABLE OF CONTENTS	ix
LIST OF FIGURES	xvii
LIST OF TABLES	xxiii
LIST OF SCHEMES.....	xxix
LIST OF ABBREVIATIONS.....	xxx
CHAPTER 1	1
<i>Molecular Machines</i>	1
1.1 INTRODUCTION.....	1
1.2 SPONTANEOUS MOTION	2
1.3 OPENING, CLOSING AND TRANSLOCATION.....	4
1.4 ROTARY MOTION	5
1.5 THREADING AND DETHREADING OF PSEUDOROTAXANES.....	6
1.6 LINEAR MOVEMENTS IN ROTAXANES	9
1.7 CIRCUMROTATIONAL MOVEMENTS IN CATENANES	16
1.8 MOLECULAR MACHINES AT WORK	18
1.9 THE LOEB MOTIF	21
1.10 SCOPE OF THESIS.....	23
CHAPTER 2	25
<i>Flip-Switches</i>	25

2.1 INTRODUCTION	25
2.2 SYNTHESIS AND CHARACTERIZATION	26
2.2.1 Synthesis	26
2.2.2 ¹ H NMR Spectroscopy.....	29
2.3 PROOF OF THE “FLIPPING” PHENOMENON	30
2.3.1 Variable Temperature ¹ H NMR Experiments.....	30
2.3.2 Rate Analysis	34
2.3.3 Increasing the activation energy	37
2.4 TRULY UNSYMMETRICAL [2]ROTAXANES: FLIP-SWITCHES	39
2.4.1 Establishing a Room Temperature Method	40
2.4.2 Determination of Relative Populations for Unsymmetrical [2]Rotaxanes	42
2.4.3 Manipulation of the Relative Population Distributions	45
2.5 SUMMARY AND CONCLUSIONS.....	46
2.6 EXPERIMENTAL	48
2.6.1 General Comments.....	48
2.6.2 Synthesis of 2-1⁺	49
2.6.3 Synthesis of 2-2²⁺	50
2.6.4 Synthesis of 2-3²⁺	51
2.6.5 Synthesis of 2-4²⁺	53
2.6.6 Synthesis of 2-5²⁺	54
2.6.7 Synthesis of 2-6⁴⁺	55
2.6.8 Synthesis of [2-6C24C8] ⁴⁺	56
2.6.9 Synthesis of [2-6CB24C8] ⁴⁺	57

2.6.10 Synthesis of [2-6CDB24C8] ⁴⁺	59
2.6.11 Synthesis of [2-6CBN24C8] ⁴⁺	61
2.6.12 Synthesis of [2-6CN24C8] ⁴⁺	63
2.6.13 Synthesis of [2-6CDN24C8] ⁴⁺	65
2.6.14 Synthesis of 2-7 ³⁺	67
2.6.15 Synthesis of [2-7C24C8] ³⁺	69
2.6.16 Synthesis of [2-7CB24C8] ³⁺	71
2.6.17 Synthesis of [2-7CDB24C8] ³⁺	73
2.6.18 Synthesis of [2-7CBN24C8] ³⁺	75
2.6.19 Synthesis of [2-7CN24C8] ³⁺	77
2.6.20 Synthesis of [2-7CDN24C8] ³⁺	79
2.6.21 Synthesis of 2-8 ³⁺	81
2.6.22 Synthesis of [2-8CB24C8] ³⁺	83
2.6.23 Synthesis of [2-8CDB24C8] ³⁺	85
2.6.24 Synthesis of [2-8CBN24C8] ³⁺	87
2.6.25 Synthesis of [2-8CN24C8] ³⁺	89
2.6.26 Synthesis of [2-8CDN24C8] ³⁺	91
2.6.27 Synthesis of 2-9 ⁴⁺	93
2.6.28 Synthesis of [2-9CDB24C8] ⁴⁺	95
2.6.29 Synthesis of [2-9CBN24C8] ⁴⁺	97
2.6.30 Synthesis of [2-9CN24C8] ⁴⁺	99

2.6.31 Synthesis of [2-9C _{DN} 24C8] ⁴⁺	101
2.6.32 Synthesis of [2-10C _{BN} 24C8] ⁴⁺	103
CHAPTER 3	105
<i>An Intramolecular Charge Transfer [2]Pseudorotaxane Switch</i>	105
3.1 INTRODUCTION.....	105
3.2 SYNTHESIS AND STRUCTURAL CHARACTERIZATION	107
3.2.1 Synthesis	107
3.2.2 X-ray Characterization.....	108
3.2.3 Molecular Orbital Analysis.....	110
3.3 RESULTS AND DISCUSSION OF THE PSEUDOROTAXANE STUDIES.....	111
3.4 SUMMARY AND CONCLUSIONS.....	114
3.5 EXPERIMENTAL	116
3.5.1 General Comments.....	116
3.5.2 Synthesis of 4-(4'- <i>N,N</i> -dimethylaminophenyl)pyridine (3-1).....	117
3.5.3 Synthesis of [4-(4'- <i>N,N</i> -dimethylaminophenyl)pyridinium]ethylbromide (3-2 ⁺)	118
3.5.4 Synthesis of Compound 3-3a ²⁺	120
3.5.5 Synthesis of Compound 3-4	123
3.5.6 Synthesis of Compound 3-5a ²⁺	124
CHAPTER 4	127
<i>N-Benzylanilinium [2]Pseudorotaxanes</i>	127
4.1 INTRODUCTION.....	127
4.2 SYNTHESIS AND CHARACTERIZATION	128

4.2.1 - Synthesis	128
4.2.2 – X-ray Crystallography.....	130
4.3 PSEUDOROTAXANE FORMATION.....	130
4.4 SUMMARY AND CONCLUSIONS.....	144
4.5 EXPERIMENTAL	145
4.5.1 General Comments.....	145
4.5.2 Synthesis of Compound HBnAnH [4-1].....	145
4.5.3 Synthesis of Compound MeOBnAnOMe [4-2].....	147
4.5.4 Synthesis of MeOBnAnCF₃ [4-3].....	149
4.5.5 Synthesis of MeOBnAnNO₂ [4-4].....	151
4.5.6 Synthesis of CF₃BnAnOMe [4-5].....	153
4.5.7 Synthesis of CF₃BnAnCF₃ [4-6].....	155
4.5.8 Synthesis of CF₃BnAnNO₂ [4-7].....	157
4.5.9 Synthesis of NO₂BnAnOMe [4-8].....	159
4.5.10 Synthesis of NO₂BnAnCF₃ [4-9].....	161
4.5.11 Synthesis of NO₂BnAnNO₂ [4-10].....	163
4.5.12 Synthesis of 3,5-BisCF₃BnAnOMe [4-11].....	165
4.5.13 Synthesis of 3,5-BisCF₃BnAnCF₃ [4-12].....	167
4.5.14 Synthesis of 3,5-BisCF₃BnAnNO₂ [4-13].....	169
4.5.15 Synthesis of C₆F₅BnAnOMe [4-14].....	171
4.5.16 Synthesis of C₆F₅BnAnCF₃ [4-15].....	173
4.5.17 Synthesis of C₆F₅BnAnNO₂ [4-16].....	175
CHAPTER 5	177
<i>[2]Rotaxane Molecular Shuttles</i>	177

5.1 INTRODUCTION.....	177
5.2 SYNTHESIS AND STRUCTURAL CHARACTERIZATION	179
5.2.1 Synthesis	179
5.2.2 ^1H NMR Spectroscopy.....	181
5.2.3 X-ray Crystallography	182
5.3 ACID/BASE SHUTTling PART I.....	184
5.3.1 ^1H NMR Spectroscopy.....	184
5.3.2 ^{19}F NMR Spectroscopy	187
5.3.3 UV-Visible Spectroscopy	189
5.4 ACID/BASE SHUTTling PART II.....	192
5.4.1 ^1H NMR Spectroscopy.....	192
5.4.2 UV-Visible Spectroscopy	194
5.4.3 Fluorescence Spectroscopy	195
5.5 SUMMARY AND CONCLUSIONS.....	197
5.6 EXPERIMENTAL	198
5.6.1 General Comments.....	198
5.6.2 Synthesis of Compound 5-1	198
5.6.3 Synthesis of Compound 5-2⁺	200
5.6.4 Synthesis of Compound 5-3	201
5.6.5 Synthesis of Compound 5-4²⁺ and 5-5²⁺	203
5.6.6 Synthesis of Compound 5-6	207
5.6.7 Synthesis of Compound 5-7	208
CHAPTER 6	210
[2]Catenane Circumrotational Shuttle	210

6.1 INTRODUCTION.....	210
6.2 SYNTHESIS AND STRUCTURAL CHARACTERIZATION	211
6.2.1 Synthesis	211
6.2.2 ¹ H NMR Spectroscopy.....	214
6.2.3 Mass Spectrometry.....	216
6.3 ACID/BASE SHUTTLING.....	218
6.3.1 ¹ H NMR Spectroscopy.....	218
6.3.2 [2]Pseudorotaxane Model Compound Study	219
6.3.3 UV-Visible Spectroscopy	221
6.4 SUMMARY AND CONCLUSIONS.....	223
6.5 EXPERIMENTAL	224
6.5.1 General Comments.....	224
6.5.2 Synthesis of Compound 6-1	224
6.5.3 Synthesis of Compound 6-2	225
6.5.4 Synthesis of Compound 6-3	227
6.5.5 Synthesis of Compound 6-4	228
6.5.6 Synthesis of Compound 6-5⁴⁺	229
6.5.7 Synthesis of Compound 6-6a⁶⁺	231
6.5.8 Synthesis of Compound 6-7a²⁺	234
CHAPTER 7	235
<i>Towards [2]Rotaxane Functional Materials</i>	<i>235</i>
7.1 INTRODUCTION.....	235
7.2 FUTURE DIRECTIONS OF STUDY	235
7.2.1 Surface Studies.....	235

7.2.2 MORF's	237
7.3 PROGRESS MADE TO THIS END.....	238
7.3.1 Surface Studies.....	238
7.3.2 MORFs.....	241
7.4 SYNTHESIS AND STRUCTURAL CHARACTERIZATION	242
7.4.1 Synthesis	242
7.4.2 ¹ H NMR Spectroscopy.....	244
7.4.3 Infrared Spectroscopy	245
7.5 SUMMARY AND CONCLUSIONS.....	247
7.6 EXPERIMENTAL	248
7.6.1 General Comments.....	248
7.6.2 Synthesis of Compound 7-1.....	248
7.6.3 Synthesis of Compound 7-2.....	250
7.6.4 Synthesis of Compound 7-3.....	251
7.6.5 Synthesis of Compound 7-4.....	252
7.6.6 Synthesis of Compound 7-5.....	253
7.6.7 Synthesis of Compound 7-6 ²⁺	254
7.6.8 Synthesis of Compound 7-7 ²⁺	256
7.6.9 Synthesis of Compound 7-8 ²⁺	258
REFERENCES	260
VITA AUCTORIS	271

LIST OF FIGURES

Figure 1.1 – Nanoscopic gyroscope designed by Garcia-Garibay <i>et al.</i>	3
Figure 1.2 – Negative allosteric hydrogen bonding receptor for uracil studied by Branda <i>et al.</i>	4
Figure 1.3 – Unidirectional molecular rotor designed by Feringa <i>et al.</i>	5
Figure 1.4 – Illustration of complexed [2]pseudorotaxane and its uncomplexed components.	6
Figure 1.5 – Plug and socket pseudorotaxane system investigated by Balzani <i>et al.</i>	7
Figure 1.6 - Folding/unfolding pseudorotaxane system demonstrated by Kim <i>et al.</i>	8
Figure 1.7– [2]Rotaxane showing linear movement of the ring on the thread.	9
Figure 1.8 – Illustration of a) threading/capping, b) slipping and c) clipping methods for rotaxane formation.	10
Figure 1.9 – Non-degenerate molecular shuttle.....	11
Figure 1.10 –Molecular muscle system studied by Sauvage <i>et al.</i>	12
Figure 1.11 – Truth tables for NOT, AND and OR logic gates.....	13
Figure 1.12 – Binary addition.	13
Figure 1.13 – [2]Rotaxane molecular half-adder described by Hien <i>et al.</i> ³³	14
Figure 1.14 – Two co-conformations of a [2]catenane circumrotational switch.....	17
Figure 1.15 – [2]Catenane capable of reversible unidirectional circumrotation designed by Leigh <i>et al.</i>	18
Figure 1.16 – Structural and graphical representation of a palindromic molecular muscle [3]rotaxane constructed by Stoddart <i>et al.</i>	19

Figure 1.17 – Graphical representation of the bending action of a cantilever due to the contraction of the palindromic molecular muscle.....	20
Figure 1.18 – [2]Pseudorotaxane of paraquat ²⁺ and BPP34C10	21
Figure 1.19 – Comparison of N ⁺ ...N ⁺ distances between paraquat ²⁺ and 1,2-bis(pyridinium)ethane ²⁺	22
Figure 1.20 – Newman projection top view (top) and side view (bottom) showing non-covalent interactions between a 1,2-bis(dipyridinium)ethane ⁴⁺ capped thread and DB24C8	22
Figure 2.1 – Illustration representing the two co-conformations of a flip-switch.	26
Figure 2.2 – ¹ H NMR spectra of a) 2-6⁴⁺ and b) [2-6cDB24C8] ⁴⁺ in CD ₃ CN.....	29
Figure 2.3 – Symmetrical thread 2-6⁴⁺ and unsymmetrical crown ether BN24C8	30
Figure 2.4 – Two possible orientations of BN24C8 for [2-6cBN24C8] ⁴⁺	31
Figure 2.5 – Variable temperature ¹ H NMR spectra of [2-6cBN24C8] ⁴⁺ in 9:1 CD ₂ Cl ₂ :CD ₃ CN. Subscripts B and N denote the <i>benzo</i> (B) and <i>naphtho</i> (N) ends of the molecule.....	32
Figure 2.6 – Room temperature (top) and limiting (bottom) ¹ H NMR spectra of [2-6cN24C8] ⁴⁺ in CD ₂ Cl ₂	34
Figure 2.7 – VT ¹ H NMR spectra showing proton resonances b and c from [2-6cBN24C8] ⁴⁺	35
Figure 2.8 – Selected experimental (top) and calculated (bottom) spectra for proton b of [2-6cBN24C8] ⁴⁺	36
Figure 2.9 – Arrhenius plot for [2-6cBN24C8] ⁴⁺	37
Figure 2.10 – Labeling scheme for [2-10cBN24C8] ⁴⁺	38

Figure 2.11 – A ball-and-stick representation of the X-ray structure for the cationic portion of the [2]rotaxane $[2-10\text{cBN}24\text{C}8]^{4+}$	39
Figure 2.12 – The partial ^1H NMR spectra of $[2-6\text{cDB}24\text{C}8]^{4+}$, $[2-6\text{cDN}24\text{C}8]^{4+}$ and $[2-6\text{cBN}24\text{C}8]^{4+}$ at 30°C in CD_3CN . Subscripts B and N denote the <i>benzo</i> (B) and <i>naphtho</i> (N) ends of the molecule, the numbering schemes are outlined in Scheme 2.3. .	41
Figure 2.13 – ^1H NMR spectrum of a combination of rotaxanes $[2-6\text{cDB}24\text{C}8]^{4+}$, $[2-6\text{cDN}24\text{C}8]^{4+}$ and $[2-6\text{cBN}24\text{C}8]^{4+}$ at 30°C in CD_3CN at 2.0×10^{-3} M each.	41
Figure 2.14 – Pictorial representation of isomer ratio determination based on room temperature ^1H NMR spectra.....	42
Figure 2.15 – A ball-and-stick representation of the X-ray structure for the cationic portion on the [2]rotaxane $[2-7\text{cBN}24\text{C}8]^{3+}$	44
Figure 3.1 – Dicationic thread $3-3\text{a}^{2+}$ can be represented by two possible resonance forms	107
Figure 3.2 – X-ray structures of $3-3\text{a}^{2+}$ (top) and $3-3\text{b}^{4+}$ (bottom) showing the atom labeling scheme and bond distances.	109
Figure 3.3 – HOMO/LUMO diagrams for $3-3\text{a}^{2+}$, $3-3\text{b}^{4+}$ and $3-6^{2+}$	110
Figure 3.4 – DFT calculated (B3LYP) electron distributions for (top to bottom) the dication bis(4-phenylpyridinium)ethane $3-6^{2+}$, thread $3-3\text{a}^{2+}$, and protonated thread $3-3\text{b}^{4+}$	111
Figure 3.5 – UV-visible absorption spectra of a 1:1 mixture of $3-3\text{a}^{2+}$ with DB24C8 (yellow) and $3-3\text{b}^{3+}$ with DB24C8 (blue) and recorded in CD_3CN at a concentration of 1.0×10^{-5} M.....	113

Figure 3.6 – Schematic representation of the threading and dethreading process initiated by alternating acid and base.	115
Figure 4.1 – <i>N,N</i> -dibenzylammonium (left), <i>N</i> -benzylanilinium (middle), bis(pyridinium)ethane (right) [2]pseudorotaxanes with DB24C8	128
Figure 4.2 – Ball-and-stick representation of the X-ray structure of CF₃BnAnOMe [4-5·H]⁺ showing an anti conformation: dihedral angle = 171.8° (carbon = black, oxygen = red, nitrogen = blue, fluorine = yellow, hydrogen = white).	130
Figure 4.3 – Titration curve for CF₃BnAnOMe (4-5)	131
Figure 4.4 – ¹ H NMR spectra of [CF₃BnAnCF₃][OTf] (top) and [CF₃BnAnCF₃⊂DB24C8][OTf] (bottom) in CD ₃ CN at 25°C; “c” is for complexed and “uc” is for uncomplexed.	133
Figure 4.5 - EXSY NMR spectrum of [3,5-BisCF₃BnAnOMe⊂DB24C8][OTf]	133
Figure 4.6 – Schematic of complexed and uncomplexed CH ₂ peaks.	137
Figure 4.7 – Ball and Stick representation of the X-ray structure of [CF₃BnAnCF₃⊂DB24C8]⁺ (carbon = black, oxygen = red, nitrogen = blue, fluorine = yellow).	142
Figure 4.8 – Ball and Stick representation of the X-ray structure of [HBnAnH⊂DB24C8]⁺ (carbon = black, oxygen = red, nitrogen = blue).....	143
Figure 4.9 – Ball and Stick representation of the X-ray structure of [MeOBnAnOMe⊂DB24C8]⁺ (carbon = black, oxygen = red, nitrogen = blue).....	144
Figure 5.1 – Degenerate [2]rotaxane molecular shuttle.	178
Figure 5.2 – Non-degenerate [2]rotaxane molecular shuttle.....	178
Figure 5.3 – Illustration of proposed [2]rotaxane molecular shuttle.	179

Figure 5.4 – Partial ^1H NMR spectra of a) capped thread 5-5a $^{2+}$ and b) [2]rotaxane 5-4a $^{2+}$ in CD_3CN at 500 MHz.	182
Figure 5.5 – X-ray crystal structure of [5-4a][OTf] $_2$ rotaxane; black = carbon, blue = nitrogen, red = oxygen, fluorine = green. Hydrogen atoms and triflate anions have been omitted for clarity.	183
Figure 5.6 – ^1H NMR spectra of a) 5-4a $^{2+}$ and b) 5-4b $^{3+}$ in CD_3CN at 500 MHz and 30°C.	185
Figure 5.7 – ^1H NMR spectra of a) 5-4a $^{2+}$ and b) 5-4b $^{3+}$ in CD_2Cl_2 at 500 MHz and 30°C.	185
Figure 5.8 – Illustration showing relationship between structure and ^{19}F chemical shift.	189
Figure 5.9 – UV-visible spectra of 5-4a $^{2+}$ (yellow) and 5-4b $^{3+}$ (black) [2]rotaxanes in CH_2Cl_2	191
Figure 5.10– UV-visible spectra of 5-4a $^{2+}$ (yellow) and 5-4b $^{3+}$ (black) [2]rotaxanes in CH_3CN	191
Figure 5.11 – ^1H NMR spectrum of a) 5-7a $^{2+}$ and b) 5-7b $^{3+}$ in CD_3CN at 500 MHz and 30°C.	193
Figure 5.12 – UV-visible spectrum of 5-7a $^{2+}$ (yellow) and 5-7b $^{3+}$ (black) OTf in CH_2Cl_2	194
Figure 5.13 – UV-visible spectrum of 5-7a $^{2+}$ (yellow) and 5-7b $^{3+}$ (black) OTf in CH_3CN	195
Figure 5.14 – Fluorescence emission spectra of 5-7a $^{2+}$ (yellow) and 5-7b $^{3+}$ (black) in CH_3CN at 1.0×10^{-5} M.	196

Figure 5.15 – Fluorescence emission spectra of 5-7a²⁺ (yellow) and 5-7b³⁺ (black) in CH ₂ Cl ₂ at 1.0 × 10 ⁻⁵ M.....	196
Figure 6.1 – Illustration of a [2]catenane molecular switch.	211
Figure 6.2 – Proton assignments for 6-6a⁶⁺	215
Figure 6.3 – ¹ H NMR spectrum of 6-6a⁶⁺ in CD ₃ CN.	215
Figure 6.4 – ESI-Mass spectra of experimental data for a) 6-6a²⁺ , b) 6-6a³⁺ , c) 6-6a⁴⁺ , d) 6-6a⁵⁺	217
Figure 6.5 – ¹ H NMR spectra of a) non-protonated (6-6a⁶⁺) and b) protonated (6-6b⁷⁺) in CD ₃ CN at room temperature.....	219
Figure 6.6 – ¹ H NMR spectra in CD ₃ CN of a) unprotonated model compound 6-7a²⁺ and b) a mixture of unprotonated model compound 6-7a²⁺ and DB24C8	220
Figure 6.7 – ¹ H NMR spectra in CD ₃ CN at 2.0 × 10 ⁻³ M of a) protonated model compound 6-7b³⁺ and b) a mixture of protonated model compound 6-7b³⁺ and DB24C8	221
Figure 6.8 – UV-visible spectra of 2.0 × 10 ⁻⁵ M CH ₃ CN solutions of non-protonated 6-6a⁶⁺ (yellow) and protonated 6-6b⁷⁺ (black).	222
Figure 7.1 – Controlling the wettability of a surface using SAMs of rotaxanes.....	237
Figure 7.2 – Cartoon schematic of rotaxanes 7-7a²⁺ and 7-7b³⁺	239
Figure 7.3 – Layer by layer approach to monolayer formation.	240
Figure 7.4 – ¹ H NMR spectrum of 7-7²⁺ in CD ₃ CN at 500 MHz and 30°C.	244
Figure 7.5 – ¹ H NMR spectrum of 7-8²⁺ in CD ₃ CN at 500 MHz and 30°C.	245
Figure 7.6 – IR spectrum of 7-2	246
Figure 7.7 – IR spectrum of 7-5	246

LIST OF TABLES

Table 1.1 – Results for absorbance and fluorescence data for the four isomers of [2]rotaxane.....	16
Table 1.2 – Truth table for [2]rotaxane molecular half adder.....	16
Table 2.1 - Isomer ratios determined from ^1H NMR data for [2]rotaxanes in CD_3CN	43
Table 2.2 – Ratios of co-conformational isomers determined for $[\mathbf{2-9cBN24C8}]^{4+}$ from ^1H NMR data in various solvents.....	46
Table 2.3 – ^1H NMR of $[\mathbf{2-1}][\text{Br}]$ in D_2O . $\text{MW}_{\text{Br}} = 344.058$ g/mol.....	49
Table 2.4 – ^1H NMR of $[\mathbf{2-1}][\text{BF}_4]$ in CD_3CN . $\text{MW}_{\text{BF}_4} = 350.946$ g/mol.....	49
Table 2.5 – ^1H NMR of $[\mathbf{2-2}][\text{Br}]_2$ in D_2O . $\text{MW}_{\text{Br}} = 500.229$ g/mol.....	50
Table 2.6 - ^1H NMR of $[\mathbf{2-2}][\text{OTf}]_2$ in CD_3CN . $\text{MW}_{\text{OTf}} = 638.559$ g/mol.....	50
Table 2.7 – ^1H NMR of $[\mathbf{2-3}][\text{Br}]_2$ in D_2O . $\text{MW}_{\text{Br}} = 451.198$ g/mol.....	51
Table 2.8 – ^1H NMR of $[\mathbf{2-3}][\text{OTf}]_2$ in CD_3CN . $\text{MW}_{\text{OTf}} = 589.528$ g/mol.....	52
Table 2.9 – ^1H NMR of $[\mathbf{2-4}][\text{OTf}]_2$ in CD_3CN . $\text{MW}_{\text{OTf}} = 617.582$ g/mol.....	53
Table 2.10 – ^1H NMR of $[\mathbf{2-5}][\text{OTf}]_2$ in CD_3CN . $\text{MW}_{\text{OTf}} = 688.618$ g/mol.....	54
Table 2.11 – ^1H NMR of $[\mathbf{2-6}][\text{OTf}]_4$ in CD_3CN . $\text{MW}_{\text{OTf}} = 1231.171$ g/mol.....	55
Table 2.12 – ^1H NMR $[\mathbf{2-6c24C8}][\text{OTf}]_4$ in CD_3CN . $\text{MW}_{\text{OTf}} = 1583.592$ g/mol.....	56
Table 2.13 ^1H NMR of $[\mathbf{2-6cB24C8}][\text{OTf}]_4$ in CD_3CN . $\text{MW}_{\text{OTf}} = 1631.634$ g/mol.....	58
Table 2.14 – ^1H NMR of $[\mathbf{2-6cDB24C8}][\text{OTf}]_4$ in CD_3CN . $\text{MW}_{\text{OTf}} = 1679.677$ g/mol.....	60
Table 2.15 – ^1H NMR of $[\mathbf{2-6cBN24C8}][\text{OTf}]_4$ in CD_3CN . $\text{MW}_{\text{OTf}} = 1729.736$ g/mol.....	62
Table 2.16 – ^1H NMR of $[\mathbf{2-6cN24C8}][\text{OTf}]_4$ in CD_3CN . $\text{MW}_{\text{OTf}} = 1681.693$ g/mol.....	64
Table 2.17 – ^1H NMR of $[\mathbf{2-6cDN24C8}][\text{OTf}]_4$ in CD_3CN . $\text{MW}_{\text{OTf}} = 1779.794$ g/mol.....	66
Table 2.18 – ^1H NMR of $[\mathbf{2-7}][\text{OTf}]_3$ in CD_3CN . $\text{MW}_{\text{OTf}} = 885.834$ g/mol.....	68

Table 2.19 – ^1H NMR of [2-7c24C8][OTf] ₃ in CD ₃ CN. MW _{OTf} = 1238.2548 g/mol.....	70
Table 2.20 – ^1H NMR of [2-7cB24C8][OTf] ₃ in CD ₃ CN. MW _{OTf} = 1286.298 g/mol....	72
Table 2.21 – ^1H NMR of [2-7cDB24C8][OTf] ₃ in CD ₃ CN. MW _{OTf} = 1334.340g/mol..	74
Table 2.22 – ^1H NMR of [2-7cBN24C8][OTf] ₃ in CD ₃ CN. MW _{OTf} = 1384.399 g/mol.	76
Table 2.23 – ^1H NMR of [2-7cN24C8][OTf] ₃ in CD ₃ CN. MW _{OTf} = 1336.356 g/mol....	78
Table 2.24 – ^1H NMR of [2-7cDN24C8][OTf] ₃ in CD ₃ CN. MW _{OTf} = 1434.458g/mol..	80
Table 2.25 – ^1H NMR of [2-8][OTf] ₃ in CD ₃ CN. MW _{OTf} = 913.887 g/mol	82
Table 2.26 – ^1H NMR of [2-8cB24C8][OTf] ₃ in CD ₃ CN. MW _{OTf} = 1314.351 g/mol....	84
Table 2.27 – ^1H NMR of [2-8cDB24C8][OTf] ₃ in CD ₃ CN. MW _{OTf} = 1362.394 g/mol.	86
Table 2.28 – ^1H NMR of [2-8cBN24C8][OTf] ₃ in CD ₃ CN. MW _{OTf} = 1412.452 g/mol.	88
Table 2.29 – ^1H NMR of [2-8cN24C8][OTf] ₃ in CD ₃ CN. MW _{OTf} = 1364.409 g/mol....	90
Table 2.30 – ^1H NMR of [2-8cDN24C8][OTf] ₃ in CD ₃ CN. MW _{OTf} = 1462.511 g/mol.	92
Table 2.31 – ^1H NMR of [2-9][OTf] ₄ in CD ₃ CN. MW _{OTf} = 1281.230 g/mol	94
Table 2.32 – ^1H NMR of [2-9cDB24C8][OTf] ₄ in CD ₃ CN. MW _{OTf} = 1729.736 g/mol.	96
Table 2.33 – ^1H NMR of [2-9cBN24C8][OTf] ₄ in CD ₃ CN. MW _{OTf} = 1779.794 g/mol.	98
Table 2.34 – ^1H NMR of [2-9cN24C8][OTf] ₄ in CD ₃ CN. MW _{OTf} = 1731.752 g/mol..	100
Table 2.35 – ^1H NMR of [2-9cDN24C8][OTf] ₄ in CD ₃ CN. MW _{OTf} = 1829.853 g/mol	
.....	102
Table 2.36 – ^1H NMR of [2-10cBN24C8][OTf] ₄ in CD ₃ CN. MW _{OTf} = 1849.667 g/mol	
.....	104
Table 3.1 – Comparison of Bond Distances in 3-3a ²⁺ and 3-3b ⁴⁺ . ^a	109
Table 3.2 – Association Constants, K _{assoc} and ΔG° values for 3-3a ²⁺ – 3-7 ²⁺ with DB24C8 in CD ₃ CN (2.0 × 10 ⁻³ M) at 298 K.....	112

Table 3.3 – Logic table for ICT pseudorotaxane system.	115
Table 3.4 – ^1H NMR of 3-1 in CD_3CN . $\text{MW} = 198.264$ g/mol	117
Table 3.5 – ^1H NMR of [3-2][Br] in D_2O . $\text{MW}_{\text{Br}} = 386.125$ g/mol	118
Table 3.6 – ^1H NMR of [3-2][OTf] in CD_3CN . $\text{MW}_{\text{OTf}} = 455.290$ g/mol	119
Table 3.7 – ^1H NMR of [3-3a][OTf]$_2$ in CD_3CN . $\text{MW}_{\text{OTf}} = 722.719$ g/mol	120
Table 3.8 – ^{13}C NMR of [3-3a][OTf]$_2$ in CD_3CN	121
Table 3.9 – ^1H NMR of [3-3b][OTf]$_3$ in CD_3CN . $\text{MW}_{\text{OTf}} = 1022.873$ g/mol	122
Table 3.10 – ^1H NMR of [3-4] in CD_3CN . $\text{MW} = 198.264$ g/mol	123
Table 3.11 – ^1H NMR of [3-5a][OTf]$_2$ in CD_3CN . $\text{MW}_{\text{OTf}} = 722.719$ g/mol	124
Table 3.12 – ^{13}C NMR of [3-5a][OTf]$_2$ in CD_3CN	125
Table 3.13 – ^1H NMR of [3-5b][OTf]$_3$ in CD_3CN . $\text{MW}_{\text{OTf}} = 1022.873$ g/mol	126
Table 4.1 - Summary of K_a 's of the <i>N</i> -benzylanilinium threads.	132
Table 4.2 - Summary of Changes in Chemical Shift ($\Delta\delta$, ppm) of the [2]Pseudorotaxanes Relative to the Free Threads. ^a	135
Table 4.3 – Summary of experimental (in red) and calculated (in black) Equilibrium Constants with DB24C8	138
Table 4.4 Summary of experimental (in red) and calculated (in black) Equilibrium Constants with 24C8	139
Table 4.5 – ESI-TOF calculated and found values for [2]pseudorotaxanes.	141
Table 4.6 – ^1H NMR of [4-1] in CD_3CN . $\text{MW} = 183.241$ g/mol	146
Table 4.7 – ^1H NMR of [4-1][OTf] in CD_3CN . $\text{MW}_{\text{OTf}} = 333.317$ g/mol	146
Table 4.8 – ^1H NMR of [4-2] in CD_3CN . $\text{MW} = 243.291$ g/mol	147
Table 4.9 – ^1H NMR of [4-2][OTf] in CD_3CN . $\text{MW}_{\text{OTf}} = 393.367$ g/mol	148
Table 4.10 – ^1H NMR of [4-3] in CD_3CN . $\text{MW} = 281.264$ g/mol	149

Table 4.11 – ^1H NMR of [4-3][OTf] in CD_3CN . $\text{MW}_{\text{OTf}} = 431.340$ g/mol.....	150
Table 4.12 – ^1H NMR of [4-4] in CD_3CN . $\text{MW} = 258.266$ g/mol.....	151
Table 4.13 – ^1H NMR of [4-4][OTf] in CD_3CN . $\text{MW}_{\text{OTf}} = 408.342$ g/mol.....	152
Table 4.14 – ^1H NMR of [4-5] in CD_3CN . $\text{MW} = 281.264$ g/mol.....	153
Table 4.15 – ^1H NMR of [4-5][OTf] in CD_3CN . $\text{MW}_{\text{OTf}} = 431.340$ g/mol.....	154
Table 4.16 – ^1H NMR of [4-6] in CD_3CN . $\text{MW} = 319.237$ g/mol.....	155
Table 4.17 – ^1H NMR of [4-6][OTf] in CD_3CN . $\text{MW}_{\text{OTf}} = 469.313$ g/mol.....	156
Table 4.18 – ^1H NMR of [4-7] in CD_3CN . $\text{MW} = 296.239$ g/mol.....	157
Table 4.19 – ^1H NMR of [4-7][OTf] in CD_3CN . $\text{MW}_{\text{OTf}} = 446.315$ g/mol.....	158
Table 4.20 – ^1H NMR of [4-8] in CD_3CN . $\text{MW} = 258.266$ g/mol.....	159
Table 4.21 – ^1H NMR of [4-8][OTf] in CD_3CN . $\text{MW}_{\text{OTf}} = 408.342$ g/mol.....	160
Table 4.22 – ^1H NMR of [4-9] in CD_3CN . $\text{MW} = 296.239$ g/mol.....	161
Table 4.23 – ^1H NMR of [4-9][OTf] in CD_3CN . $\text{MW}_{\text{OTf}} = 446.315$ g/mol.....	162
Table 4.24 – ^1H NMR of [4-10] in CD_3CN . $\text{MW} = 273.241$ g/mol.....	163
Table 4.25 – ^1H NMR of [4-10][OTf] in CD_3CN . $\text{MW}_{\text{OTf}} = 423.317$ g/mol.....	164
Table 4.26 – ^1H NMR of [4-11] in CD_3CN . $\text{MW} = 349.262$ g/mol.....	165
Table 4.27 – ^1H NMR of [4-11][OTf] in CD_3CN . $\text{MW}_{\text{OTf}} = 499.311$ g/mol.....	166
Table 4.28 – ^1H NMR of [4-12] in CD_3CN . $\text{MW} = 387.235$ g/mol.....	167
Table 4.29 – ^1H NMR of [4-12][OTf] in CD_3CN . $\text{MW}_{\text{OTf}} = 537.261$ g/mol.....	168
Table 4.30 – ^1H NMR of [4-13] in CD_3CN . $\text{MW} = 364.243$ g/mol.....	169
Table 4.31 – ^1H NMR of [4-13][OTf] in CD_3CN . $\text{MW}_{\text{OTf}} = 514.313$ g/mol.....	170
Table 4.32 – ^1H NMR of [4-14] in CD_3CN . $\text{MW} = 303.221$ g/mol.....	171
Table 4.33 – ^1H NMR of [4-14][OTf] in CD_3CN . $\text{MW}_{\text{OTf}} = 453.297$ g/mol.....	172
Table 4.34 – ^1H NMR of [4-15] in CD_3CN . $\text{MW} = 341.194$ g/mol.....	173

Table 4.35 – ^1H NMR of [4-15][OTf] in CD_3CN . $\text{MW}_{\text{OTf}} = 491.270$ g/mol.....	173
Table 4.36 – ^1H NMR of [4-16] in CD_3CN . $\text{MW}_{\text{OTf}} = 318.196$ g/mol	175
Table 4.37 – ^1H NMR of [4-16][OTf] in CD_3CN . $\text{MW}_{\text{OTf}} = 468.272$ g/mol.....	175
Table 5.1 – Comparison of ^1H NMR Chemical Shifts in CD_2Cl_2	187
Table 5.2 – Summary of ^{19}F chemical shifts for capped thread (5-5) and rotaxane (5-4)	188
Table 5.3 – Summary of UV-vis data for 5-5a $^{2+}$ capped thread and 5-4a $^{2+}$ rotaxane	190
Table 5.4 – Summary of UV-visible data for 5-7a $^{2+}$	194
Table 5.5 – ^1H NMR of 5-1 in CDCl_3 . $\text{MW} = 170.205$ g/mol.....	199
Table 5.6 – ^1H NMR of 5-1 in CD_3CN	199
Table 5.7 – ^1H NMR of [5-2][Br] in D_2O . $\text{MW}_{\text{Br}} = 358.073$ g/mol.....	200
Table 5.8 – ^1H NMR of [5-2][OTf] in CD_3CN . $\text{MW}_{\text{OTf}} = 427.233$ g/mol	200
Table 5.9 – ^1H NMR of [5-3][Br] $_2$ in D_2O . $\text{MW}_{\text{Br}} = 465.022$ g/mol.....	201
Table 5.10 – ^1H NMR of [5-3][OTf] $_2$ in CD_3CN . $\text{MW}_{\text{OTf}} = 603.540$ g/mol.....	202
Table 5.11 – ^1H NMR of [5-4][OTf] $_2$ in CD_3CN . $\text{MW}_{\text{OTf}} = 1278.180$ g/mol.....	204
Table 5.12 – ^1H NMR of [5-5][OTf] $_2$ in CD_3CN . $\text{MW}_{\text{OTf}} = 829.673$ g/mol.....	205
Table 5.13 – ^1H NMR of [5-5][OTf] $_3$ in CD_3CN . $\text{MW}_{\text{OTf}} = 829.673$ g/mol.....	206
Table 5.14 – ^1H NMR of [5-6] in CD_3CN . $\text{MW} = 271.152$ g/mol	207
Table 5.15 – ^1H NMR of [5-7][OTf] $_2$ in CD_3CN . $\text{MW}_{\text{OTf}} = 1242.301$ g/mol.....	209
Table 6.1 – Summary of chemical shift comparisons between 6-6a $^{6+}$ and model compounds 6-5 $^{4+}$ and 6-7 $^{2+}$	216
Table 6.2 – Calculated and found exact masses for compound [6-6a][OTf] $_6$	218
Table 6.3 – ^1H NMR of 6-1 in CD_3CN . $\text{MW} = 341.0411$ g/mol.....	224
Table 6.4 – ^1H NMR of 6-2 in CD_3CN . $\text{MW} = 337.417$ g/mol	226

Table 6.5 – ^1H NMR of 6-3 in CD_3CN . MW = 258.357 g/mol	227
Table 6.6 – ^1H NMR of 6-4 in CD_3CN . MW = 416.149 g/mol	228
Table 6.7 – ^1H NMR of [6-5][OTf]₄ in CD_3CN . MW _{OTf} = 1609.188 g/mol	230
Table 6.8 – ^1H NMR of [6-6][OTf]₆ in CD_3CN . MW _{OTf} = 2533.441 g/mol	232
Table 6.9 – ^1H NMR of [6-7][OTf] in CD_3CN . MW _{OTf} = 817.816 g/mol	234
Table 7.1 – ^1H NMR of 7-1 in CD_3CN . MW = 310.352 g/mol	249
Table 7.2 – ^1H NMR of 7-2 in DMSO-d_6 . MW = 353.374 g/mol	250
Table 7.3 – ^1H NMR of 7-3 in CD_3CN . MW = 323.390 g/mol	251
Table 7.4 – ^1H NMR of 7-4 in CD_3CN . MW = 402.287 g/mol	252
Table 7.5 – ^1H NMR of 7-5 in CD_3CN . MW = 397.492 g/mol	253
Table 7.6 – ^1H NMR of [7-6][Br]₂ in D_2O . MW _{Br} = 668.424 g/mol	254
Table 7.7 – ^1H NMR of [7-6][OTf]₂ in CD_3CN . MW _{OTf} = 806.754 g/mol	255
Table 7.8 – ^1H NMR of [7-7][OTf]₂ in CD_3CN . MW _{OTf} = 1445.500 g/mol	257
Table 7.9 – ^1H NMR of [7-8][OTf]₂ in CD_3CN . MW _{OTf} = 1576.635 g/mol	259

LIST OF SCHEMES

Scheme 2.1 – Synthetic route for threads.	26
Scheme 2.2 – Representative synthesis of a [2]rotaxane molecular flip-switch.....	28
Scheme 2.3 – Labeling scheme for Chapter 2.	28
Scheme 3.1 – Numbering scheme for compounds in Chapter 3.....	106
Scheme 3.2 – Synthesis of threads 3-3a²⁺ and 3-3b⁴⁺	108
Scheme 4.1 - Synthesis of benzylanilinium threads.	129
Scheme 4.2 – Derivation of Uncomplexed Protonated Thread [HA].	136
Scheme 4.3 – Correction for actual initial concentration of protonated thread	137
Scheme 5.1 – Synthetic scheme for the synthesis of the [2]rotaxane molecular shuttles 5-4a²⁺ and 5-7a²⁺	181
Scheme 5.2 – Labeling scheme for [2]rotaxane molecular shuttle acid/base switch 5-4a²⁺ and 5-4b³⁺	184
Scheme 5.3 – Labeling scheme for molecular shuttles 5-7a²⁺ and 5-7b³⁺	193
Scheme 6.1 – Synthesis of [2]catenane 6-6⁶⁺	213
Scheme 7.1 – Synthetic scheme for [2]rotaxanes molecular shuttles.	243

LIST OF ABBREVIATIONS

24C8	24-crown-8 ether
Å	Angstrom
B24C8	Benzo-24-crown-8 ether
BN24C8	Benzonaphtho-24-crown-8 ether
BPP34C10	Bisparaphenylene-34-crown-10 ether
CBPQT⁴⁺	Cyclobis(paraquat- <i>p</i> -phenylene)
CB[8]	Cucurbit[8]uril
COSY	Correlation Spectroscopy
DB24C8	Dibenzo-24-crown-8 ether
DFT	Density Functional Theory
DN24C8	Dinaphtho-24-crown-8 ether
DS-EE	Dynamic State, E,E isomer
D-π-A-π-D	Donor- π -Acceptor- π -Donor
E_a	Activation Energy
EDG	Electron Donating Group
ESI-TOF	Electrospray Ionization-Time-of-Flight
EWG	Electron Withdrawing Group
EXSY	Exchange Spectroscopy
HETCOR	Heteronuclear Correlation Spectroscopy
HOMO	Highest Occupied Molecular Orbital
HR-MS	High Resolution Mass Spectrometry
Hz	Hertz

ICT	Intramolecular Charge Transfer
K	Kelvins
K_a	Acidity Constant
K_{assoc}	Association Constant
kJ/mol	Kilojoules per mole
LUMO	Lowest Unoccupied Molecular Orbital
MOF	Metal Organic Framework
MORFs	Metal Organic Rotaxane Frameworks
N24C8	Naphtho-24-crown-8 ether
OTf	Trifluoromethanesulfonate ion
pN	Piconewtons
ppm	parts per million
PSS	Photostationary State
R	Gas Constant
SAM	Self-Assembled Monolayer
T	Temperature
<i>t</i>	tertiary
T_c	Coalescence Temperature
<i>tert</i>	tertiary
TLC	Thin Layer Chromatography
TTF	Tetrathiofulvalene
Triflate	Trifluoromethanesulfonate ion
VT	Variable Temperature

CHAPTER 1

Molecular Machines

1.1 INTRODUCTION

Interest in molecular machines was prompted by Feynman's famous speech "There's Plenty of Room at the Bottom" where he suggested the possibility of directly manipulating and controlling individual atoms. His talk inspired the "Bottom-Up Approach" to nanotechnology whereby molecular devices and machines are constructed molecule-by-molecule to make individual components which are then connected together to make more complex systems. Today, the design and synthesis of nanoscale species that are capable of controlled mechanical motions is the focus of research groups worldwide.

In the macroscopic world, a device is something designed for a particular purpose and a machine is a device that consists of interrelated parts that work together to achieve a particular function.¹ In molecular terms, a device consists of a number of discrete molecular entities designed to perform a particular function. A molecular machine is a type of molecular device where the component parts move relative to one another as the result of an external stimulus.²

Today, the literature describes many systems that behave as molecular devices and machines whose inspirations are found in their macroscopic counterparts. As with macroscopic machines, an energy input is required to give rise to a measurable output. The energy input can be thermal, chemical, electrochemical or photochemical. The output

can be any type of measurable signal. The types of mechanical motions can be divided into six groups:

1. Spontaneous
2. Opening, Closing and Translocation
3. Rotary
4. Threading/Dethreading
5. Linear
6. Circumrotational

The feature that makes these molecular motions significant is that they all describe a motion with a particular direction. The motors in a molecular machine consist of a stationary part and a mobile part. The movement of the mobile part with respect to the stationary part describes the work performed by the motor. Work is defined as the amount of force required to induce a displacement in a particular direction.¹

The molecular systems described in this introductory chapter are only representative examples of what is available in the literature.

1.2 SPONTANEOUS MOTION

Molecular machines that move spontaneously are influenced by Brownian motion. Brownian motion is the random movement of particles that result from the bombardment of molecules by the liquid or gas medium. Some machines that are included under this heading are gears,^{3, 4} turnstiles,⁵ brakes,^{6, 7} ratchets,⁸ and gyroscopes.⁹⁻¹³ Spontaneous motion occurs in all molecules, such as rotation about a carbon-carbon single bond. Examination of a simple molecular gyroscope illustrates what is meant by spontaneous

motion. In this example, an alkyne-aryl-alkyne axle, the rotor (shown in red), is encased by a rigid triptycyl framework, referred to as the stator (shown in blue) (Figure 1.1).¹⁰

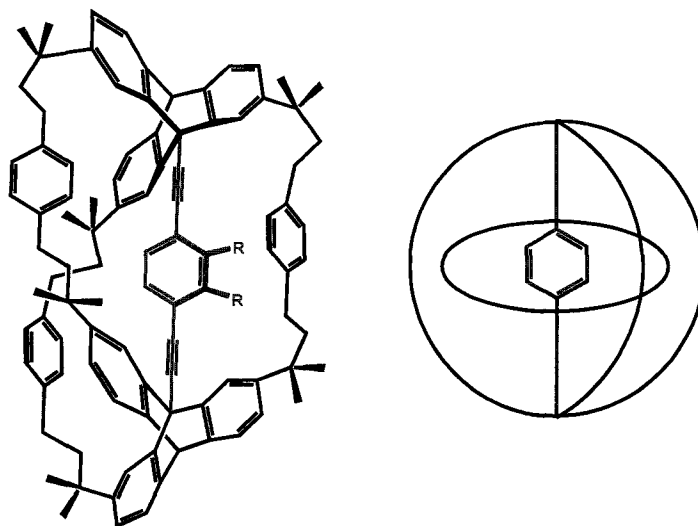


Figure 1.1 – Nanoscopic gyroscope designed by Garcia-Garibay *et al.*

The authors suggested that when $R = F$, the difluorobenzene unit should be able to reorient freely since it is sterically shielded from contact with other molecules in the environment. Calculations using the AM1 method predicted that rotation about the triptycyl-alkyne and aryl-alkyne bond (*i.e.* the axle) is essentially frictionless. In solution, ^1H NMR experiments showed the compound with $R = \text{H}$ has three-fold symmetry for the triptycyl framework and two-fold symmetry for the 1,4-phenylene ring in the middle suggesting free rotation about the aryl-alkyne single bonds. Unfortunately, interdigitation of adjacent molecules in the solid state prevents free rotation of the central axle. The authors suggest that with the addition of bulky groups in key positions on the framework, interdigitation may be prevented allowing the internal rod to rotate freely. Although movement in this system is not really in a specific direction, it is still considered a

molecular device since the axle is rotating freely with respect to the “stationary” triptycyl stator.

1.3 OPENING, CLOSING AND TRANSLOCATION

Molecular systems categorized by opening, closing and translocation movements cover a very broad area of molecular motors and devices. This category is based on structural changes to a molecular system as the result of a chemical input that cause a molecule to open, close or transport another molecule. These are functions related to recognition, assembly/disassembly, transport, catalysis and signal transfer. Typical molecular machines that may be categorized here would be: allosteric systems,¹⁴⁻¹⁶ tweezers¹⁷ and ion channels.¹⁸⁻²⁰ Allosteric systems are characterized by a binding event at one part of the molecule that causes a conformational change in another part of the

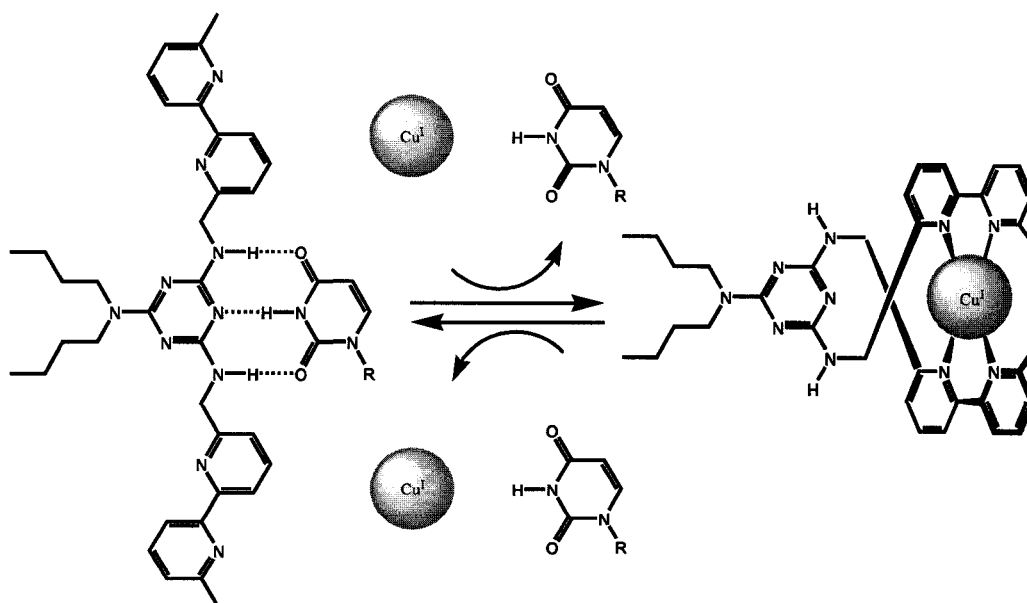


Figure 1.2 – Negative allosteric hydrogen bonding receptor for uracil studied by Branda *et al.*

molecule. Conformational change at the second site may enhance (positive allostery) or impair (negative allostery) binding of a second substrate at this site. An elegant example of negative allostery was demonstrated by Branda and coworkers using the compound shown in Figure 1.2.¹⁶ In this example, the molecule is a receptor for imide guests, such as uracil. Addition of Cu(I) causes the bipyridine arms to come together forming metal-ligand coordination bonds. This rearrangement destroys the hydrogen bonding surface for the guest, thus displacing the uracil. Removal of the Cu(I) restores the receptor to its original conformation and hence its uracil binding affinity.

1.4 ROTARY MOTION

Rotary machines are distinguished by repetitive rotation in one direction due to the input of an external stimulus. A system which achieves 360° unidirectional rotation has been described by Feringa *et al.* consisting of a sterically overcrowded alkene which

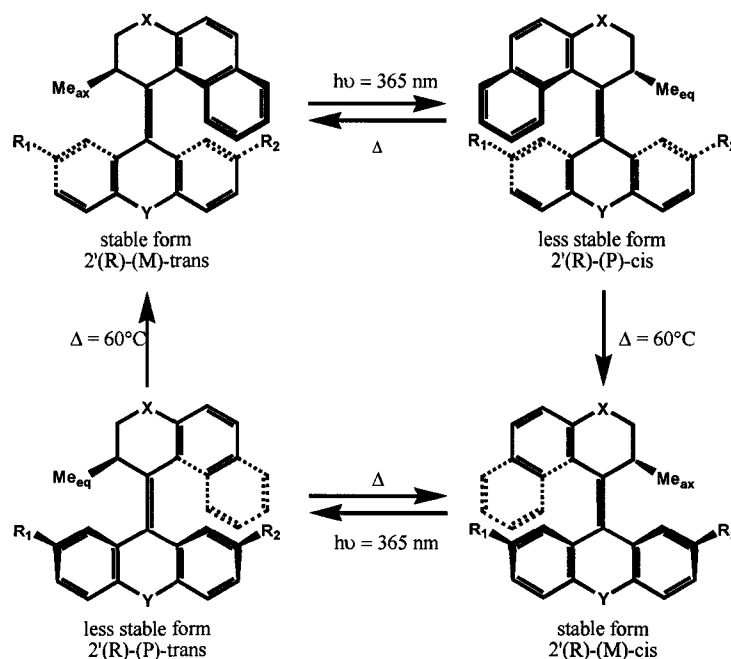


Figure 1.3 – Unidirectional molecular rotor designed by Feringa *et al.*

results in the helical arrangement of the fused arene rings.²¹⁻²³ The chiral groups are essential for the observed unidirectional rotation and dictate whether clockwise or counterclockwise rotation is observed. The 360° rotation is achieved by two *cis-trans* photoisomerizations and two thermal controlled helicity inversions. A schematic of events is given in Figure 1.3.²²

1.5 THREADING AND DETHREADING OF PSEUDOROTAXANES

Threading and dethreading movements specifically refer to supramolecular complexes called pseudorotaxanes. These complexes are composed of a minimum of two distinct components: a linear molecule, referred to as the thread, and a ring whose cavity is large enough to allow the thread to penetrate (Figure 1.4). Design of these host-guest systems requires that interactions exist between the two components that encourage their complexation. Pseudorotaxanes are formed under thermodynamic control and are driven by one or a combination of weak non-covalent interactions that define supramolecular complexes: hydrophobic interactions, electrostatic interactions (ion-ion, ion-dipole, dipole-dipole), hydrogen bonding, π - π stacking (face-to-face and edge-to face), metal coordination and van der Waals forces. To reverse the threading process, the non-covalent forces holding the complex together must be disrupted. This can be accomplished using chemical, photochemical or electrochemical stimuli.

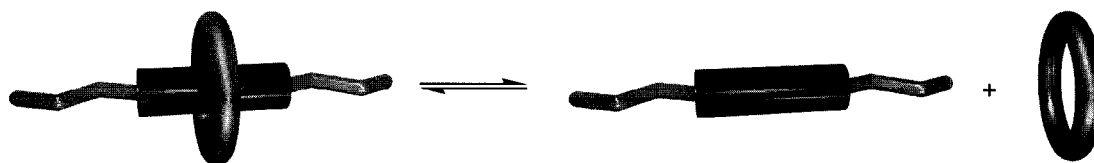


Figure 1.4 – Illustration of complexed [2]pseudorotaxane and its uncomplexed components.

The complexation/decomplexation of the pseudorotaxane shown in Figure 1.5 is chemically controlled using acid and base. Pseudorotaxane formation only occurs when the amine group on the thread is protonated. Complexation is driven by strong $NH\cdots O$ hydrogen bonding interactions between the amine hydrogen atoms of the thread and the oxygen atoms of the ring. This particular system is interesting not only for the threading/dethreading aspect, but also due to the energy transfer that occurs when the pseudorotaxane is intact. The binaphthyl unit on the crown ether absorbs light at 241 nm, 282 nm and 336 nm and fluoresces at 370 nm. Conversely, the anthracenyl unit on the thread absorbs light at 372 nm and fluoresces at 423 nm. When the anthracenyl thread is unprotonated there is no complexation with the crown ether. Irradiation using $\lambda = 282$ nm results in emission with $\lambda_{\max} = 370$ nm. Addition of acid results in complexation of the

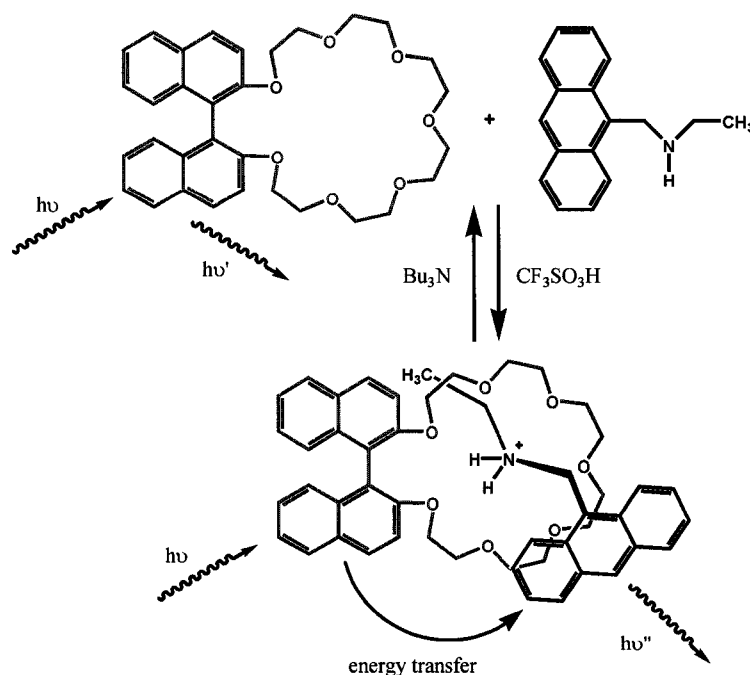


Figure 1.5 – Plug and socket pseudorotaxane system investigated by Balzani *et al.*

thread and crown and irradiation using $\lambda = 282$ nm results in the quenching of the 370 nm emission, but sensitization of emission at 423 nm. Addition of base deprotonates the thread causing dethreading and thus excitation of the binaphthyl unit results in the reappearance of the binaphthyl fluorescence and disappearance of the anthracenyl fluorescence.²⁴

Pseudorotaxanes have been exploited in ways other than threading/dethreading of a complex. Kim *et al.* devised a system using cucurbit[8]uril (CB[8]) as the ring and a hexamethylene bridged bis(viologen) as the thread, where the switching is electrochemically controlled (Figure 1.6).²⁵ In water, hydrophobic interactions between the bridging alkyl chain and the inner cavity of CB[8], along with stabilizing ion-dipole interactions between the pyridinium nitrogen atoms and the CB[8] oxygen atoms around the perimeter of the ring, drive the formation of the pseudorotaxane. Two-electron

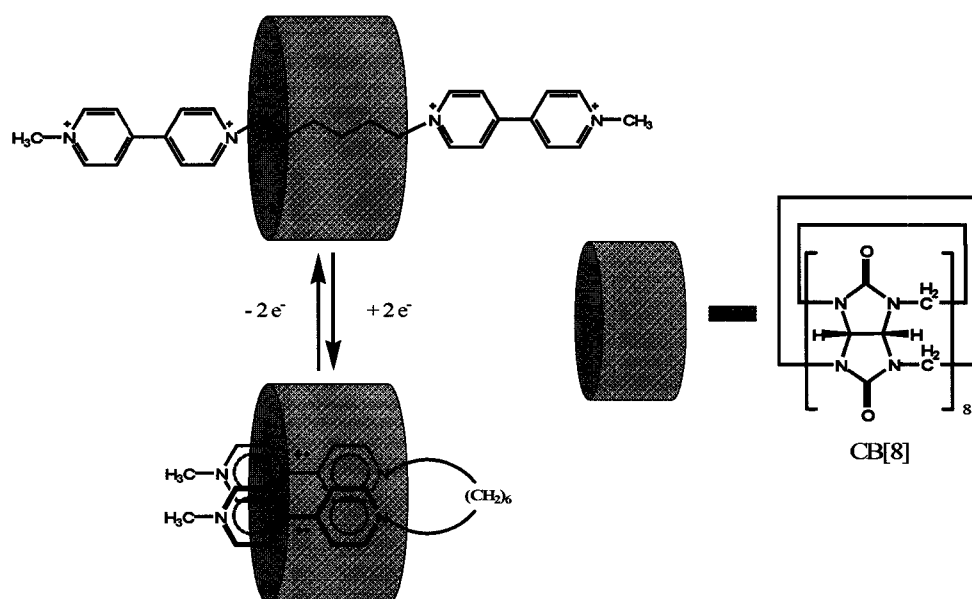


Figure 1.6 - Folding/unfolding pseudorotaxane system demonstrated by Kim *et al.*

reduction of the bis(viologen) thread results in two radical cation viologen terminal units. Consequently, intramolecular pairing of the radical ions inside the **CB[8]** ring results in the formation of a loop by the thread. Unfolding of the thread back to its linear conformation is accomplished by a two-electron oxidation.

1.6 LINEAR MOVEMENTS IN ROTAXANES

Rotaxanes are compounds that consist of a linear thread component that is capped on both ends with bulky groups and a macrocyclic ring. The ring encircles the thread, as it does in a pseudorotaxane, but the bulky capping groups prevent the ring from sliding off the end of the thread. In this way, the ring and the capped thread are mechanically linked together. Exploitation of this mechanical linkage allows for linear movement of one component with respect to the other (Figure 1.7). The nomenclature for such systems places the number of mechanically linked components in square brackets in front of the word rotaxane: [n]rotaxane. In the example shown in Figure 1.7, a single capped thread encircled by one ring is referred to as a [2]rotaxane.

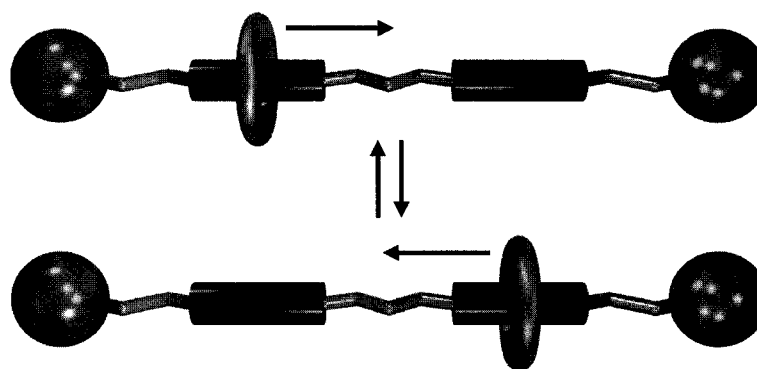


Figure 1.7– [2]Rotaxane showing linear movement of the ring on the thread.

Three methods exist for rotaxane formation: a) threading followed by capping,²⁶ b) slipping,^{27, 28} and c) clipping.²⁹ All methods require the design to include necessary

components that are capable of non-covalent interactions to draw together the thread and ring entities, an action referred to as “templating”. The threading followed by capping method, which is the most widely used, involves forming the pseudorotaxane between the thread and ring, followed by covalently attaching bulky capping groups to either end of the thread to prevent the ring from dethreading. In the slipping method, the capped thread is synthesized first, followed by slipping of the ring over a carefully designed bulky end by providing the necessary amount of energy to the system. Clipping also begins with an intact capped thread, however an open ‘ring’ associates with the thread and then is closed by covalent modification. Each method is represented pictorially in Figure 1.8.

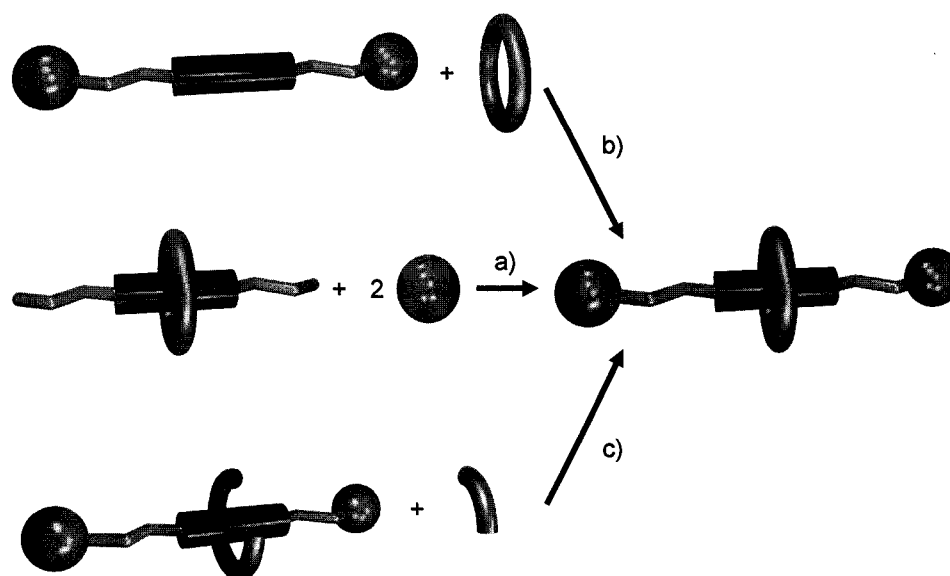


Figure 1.8 – Illustration of a) threading/capping, b) slipping and c) clipping methods for rotaxane formation.

A molecular shuttle is a rotaxane with two or more distinct recognition sites on the thread for the ring to occupy (Figure 1.9). Ideally, the ring prefers to reside at one site over the other due to stronger, non-covalent interactions. This is, therefore, the most

stable conformation and is referred to as State 0. External stimulus either destroys the interactions at this site or enhances the interactions at the other site, causing the ring to 'shuttle'; this is referred to as State 1. Reversing the effects caused by the external stimulus should direct the ring to return to its 'resting state'.

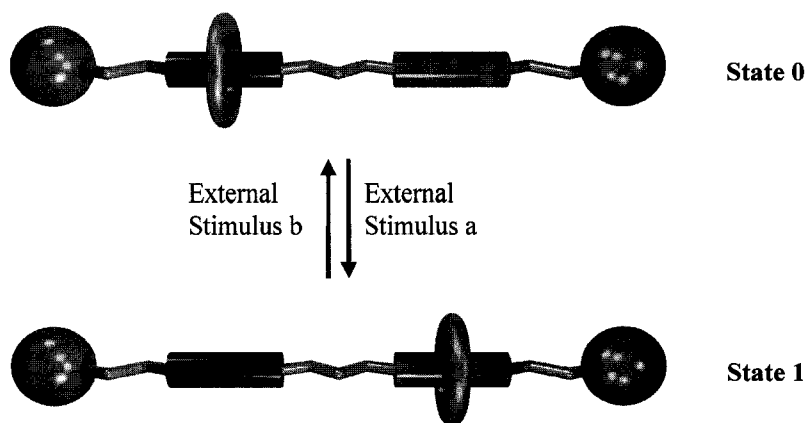


Figure 1.9 – Non-degenerate molecular shuttle.

The [2]rotaxane molecular shuttle illustrated in Figure 1.10 is not a typical system as the ring and the thread are covalently linked together.³⁰ On the thread portion there is a phenanthroline binding site and a terpyridine binding site and on the ring portion there is a phenanthroline binding site. In the presence of copper(I), which templates and assembles the supramolecular species, the thread of one molecule penetrates the ring of a second molecule, forming a hermaphroditic dimer complex. Bulky capping groups are added to prevent dethreading during demetallation of the copper(I) and remetallation with zinc(II). Copper(I), which prefers a four coordinate geometry, binds to the phenanthroline fragments on the thread and ring. This results in an extended co-conformation that stretches ~ 83 Å. Treatment with KCN extracts the copper(I) and addition of $\text{Zn}(\text{NO}_3)_2$, which prefers a five-coordinate geometry, results in the zinc(II) coordinating to the phenanthroline on the ring and the terpyridine on the thread. This causes the contraction

of the whole system to ~ 65 Å. The process can be reversed to the extended scenario by the addition of excess $[\text{Cu}(\text{CH}_3\text{CN})_4][\text{PF}_6]_2$. The expansion and contraction motion is reminiscent of myosin moving along actin filaments in muscles.³¹

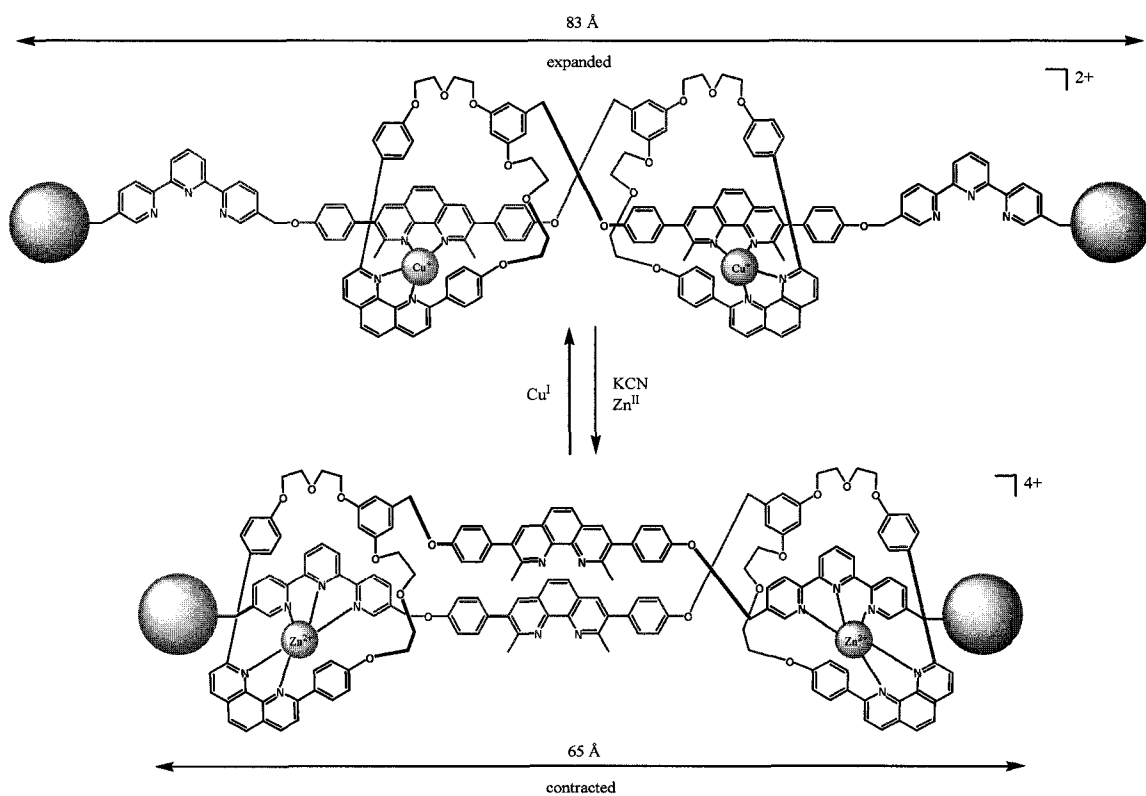


Figure 1.10 –Molecular muscle system studied by Sauvage *et al.*

The translational movements in rotaxanes can also be coupled to other properties selectively incorporated into the design of the system. One particular area this is likely to find application is in digital information processing, which is based on binary digits (1 and 0) and logic gates.³² Logic gates are the elementary building blocks of digital circuits, with the simplest consisting of two inputs and one output. A threshold value is arbitrarily set; inputs below the threshold are represented by ‘0’ and inputs above the threshold are represented by ‘1’. The three basic logic gates are NOT, AND and OR gates; other logic gates can be obtained by using combinations of these three. The NOT gate, also known as

an inverter, changes an input of 1 to an output of 0. The AND gate gives an output of 1 only if both inputs are 1, otherwise the output is 0. The OR gate gives an output of 1 if either input or both inputs are 1. The associated truth tables are shown in Figure 1.11.

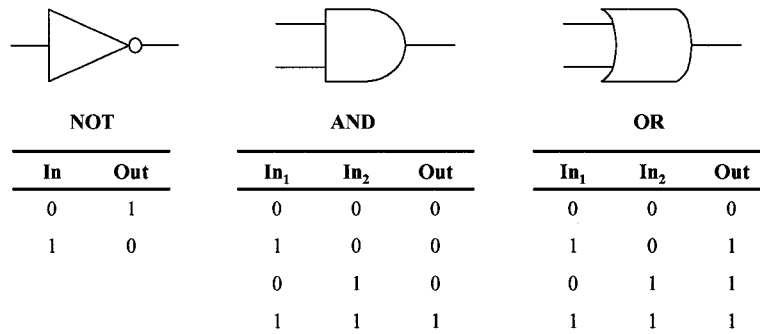


Figure 1.11 – Truth tables for NOT, AND and OR logic gates.

A half-adder is a combination of an XOR gate and an AND gate that is used to add binary numbers. The XOR gate generates the “SUM” digit and the AND gate generates the “CARRY” digit (Figure 1.12).

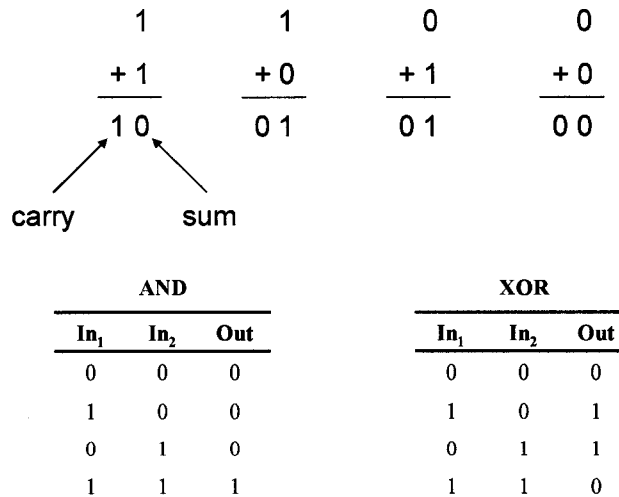


Figure 1.12 – Binary addition.

The rotaxane system depicted in Figure 1.13 is an example of a half-adder.³³ It is comprised of an α -cyclodextrin (α -CD) macrocycle mechanically linked to a thread

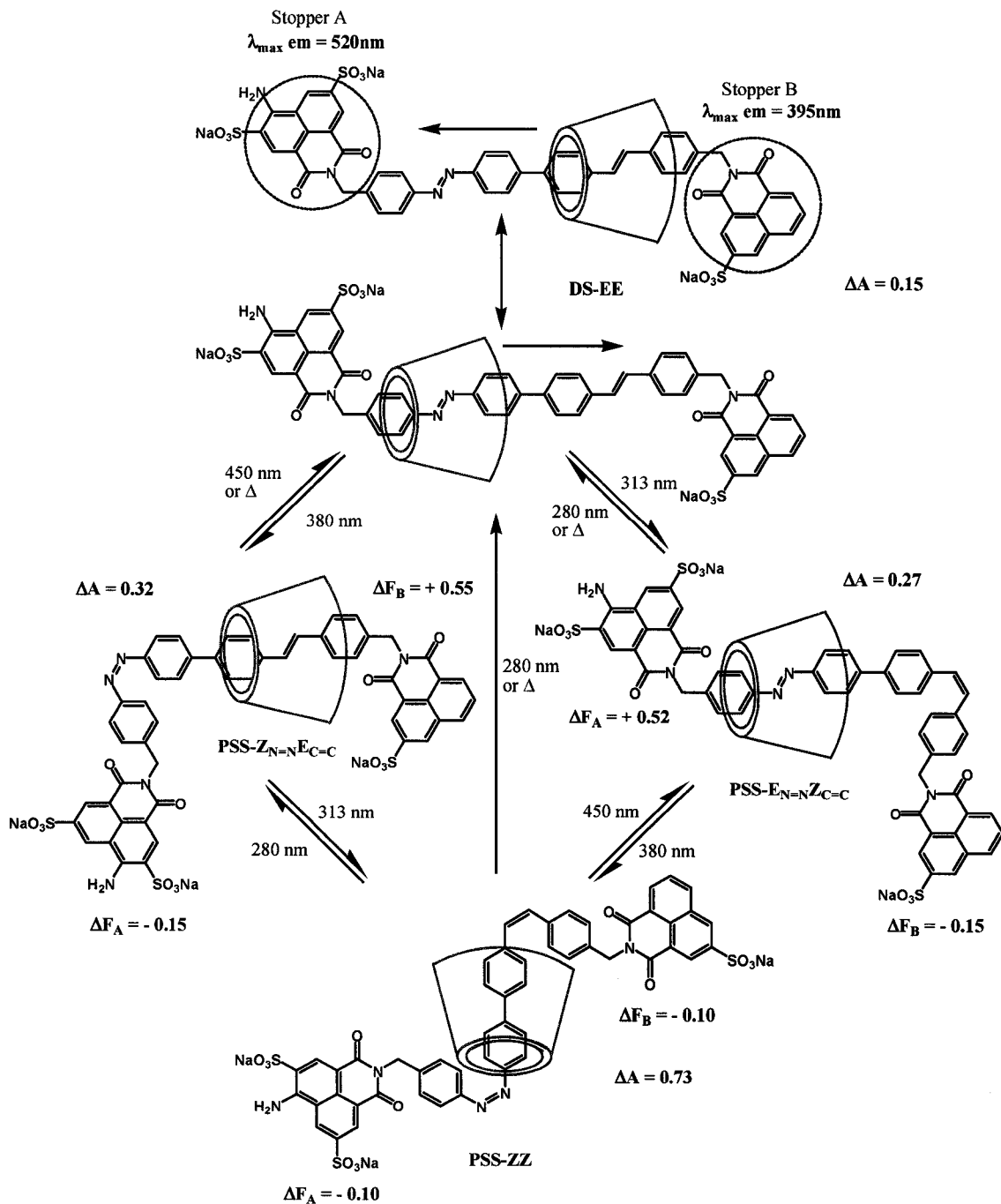


Figure 1.13 – [2]Rotaxane molecular half-adder described by Hien et al.³³

bearing two photoswitchable binding sites: an azobenzene site and a stilbene site. The bulky capping groups are two fluorescent naphthalimide groups, Stopper A and Stopper B. Using different wavelengths of light, the two recognition sites can be individually addressed. The azobenzene is switched from isomer E to Z using $\lambda = 380$ nm and the stilbene is switched from isomer E to Z using $\lambda = 313$ nm. The [2]rotaxane absorbs at $\lambda = 270$ nm and $\lambda = 350$ nm with an isosbestic point at $\lambda = 301$ nm. Stopper A fluoresces at $\lambda_{\text{max}} = 520$ nm and Stopper B fluoresces at $\lambda = 395$ nm. In the initial E,E isomer, the α -CD shuttles between both the azobenzene and stilbene sites (**DS-E_{N=N}E_{C=C}**; **DS** means dynamic state). Photoisomerization using $\lambda = 380$ nm converts the azobenzene from E to Z, causing α -CD to reside at the stilbene site (**PSS-Z_{N=N}E_{C=C}**; **PSS** means photostationary state). Alternatively, photoisomerization of the **DS-E_{N=N}E_{C=C}** isomer using $\lambda = 313$ nm converts the stilbene from E to Z, causing α -CD to reside at the azobenzene site (**PSS-E_{N=N}Z_{C=C}**). Photoisomerization of **PSS-Z_{N=N}E_{C=C}** with $\lambda = 313$ nm produces **PSS-Z_{N=N}Z_{C=C}**, likewise irradiation of **PSS-E_{N=N}Z_{C=C}** with $\lambda = 380$ nm also produces **PSS-Z_{N=N}Z_{C=C}**. Since α -CD cannot reside at either the azobenzene or stilbene site, it encircles the biphenyl group between the two sites. The position of the macrocycle α -CD affects the absorbance of the other conformations; the absorbance at $\lambda = 270$ nm increases and the absorbance at $\lambda = 350$ nm decreases. The magnitude of the change in absorbance is measured by: $\Delta A = \frac{|Abs_{(270)} - Abs_{(350)}|}{Abs_{(301)}}$. The position of the macrocycle α -CD also affects the fluorescence of Stopper A and Stopper B. The presence of α -CD near the fluorescent stopper hinders vibrations and rotations of the methylene bonds between the stopper and the recognition site, resulting in increased fluorescence. The percent by which the fluorescence increases or decreases with respect to the **DS-E_{N=N}E_{C=C}** is measured as

ΔF . In terms of logic expressions, the inputs are assigned as $\lambda = 380$ nm and $\lambda = 313$ nm and the outputs are assigned as ΔA and ΔF . Results are summarized in Table 1.1.

Table 1.1 – Results for absorbance and fluorescence data for the four isomers of [2]rotaxane.

	ΔA	ΔF
DS-EE	0.15	0.10
PSS-Z_{N=N}E_{C=C}	0.32	0.55
PSS-E_{N=N}Z_{C=C}	0.27	0.52
PSS-Z_{N=N}Z_{C=C}	0.73	0.43

Setting the threshold for ΔA at 0.70 means that only under the condition that produces isomer **PSS-Z_{N=N}Z_{C=C}** (when both inputs are used) would give a value of 1. This meets the necessary conditions for an AND gate. Setting the threshold for ΔF at 0.50 means that conditions producing either **PSS-Z_{N=N}E_{C=C}** (when $\lambda = 380$ nm is used) or **PSS-E_{N=N}Z_{C=C}** (when $\lambda = 313$ nm is used) gives an output of 1. This meets the necessary conditions for an XOR gate.(Table 1.2)

Table 1.2 – Truth table for [2]rotaxane molecular half adder.

In₁ (380 nm)	In₂ (313nm)	Out₁ ΔA (AND gate) n_c	Out₁ ΔF (XOR gate) n_s	Binary Sum
0	0	0	0	00
1	0	0	1	01
0	1	0	1	01
1	1	1	0	10

1.7 CIRCUMROTATIONAL MOVEMENTS IN CATENANES

A catenane is a species consisting of two or more interlocked macrocyclic components held together by mechanical bonds that prevent their dissociation (Figure

1.14). They are generally formed using a template-directed clipping synthesis whereby one ring is intact while the other is a 'U-shaped' component. After forming a pseudorotaxane complex, the 'U-shaped' portion is closed by covalent modification. Similar to a molecular shuttle, if one ring contains two recognition sites, the other ring can be controllably switched between the two sites.

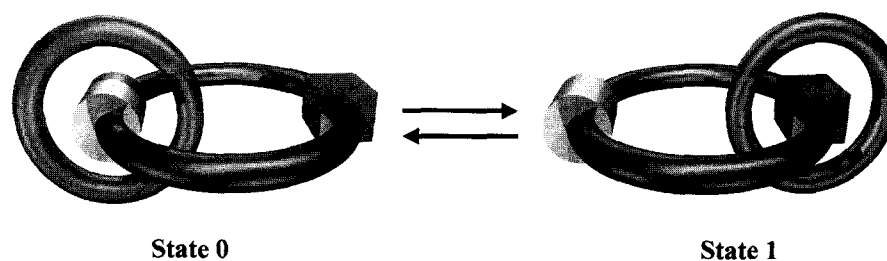


Figure 1.14 – Two co-conformations of a [2]catenane circumrotational switch.

Leigh *et al.* designed a catenane system where, not only is there control over switching between recognition sites, but also in which direction one ring moves around the other (Figure 1.15).³⁴ In this [2]catenane, the two recognition sites on the one ring are fumaramide and succinamide (blue). Fumaramide (E-configuration) can be photochemically switched to the maleamide isomer (Z-configuration). Other features to this ring are the two bulky blocking groups, dimethyl-*t*-butylsiloxy and trityl, which are located on either side of the succinamide fragment. The second ring (red) has two isophthalamide components that are capable of hydrogen bonding with the carbonyl groups of the fumaramide, succinamide and maleamide fragments on the other ring. The isophthalamide ring prefers the possible recognition sites in the order from greatest to least: fumaramide, succinamide then maleamide. When fumaramide is photochemically switched to maleamide, the isophthalamide ring would prefer to shuttle to the succinamide site. The bulky blocking groups prevent this, thus the isophthalamide ring is

forced to remain at the maleamide site. Removal of the silyl group allows the isophthalamide ring to move to the succinamide site. Re-silylation replaces the bulky blocking group so that when maleamide is photoisomerized back to fumaramide, and the trityl group removed, the isophthalamide ring will have completed a 360° rotation in a clockwise direction as illustrated in Figure 1.15. Had the sequence of events been carried out in the reverse order, a clockwise 360° rotation would have occurred.

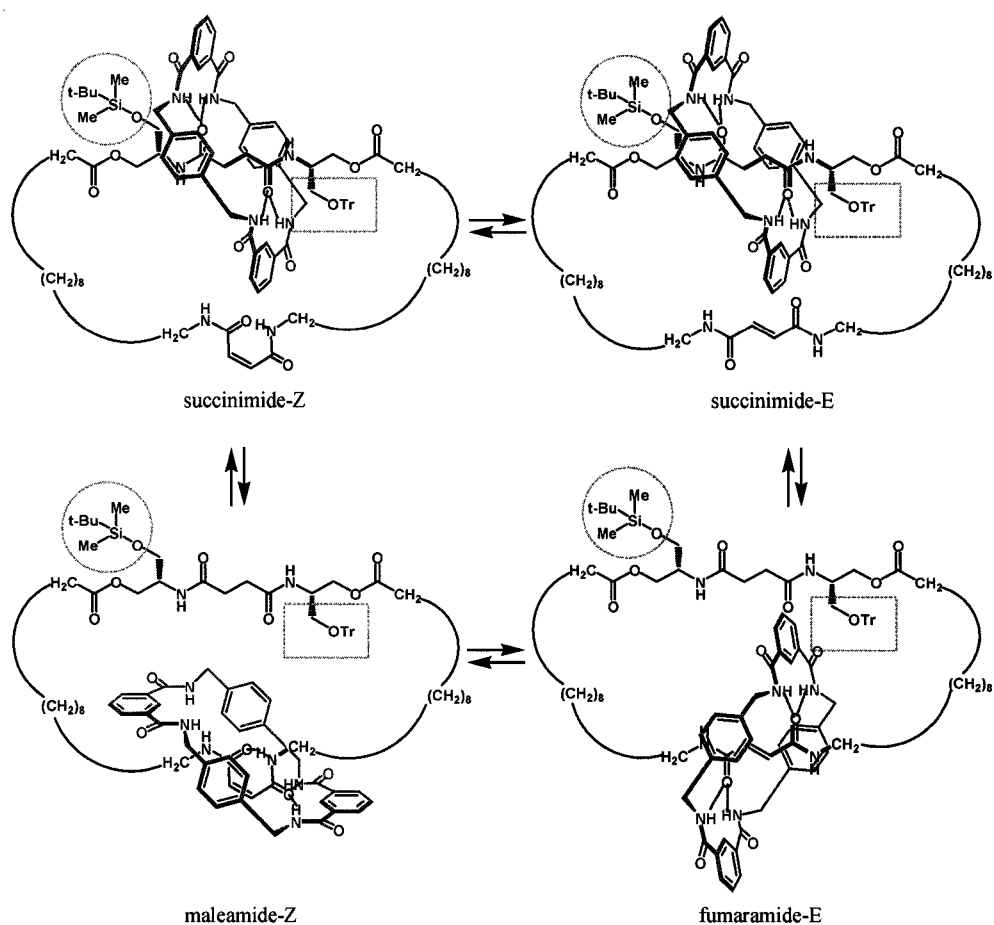


Figure 1.15 – [2]Catenane capable of reversible unidirectional circumrotation designed by Leigh *et al.*

1.8 MOLECULAR MACHINES AT WORK

The systems described so far have all been in solution. In order to make molecular machines and motors into functional materials, they need to be interfaced to the

macroscopic world in an ordered fashion. To accomplish this, nanomachines will need to be organized at an interface, deposited on surfaces, immobilized on membranes or in crystal lattices. By organizing molecular assemblies in one of these ways, their movements may behave coherently and be addressed on the nanometer scale.

In a remarkable example of molecular machines performing measurable mechanical work, Stoddart and co-workers used self-assembled monolayers (SAMs) of a bistable [3]rotaxane molecular shuttle system to bend a cantilever. Figure 1.16 illustrates the palindromic molecular shuttling system whose movements are also reminiscent of a biological muscle.³⁵

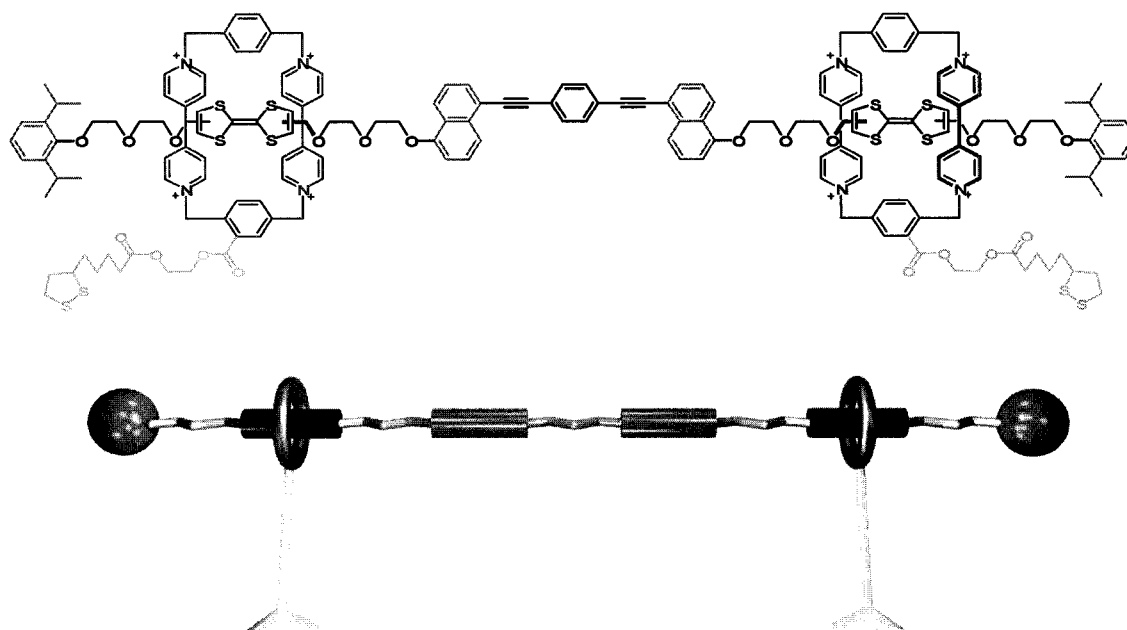


Figure 1.16 – Structural and graphical representation of a palindromic molecular muscle [3]rotaxane constructed by Stoddart *et al.*

The thread portion consists of two pairs of distinct recognition sites for the cyclobis(paraquat-p-phenylene)⁴⁺ (CBPQT⁴⁺) macrocycle: a naphthalene fragment and a

tetrathiofulvalene (**TTF**). Both sites are electron rich, but the electron poor **CBPQT**⁴⁺ has a higher affinity for the **TTF** site. One- or two-electron oxidation of the **TTF** unit causes electrostatic repulsion of the positively charged macrocycle, forcing it to the less favourable naphthalene site. Reducing **TTF** back to its neutral state returns the system back to its thermodynamically favoured state. The distance between the two macrocycles changes from 4.2 nm (in the extended state) to 1.4 nm (in the contracted state). The macrocycles are functionalized with disulfide groups which allow them to be adsorbed onto a gold surface (Figure 1.17). Cantilevers that were evaporated with gold were used to form self-assembled monolayers of the [3]rotaxane bistable shuttles. Stress on the cantilever caused by the oxidation of the **TTF** and the moving of **CBPQT**⁴⁺ to the inner naphthalene site was monitored by the change in the deflection of a laser beam focused on the cantilevers.

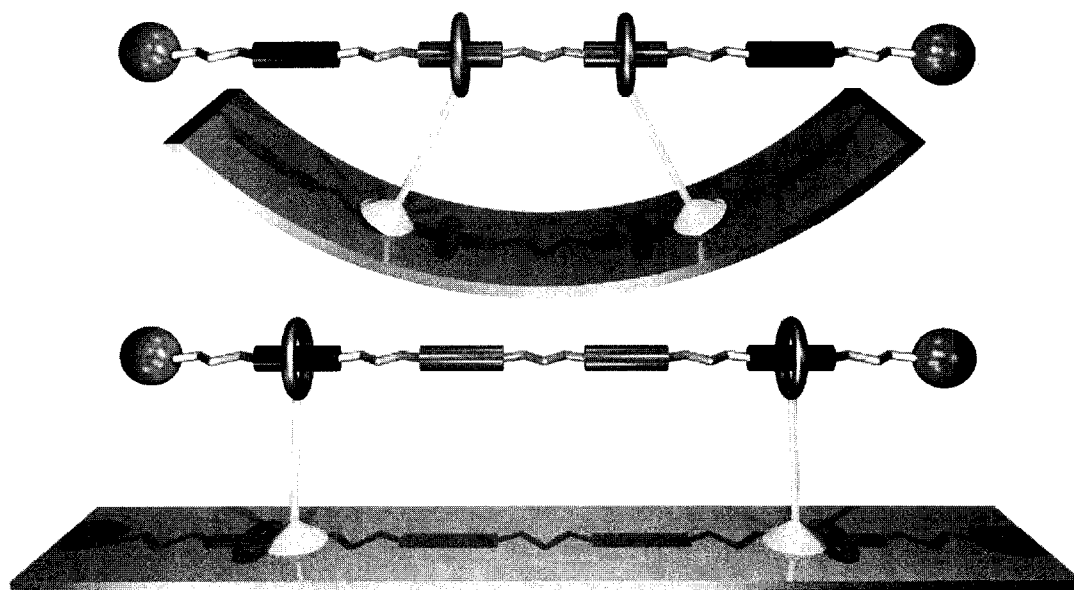


Figure 1.17 – Graphical representation of the bending action of a cantilever due to the contraction of the palindromic molecular muscle.

The mechanical bending of the cantilevers was observed over 25 cycles of oxidation/reduction. The mean molecular force associated with the bending of the cantilever was calculated based on Coulomb's Law and was found to be in the range of 14 - 21 pN.

1.9 THE LOEB MOTIF

In the late 1980s, Stoddart and co-workers discovered that bis(paraphenylene)-34-crown-10 ether (**BPP34C10**) formed a pseudorotaxane complex with paraquat²⁺ (Figure 1.18).³⁶ It was noted that the binding of paraquat²⁺ with **BPP34C10** was attributed to i) charge transfer between the hydroquinol rings of the crown with the pyridinium rings of paraquat²⁺, ii) paraquat²⁺ being tilted by 62° from the perpendicular so as to maximize N⁺...O interactions between the pyridinium nitrogen atoms and the crown ether oxygen atoms and iii) the weak CH...O hydrogen bond interactions between the guest and the receptor.

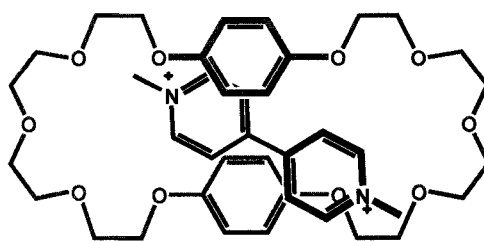


Figure 1.18 – [2]Pseudorotaxane of paraquat²⁺ and BPP34C10.

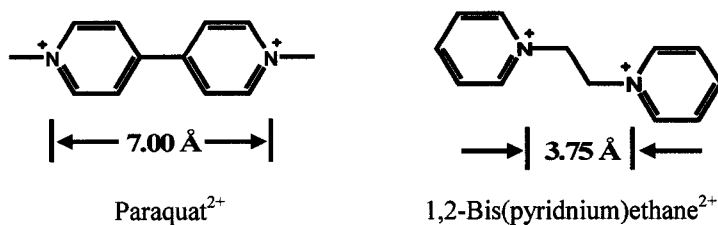


Figure 1.19 – Comparison of $N^+ \cdots N^+$ distances between paraquat²⁺ and 1,2-bis(pyridinium)ethane²⁺.

The $N^+ \cdots N^+$ distance in paraquat²⁺ is 7.00 Å. 1,2-Bis(pyridinium)ethane²⁺ is an isomeric form of paraquat²⁺, however the positive charge distribution is much more concentrated with an $N^+ \cdots N^+$ distance of 3.75 Å (Figure 1.19).³⁷ Loeb and Wisner established that 1,2-bis(pyridinium)ethane²⁺ is capable of forming [2]pseudorotaxane complexes with the macrocycle 24-crown-8 ether (**24C8**) and its derivatives. Solution ¹H NMR spectroscopic studies and X-ray crystallographic data indicated that complexation is driven by several non-covalent interactions, namely: i) $N^+ \cdots O$ ion-dipole interactions, ii) eight weak $CH \cdots O$ hydrogen bonds and iii) π - π stacking interactions (Figure 1.20).^{37,38}

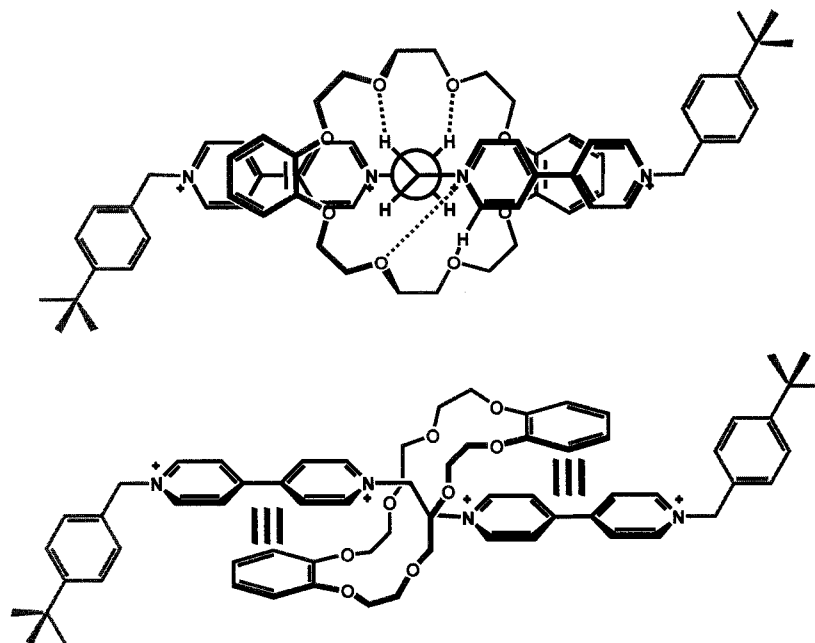


Figure 1.20 – Newman projection top view (top) and side view (bottom) showing non-covalent interactions between a 1,2-bis(dipyridinium)ethane⁴⁺ capped thread and DB24C8.

The 1,2-bis(pyridinium)ethane/24C8 motif has proven to be a versatile system. It has been used for the formation of [2]pseudorotaxanes,³⁷⁻³⁹ [2]rotaxanes,⁴⁰⁻⁴³ [3]rotaxanes,⁴⁴ [3]catenanes,⁴⁵ molecular shuttles,⁴⁶ branched [n]rotaxanes, (n=2-4),⁴⁷ dendrimeric rotaxanes⁴⁸ and metal organic rotaxane frameworks (MORFs).⁴⁹

1.10 SCOPE OF THESIS

In this thesis, a broad range of topics will be covered, each touching on different aspects of the types of mechanical motion that have been described in this introductory chapter on molecular machines.

It has been previously established, by the Loeb group, that the 1,2-bis(pyridinium)ethane binding site relies on the two positive charges at the pyridinium nitrogen atoms to generate non-covalent interactions with 24-crown-8 macrocycles; the pyridinium nitrogen atoms are involved in ion-dipole interactions with the crown ether, they render the ethylene protons and the *ortho* pyridinium protons acidic enough that they can form relatively weak hydrogen bonds and lastly they make the linear thread electron poor.

To begin this thesis, in **Chapter 2**, a new type of mechanical motion is described which has been coined a mechanical “Flip-Switch”, using a single recognition motif based on the previously mentioned 1,2-bis(pyridinium)ethane binding site and several different macrocycles. In **Chapter 3**, it will be shown how the binding capabilities of the bis(pyridinium)ethane site can be effectively turned *OFF* by an intramolecular charge transfer (ICT) and then be turned back *ON* by shutting off the ICT. The Loeb motif has also been exploited in conjunction with a new recognition site, *N*-benzylanilinium, in an effort to develop bistable molecular machines. A detailed study of the new binding site,

its properties and complexation abilities with 24-crown-8 macrocycles is presented in **Chapter 4**. A new molecular system, based on the structural similarities of these two recognition sites, has been designed and synthesized whereby both structural motifs can be combined into a single molecular architecture with only slight modifications to the existing framework. The versatility of this approach will be demonstrated by the bistable [2]rotaxane molecular shuttles described in **Chapter 5**, modification into a [2]catenane circumrotational shuttle in **Chapter 6**, and finally into systems that have potential to be transformed into functional materials, which is discussed in **Chapter 7**.

For each particular system, a description of the movement of one component with respect to the other, the input used to manipulate the movement, and the way in which the movement is monitored, will be presented and discussed.

CHAPTER 2

Flip-Switches

2.1 INTRODUCTION

The (1,2-bis(dipyridinium)ethane) \subset (24-crown-8) or Loeb motif has proven to be a versatile recognition template for the formation of interlocked and interpenetrated molecules. This chapter describes the use of this interaction to illustrate a new type of motion with a set of previously unexplored isomers. These co-conformations operate at a single recognition site, where the relative positioning of the two interlocked components produces two positional isomers such that their inter-conversion is reminiscent of a “flip-switch”. The term “flip” is used herein to visualize the resultant change in relative positions of the two components rather than as a statement of the actual mechanism of reorientation.⁵⁰

Figure 2.1 illustrates the two co-conformations. On the thread portion of the rotaxane, there is a green sphere on one end and a blue sphere on the other end. Similarly, the macrocycle also has a green cylinder on one end and a blue cylinder on the other end. Two co-conformations exist: (i) when the green cylinder on the macrocycle is over the green sphere on the thread and (ii) when the green cylinder on the macrocycle is over the blue sphere on the thread. This chapter focuses on proving the existence of the two co-conformations, showing how one co-conformation may be preferred over the other as well as demonstrating the manipulation of the ratio of co-conformations by external perturbation.

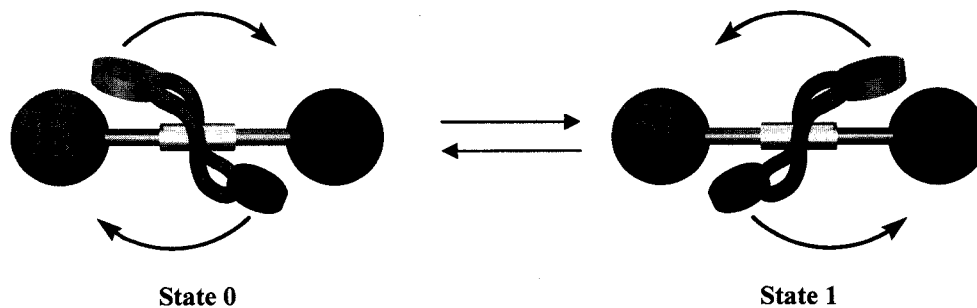
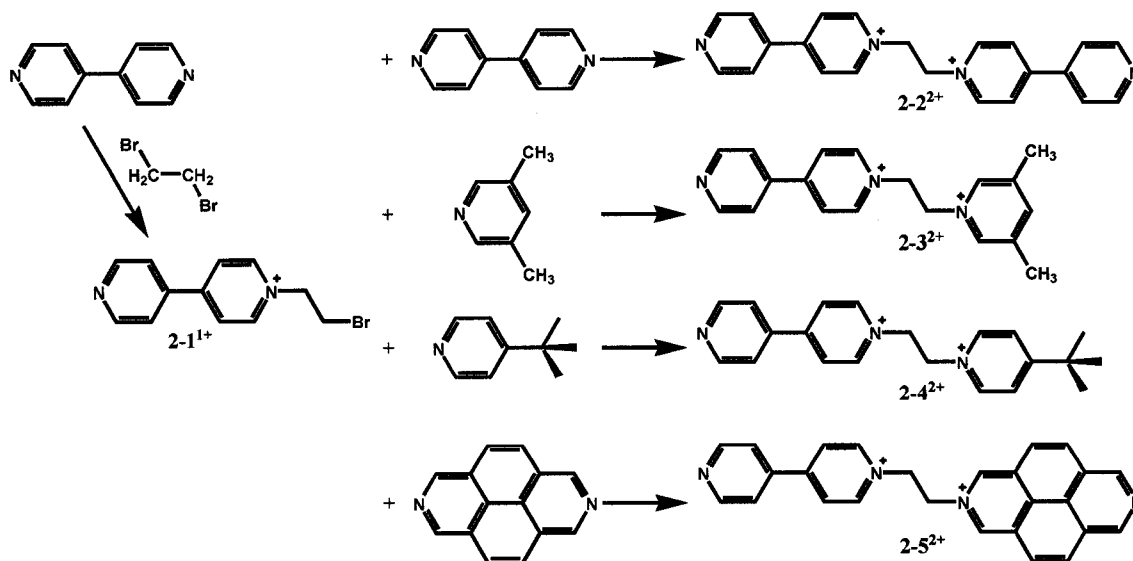


Figure 2.1 – Illustration representing the two co-conformations of a flip-switch.

2.2 SYNTHESIS AND CHARACTERIZATION

2.2.1 Synthesis

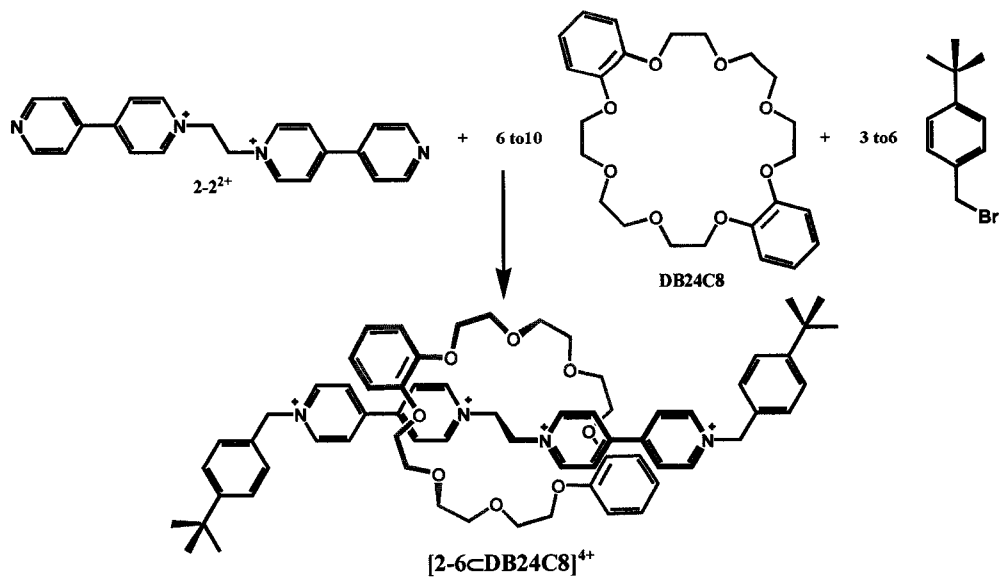
Each of the [2]rotaxane molecular flip-switches was synthesized in a similar manner. Compound **2-1¹⁺** was refluxed with the corresponding pyridine to generate the threads **2-2²⁺** - **2-5²⁺** (Scheme 2.1). Each thread was isolated as the bromide salt and subsequently anion exchanged to the triflate salt.



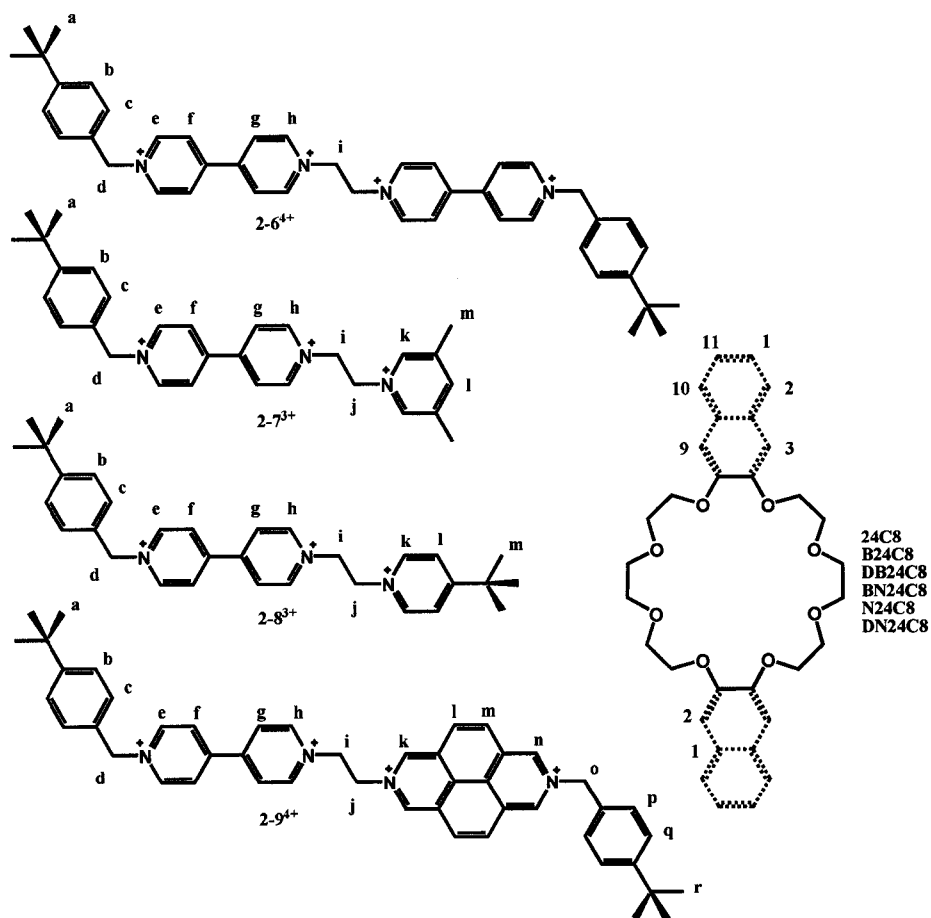
Scheme 2.1 – Synthetic route for threads.

To synthesize the [2]rotaxanes one equivalent of thread was reacted with six to ten equivalents of appropriate crown ether and three to six equivalents of *tert*-butylbenzyl bromide (Scheme 2.2). Two different reaction conditions were used: (i) dissolving all reactants in CH₃CN, stirring for three to five days at room temperature and then filtering the resulting precipitate or ii) dissolving all reactants in a two phase mixture of CH₃NO₂/H₂O, adding NaOTf to the H₂O layer, stirring for three to five days at room temperature, subsequent removal of H₂O layer, washing of the CH₃NO₂ layer several times with H₂O, evaporating the CH₃NO₂ followed by column chromatography on the residue. Using the first method did not always yield the [2]rotaxane directly, thus it was necessary to purify the residue from the CH₃CN filtrate by column chromatography. The [2]rotaxanes that precipitated from CH₃CN solution were isolated as the bromide salt by vacuum filtration and then anion exchanged to the corresponding triflate salt. Capped threads were also synthesized using method (i) but without the addition of crown ether. Synthesis of the capped threads made possible analysis of the non-covalent interactions in the [2]rotaxanes by comparing the ¹H NMR chemical shifts of both species in the same solvent. The **24C8** derivatives were synthesized according to modified literature procedures.^{51, 52}

The labeling scheme for this chapter is outlined in Scheme 2.3. For the purpose of clarity, the rotaxanes will be represented by capped thread number followed by the corresponding crown, for example [2-6cDB24C8]⁴⁺. When referring to the capped thread species, only the number of the thread will be used. All rotaxanes and capped threads have been converted to the triflate anion species.



Scheme 2.2 – Representative synthesis of a [2]rotaxane molecular flip-switch.



Scheme 2.3 – Labeling scheme for Chapter 2.

2.2.2 ^1H NMR Spectroscopy

One of the simplest [2]rotaxanes that can be made with the bis(pyridinium)ethane binding motif and which displays the effect of all three non-covalent interactions responsible for the initial self-assembly is $[2\text{-}6\text{cDB}24\text{C}8]^{4+}$. Figures 2.2a and 2.2b show the ^1H NMR spectra in CD_3CN of $2\text{-}6^{4+}$ and $[2\text{-}6\text{cDB}24\text{C}8]^{4+}$. Chemical shift differences between the capped thread and [2]rotaxane indicate the influence of the non-covalent

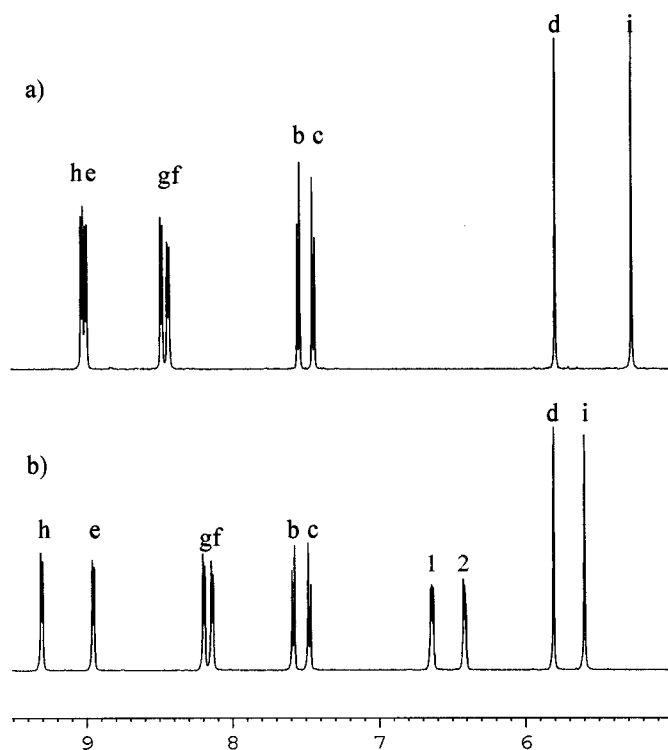


Figure 2.2 – ^1H NMR spectra of a) $2\text{-}6^{4+}$ and b) $[2\text{-}6\text{cDB}24\text{C}8]^{4+}$ in CD_3CN .

interactions between the thread and the crown ether. The ethylene protons of the recognition site, **i**, and the *ortho*-pyridinium protons, **h**, are involved in hydrogen bonding interactions with the oxygen atoms of the crown ether. As a result, they shift downfield by ~ 0.30 ppm which is typical of protons involved in this type of non-covalent interaction. Conversely, the *meta*-pyridinium protons, **f** and **g**, shift upfield ~ 0.30 ppm

due to π -stacking interactions between the electron rich catechol rings of the crown ether and the electron poor pyridinium rings of the thread. At the same time, the crown ether catechol protons also shift upfield for the same reason. Other protons on the thread, such as **b**, **c** and **d**, do not shift significantly as they are not directly involved in any non-covalent interactions with the crown ether. Proton **e** is only significantly affected in the presence of *naphtho* rings on the crown ether.

2.3 PROOF OF THE “FLIPPING” PHENOMENON

2.3.1 Variable Temperature ^1H NMR Experiments

To confirm the existence of the flipping phenomenon, the symmetrical thread **2-6⁴⁺** was used with the unsymmetrical crown ether **BN24C8**. The use of the terms ‘symmetrical’ and ‘unsymmetrical’ is meant to indicate whether the two ends of the molecule as viewed through a mirror plane located between (i) the carbon atoms of the ethylene bridge for the thread or the rotaxane or (ii) between the second and third oxygen atoms of the ethereal arms of the crown ether, have the same or different substituents, respectively (Figure 2.3).

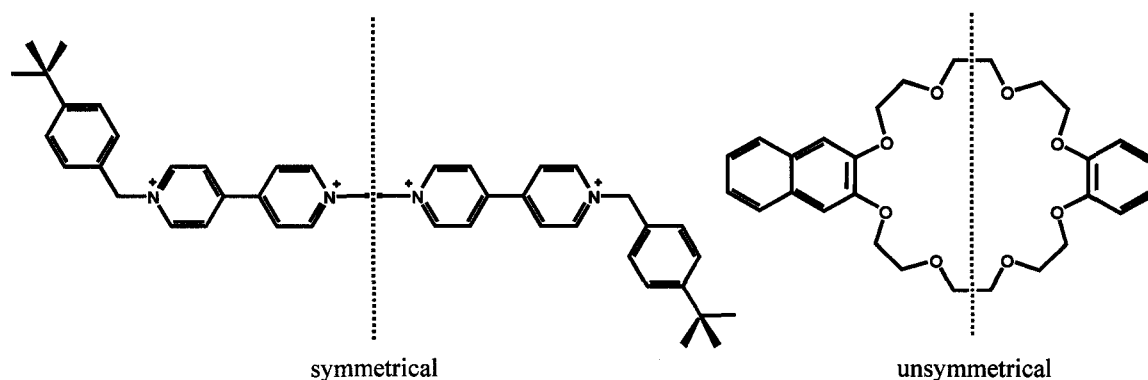


Figure 2.3 – Symmetrical thread 2-6⁴⁺ and unsymmetrical crown ether BN24C8.

Figure 2.4 shows the two possible orientations of the ring for this rotaxane. In State 0, the *naphtho* ring of the crown ether is located over the blue dipyrindinium end and the *benzo* ring over the green dipyrindinium end. In State 1, the ring has flipped so that the *naphtho* ring is over the green dipyrindinium and the *benzo* ring is over the blue dipyrindinium.

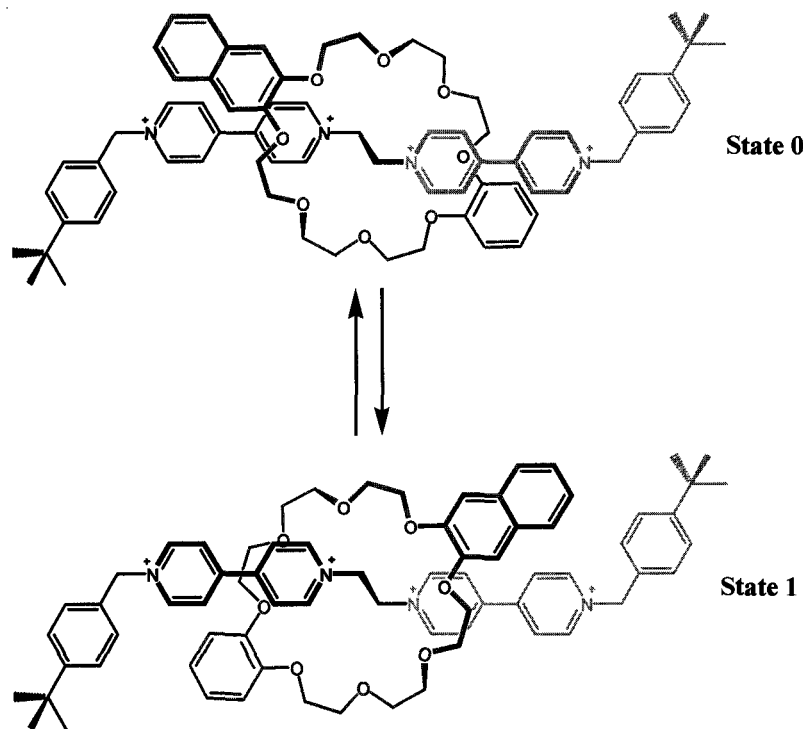


Figure 2.4 – Two possible orientations of BN24C8 for $[2-6\subset\text{BN24C8}]^{4+}$.

Since both sides of the thread are equivalent, and the *naphtho* ring does not prefer the blue dipyrindinium rings any more than the green dipyrindinium rings, this particular example is considered degenerate. By definition, these must have equal populations since they are simply different ends of the same molecule. Variable Temperature (VT) NMR is a simple technique used for studying dynamic processes, such as conformational changes. Figure 2.5 shows that at 30°C, the aromatic portion of the spectrum of $[2-6\subset\text{BN24C8}]^{4+}$

in CD_2Cl_2 exhibits four averaged peaks representing the eight different types of dipyrindyl protons. This is the result of a rapid end-to-end exchange of the aromatic rings of the crown ether relative to the thread. As the temperature is lowered, the peaks, which started as sharp doublets, begin to broaden. Coalescence occurs at $\sim -45^\circ\text{C}$, when the peaks

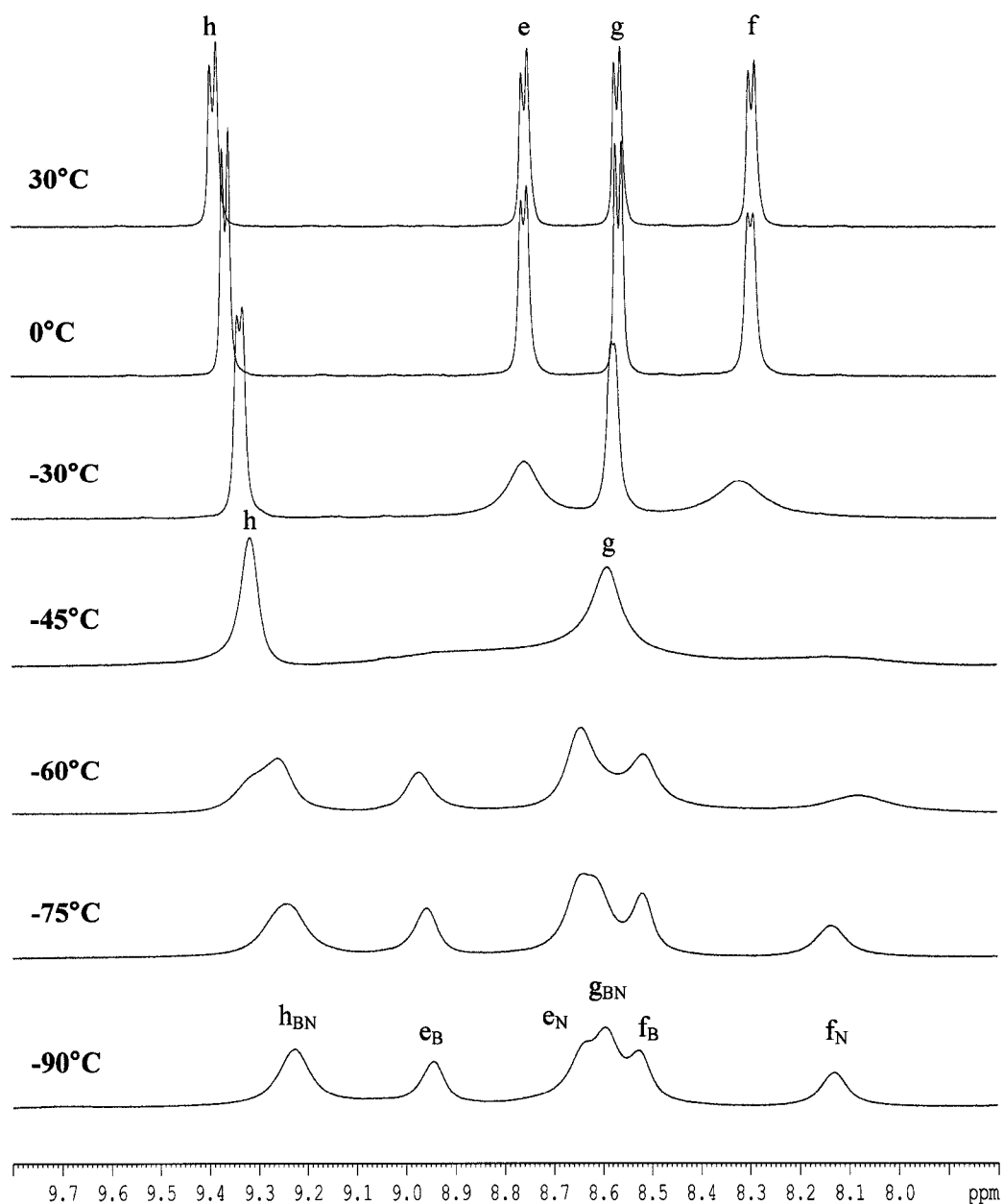


Figure 2.5 – Variable temperature ^1H NMR spectra of $[2-6\text{cBN}24\text{C}8]^{4+}$ in 9:1 $\text{CD}_2\text{Cl}_2:\text{CD}_3\text{CN}$. Subscripts B and N denote the *benzo* (B) and *naphtho* (N) ends of the molecule.

representing protons **e** and **f** are flattened into the baseline as the rate of flipping approaches that of the NMR timescale. The limiting spectrum of the same compound at -90°C shows six broad, but distinct peaks. Peak broadening is a consequence of the increase in viscosity of the solvent, CD₂Cl₂, as the temperature approaches its freezing point at -95°C and the fact these relatively large molecules are tumbling more slowly since the solution has less thermal energy.

Closer examination of the environments of each of the protons provides a rationalization for the appearance of the limiting spectrum. The inner protons labeled **h** and **g** (Scheme 2.3) are consistently shielded by either the *benzo* aromatic ring or the inner portion of the *naphtho* aromatic ring of **BN24C8**. As a result, the peaks representing these protons do not split since their immediate environments are not sufficiently different. However, the outer dipyridyl protons, labeled **e** and **f**, do experience significantly different amounts of shielding depending on the presence or absence of the larger *naphtho* ring. When the *naphtho* ring is present, the protons are shielded and hence are shifted upfield due to ring current effects. When the *naphtho* ring is absent (*i.e.* located over the other “side” of the thread) the protons are deshielded and hence are positioned further downfield compared to the averaged peaks of the room temperature spectrum. The chemical shift difference ($\Delta\delta$) is ~ 0.30 ppm, which is in the range previously observed and discussed for protons involved in π -stacking in the rotaxanes compared to the protons in the capped threads.^{37,38,40}

To add further evidence of the existence of this interconversion, the same VT ¹H NMR experiment was performed on the **[2-6cN24C8]⁴⁺** rotaxane. Examination of the room temperature spectrum again shows an average set of peaks. Upon cooling to -75°C,

eight distinct peaks become evident, one for each type of dipyriddy proton on the different ends of the molecule (Figure 2.6). In this rotaxane, all dipyriddy protons sense a dramatic change in environment; *i.e.* either there is an aromatic ring present over the protons or there is not. Thus, dipyriddy protons on one end of the thread experience shielding, while the other end has no shielding.

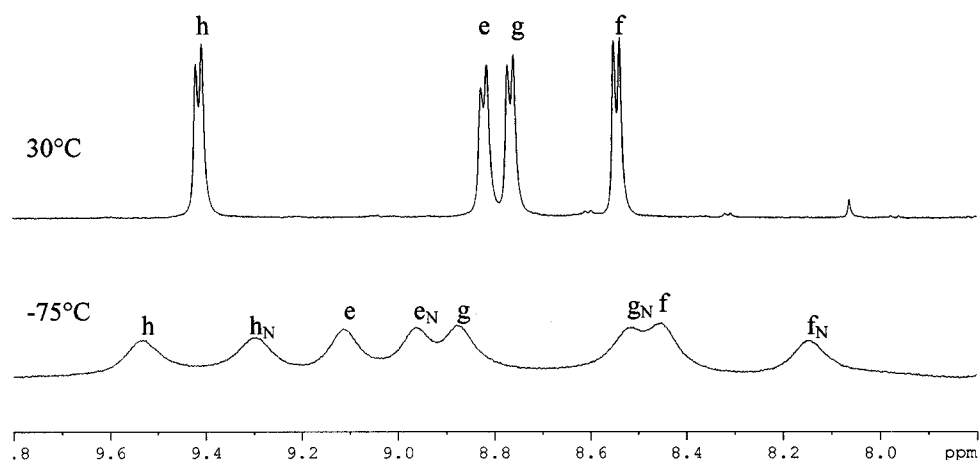


Figure 2.6 – Room temperature (top) and limiting (bottom) ¹H NMR spectra of [2-6cN24C8]⁴⁺ in CD₂Cl₂.

To summarize, the room temperature ¹H NMR spectra of the [2]rotaxanes, [2-6cBN24C8]⁴⁺ and [2-6cN24C8]⁴⁺, both show an average set of resonances for the dipyriddy protons, e, f, g and h. Conversely, the low temperature spectra reveal two sets of distinct dipyriddy resonances. The presence of two sets of peaks in the limiting spectra gives direct evidence to support the existence of two distinct orientations of the crown ether ring relative to the pyridinium thread.

2.3.2 Rate Analysis

The end-to-end interchanging of the flip-switch is a dynamic process and the rate of the process is temperature dependent. The rates for the “flipping” phenomenon can be

determined by performing full lineshape analysis on experimental variable temperature ^1H NMR spectra. The data collected at each temperature were fitted to a calculated

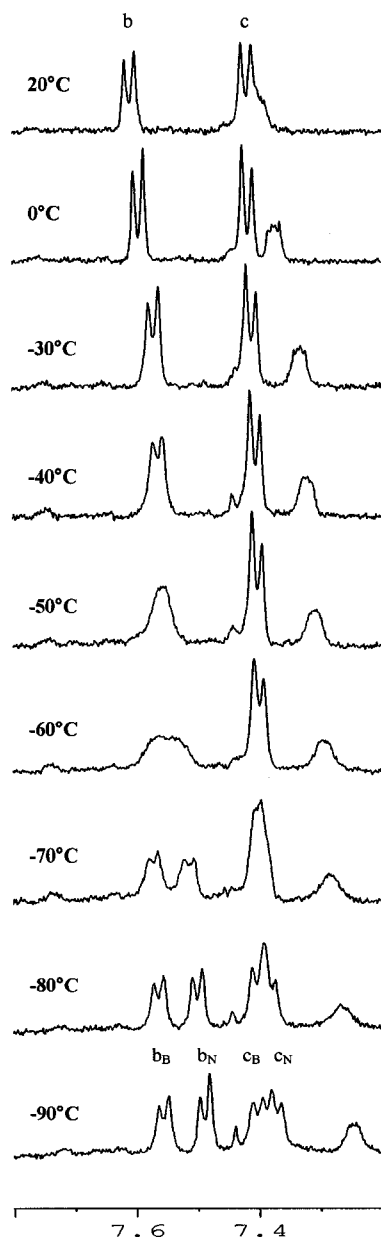


Figure 2.7 – VT ^1H NMR spectra showing proton resonances b and c from $[\text{2-6cBN24C8}]^{4+}$.

spectrum generated using the software gNMR. From the simulations, rate constants and activation parameters can be extracted. The VT ^1H NMR experiment for

[2-6C_{BN}24C8]⁴⁺ was used to obtain this data using the peaks corresponding to the **b** protons of the thread, the outer protons on the *tert*-butylbenzyl stopper (Scheme 2.2). The dipyriddy peaks are not suitable for these simulations because the peaks in the low temperature spectra are too broad. Figure 2.7 illustrates both *tert*-butylbenzyl peaks, **b** and **c**, splitting from one doublet at room temperature into two doublets at low temperature in the expected 1:1 ratio. This suggests that the *tert*-butylbenzyl aromatic ring, although not involved in face-to-face π -stacking with the crown ether aromatic rings, must be involved in edge-to-face π -stacking interactions since it senses the difference between a *naphtho* ring and a *benzo* ring of the crown ether.

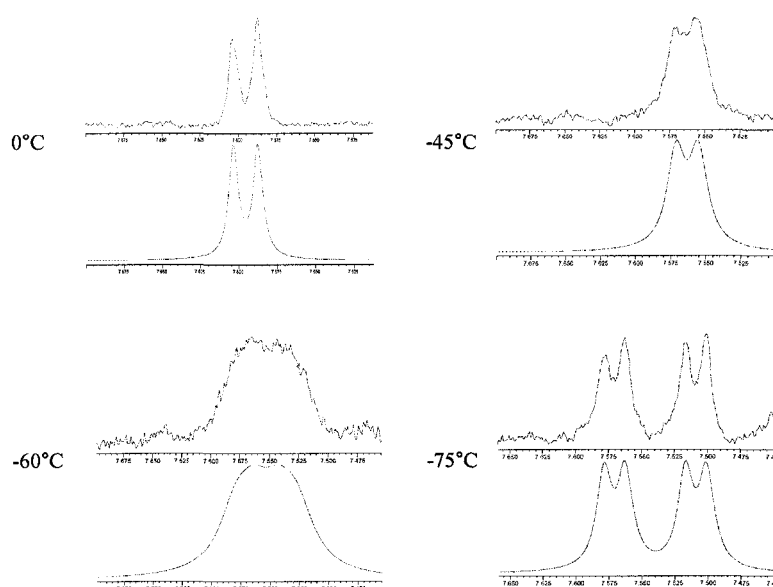


Figure 2.8 – Selected experimental (top) and calculated (bottom) spectra for proton **b** of [2-6C_{BN}24C8]⁴⁺.

Selected simulations at different temperatures are shown in Figure 2.8. The calculations iterate on four variables: the chemical shift of **b_N**, the chemical shift of **b_B**, the line width of the peaks, **w** (in Hz) and the rate constant, **k**. The natural log of the rate

constants are plotted against $1/T$ (in K) to give a slope that is equal to $-E_a/R$, where E_a is the energy barrier (activation energy) and R is the gas constant ($8.314 \text{ J K mol}^{-1}$) (Figure 2.9). Based on the simulations, the rate of the “end-to-end” exchange for $[2\text{-}6\text{-cBN}24\text{C}8]^{4+}$ was calculated to be $6.8 \times 10^3 \text{ s}^{-1}$ at 298 K with an energy barrier of 29 kJ/mol.

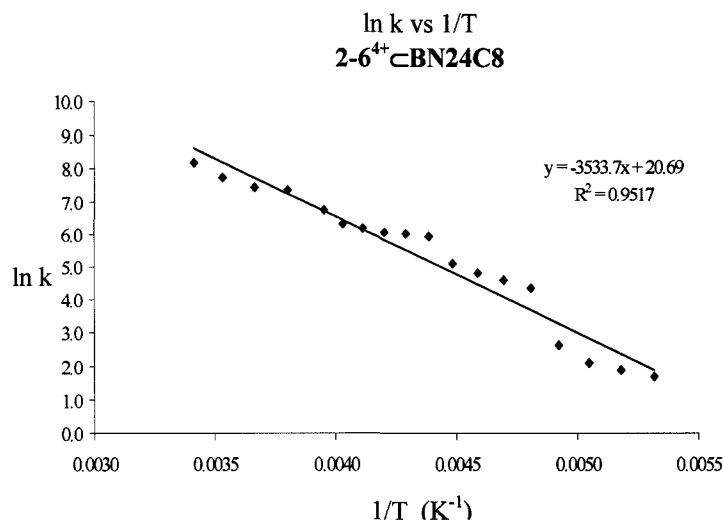


Figure 2.9 – Arrhenius plot for $[2\text{-}6\text{-cBN}24\text{C}8]^{4+}$.

The rate for $[2\text{-}6\text{-cN}24\text{C}8]^{4+}$ could not be calculated using the full lineshape analysis because the peaks of the *t*-butylbenzyl protons were too broad in the limiting spectra.

2.3.3 Increasing the activation energy

To raise the energetic barrier, one or more of the interactions between the thread and the crown would have to be enhanced. One possibility is to make the crown ether aromatic rings more electron rich or the thread more electron poor. Attempts were made to synthesize a thread using pyridine-3,5-dimethyl ester so that electron withdrawing groups were directly bonded to the pyridinium ring. Unfortunately, alkylation was unsuccessful because the nucleophilicity of the nitrogen was affected by the electron

withdrawing effects of the dimethyl ester groups. Attempts to oxidize $2\text{-}3^{2+}$ to the dicarboxylic acid substituted thread, but oxidation using KMnO_4 destroyed the ethylene bridge. Therefore, in an attempt to increase the activation energy, 3,5-bis(methoxycarbonyl)benzyl bromide was incorporated as a stopper in place of *t*-butylbenzyl bromide. The new stopper was synthesized according to a modified literature procedure⁵³ and incorporated into the [2]rotaxane $[2\text{-}10\text{cBN}24\text{C}8]^{4+}$ (Figure 2.10) using the same synthetic methodology outlined in Scheme 2.1. The expectation was that the ester groups on the stopper would have an electron withdrawing effect on the pyridinium rings of the thread and therefore increase the electrostatic interaction between the electron rich catechol rings of the crown and the electron poor pyridinium rings of the thread. Variable temperature ^1H NMR was used to assess any change in activation energy when compared to the original [2]rotaxane $[2\text{-}6\text{cBN}24\text{C}8]^{4+}$. The expectation was that an increase in activation energy would be indicated by a higher coalescence temperature (T_c).

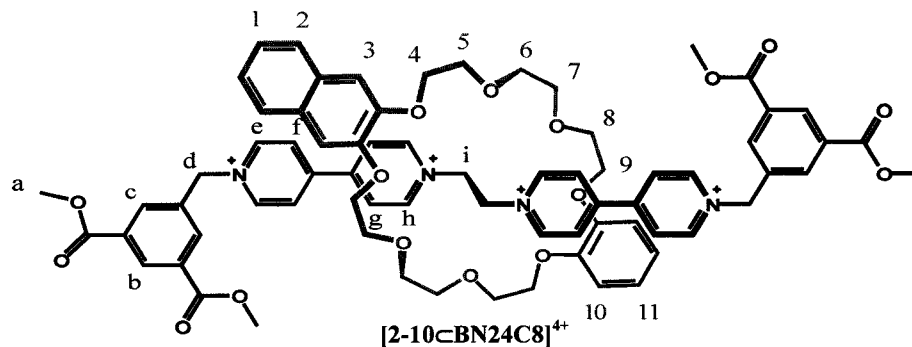


Figure 2.10 – Labeling scheme for $[2\text{-}10\text{cBN}24\text{C}8]^{4+}$.

Unfortunately, coalescence occurred at $\sim 45^\circ\text{C}$, around the same temperature as noted for $[2\text{-}6\text{cBN}24\text{C}8]^{4+}$. Efforts to establish rate constants and an activation energy by

fitting the VT ^1H NMR spectra to calculated spectra using gNMR were also unsuccessful. However, the similarity of coalescence temperatures does suggest that the energy barriers of the two flip-switches are similar and the ester groups are too remote to be effective.

Crystals suitable for single crystal X-ray structural determination were grown by slow evaporation of an CH_3CN solution of $[\mathbf{2-10cBN24C8}]^{4+}$ (Figure 2.11).

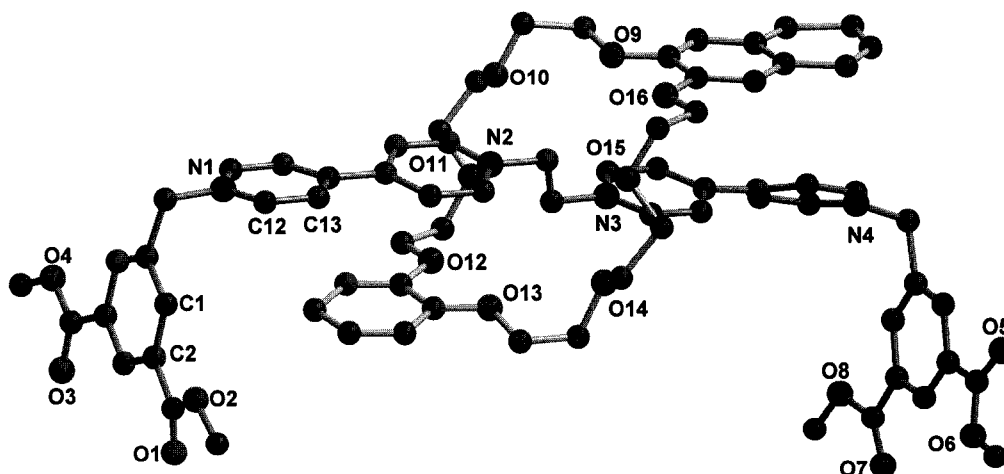


Figure 2.11 – A ball-and-stick representation of the X-ray structure for the cationic portion of the [2]rotaxane $[\mathbf{2-10cBN24C8}]^{4+}$.

2.4 TRULY UNSYMMETRICAL [2]ROTAXANES: FLIP-SWITCHES

The [2]rotaxane $[\mathbf{2-6cBN24C8}]^{4+}$ represents a simple flip-switch containing a ring with two different aromatic groups. To introduce non-degeneracy into the flip-switch system, both an unsymmetrical thread and an unsymmetrical ring are required. The simplest way to make the threads unsymmetrical about the ethylene bridge is to incorporate different pyridines. Both 3,5-lutidine and 4-*t*-butylpyridine are commercially available, and 2,7-diazapyrene can be prepared in three steps.⁵⁴ These compounds were used to synthesize threads $\mathbf{2-3}^{2+}$, $\mathbf{2-4}^{2+}$ and $\mathbf{2-5}^{2+}$ (Scheme 2.1), which were subsequently used to make [2]rotaxanes by combining $\mathbf{2-7}^{3+}$, $\mathbf{2-8}^{3+}$ and $\mathbf{2-9}^{4+}$ with the six 24C8

derivatives: **24C8**, **B24C8**, **DB24C8**, **BN24C8**, **N24C8** and **DN24C8** (Scheme 2.2). In cases where the crown ether is **B24C8**, **BN24C8** or **N24C8**, there exists the possibility of differences in the relative populations between the two co-conformations.

Ideally, it would be possible to record the limiting low temperature spectra and integrate the appropriate peaks for each pyridyl proton to determine the relative populations. Unfortunately, limited solubility of these compounds in CD_2Cl_2 as well as rapid chemical exchange of the co-conformations at the lowest temperatures accessible in CD_2Cl_2 (freezing point = -95°C) prevented use of this method.

2.4.1 Establishing a Room Temperature Method

At room temperature, the chemical shifts of the dipyriddy protons **e** and **f** in $[\text{2-6cBN24C8}]^{4+}$ are a weighted average of the positions observed for the same protons in the [2]rotaxanes $[\text{2-6cDB24C8}]^{4+}$ and $[\text{2-6cDN24C8}]^{4+}$. By definition, the isomer ratio for $[\text{2-6cBN24C8}]^{4+}$ rotaxane must be 50:50. The inner pyridinium protons, **g** and **h**, have essentially the same chemical shift in all three rotaxanes since their shielded environment does not change regardless of which crown is present (Figure 2.12).

To verify that this result was unaffected by external conditions or concentration, all three rotaxanes were dissolved together in 1 mL of CD_3CN at 2.0×10^{-3} M. Figure 2.13 validates the previous result since the chemical shifts of both experiments are identical; the resonance of proton **e** in the **BN24C8** rotaxane is at the average of the positions for the same proton **e** in the **DB24C8** and **DN24C8** rotaxanes.

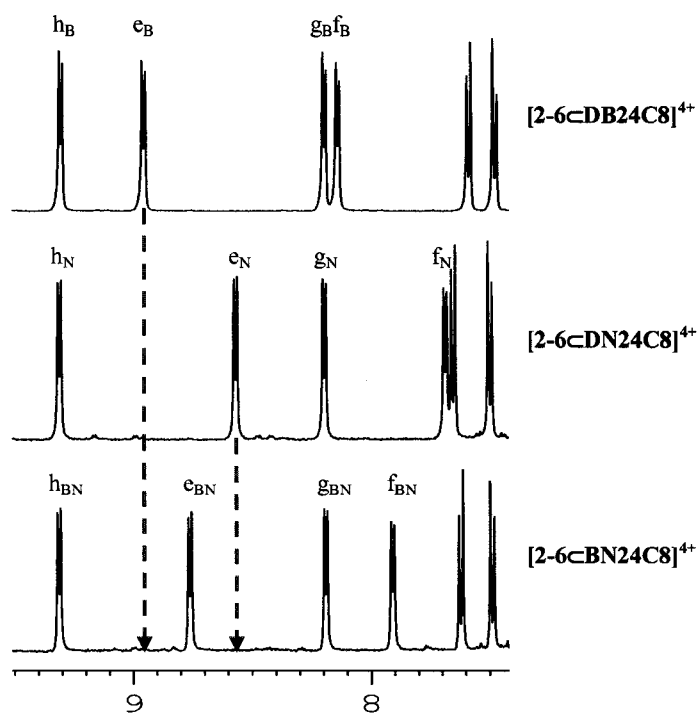


Figure 2.12 – The partial ^1H NMR spectra of $[2-6\subset\text{DB24C8}]^{4+}$, $[2-6\subset\text{DN24C8}]^{4+}$ and $[2-6\subset\text{BN24C8}]^{4+}$ at 30°C in CD_3CN . Subscripts B and N denote the *benzo* (B) and *naphtho* (N) ends of the molecule, the numbering schemes are outlined in Scheme 2.3.

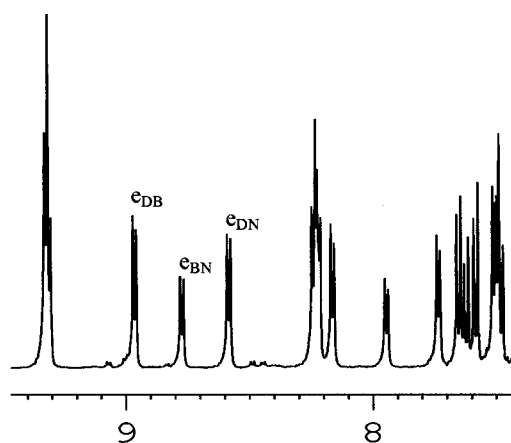


Figure 2.13 – ^1H NMR spectrum of a combination of rotaxanes $[2-6\subset\text{DB24C8}]^{4+}$, $[2-6\subset\text{DN24C8}]^{4+}$ and $[2-6\subset\text{BN24C8}]^{4+}$ at 30°C in CD_3CN at 2.0×10^{-3} M each.

2.4.2 Determination of Relative Populations for Unsymmetrical [2]Rotaxanes

Figure 2.14 illustrates the idea behind the room temperature method. The top spectrum (a) describes the scenario discussed above for rotaxane $[2-6\text{-cBN24C8}]^{4+}$, where the resonance of the **e** proton lies between the limiting shifts for the same proton in the **DN24C8** and **DB24C8** rotaxanes. The middle spectrum (b) describes the scenario where the chemical shift of the **e** proton in an unsymmetrical **BN24C8** rotaxane is closer to the limiting shift of the **e** proton for the **DN24C8** rotaxane. This suggests that the character of the **e** proton of the **BN24C8** rotaxane is closer to the character of the **e** proton in the **DN24C8** rotaxane, thus the *naphtho* group must be residing ovetop of the dipyridyl group the majority of the time. The opposite of this is described in the bottom spectrum (c) where the average shift of the **e** proton of the unsymmetrical **BN24C8** rotaxane is closer to the limiting shift of the **e** proton in the **DB24C8** rotaxane. In this case, the *benzo* group is residing over the dipyridyl group the majority of the time.

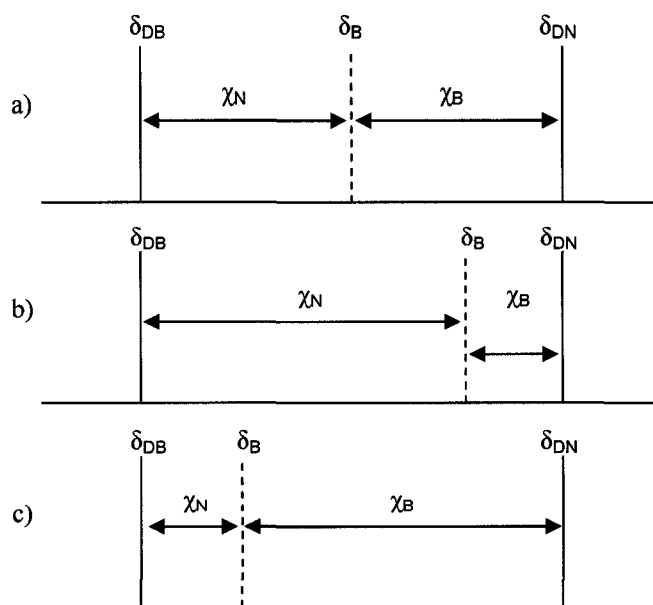


Figure 2.14 – Pictorial representation of isomer ratio determination based on room temperature ^1H NMR spectra.

The room temperature resonances representing the weighted averages for protons e_B and e_N in $[2-7\text{cBN}24\text{C}8]^{3+}$, $[2-8\text{cBN}24\text{C}8]^{3+}$ and $[2-9\text{cBN}24\text{C}8]^{4+}$ were compared to the limiting shifts for these same protons in the analogous rotaxanes $[2-6\text{cDB}24\text{C}8]^{4+}$ and $[2-6\text{cDN}24\text{C}8]^{4+}$ to determine the ratio of co-conformational isomers in these compounds in CD_3CN (Table 2.1). This method shows that in CD_3CN , the larger *naphtho* group prefers π -stacking with the 4,4'-dipyridinium group rather than the 3,5-lutidinium ($2-7^{3+}$), 4-*t*-butylpyridinium ($2-8^{3+}$) or 4,7-diazapyrenium ($2-9^{4+}$) groups. For $[2-7\text{cBN}24\text{C}8]^{3+}$ and $[2-8\text{cBN}24\text{C}8]^{3+}$ this is probably due to the increased steric interactions between the methyl or *t*-butyl substituents and the larger *naphtho* group compared to the smaller *benzo* group.

Table 2.1 - Isomer ratios determined from ^1H NMR data for [2]rotaxanes in CD_3CN .

[2]rotaxane	Isomer Ratio ^a
	N/DP:B/DP
$[2-6\text{cBN}24\text{C}8]^{4+}$	50:50 ^b
$[2-7\text{cBN}24\text{C}8]^{3+}$	57:43
$[2-8\text{cBN}24\text{C}8]^{3+}$	79:21
$[2-9\text{cBN}24\text{C}8]^{4+}$	60:40
	N/DP:-/DP
$[2-6\text{cN}24\text{C}8]^{4+}$	47:53 ^b
$[2-7\text{cN}24\text{C}8]^{3+}$	67:33
$[2-8\text{cN}24\text{C}8]^{3+}$	91:9
$[2-9\text{cN}24\text{C}8]^{4+}$	66:34
	B/DP:-/DP
$[2-6\text{cB}24\text{C}8]^{4+}$	50:50 ^b
$[2-7\text{cB}24\text{C}8]^{3+}$	49:51
$[2-8\text{cB}24\text{C}8]^{3+}$	82:18
$[2-9\text{cB}24\text{C}8]^{4+}$	^c

^a N/DP indicates *naphtho* π -stacked with 4,4'-dipyridinium, B/DP *benzo* π -stacked with 4,4'-dipyridinium and -/DP nothing stacked with 4,4'-dipyridinium. Errors for ratios are estimated to be <5%. ^b By definition the isomer ratios for $[2-6\text{cBN}24\text{C}8]^{4+}$, $[2-6\text{cN}24\text{C}8]^{4+}$, $[2-6\text{cB}24\text{C}8]^{4+}$ are 50:50. ^c It was not possible to calculate a value for $[2-9\text{cB}24\text{C}8]^{4+}$ it was not be prepared in sufficient yield and purity.

Similar trends are seen when **N24C8** and **B24C8** rotaxanes are used as the unsymmetrical crown ethers. The chemical shifts of the **e** protons in rotaxanes $[2-6\subset 24C8]^{4+}$ and $[2-6\subset DN24C8]^{4+}$ were used for the limiting shifts for the rotaxanes with **N24C8** as the unsymmetrical crown ether, whereas the chemical shifts of the **e** protons in $[2-6\subset 24C8]^{4+}$ and $[2-6\subset DB24C8]^{4+}$ were used when comparing to rotaxanes with **B24C8**. Again, the dramatic preference for the *naphtho* group to be associated with the dipyridyl group in the case where the other end is *t*-butyl is attributed to steric interactions with the aromatic ring of the crown ether.

The X-ray crystal structure of $[2-7\subset BN24C8]^{3+}$ (Figure 2.15), gives solid state evidence to support the results of the solution studies. In the solid state, *naphtho* lies over the 4,4'-dipyridinium group and *benzo* over the 3,5-lutidinium ring. It appears that the *benzo* ring can fit between the methyl groups whereas the *naphtho* group may encounter unfavourable steric interactions. This effect would be even more pronounced in $[2-8\subset BN24C8]^{3+}$ and $[2-8\subset N24C8]^{3+}$ since the *t*-butyl group is not only much bulkier than the methyl groups of lutidine, but is also located in the para position where it would have a more severe steric interaction with the *naphtho* aromatic ring of the crown ether.

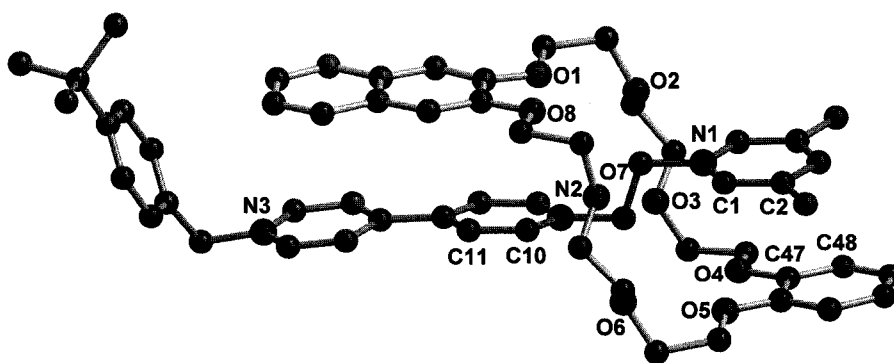


Figure 2.15 – A ball-and-stick representation of the X-ray structure for the cationic portion on the [2]rotaxane $[2-7\subset BN24C8]^{3+}$.

2.4.3 Manipulation of the Relative Population Distributions

Since the populations of the two isomers seem to be dependent on the relative degrees of π -stacking available, it was of interest to try to manipulate the populations. Hunter has shown that changing solvent polarity can have a profound influence on intramolecular face-to-face π -stacking between aromatic rings.^{55, 56} Others have used solvent polarity to control co-conformational changes in molecular shuttles.⁵⁷⁻⁵⁹ [2]Rotaxane [2-9CBN24C8]⁴⁺ was chosen for this study as it contains two different planar pyridinium groups of different surface area and offers no negative steric contributions. Table 2.2 contains data for [2-9CBN24C8]⁴⁺ in CD₃CN, CD₂Cl₂, CD₃OD, (CD₃)₂CO, CD₃NO₂, (CD₃)₂SO and D₂O and demonstrates that the ratio of co-conformational isomers can indeed be tuned by a simple external perturbation such as solvent polarity. Solvent polarity is quantified using the parameter Z .^{60, 61} The solvophobic description of aromatic interactions suggests that polar solvents are unable to properly solvate aromatic surfaces, enhancing π -stacking interactions in polar solvents. In non-polar solvents, aromatic surfaces are better solvated, however, electrostatic interactions can have an increased impact.⁵⁶ In these molecular flip-switches, both π -stacking and electrostatic interactions are contributing to the overall stability of the system. The ratio of isomers shows an increase in π -stacking of the naphtho group with the 4,4'-dipyridinium group in the more polar solvents. This is consistent with observed trends and shows that the naphtho-dipyridinium combination is the more favourable interaction. The observed anomaly of the isomer ratio in CD₂Cl₂ of 59:41 is attributed to enhanced electrostatic interactions in the non-polar solvent, similar to observations made in Hunter's study.⁵⁶

Table 2.2 – Ratios of co-conformational isomers determined for [2-9C₂BN24C8]⁴⁺ from ¹H NMR data in various solvents.

N/DP : B/DP Isomer Ratio	Solvent System	Z (kcal/mol)
82:18	(CD ₃) ₂ SO	71.1
71:29	(CD ₃) ₂ CO	65.7
70:30	D ₂ O	94.6
65:35	CD ₃ OD	83.6
60:40	CD ₃ CN	71.3
58:42	CD ₃ NO ₂	71.2
59:41	CD ₂ Cl ₂	64.2

^a The OTf salt of the thread was used for all solvents except D₂O for which the chloride salt was used. ^b Z, solvent polarity parameters. ^{60, 61}.

2.5 SUMMARY AND CONCLUSIONS

In summary, a new type of flipping mechanical motion in interlocked molecules has been described. The existence of co-conformations that are the result of this flipping phenomenon has been confirmed by variable temperature ¹H NMR spectroscopy. Limiting ¹H NMR spectra of rotaxanes [2-6C₂BN24C8]⁴⁺ and [2-6C₂N24C8]⁴⁺ show six and eight distinct proton resonances, respectively, representing dipyrindyl protons on opposite ends of the thread which implies that the two ends are distinct. Using full lineshape analysis on experimental VT NMR spectra, the rate constant (k) for the reorientation of the crown ether in [2-6C₂BN24C8]⁴⁺ was determined to be $6.8 \times 10^3 \text{ s}^{-1}$ at 25°C with an energy barrier of 29 kJ/mol.

To improve on this system, the non-covalent interactions between the crown ether and the thread must be enhanced and the rate of flipping must be decreased. Addition of methyl groups to the ethereal arms on the crown ether may have the effect of slowing the rate. Negatively charged sulfonate groups appended to the aromatic rings of the crown ether would serve as a counterion to the cationic thread, and it should also increase the

electrostatic interaction between the electron rich crown ether and electron poor thread. It would also be necessary to find a way to control the motion by an external perturbation. Addition of a dimethylamino group to the crown ether would provide a site for protonation/deprotonation that would allow control over the change in the electron density of the aromatic ring to which it is attached from electron rich to electron poor. This may be a means to cause electrostatic repulsion/attraction if one ring on the thread is electron poor and the other is electron rich. Further studies are necessary to improve the feasibility of the molecular flip-switch.

2.6 EXPERIMENTAL

2.6.1 General Comments

Sodium trifluoromethanesulfonate, 4,4'-dipyridyl, 1,2-dibromoethane, 3,5-lutidine, 4-*tert*-butylpyridine, 4-*tert*-butylbenzylbromide and **DB24C8** were purchased from Aldrich and used as received. Deuterated solvents were obtained from Cambridge Isotope Laboratories and used as received. Solvents were dried using an Innovative Technologies Solvent Purification System. Thin Layer Chromatography (TLC) was performed using Merck Silica gel 60 F₂₅₄ plates and viewed under UV light. Column chromatography was performed using Silicycle Ultra Pure Silica Gel (230 – 400 mesh). ¹H NMR and 2-D experiments were performed on a Brüker Avance 500 instrument operating at 500.1 MHz. The deuterated solvent was used as the lock and the residual solvent or TMS as the internal reference. Conventional 2-D NMR experiments (¹H-¹H COSY) were conducted and used to help assign all peaks. High resolution mass spectrometry (HR-MS) experiments were performed on a Micromass LCT Electrospray (ESI) time-of-flight (TOF) Mass Spectrometer. Solutions of 50-100 ng/μL were prepared in CH₃CN (unless otherwise indicated), and injected for analysis at a rate of 5 μL/min using a syringe pump.

2.6.2 Synthesis of 2-1⁺

4,4'-Dipyridyl (5.00 g, 0.0320 mol) was dissolved in 1,2-dibromoethane (150 mL) and refluxed for three hours. The solution was filtered hot and the resulting precipitate washed with cold ethanol. The precipitate was collected and recrystallized from ethanol to yield a yellow crystalline powder (10.32 g, 94%).

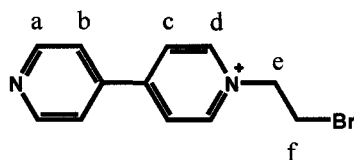


Table 2.3 – ¹H NMR of [2-1][Br] in D₂O. MW_{Br} = 344.058 g/mol

Proton	δ (ppm)	Multiplicity	# Protons	J (Hz)
a	8.68	d	2	³ J _{ab} = 6.36
b	7.87	d	2	³ J _{ba} = 6.36
c	8.35	d	2	³ J _{cd} = 6.77
d	8.93	d	2	³ J _{dc} = 6.77
e	4.99	t	2	³ J _{ef} = 5.70
f	3.92	t	2	³ J _{fe} = 5.70

Table 2.4 – ¹H NMR of [2-1][BF₄] in CD₃CN. MW_{BF₄} = 350.946 g/mol

Proton	δ (ppm)	Multiplicity	# Protons	J (Hz)
a	8.84	d	2	³ J _{ab} = 6.06
b	7.82	d	2	³ J _{ba} = 6.06
c	8.38	d	2	³ J _{cd} = 6.54
d	8.84	d	2	³ J _{dc} = 6.54
e	4.97	t	2	³ J _{ef} = 5.86
f	3.97	t	2	³ J _{fe} = 5.86

2.6.3 Synthesis of 2-2²⁺

[2-1][Br] (2.00 g, 0.00581 mol) and 4,4'-dipyridyl (3.00 g, 0.0192 mol) were dissolved in absolute ethanol (80 mL) and refluxed for five days. The solution was filtered hot and the resulting precipitate washed with cold ethanol. The precipitate was collected and stirred in CHCl₃ to yield a beige powder (1.23 g, 42 %). The bromide salt was anion exchanged to the triflate salt by heating the bromide salt in water and adding NaOTf. The resulting precipitate was collected by filtration (1.48 g, 94 %).

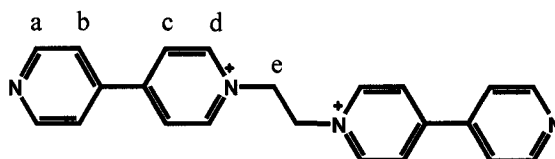


Table 2.5 – ¹H NMR of [2-2][Br]₂ in D₂O. MW_{Br-} = 500.229 g/mol

Proton	δ (ppm)	Multiplicity	# Protons	J (Hz)
a	8.77	d	4	³ J _{ab} = 4.48
b	7.90	d	4	³ J _{ba} = 4.48
c	8.48	d	4	³ J _{cd} = 5.65
d	8.98	d	4	³ J _{dc} = 5.65
e	5.40	s	4	--

Table 2.6 - ¹H NMR of [2-2][OTf]₂ in CD₃CN. MW_{OTf-} = 638.559 g/mol

Proton	δ (ppm)	Multiplicity	# Protons	J (Hz)
a	8.80	d	4	³ J _{ab} = 6.63
b	8.39	d	4	³ J _{ba} = 6.63
c	7.81	d	4	³ J _{cd} = 5.82
d	8.87	d	4	³ J _{dc} = 5.82
e	5.18	s	4	--

2.6.4 Synthesis of 2-3²⁺

[2-1][Br] (2.50 g, 0.00727 mol) and 3,5-lutidine (3.89 g, 0.0363 mol) were dissolved in absolute ethanol (80 mL) and refluxed overnight. The solution was cooled and placed in the freezer overnight. The resulting precipitate was filtered and washed with cold ethanol. The precipitate was collected and stirred in CHCl₃ to yield a beige powder (1.66g, 51 %). The bromide salt was anion exchanged to the triflate salt by heating the bromide salt in water and adding NaOTf. The resulting precipitate was collected by filtration (1.98 g, 91 %).

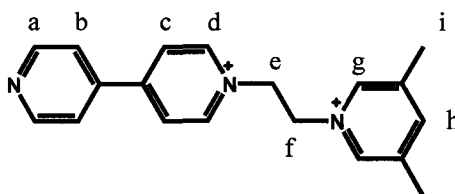


Table 2.7 – ¹H NMR of [2-3][Br]₂ in D₂O. MW_{Br-} = 451.198 g/mol

Proton	δ (ppm)	Multiplicity	# Protons	J (Hz)
a	8.74	d	2	³ J _{ab} = 4.96
b	7.87	d	2	³ J _{ba} = 4.96
c	8.43	d	2	³ J _{cd} = 6.12
d	8.86	d	2	³ J _{dc} = 6.12
e	5.30	t	2	³ J _{ef} = 6.08
f	5.21	t	2	³ J _{fe} = 6.08
g	8.46	s	2	--
h	8.28	s	1	--
i	2.42	s	6	--

Table 2.8 – ^1H NMR of [2-3][OTf]₂ in CD₃CN. MW_{OTf} = 589.528 g/mol

Proton	δ (ppm)	Multiplicity	# Protons	J (Hz)
a	8.86	d	2	$^3J_{ab} = 5.85$
b	7.82	d	2	$^3J_{ba} = 5.85$
c	8.38	d	2	$^3J_{cd} = 6.83$
d	8.82	d	2	$^3J_{dc} = 6.83$
e	5.16	t	2	$^3J_{ef} = 6.50$
f	5.07	t	2	$^3J_{fe} = 6.50$
g	8.48	s	2	--
h	8.24	s	1	--
i	2.47	s	6	--

2.6.5 Synthesis of 2-4²⁺

[2-1][BF₄] (2.00 g, 0.00570 mol) and 4-*t*-butylpyridine (3.85 g, 0.0285 mol) were dissolved in CH₃CN (80 mL) and refluxed overnight. The solution was cooled and filtered and the precipitate was washed with CH₃CN. The precipitate was collected and stirred in CHCl₃ to yield a beige powder (2.25 g, 82 %). The bromide salt was anion exchanged to the triflate salt by heating the bromide salt in water and adding NaOTf. The resulting precipitate was collected by filtration (2.88 g, 91 %).

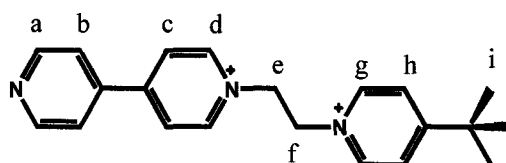


Table 2.9 – ¹H NMR of [2-4][OTf]₂ in CD₃CN. MW_{OTf} = 617.582 g/mol

Proton	δ (ppm)	Multiplicity	# Protons	J (Hz)
a	8.87	d	2	³ J _{ab} = 5.90
b	7.81	d	2	³ J _{ba} = 5.90
c	8.39	d	2	³ J _{cd} = 6.63
d	8.82	d	2	³ J _{dc} = 6.63
e	5.14	t	2	³ J _{ef} = 5.70
f	5.10	t	2	³ J _{fe} = 5.70
g	8.63	d	2	³ J _{gh} = 6.70
h	8.07	d	2	³ J _{hg} = 6.70
i	1.41	s	9	--

2.6.6 Synthesis of 2-5²⁺

[2-2][BF₄] (0.371 g, 0.00106 mol) and 2,7-diazapyrene (0.240 g, 0.0118 mol) were dissolved in propionitrile (80 mL) and refluxed for seven days. The solution was cooled and the resulting precipitate was filtered and washed with CH₂Cl₂. The precipitate was collected and stirred in CH₂Cl₂ again and filtered to yield a beige powder (0.140 g, 24 %). The bromide salt was anion exchanged to the triflate salt by heating the bromide salt in water and adding NaOTf. The resulting precipitate was collected by filtration (0.150 g, 86 %).

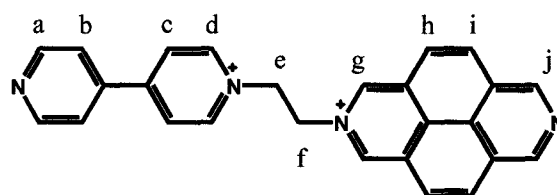


Table 2.10 – ¹H NMR of [2-5][OTf]₂ in CD₃CN. MW_{OTf} = 688.618 g/mol

Proton	δ (ppm)	Multiplicity	# Protons	J (Hz)
a	8.85	d	2	³ J _{ab} = 6.09
b	7.78	d	2	³ J _{ba} = 6.09
c	8.34	d	2	³ J _{cd} = 6.76
d	8.80	d	2	³ J _{dc} = 6.76
e	5.40	t	2	³ J _{ef} = 6.46
f	5.62	t	2	³ J _{fe} = 6.46
g	9.68	s	2	--
h	8.74	d	2	³ J _{hi} = 9.12
i	8.53	d	2	³ J _{ih} = 9.12
j	9.89	s	2	--

2.6.7 Synthesis of 2-6⁴⁺

[2-2][OTf]₂ (0.100 g, 1.57 × 10⁻⁴ mol) and *t*-butylbenzyl bromide (0.213g, 9.40 × 10⁻⁴ mol) were dissolved in CH₃CN and stirred for five days. The precipitate that formed was filtered and the filtrate evaporated. The filtrate was stirred in CH₂Cl₂ to get rid of excess *t*-butylbenzyl bromide. The resulting precipitate was filtered and combined with the first precipitate and all dissolved in H₂O. NaOTf was added to the solution resulting in precipitation of the product as the triflate salt. The white precipitate was collected by vacuum filtration (0.110 g, 57 %). ESI-MS: *m/z* [2-6 - OTf]⁺ calc. 1081.2596, found 1081.2567.

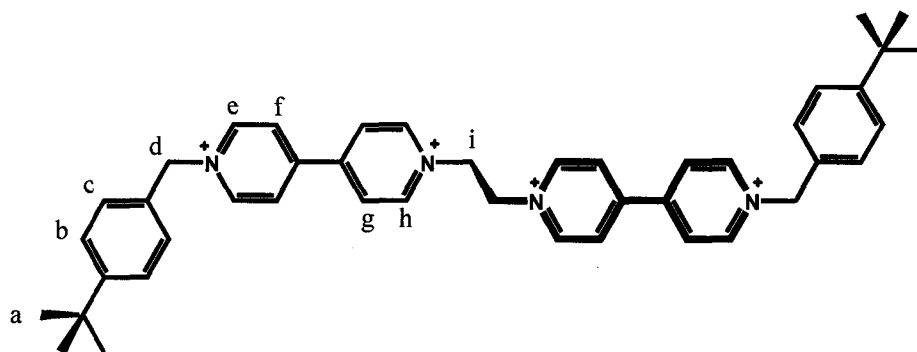


Table 2.11 – ¹H NMR of [2-6][OTf]₄ in CD₃CN. MW_{OTf} = 1231.171 g/mol

Proton	δ (ppm)	Multiplicity	# Protons	J (Hz)
a	1.32	s	18	--
b	7.54	d	4	³ J _{bc} = 8.38
c	7.44	d	4	³ J _{cb} = 8.38
d	5.79	s	4	--
e	9.00	d	4	³ J _{ef} = 6.74
f	8.43	d	4	³ J _{fe} = 6.74
g	8.48	d	4	³ J _{gh} = 6.68
h	9.03	d	4	³ J _{hg} = 6.68
i	5.27	s	4	--

2.6.8 Synthesis of [2-6C24C8]⁴⁺

[2-2][OTf]₂ (0.181 g, 2.84×10^{-4} mol), **24C8** (1.00 g, 2.84×10^{-3} mol) and *t*-butylbenzyl bromide (0.387g, 1.70×10^{-3} mol) were dissolved in CH₃CN and stirred for five days. The solution was filtered and the filtrate evaporated. The filtrate was stirred in toluene to get rid of excess crown and *t*-butylbenzyl bromide. This was filtered and the filtrate evaporated. The residue was dissolved in CH₂Cl₂ and the resulting precipitate collected by vacuum filtration. (0.075 g, 17 %) **ESI-MS**: *m/z* [2-6C24C8 - OTf]⁺ calc. 1433.4688, found 1433.4634.

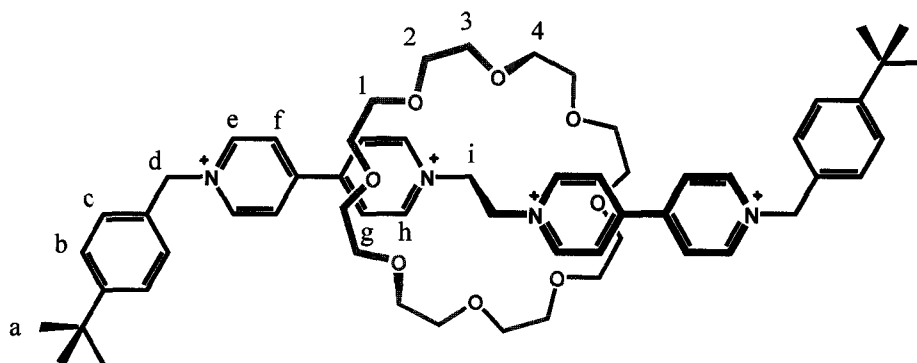


Table 2.12 – ¹H NMR [2-6C24C8][OTf]₄ in CD₃CN. MW_{OTf} = 1583.592 g/mol

Proton	δ (ppm)	Multiplicity	# Protons	J (Hz)
a	1.32	s	18	--
b	7.56	d	4	³ J _{bc} = 8.32
c	7.48	d	4	³ J _{cb} = 8.32
d	5.83	s	4	--
e	9.05	d	4	³ J _{ef} = 6.65
f	8.51	d	4	³ J _{fe} = 6.65
g	8.57	d	4	³ J _{gh} = 6.69
h	9.32	d	4	³ J _{hg} = 6.69
i	5.44	s	4	--
1-4	3.51	s	32	--

2.6.9 Synthesis of [2-6c-B24C8]⁴⁺

[2-2][OTf]₂ (0.200 g, 3.13×10^{-4} mol), B24C8 (0.753 g, 1.88×10^{-3} mol) and *t*-butylbenzyl bromide (0.427g, 1.88×10^{-3} mol) were dissolved in a two layer solution of CH₃NO₂/NaOTf_(aq) (20 mL, 3:1) and stirred for five days. The two layers were separated and the MeNO₂ layer washed twice with water, then subsequently dried with MgSO₄. The CH₃NO₂ solution was filtered and the solvent evaporated. The product was purified by column chromatography (SiO₂) using CH₃OH:2M NH₄Cl (aq): CH₃NO₂ (7:2:1) as the eluent. Like fractions were combined and the solvent evaporated. The residue was dissolved in CH₃NO₂ and H₂O and NaOTf added to anion exchange the rotaxane. The layers were separated and the organic layer dried with MgSO₄ and filtered. The CH₃NO₂ was evaporated yielding an orange solid ($R_f = 0.31$, 0.167 g, 33 %).

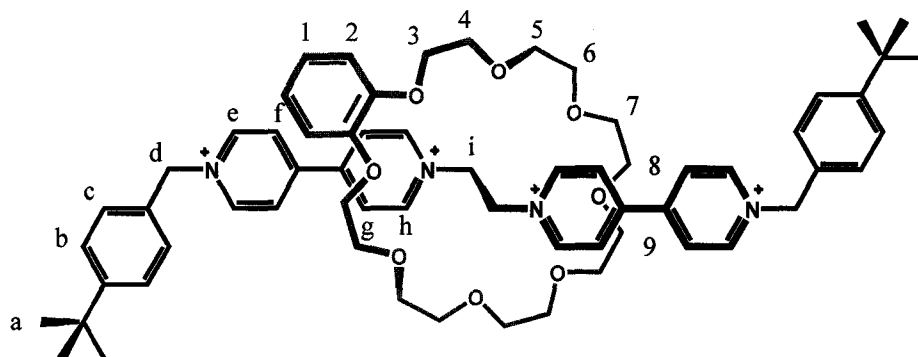


Table 2.13 ^1H NMR of [2-6c-B24C8][OTf] $_4$ in CD_3CN . $\text{MW}_{\text{OTf}} = 1631.634$ g/mol

Proton	δ (ppm)	Multiplicity	# Protons	J (Hz)
a	1.33	s	18	--
b	7.57	d	4	$^3J_{bc} = 8.26$
c	7.48	d	4	$^3J_{cb} = 8.26$
d	5.82	s	4	--
e	9.00	d	4	$^3J_{ef} = 6.46$
f	8.31	d	4	$^3J_{fe} = 6.46$
g	8.36	d	4	$^3J_{gh} = 6.53$
h	9.29	d	4	$^3J_{hg} = 6.53$
i	5.48	s	4	--
1	6.69	dd	4	$J_{\text{meta}} = 3.58; J_{\text{ortho}} = 5.59$
2	6.47	dd	4	$J_{\text{meta}} = 3.58; J_{\text{ortho}} = 5.59$
3-9	3.18-4.03	m	24	--

2.6.10 Synthesis of [2-6CDB24C8]⁴⁺

[2-2][OTf]₂ (0.200 g, 3.13×10^{-4} mol), DB24C8 (0.843 g, 1.88×10^{-3} mol) and *t*-butylbenzyl bromide (0.427g, 1.88×10^{-3} mol) were dissolved in a two layer solution of CH₃NO₂/NaOTf_(aq) (20 mL, 3:1) and stirred for five days. The two layers were separated and the CH₃NO₂ layer washed twice with water, then subsequently dried with MgSO₄. The CH₃NO₂ solution was filtered and the solvent evaporated. The product was purified by column chromatography (SiO₂) using CH₃OH:2M NH₄Cl (aq): CH₃NO₂ (7:2:1) as the eluent. Like fractions were combined and the solvent evaporated. The residue was dissolved in CH₃NO₂ and H₂O and NaOTf added to anion exchange the rotaxane. The layers were separated and the organic layer dried with MgSO₄ and filtered. The CH₃NO₂ was evaporated yielding an orange solid (*R*_f = 0.38, 0.340 g, 65 %) ESI-MS: *m/z* [2-6CDB24C8 - 2OTf]²⁺ calc. 690.2581, found 690.2559.

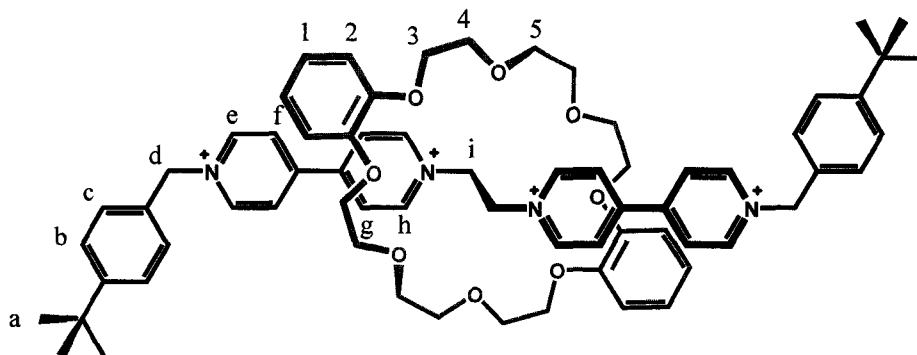


Table 2.14 – ^1H NMR of $[2\text{-}6\text{c}\text{-DB}24\text{C}8][\text{OTf}]_4$ in CD_3CN . $\text{MW}_{\text{OTf}} = 1679.677$ g/mol

Proton	δ (ppm)	Multiplicity	# Protons	J (Hz)
a	1.32	s	18	--
b	7.58	d	4	$^3J_{bc} = 8.24$
c	7.48	d	4	$^3J_{cb} = 8.24$
d	5.81	s	4	--
e	8.96	d	4	$^3J_{ef} = 6.45$
f	8.16	d	4	$^3J_{fe} = 6.45$
g	8.22	d	4	$^3J_{gh} = 6.52$
h	9.31	d	4	$^3J_{hg} = 6.52$
i	5.60	s	4	--
1	6.64	dd	4	$J_{\text{meta}} = 3.58; J_{\text{ortho}} = 5.59$
2	6.41	dd	4	$J_{\text{meta}} = 3.58; J_{\text{ortho}} = 5.59$
3-5	4.00-4.05	m	24	--

2.6.11 Synthesis of [2-6C₆BN24C8]⁴⁺

[2-2][OTf]₂ (0.200 g, 3.13×10^{-4} mol), BN24C8 (0.937g, 1.88×10^{-3} mol) and *t*-butylbenzyl bromide (0.427g, 1.88×10^{-3} mol) were dissolved in a two layer solution of CH₃NO₂/NaOTf_(aq) (20 mL, 3:1) and stirred for five days. The two layers were separated and the CH₃NO₂ layer washed twice with water, then subsequently dried with MgSO₄. The CH₃NO₂ solution was filtered and the solvent evaporated. The product was purified by column chromatography (SiO₂) using CH₃OH:2M NH₄Cl (aq):CH₃NO₂ (7:2:1) as the eluent. Like fractions were combined and the solvent evaporated. The residue was dissolved in CH₃NO₂ and H₂O and NaOTf added to anion exchange the rotaxane. The layers were separated and the organic layer dried with MgSO₄ and filtered. The CH₃NO₂ was evaporated yielding an orange solid ($R_f = 0.38$, 0.214 g, 40 %) ESI-MS: m/z [2-6C₆BN24C8 - 2OTf]²⁺ calc. 715.2660, found 715.2667.

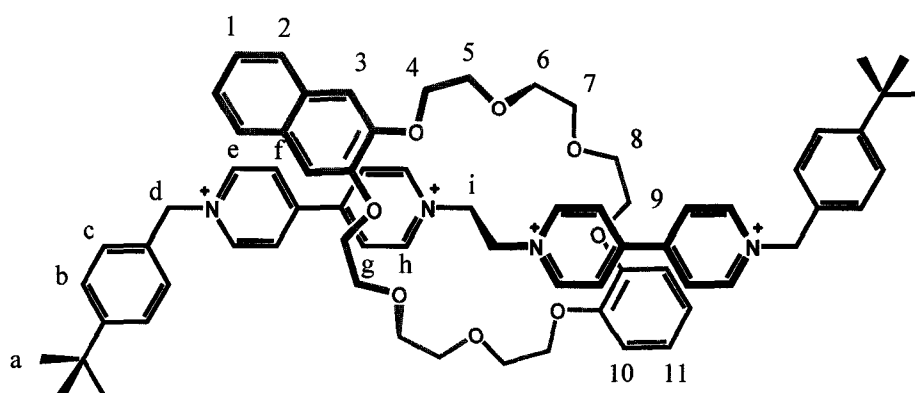


Table 2.15 – ^1H NMR of $[2\text{-}6\text{cBN}24\text{C}8][\text{OTf}]_4$ in CD_3CN . $\text{MW}_{\text{OTf}} = 1729.736$ g/mol

Proton	δ (ppm)	Multiplicity	# Protons	J (Hz)
a	1.35	s	18	--
b	7.62	d	4	$^3J_{bc} = 8.32$
c	7.49	d	4	$^3J_{cb} = 8.32$
d	5.72	s	4	--
e	8.77	d	4	$^3J_{ef} = 6.49$
f	7.93	d	4	$^3J_{fe} = 6.49$
g	8.21	d	4	$^3J_{gh} = 6.52$
h	9.32	d	4	$^3J_{hg} = 6.52$
i	5.63	s	4	--
1	6.82	dd	2	$J_{\text{meta}} = 3.20; J_{\text{ortho}} = 6.07$
2	7.30	dd	2	$J_{\text{meta}} = 3.20; J_{\text{ortho}} = 6.07$
3	6.98	s	2	--
4-9	4.01-4.18	m	24	--
10	6.37	dd	2	$J_{\text{meta}} = 3.69; J_{\text{ortho}} = 5.85$
11	6.63	dd	2	$J_{\text{meta}} = 3.69; J_{\text{ortho}} = 5.85$

2.6.12 Synthesis of [2-6C-N24C8]⁴⁺

[2-2][OTf]₂ (0.200 g, 3.13×10^{-4} mol), N24C8 (0.847 g, 1.88×10^{-3} mol) and *t*-butylbenzyl bromide (0.427g, 1.88×10^{-3} mol) were dissolved in a two layer solution of CH₃NO₂/NaOTf_(aq) (20 mL, 3:1) and stirred for five days. The two layers were separated and the CH₃NO₂ layer washed twice with water, then subsequently dried with MgSO₄. The CH₃NO₂ solution was filtered and the solvent evaporated. The product was purified by column chromatography (SiO₂) using CH₃OH:2M NH₄Cl (aq):CH₃NO₂ (7:2:1) as the eluent. Like fractions were combined and the solvent evaporated. The residue was dissolved in CH₃NO₂ and H₂O and NaOTf added to anion exchange the rotaxane. The layers were separated and the organic layer dried with MgSO₄ and filtered. The CH₃NO₂ was evaporated yielding an orange solid (*R*_f = 0.31, 0.117 g, 22 %) **ESI-MS**: *m/z* [2-6C-N24C8 - 2OTf]²⁺ calc. 691.2659, found 691.2656.

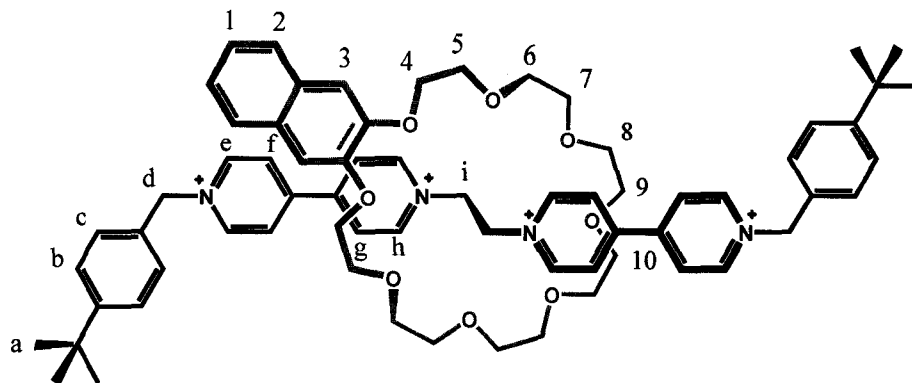


Table 2.16 – ^1H NMR of $[2\text{-}6\text{C}_{\text{N}24}\text{C}_8][\text{OTf}]_4$ in CD_3CN . $\text{MW}_{\text{OTf}} = 1681.693$ g/mol

Proton	δ (ppm)	Multiplicity	# Protons	J (Hz)
a	1.33	s	18	--
b	7.61	d	4	$^3J_{\text{bc}} = 8.26$
c	7.49	d	4	$^3J_{\text{cb}} = 8.26$
d	5.74	s	4	--
e	8.81	d	4	$^3J_{\text{ef}} = 6.46$
f	8.11	d	4	$^3J_{\text{fe}} = 6.46$
g	8.38	d	4	$^3J_{\text{gh}} = 6.53$
h	9.31	d	4	$^3J_{\text{hg}} = 6.53$
i	5.51	s	4	--
1	6.86	d	2	$J_{\text{meta}} = 3.58; J_{\text{ortho}} = 5.59$
2	7.32	d	2	$J_{\text{meta}} = 3.58; J_{\text{ortho}} = 5.59$
3	7.00	s	2	--
4-10	3.10-4.18	m	24	--

2.6.13 Synthesis of [2-6cDN24C8]⁴⁺

[2-2][OTf]₂ (0.200 g, 3.13×10^{-4} mol), DN24C8 (1.03g, 1.88×10^{-3} mol) and *t*-butylbenzyl bromide (0.427g, 1.88×10^{-3} mol) were dissolved in a two layer solution of CH₃NO₂/NaOTf_(aq) (20 mL, 3:1) and stirred for five days. The two layers were separated and the CH₃NO₂ layer washed twice with water, then subsequently dried with MgSO₄. The CH₃NO₂ solution was filtered and the solvent evaporated. The product was purified by column chromatography (SiO₂) using CH₃OH:2M NH₄Cl (aq):CH₃NO₂ (7:2:1) as the eluent. Like fractions were combined and the solvent evaporated. The residue was dissolved in CH₃NO₂ and H₂O and NaOTf added to anion exchange the rotaxane. The layers were separated and the organic layer dried with MgSO₄ and filtered. The CH₃NO₂ was evaporated yielding an orange solid ($R_f = 0.38$, 0.190 g, 34 %) **ESI-MS**: m/z [2-6cDN24C8 - 2OTf]²⁺⁺ calc. 740.2738, found 740.2751.

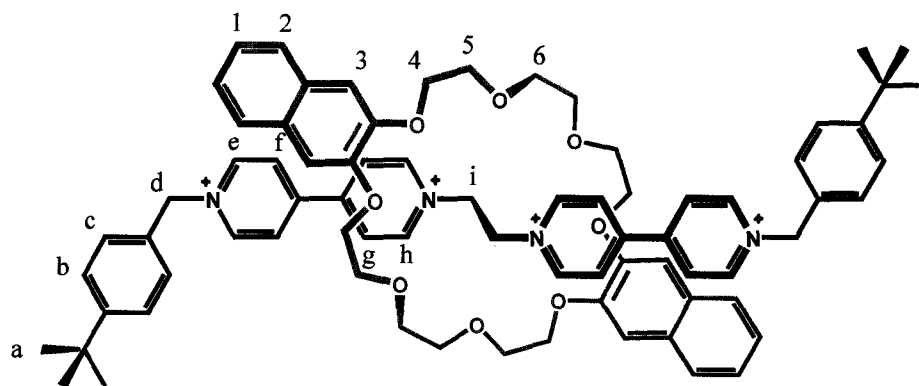


Table 2.17 – ^1H NMR of $[2\text{-}6\text{cDN}24\text{C}8][\text{OTf}]_4$ in CD_3CN . $\text{MW}_{\text{OTf}} = 1779.794$ g/mol

Proton	δ (ppm)	Multiplicity	# Protons	J (Hz)
a	1.37	s	18	--
b	7.65	d	4	$^3J_{bc} = 8.29$
c	7.50	d	4	$^3J_{cb} = 8.29$
d	5.66	s	4	--
e	8.57	d	4	$^3J_{ef} = 6.44$
f	7.70	d	4	$^3J_{fe} = 6.44$
g	8.20	d	4	$^3J_{gh} = 6.51$
h	9.32	d	4	$^3J_{hg} = 6.51$
i	5.64	s	4	--
1	6.85	dd	4	$J_{\text{meta}} = 3.20; J_{\text{ortho}} = 5.94$
2	7.29	dd	4	$J_{\text{meta}} = 3.15; J_{\text{ortho}} = 5.94$
3	6.98	s	4	--
4-6	4.11-4.19	m	24	--

2.6.14 Synthesis of 2-7³⁺

[2-3][OTf]₂ (0.100 g, 1.70×10^{-4} mol) and *t*-butylbenzyl bromide (0.115g, 5.09×10^{-4} mol) were dissolved in a CH₃CN and stirred for five days. The precipitate that formed was filtered and the filtrate evaporated. The filtrate was stirred in CH₂Cl₂ to remove excess *t*-butylbenzyl bromide. The resulting precipitate was filtered and combined with the first precipitate and all dissolved in H₂O. NaOTf was added to the solution resulting in precipitation of the product as the triflate salt. The white precipitate was collected by vacuum filtration. (0.0800 g, 53 %) **ESI-MS**: *m/z* [2-7 - OTf]⁺ calc. 736.1944, found 736.1932.

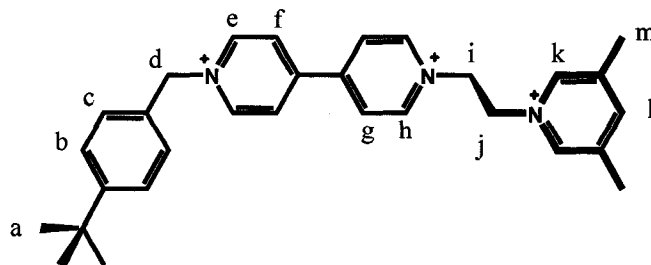


Table 2.18 – ^1H NMR of [2-7][OTf]₃ in CD₃CN. MW_{OTf} = 885.834 g/mol

Proton	δ (ppm)	Multiplicity	# Protons	J (Hz)
a	1.30	s	9	--
b	7.54	d	2	$^3J_{bc} = 8.36$
c	7.45	d	2	$^3J_{cb} = 8.36$
d	5.80	s	2	--
e	9.01	d	2	$^3J_{ef} = 6.75$
f	8.42	d	2	$^3J_{fe} = 6.75$
g	8.46	d	2	$^3J_{gh} = 6.82$
h	9.23	d	2	$^3J_{hg} = 6.82$
i	5.32	t	2	$^3J_{ij} = 6.90$
j	5.14	t	2	$^3J_{ji} = 6.90$
k	8.73	s	2	--
l	8.23	s	1	--
m	2.48	s	6	--

2.6.15 Synthesis of [2-7C24C8]³⁺

[2-3][OTf]₂ (0.134 g, 2.27×10^{-4} mol), **24C8** (0.800 g, 2.27×10^{-3} mol) and *t*-butylbenzyl bromide (0.155 g, 6.81×10^{-4} mol) were dissolved in CH₃CN and stirred for five days. The solution was filtered and the filtrate evaporated. The filtrate was stirred in toluene to get rid of excess crown and *t*-butylbenzyl bromide. This was filtered and the filtrate evaporated. The residue was purified by preparative TLC using 7:4:3 CH₃OH:CH₃NO₂:2M NH₄Cl. The band with R_f = 0.76 was collected and the compound isolated using the same eluent to extract the product from the silica gel. The solvents were evaporated and the residue dissolved in a two phase CH₃NO₂/NaOTf_(aq) mixture. The CH₃NO₂ layer was washed two times with water, then dried with MgSO₄, filtered and evaporated to yield [2-7C24C8]³⁺ as white powder. (0.0200 g, 7 %) ESI-MS: *m/z* [2-7C24C8 - OTf]⁺ calc. 1088.4041, found 1088.4034.

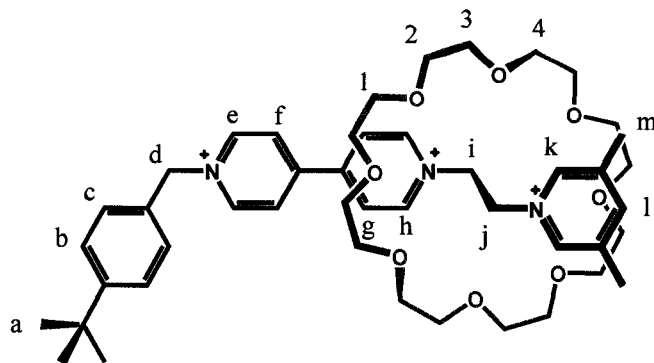


Table 2.19 – ^1H NMR of $[2\text{-}7\text{C}24\text{C}8][\text{OTf}]_3$ in CD_3CN . $\text{MW}_{\text{OTf}} = 1238.2548$ g/mol

Proton	δ (ppm)	Multiplicity	# Protons	J (Hz)
a	1.32	s	9	--
b	7.56	d	2	$^3J_{bc} = 8.34$
c	7.47	d	2	$^3J_{cb} = 8.34$
d	5.82	s	2	--
e	9.03	d	2	$^3J_{ef} = 6.68$
f	8.47	d	2	$^3J_{fe} = 6.68$
g	8.51	d	2	$^3J_{gh} = 6.79$
h	9.27	d	2	$^3J_{hg} = 6.79$
i	5.35	m	2	--
j	5.23	m	2	--
k	8.74	s	2	--
l	8.24	s	1	--
m	2.55	s	6	--
1-4	3.48	m	32	--

2.6.16 Synthesis of [2-7cB24C8]³⁺

[2-3][OTf]₂ (0.100 g, 1.70×10^{-4} mol), B24C8 (0.288 g, 7.19×10^{-4} mol) and *t*-butylbenzyl bromide (0.116g, 5.09×10^{-4} mol) were dissolved in CH₃CN and stirred for five days. The solution was filtered and the filtrate evaporated. The filtrate was stirred in toluene to get rid of excess crown. This was filtered and the filtrate evaporated. The residue was purified by column chromatography (SiO₂) using CH₃OH:2M NH₄Cl (aq): CH₃NO₂ (7:2:1) as the eluent. Like fractions were combined and the solvent evaporated. The residue was dissolved in CH₃NO₂ and H₂O and NaOTf added to anion exchange the rotaxane. The layers were separated and the organic layer dried with MgSO₄ and filtered. The CH₃NO₂ was evaporated yielding an orange solid ($R_f = 0.43$, 0.0590 g, 27 %) ESI-MS: m/z [2-7cB24C8 - 2OTf]²⁺ calc. 1136.4041, found 1136.4047.

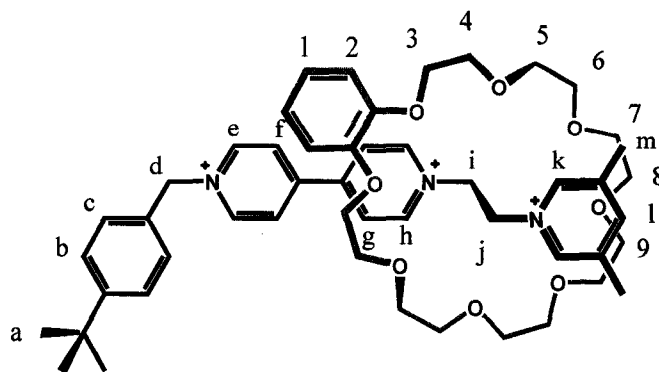


Table 2.20 – ^1H NMR of [2-7cB24C8][OTf]₃ in CD₃CN. MW_{OTf} = 1286.298 g/mol

Proton	δ (ppm)	Multiplicity	# Protons	J (Hz)
a	1.32	s	9	--
b	7.56	d	2	$^3J_{bc} = 8.38$
c	7.49	d	2	$^3J_{cb} = 8.38$
d	5.82	s	2	--
e	9.03	d	2	$^3J_{ef} = 6.81$
f	8.35	d	2	$^3J_{fe} = 6.81$
g	8.38	d	2	$^3J_{gh} = 6.83$
h	9.27	d	2	$^3J_{hg} = 6.83$
i	5.39	s	2	--
j	5.30	s	2	--
k	8.68	s	2	--
l	8.07	s	1	--
m	2.44	s	6	--
1	6.75	dd	2	$J_{meta} = 3.58; J_{ortho} = 5.95$
2	6.61	dd	2	$J_{meta} = 3.58; J_{ortho} = 5.95$
3-9	3.23-3.95	m	28	--

2.6.17 Synthesis of [2-7CDB24C8]³⁺

[2-3][OTf]₂ (0.200 g, 3.48×10^{-4} mol), **DB24C8** (0.935g, 2.09×10^{-3} mol) and *t*-butylbenzyl bromide (0.237g, 1.04×10^{-3} mol) were dissolved in a two layer solution of CH₃NO₂/NaOTf_(aq) (20 mL, 3:1) and stirred for five days. The two layers were separated and the MeNO₂ layer washed twice with water, then subsequently dried with MgSO₄. The CH₃NO₂ solution was filtered and the solvent evaporated. The product was purified by column chromatography (SiO₂) using CH₃OH:2M NH₄Cl (aq):CH₃NO₂ (7:2:1) as the eluent. Like fractions were combined and the solvent evaporated. The residue was dissolved in CH₃NO₂ and H₂O and NaOTf added to anion exchange the rotaxane. The layers were separated and the organic layer dried with MgSO₄ and filtered. The CH₃NO₂ was evaporated yielding an orange solid ($R_f = 0.54$, 0.190 g, 41 %) **ESI-MS: m/z [2-7CDB24C8 - OTf]⁺ calc. 1184.4041, found 1184.4028.**

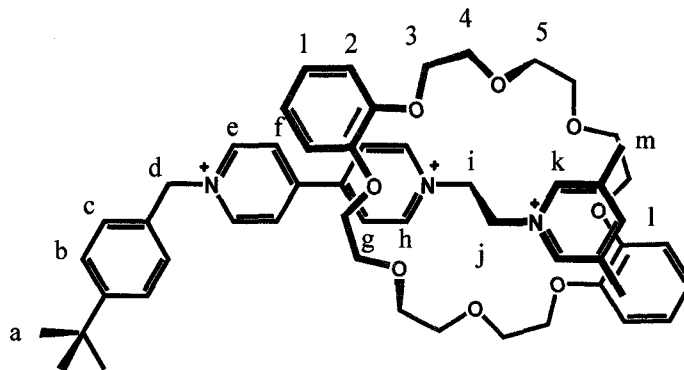


Table 2.21 – ^1H NMR of [2-7cDB24C8][OTf]₃ in CD₃CN. MW_{OTf} = 1334.340g/mol

Proton	δ (ppm)	Multiplicity	# Protons	J (Hz)
a	1.32	s	9	--
b	7.58	d	2	$^3J_{bc} = 8.27$
c	7.47	d	2	$^3J_{cb} = 8.27$
d	5.80	s	2	--
e	8.97	d	2	$^3J_{ef} = 6.48$
f	8.12	d	2	$^3J_{fe} = 6.48$
g	8.16	d	2	$^3J_{gh} = 6.49$
h	9.34	d	2	$^3J_{hg} = 6.49$
i	5.49	m	2	--
j	5.36	m	2	--
k	8.57	s	2	--
l	7.76	s	1	--
m	2.26	s	6	--
1	6.71	dd	4	$J_{meta} = 3.53; J_{ortho} = 5.81$
2	6.64	dd	4	$J_{meta} = 3.53; J_{ortho} = 5.81$
3-5	3.91-4.08	m	24	--

2.6.18 Synthesis of [2-7cBN24C8]³⁺

[2-3][OTf]₂ (0.200 g, 3.39×10^{-4} mol), **BN24C8** (0.676 g, 0.00135 mol) and *t*-butylbenzyl bromide (0.231 g, 0.00102 mol) were dissolved in a two layer solution of CH₃NO₂/NaOTf_(aq) (20 mL, 3:1) and stirred for five days. The two layers were separated and the CH₃NO₂ layer washed twice with water, then subsequently dried with MgSO₄. The CH₃NO₂ solution was filtered and the solvent evaporated. The product was purified by column chromatography (SiO₂) using CH₃OH:2M NH₄Cl (aq):CH₃NO₂ (7:2:1) as the eluent. Like fractions were combined and the solvent evaporated. The residue was dissolved in CH₃NO₂ and H₂O and NaOTf added to anion exchange the rotaxane. The layers were separated and the organic layer dried with MgSO₄ and filtered. The CH₃NO₂ was evaporated yielding an orange solid ($R_f = 0.54$, 0.168 g, 36 %) **ESI-MS: m/z [2-7cBN24C8 - OTf]⁺ calc. 1234.4198, found 1234.4169.**

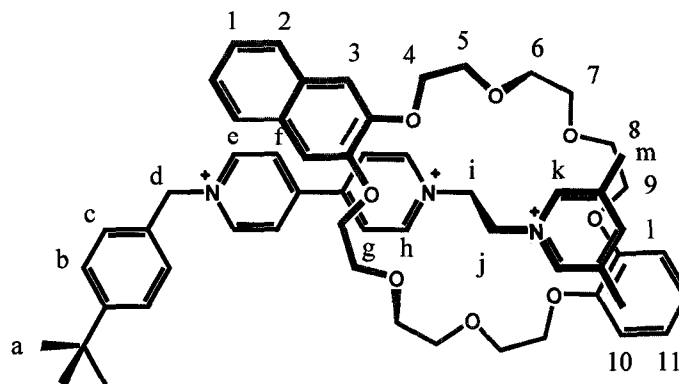


Table 2.22 – ^1H NMR of $[2\text{-}7\text{cBN}24\text{C}8][\text{OTf}]_3$ in CD_3CN . $\text{MW}_{\text{OTf}} = 1384.399$ g/mol

Proton	δ (ppm)	Multiplicity	# Protons	J (Hz)
a	1.32	s	9	--
b	7.58	d	2	$^3J_{bc} = 8.27$
c	7.47	d	2	$^3J_{cb} = 8.27$
d	5.80	s	2	--
e	8.97	d	2	$^3J_{ef} = 6.48$
f	8.12	d	2	$^3J_{fe} = 6.48$
g	8.16	d	2	$^3J_{gh} = 6.49$
h	9.34	d	2	$^3J_{hg} = 6.49$
i	5.50	m	2	--
j	5.36	m	2	--
k	8.57	s	2	--
l	7.76	s	1	--
m	2.35	s	6	--
1	6.71	dd	2	$J_{\text{meta}} = 3.53; J_{\text{ortho}} = 5.81$
2	6.64	dd	2	$J_{\text{meta}} = 3.53; J_{\text{ortho}} = 5.81$
3-5	4.08-3.91	m	2	--
4-9	4.37-3.92	m	24	--
10	6.65	m	2	--
11	6.69	m	2	--

2.6.19 Synthesis of [2-7C_N24C8]³⁺

[2-3][OTf]₂ (0.200 g, 3.39×10^{-4} mol), N24C8 (0.917 g, 2.04×10^{-3} mol) and *t*-butylbenzyl bromide (0.231g, 1.02×10^{-3} mol) were dissolved in CH₃CN and stirred for five days. The solution was filtered and the filtrate evaporated. The filtrate was stirred in toluene to get rid of excess crown. This was filtered and the filtrate evaporated. The residue was purified by column chromatography (SiO₂) using CH₃OH:2M NH₄Cl (aq): CH₃NO₂ (7:2:1) as the eluent. Like fractions were combined and the solvent evaporated. The residue was dissolved in CH₃NO₂ and H₂O and NaOTf added to anion exchange the rotaxane. The layers were separated and the organic layer dried with MgSO₄ and filtered. The CH₃NO₂ was evaporated yielding an orange solid ($R_f = 0.41$, 0.147 g, 33 %) **ESI-MS**: m/z [2-7C_N24C8 - OTf]⁺ calc. 1186.4233, found 1186.4203.

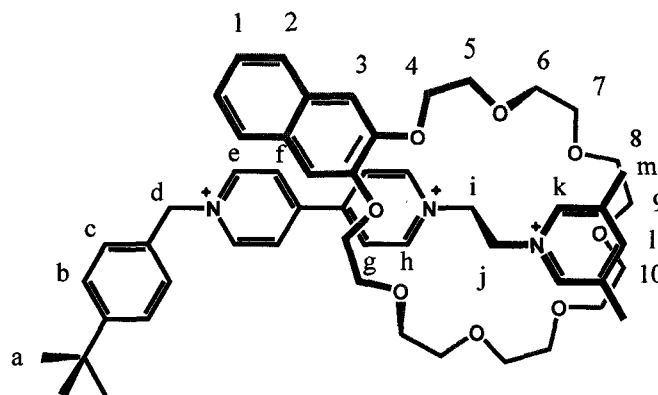
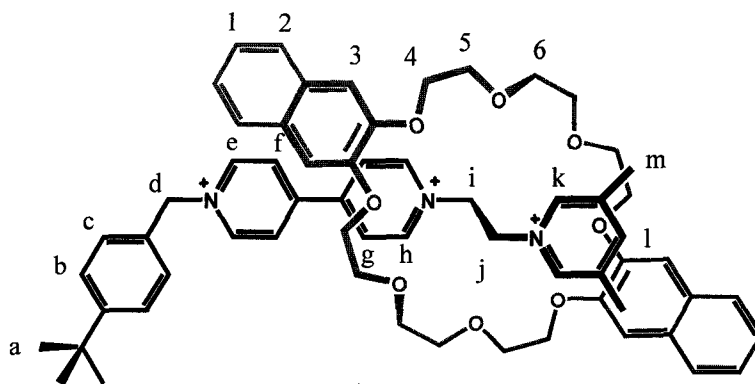


Table 2.23 – ^1H NMR of $[2\text{-}7\text{C-N}24\text{C}8][\text{OTf}]_3$ in CD_3CN . $\text{MW}_{\text{OTf}} = 1336.356$ g/mol

Proton	δ (ppm)	Multiplicity	# Protons	J (Hz)
a	1.34	s	9	--
b	7.61	d	2	$^3J_{bc} = 8.36$
c	7.53	d	2	$^3J_{cb} = 8.36$
d	5.68	s	2	--
e	8.72	d	2	$^3J_{ef} = 6.63$
f	7.92	d	2	$^3J_{fe} = 6.63$
g	8.31	d	2	$^3J_{gh} = 6.70$
h	9.20	d	2	$^3J_{hg} = 6.70$
i	5.37	s	2	--
j	5.37	s	2	--
k	8.78	s	2	--
l	8.19	s	1	--
m	2.52	s	6	--
1	6.86	dd	2	$J_{\text{meta}} = 3.25; J_{\text{ortho}} = 6.05$
2	7.36	dd	2	$J_{\text{meta}} = 3.25; J_{\text{ortho}} = 6.05$
3	7.04	s	2	--
4-10	3.14-4.42	m	28	--

2.6.20 Synthesis of [2-7cDN24C8]³⁺

[2-3][OTf]₂ (0.115 g, 2.00×10^{-4} mol), DN24C8 (0.660g, 1.20×10^{-3} mol) and *t*-butylbenzyl bromide (0.136g, 6.00×10^{-4} mol) were dissolved in a two layer solution of CH₃NO₂/NaOTf_(aq) (20 mL, 3:1) and stirred for five days. The two layers were separated and the CH₃NO₂ layer washed twice with water, then subsequently dried with MgSO₄. The CH₃NO₂ solution was filtered and the solvent evaporated. The product was purified by column chromatography (SiO₂) using CH₃OH:2M NH₄Cl (aq):CH₃NO₂ (7:2:1) as the eluent. Like fractions were combined and the solvent evaporated. The residue was dissolved in CH₃NO₂ and H₂O and NaOTf added to anion exchange the rotaxane. The layers were separated and the organic layer dried with MgSO₄ and filtered. The CH₃NO₂ was evaporated yielding an orange solid ($R_f = 0.55$, 0.157 g, 55 %) **ESI-MS**: m/z [2-7cDN24C8 - OTf]⁺ calc. 1284.4354, found 1284.4335.

Table 2.24 – ^1H NMR of $[2\text{-}7\text{cDN}24\text{C}8][\text{OTf}]_3$ in CD_3CN . $\text{MW}_{\text{OTf}} = 1434.458\text{g/mol}$

Proton	δ (ppm)	Multiplicity	# Protons	J (Hz)
a	1.37	s	9	--
b	7.66	d	2	$^3J_{bc} = 8.33$
c	7.46	d	2	$^3J_{cb} = 8.33$
d	5.59	s	2	--
e	8.41	d	2	$^3J_{ef} = 6.50$
f	7.15	d	2	$^3J_{fe} = 6.50$
g	7.80	d	2	$^3J_{gh} = 6.61$
h	9.26	d	2	$^3J_{hg} = 6.61$
i	5.49	m	2	--
j	5.49	m	2	--
k	8.76	s	2	--
l	7.87	s	1	--
m	2.39	s	6	--
1	6.98	dd	4	$J_{\text{meta}} = 3.21; J_{\text{ortho}} = 6.09$
2	7.37	dd	4	$J_{\text{meta}} = 3.21; J_{\text{ortho}} = 6.09$
3	6.96	m	4	--
4-6	4.27-3.97	m	24	--

2.6.21 Synthesis of **2-8**³⁺

[**2-4**][OTf]₂ (0.100 g, 1.62×10^{-4} mol) and *t*-butylbenzyl bromide (0.110g, 4.86×10^{-4} mol) were dissolved in CH₃CN and stirred for five days. The precipitate that formed was filtered and the filtrate evaporated. The filtrate was stirred in CH₂Cl₂ to get rid of excess *t*-butylbenzyl bromide. The resulting precipitate was filtered and combined with the first precipitate and all dissolved in H₂O. NaOTf was added to the solution resulting in precipitation of the product as the triflate salt. The white precipitate was collected by vacuum filtration. (0.0830 g, 56 %) ESI-MS: *m/z* [**2-8** - OTf]⁺ calc. 764.2263, found 764.2234.

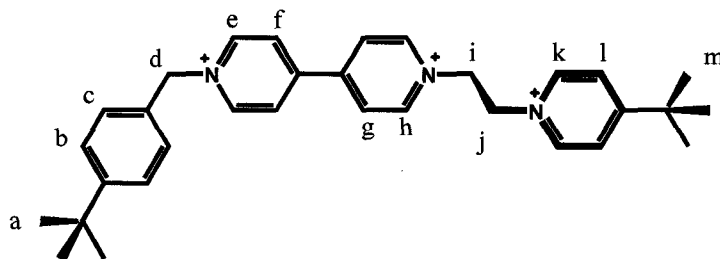


Table 2.25 – ^1H NMR of [2-8][OTf]₃ in CD₃CN. MW_{OTf} = 913.887 g/mol

Proton	δ (ppm)	Multiplicity	# Protons	J (Hz)
a	1.31	s	9	--
b	7.55	d	2	$^3J_{bc} = 8.37$
c	7.45	d	2	$^3J_{cb} = 8.37$
d	5.80	s	2	--
e	9.00	d	2	$^3J_{ef} = 6.78$
f	8.42	d	2	$^3J_{fe} = 6.78$
g	8.46	d	2	$^3J_{gh} = 6.86$
h	8.96	d	2	$^3J_{hg} = 6.86$
i	5.18	t	2	$^3J_{ij} = 6.69$
j	5.09	t	2	$^3J_{ji} = 6.69$
k	8.64	d	2	$^3J_{kl} = 6.90$
l	8.07	d	2	$^3J_{lk} = 6.90$
m	1.40	s	9	--

2.6.22 Synthesis of [2-8cB24C8]³⁺

[2-4][OTf]₂ (0.200 g, 3.24×10^{-4} mol), B24C8 (0.778 g, 1.94×10^{-3} mol) and *t*-butylbenzyl bromide (0.441g, 1.94×10^{-3} mol) were dissolved in a two layer solution of CH₃NO₂/NaOTf_(aq) (20 mL, 3:1) and stirred for five days. The two layers were separated and the CH₃NO₂ layer washed twice with water, then subsequently dried with MgSO₄. The CH₃NO₂ solution was filtered and the solvent evaporated. The product was purified by column chromatography (SiO₂) using CH₃OH:2M NH₄Cl (aq):CH₃NO₂ (7:2:1) as the eluent. Like fractions were combined and the solvent evaporated. The residue was dissolved in CH₃NO₂ and H₂O and NaOTf added to anion exchange the rotaxane. The layers were separated and the organic layer dried with MgSO₄ and filtered. The CH₃NO₂ was evaporated yielding an orange solid ($R_f = 0.46$, 0.138g, 32 %) **ESI-MS: *m/z* [2-8cB24C8 - 2OTf]²⁺ calc. 507.7414, found 507.7392.**

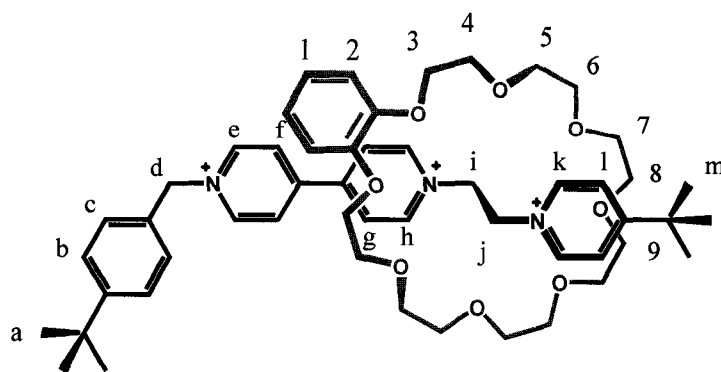


Table 2.26 – ^1H NMR of [2-8cB24C8][OTf]₃ in CD₃CN. MW_{OTf} = 1314.351 g/mol

Proton	δ (ppm)	Multiplicity	# Protons	J (Hz)
a	1.32	s	9	--
b	7.57	d	2	$^3J_{bc} = 8.29$
c	7.47	d	2	$^3J_{cb} = 8.29$
d	5.81	s	2	--
e	8.98	d	2	$^3J_{ef} = 6.54$
f	8.25	d	2	$^3J_{fe} = 6.54$
g	8.28	d	2	$^3J_{gh} = 6.65$
h	9.26	d	2	$^3J_{hg} = 6.65$
i	5.40	m	2	--
j	5.35	m	2	--
k	8.92	s	2	--
l	8.02	s	2	--
m	1.38	s	9	--
1	6.72	dd	2	$J_{meta} = 3.58; J_{ortho} = 5.68$
2	6.57	dd	2	$J_{meta} = 3.58; J_{ortho} = 5.68$
3-9	3.20-4.13	m	28	--

2.6.23 Synthesis of [2-8 \subset DB24C8]³⁺

[2-4][OTf]₂ (0.150 g, 2.43×10^{-4} mol), **DB24C8** (0.871g, 1.94×10^{-3} mol) and *t*-butylbenzyl bromide (0.166g, 7.29×10^{-4} mol) were dissolved in a two layer solution of CH₃NO₂/NaOTf_(aq) (20 mL, 3:1) and stirred for five days. The two layers were separated and the CH₃NO₂ layer washed twice with water, then subsequently dried with MgSO₄. The CH₃NO₂ solution was filtered and the solvent evaporated. The product was purified by column chromatography (SiO₂) using CH₃OH:2M NH₄Cl(aq):CH₃NO₂ (7:2:1) as the eluent. Like fractions were combined and the solvent evaporated. The residue was dissolved in CH₃NO₂ and H₂O and NaOTf added to anion exchange the rotaxane. The layers were separated and the organic layer dried with MgSO₄ and filtered. The CH₃NO₂ was evaporated yielding an orange solid (R_f = 0.51, 0.191 g, 58 %) **ESI-MS**: *m/z* [2-8 \subset DB24C8 - OTf]⁺ calc. 1212.4354, found 1212.4415

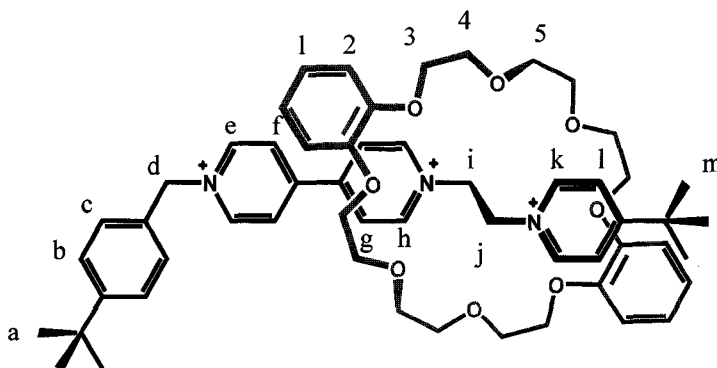


Table 2.27 – ^1H NMR of [2-8cDB24C8][OTf]₃ in CD₃CN. . MW_{OTf} = 1362.394 g/mol

Proton	δ (ppm)	Multiplicity	# Protons	J (Hz)
a	1.32	s	9	--
b	7.57	d	2	$^3J_{bc} = 8.36$
c	7.52	d	2	$^3J_{cb} = 8.36$
d	5.88	s	2	--
e	9.11	d	2	$^3J_{ef} = 6.46$
f	8.26	d	2	$^3J_{fe} = 6.46$
g	8.32	d	2	$^3J_{gh} = 6.56$
h	9.31	d	2	$^3J_{hg} = 6.56$
i	5.56	m	2	--
j	5.44	m	2	--
k	8.99	d	2	$^3J_{kl} = 6.67$
l	7.85	d	2	$^3J_{lk} = 6.67$
m	1.22	s	9	--
1	6.69	dd	4	$J_{meta} = 3.56; J_{ortho} = 5.80$
2	6.57	dd	4	$J_{meta} = 3.56; J_{ortho} = 5.80$
3-5	3.95-4.14	m	24	--

2.6.24 Synthesis of [2-8cBN24C8]³⁺

[2-4][OTf]₂ (0.150 g, 2.43×10^{-4} mol), BN24C8 (0.484 g, 9.72×10^{-4} mol) and *t*-butylbenzyl bromide (0.166g, 7.29×10^{-4} mol) were dissolved in a two layer solution of CH₃NO₂/NaOTf_(aq) (20 mL, 3:1) and stirred for five days. The two layers were separated and the CH₃NO₂ layer washed twice with water, then subsequently dried with MgSO₄. The CH₃NO₂ solution was filtered and the solvent evaporated. The product was purified by column chromatography (SiO₂) using CH₃OH:2M NH₄Cl(aq):CH₃NO₂ (7:2:1) as the eluent. Like fractions were combined and the solvent evaporated. The residue was dissolved in CH₃NO₂ and H₂O and NaOTf added to anion exchange the rotaxane. The layers were separated and the organic layer dried with MgSO₄ and filtered. The CH₃NO₂ was evaporated yielding an orange solid ($R_f = 0.56$, 0.063 g, 18 %) **ESI-MS**: m/z [2-8cBN24C8 - OTf]⁺ calc. 1262.4511, found 1262.4526.

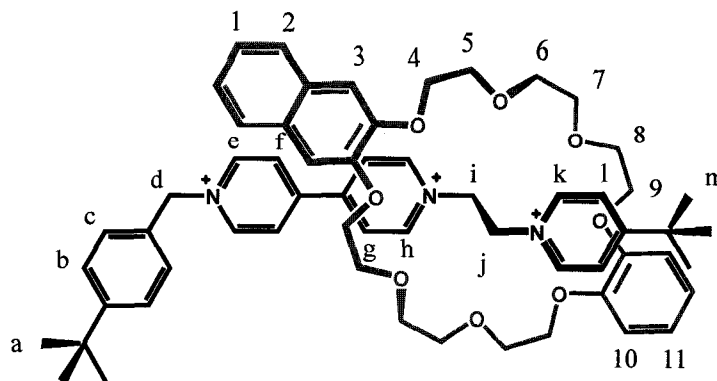


Table 2.28 – ^1H NMR of $[2\text{-}8\text{cBN}24\text{C}8][\text{OTf}]_3$ in CD_3CN . $\text{MW}_{\text{OTf}} = 1412.452$ g/mol

Proton	δ (ppm)	Multiplicity	# Protons	J (Hz)
a	1.36	s	9	--
b	7.64	d	2	$^3J_{bc} = 8.27$
c	7.49	d	2	$^3J_{cb} = 8.27$
d	5.65	s	2	--
e	9.02	d	2	$^3J_{ef} = 6.46$
f	7.91	d	2	$^3J_{fe} = 6.46$
g	7.98	d	2	$^3J_{gh} = 6.56$
h	9.28	d	2	$^3J_{hg} = 6.56$
i	5.55	m	2	--
j	5.45	m	2	--
k	8.62	d	2	$^3J_{kl} = 6.67$
l	7.62	d	2	$^3J_{lk} = 6.67$
m	1.21	s	9	--
1	6.86	dd	2	$J_{\text{meta}} = 3.22; J_{\text{ortho}} = 6.09$
2	7.34	dd	2	$J_{\text{meta}} = 3.22; J_{\text{ortho}} = 6.09$
3	6.96	s	2	--
4-9	3.93-4.32	m	24	--
10	6.58	dd	2	$J_{\text{meta}} = 3.59; J_{\text{ortho}} = 5.88$
11	6.65	dd	2	$J_{\text{meta}} = 3.59; J_{\text{ortho}} = 5.88$

2.6.25 Synthesis of [2-8cN24C8]³⁺

[2-4][OTf]₂ (0.200 g, 3.24×10^{-4} mol), N24C8 (0.874 g, 1.94×10^{-3} mol) and *t*-butylbenzyl bromide (0.441g, 1.94×10^{-3} mol) were dissolved in a two layer solution of CH₃NO₂/NaOTf_(aq) (20 mL, 3:1) and stirred for five days. The two layers were separated and the CH₃NO₂ layer washed twice with water, then subsequently dried with MgSO₄. The CH₃NO₂ solution was filtered and the solvent evaporated. The product was purified by column chromatography (SiO₂) using CH₃OH:2M NH₄Cl(aq):CH₃NO₂ (7:2:1) as the eluent. Like fractions were combined and the solvent evaporated. The residue was dissolved in CH₃NO₂ and H₂O and NaOTf added to anion exchange the rotaxane. The layers were separated and the organic layer dried with MgSO₄ and filtered. The CH₃NO₂ was evaporated yielding an orange solid ($R_f = 0.47$, 0.186 g, 42 %) **ESI-MS**: m/z [2-8cN24C8 - 2OTf]²⁺ calc. 532.7493, found 532.7515.

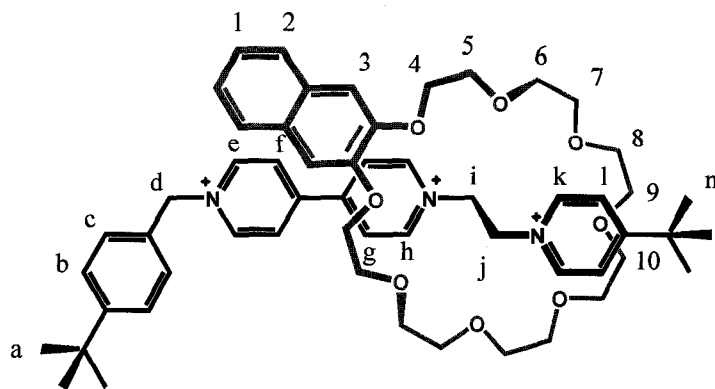


Table 2.29 – ^1H NMR of $[2\text{-}8\text{cN}24\text{C}8][\text{OTf}]_3$ in CD_3CN . $\text{MW}_{\text{OTf}} = 1364.409$ g/mol

Proton	δ (ppm)	Multiplicity	# Protons	J (Hz)
a	1.36	s	9	--
b	7.64	d	2	$^3J_{bc} = 8.25$
c	7.48	d	2	$^3J_{cb} = 8.25$
d	5.65	s	2	--
e	8.61	d	2	$^3J_{ef} = 6.49$
f	7.78	d	2	$^3J_{fe} = 6.49$
g	8.17	d	2	$^3J_{gh} = 6.60$
h	9.24	d	2	$^3J_{hg} = 6.60$
i	5.40	s	2	--
j	5.40	s	2	--
k	8.98	d	2	$^3J_{kl} = 6.70$
l	8.10	d	2	$^3J_{lk} = 6.70$
m	1.39	s	9	--
1	6.94	dd	2	$J_{\text{meta}} = 3.18; J_{\text{ortho}} = 5.96$
2	7.36	dd	2	$J_{\text{meta}} = 3.18; J_{\text{ortho}} = 5.96$
3	7.00	s	2	--
4-10	3.09-4.37	m	28	--

2.6.26 Synthesis of [2-8cDN24C8]³⁺

[2-4][OTf]₂ (0.150 g, 2.43×10^{-4} mol), DN24C8 (0.533g, 1.94×10^{-3} mol) and *t*-butylbenzyl bromide (0.166g, 7.29×10^{-4} mol) were dissolved in a two layer solution of CH₃NO₂/NaOTf_(aq) (20 mL, 3:1) and stirred for five days. The two layers were separated and the CH₃NO₂ layer washed twice with water, then subsequently dried with MgSO₄. The CH₃NO₂ solution was filtered and the solvent evaporated. The product was purified by column chromatography (SiO₂) using CH₃OH:2M NH₄Cl(aq):CH₃NO₂ (7:2:1) as the eluent. Like fractions were combined and the solvent evaporated. The residue was dissolved in CH₃NO₂ and H₂O and NaOTf added to anion exchange the rotaxane. The layers were separated and the organic layer dried with MgSO₄ and filtered. The CH₃NO₂ was evaporated yielding an orange solid ($R_f = 0.58$, 0.150 g, 42 %) **ESI-MS**: m/z [2-8cDN24C8 - OTf]⁺ calc. 1312.4667, found 1312.4719.

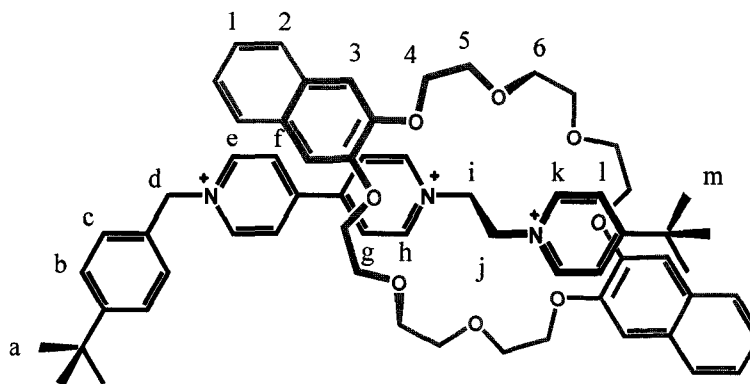


Table 2.30 – ^1H NMR of $[2\text{-}8^{\text{c}}\text{DN}24\text{C}8][\text{OTf}]_3$ in CD_3CN . $\text{MW}_{\text{OTf}} = 1462.511$ g/mol

Proton	δ (ppm)	Multiplicity	# Protons	J (Hz)
a	1.32	s	9	--
b	7.66	d	2	$^3J_{bc} = 8.34$
c	7.47	d	2	$^3J_{cb} = 8.34$
d	5.59	s	2	--
e	9.04	d	2	$^3J_{ef} = 6.67$
f	7.94	d	2	$^3J_{fe} = 6.67$
g	7.86	d	2	$^3J_{gh} = 6.67$
h	9.27	d	2	$^3J_{hg} = 6.67$
i	5.56	m	2	--
j	5.48	m	2	--
k	8.43	d	2	$^3J_{kl} = 6.56$
l	7.22	d	2	$^3J_{lk} = 6.56$
m	1.13	s	9	--
1	6.96	dd	4	$J_{\text{meta}} = 3.23; J_{\text{ortho}} = 5.96$
2	7.36	dd	4	$J_{\text{meta}} = 3.23; J_{\text{ortho}} = 5.96$
3	6.95	m	4	--
4-6	3.74-4.29	m	24	--

2.6.27 Synthesis of 2-9⁴⁺

[2-5][OTf]₂ (0.0150 g, 2.24×10^{-5} mol) and *t*-butylbenzyl bromide (0.0255g, 1.12×10^{-4} mol) were dissolved in CH₃CN and stirred for three days. The precipitate that formed was filtered and collected. The precipitate was dissolved in H₂O and NaOTf was added resulting in precipitation of the product as the triflate salt. The white precipitate was stirred in CH₂Cl₂ and collected by vacuum filtration. (0.0030 g, 10 %)

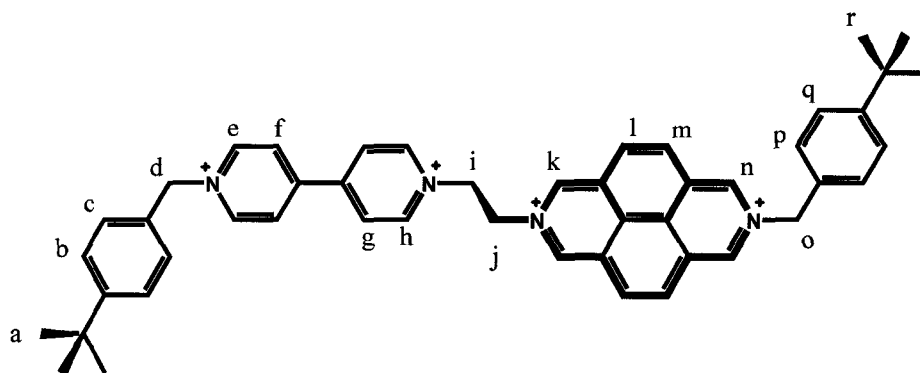


Table 2.31 – ^1H NMR of [2-9][OTf]₄ in CD₃CN. MW_{OTf} = 1281.230 g/mol

Proton	δ (ppm)	Multiplicity	# Protons	J (Hz)
a	1.32	s	9	--
b	7.53	d	2	$^3J_{bc} = 8.48$
c	7.45	d	2	$^3J_{cb} = 8.48$
d	5.79	s	2	--
e	9.00	d	2	$^3J_{ef} = 6.68$
f	8.44	d	2	$^3J_{fe} = 6.68$
g	8.48	d	2	$^3J_{gh} = 6.83$
h	9.11	d	2	$^3J_{hg} = 6.83$
i	5.53	m	2	--
j	5.76	m	2	--
k	10.16	s	2	--
l	8.87	s	2	--
m	8.87	s	2	--
n	10.03	s	2	--
o	6.26	s	2	--
p	7.56	d	2	$^3J_{pq} = 8.45$
q	7.59	d	2	$^3J_{qp} = 8.45$
r	1.32	s	9	--

2.6.28 Synthesis of [2-9CDB24C8]⁴⁺

[2-5][OTf]₂ (0.030 g, 5.47×10^{-5} mol), **DB24C8** (0.245 g, 5.47×10^{-4} mol) and *t*-butylbenzyl bromide (0.075 g, 3.28×10^{-4} mol) were dissolved in a two layer solution of CH₃NO₂/NaOTf_(aq) (20 mL, 3:1) and stirred for five days. The two layers were separated and the CH₃NO₂ layer washed twice with water, then subsequently dried with MgSO₄. The CH₃NO₂ solution was filtered and the solvent evaporated. The product was purified by column chromatography (SiO₂) using CH₃OH:2M NH₄Cl(aq):CH₃NO₂ (7:2:1) as the eluent. Like fractions were combined and the solvent evaporated. The residue was dissolved in CH₃NO₂ and H₂O and NaOTf added to anion exchange the rotaxane. The layers were separated and the organic layer dried with MgSO₄ and filtered. The CH₃NO₂ was evaporated yielding an orange solid ($R_f = 0.35$, 0.020 g, 21 %) **ESI-MS: *m/z* [2-9CDB24C8 - 3OTf]³⁺** calc. 427.1931, found 427.1943.

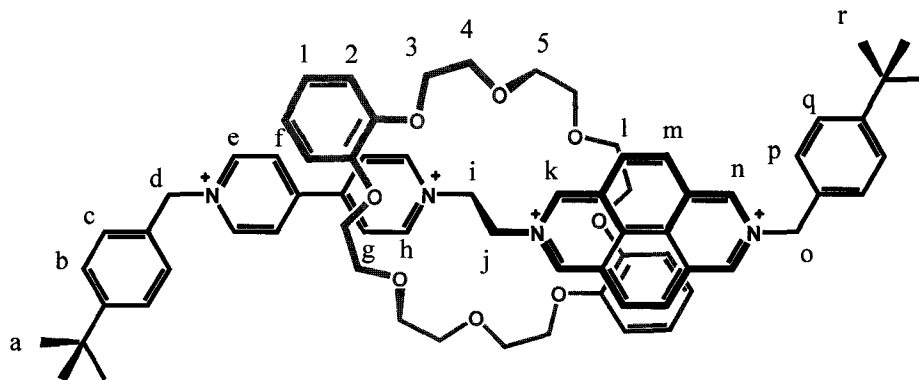


Table 2.32 – ^1H NMR of $[2\text{-}9\text{cDB}24\text{C}8][\text{OTf}]_4$ in CD_3CN . $\text{MW}_{\text{OTf}} = 1729.736$ g/mol

Proton	δ (ppm)	Multiplicity	# Protons	J (Hz)
a	1.32	s	9	--
b	7.59	d	2	$^3J_{bc} = 8.25$
c	7.49	d	2	$^3J_{cb} = 8.25$
d	5.82	s	2	--
e	8.99	d	2	$^3J_{ef} = 6.78$
f	8.24	d	2	$^3J_{fe} = 6.78$
g	8.33	d	2	$^3J_{gh} = 6.78$
h	9.41	d	2	$^3J_{hg} = 6.78$
i	5.56	m	2	--
j	6.11	m	2	--
k	10.28	s	2	--
l	8.69	d	2	$^3J_{lm} = 9.10$
m	8.73	d	2	$^3J_{ml} = 9.10$
n	9.93	s	2	--
o	6.26	s	2	--
p	7.61	d	2	$^3J_{pq} = 8.25$
q	7.67	d	2	$^3J_{qp} = 8.25$
r	1.30	s	9	--
1	6.14	dd	4	$J_{\text{meta}} = 3.80; J_{\text{ortho}} = 5.82$
2	5.81	dd	4	$J_{\text{meta}} = 3.80; J_{\text{ortho}} = 5.82$
3-5	3.86-4.30	m	24	--

2.6.29 Synthesis of [2-9CBN24C8]⁴⁺

[2-5][OTf]₂ (0.030 g, 4.37×10^{-5} mol), BN24C8 (0.218 g, 4.37×10^{-4} mol) and *t*-butylbenzyl bromide (0.060 g, 2.62×10^{-4} mol) were dissolved in a two layer solution of CH₃NO₂/NaOTf_(aq) (20 mL, 3:1) and stirred for five days. The two layers were separated and the CH₃NO₂ layer washed twice with water, then subsequently dried with MgSO₄. The CH₃NO₂ solution was filtered and the solvent evaporated. The product was purified by column chromatography (SiO₂) using CH₃OH:2M NH₄Cl(aq):CH₃NO₂ (7:2:1) as the eluent. Like fractions were combined and the solvent evaporated. The residue was dissolved in CH₃NO₂ and H₂O and NaOTf added to anion exchange the rotaxane. The layers were separated and the organic layer dried with MgSO₄ and filtered. The CH₃NO₂ was evaporated yielding an orange solid ($R_f = 0.33$, 0.021 g, 27 %) ESI-MS: m/z [2-9CBN24C8 - 3OTf]³⁺ calc. 443.8650, found 443.8601.

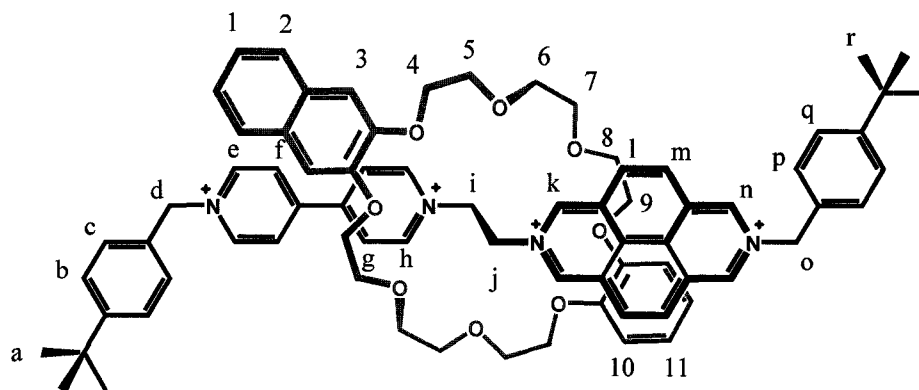


Table 2.33 – ^1H NMR of [2-9cBN24C8][OTf]₄ in CD₃CN. MW_{OTf} = 1779.794 g/mol

Proton	δ (ppm)	Multiplicity	# Protons	J (Hz)
a	1.32	s	9	--
b	7.61	d	2	$^3J_{bc} = 8.40$
c	7.50	d	2	$^3J_{cb} = 8.40$
d	5.78	s	2	--
e	8.90	d	2	$^3J_{ef} = 6.72$
f	8.18	d	2	$^3J_{fe} = 6.72$
g	8.41	d	2	$^3J_{gh} = 6.75$
h	9.48	d	2	$^3J_{hg} = 6.75$
i	5.71	m	2	--
j	6.07	m	2	--
k	10.24	s	2	--
l	8.56	d	2	$^3J_{lm} = 9.15$
m	8.67	d	2	$^3J_{ml} = 9.15$
n	9.70	s	2	--
o	6.14	s	2	--
p	7.61	d	2	$^3J_{pq} = 8.40$
q	7.74	d	2	$^3J_{qp} = 8.40$
r	1.32	s	9	--
1	6.12	dd	2	$J_{meta} = 3.22; J_{ortho} = 6.10$
2	6.53	dd	2	$J_{meta} = 3.22; J_{ortho} = 6.10$
3	6.40	m	2	--
4-9	3.93-4.23	m	24	--
10	5.75	dd	2	$J_{meta} = 3.61; J_{ortho} = 5.89$
11	6.12	dd	2	$J_{meta} = 3.61; J_{ortho} = 5.89$

2.6.30 Synthesis of [2-9C-N24C8]⁴⁺

[2-5][OTf]₂ (0.035 g, 5.08×10^{-5} mol), N24C8 (0.229 g, 5.08×10^{-4} mol) and *t*-butylbenzyl bromide (0.069g, 3.04×10^{-4} mol) were dissolved in CH₃CN and stirred for five days. The solution was filtered and the filtrate evaporated. The filtrate was stirred in toluene to get rid of excess crown and *t*-butylbenzyl bromide. This was filtered and the filtrate evaporated. The residue was subjected to prep TLC using 7:2:1 CH₃OH:2M NH₄Cl:CH₃NO₂ as the eluent. The band with R_f = 0.79 was collected and the product was extracted from the silica gel using the same eluent. (0.0190 g, 22 %)

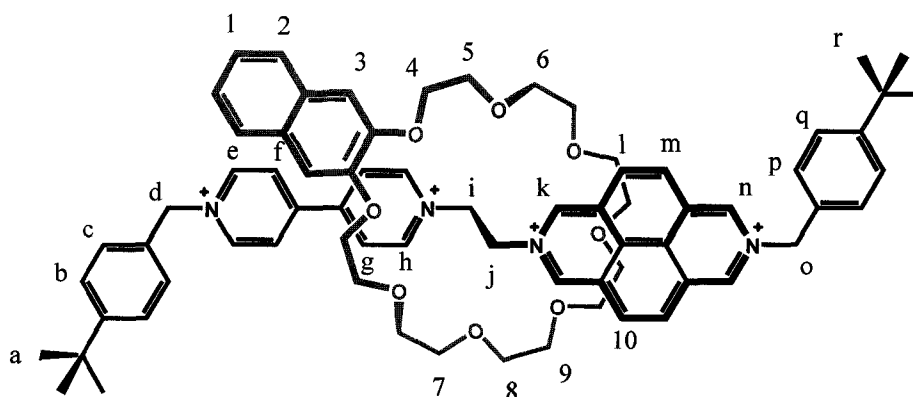


Table 2.34 – ^1H NMR of $[2\text{-}9\text{cN}24\text{C}8][\text{OTf}]_4$ in CD_3CN . $\text{MW}_{\text{OTf}} = 1731.752$ g/mol.

Proton	δ (ppm)	Multiplicity	# Protons	J (Hz)
a	1.32	s	9	--
b	7.56	d	2	$^3J_{bc} = 8.20$
c	7.51	d	2	$^3J_{cb} = 8.20$
d	5.83	s	2	--
e	9.02	d	2	$^3J_{ef} = 6.42$
f	8.46	d	2	$^3J_{fe} = 6.42$
g	8.65	d	2	$^3J_{gh} = 6.58$
h	9.47	d	2	$^3J_{hg} = 6.58$
i	5.70	m	2	--
j	5.94	m	2	--
k	10.28	s	2	--
l	8.62	d	2	$^3J_{lm} = 9.15$
m	8.72	d	2	$^3J_{ml} = 9.15$
n	9.74	s	2	--
o	6.13	s	2	--
p	7.64	d	2	$^3J_{pq} = 8.28$
q	7.73	d	2	$^3J_{qp} = 8.28$
r	1.34	s	9	--
1	6.90	m	2	--
2	6.67	m	2	--
3	6.31	s	2	--
4-10	3.38-4.30	m	28	--

2.6.31 Synthesis of [2-9cDN24C8]⁴⁺

[2-5][Br]₂ (0.030 g, 5.47×10^{-5} mol), DN24C8 (0.300 g, 5.47×10^{-4} mol) and *t*-butylbenzyl bromide (0.075 g, 3.28×10^{-4} mol) were dissolved in a two layer solution of CH₃NO₂/NaOTf_(aq) (20 mL, 3:1) and stirred for five days. The two layers were separated and the CH₃NO₂ layer washed twice with water, then subsequently dried with MgSO₄. The CH₃NO₂ solution was filtered and the solvent evaporated. The product was purified by column chromatography (SiO₂) using CH₃OH:2M NH₄Cl (aq):CH₃NO₂ (7:2:1) as the eluent. Like fractions were combined and the solvent evaporated. The residue was dissolved in CH₃NO₂ and H₂O and NaOTf added to anion exchange the rotaxane. The layers were separated and the organic layer dried with MgSO₄ and filtered. The CH₃NO₂ was evaporated yielding an orange solid ($R_f = 0.33$, 0.036 g, 36 %) **ESI-MS: *m/z* [2-9cDN24C8 - 2OTf]²⁺ calc. 765.2816, found 765.2781.**

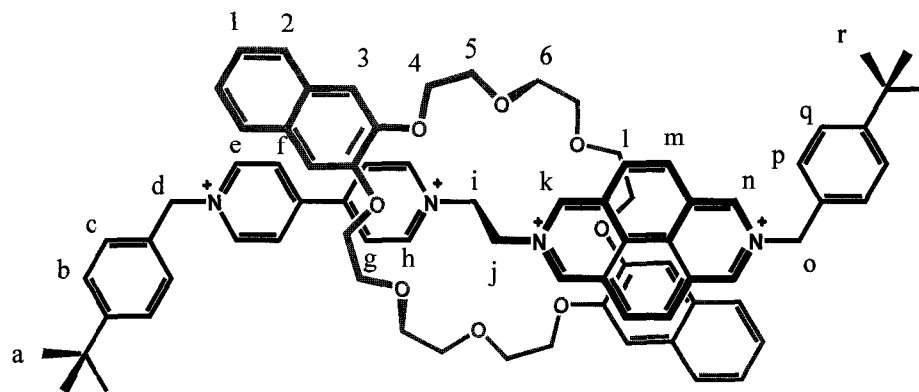


Table 2.35 – ^1H NMR of $[2\text{-}9\text{cDN}24\text{C}8][\text{OTf}]_4$ in CD_3CN . $\text{MW}_{\text{OTf}} = 1829.853$ g/mol

Proton	δ (ppm)	Multiplicity	# Protons	J (Hz)
a	1.32	s	9	--
b	7.63	d	2	$^3J_{bc} = 8.38$
c	7.51	d	2	$^3J_{cb} = 8.38$
d	5.67	s	2	--
e	8.85	d	2	$^3J_{ef} = 6.70$
f	8.20	d	2	$^3J_{fe} = 6.70$
g	8.53	d	2	$^3J_{gh} = 6.82$
h	9.53	d	2	$^3J_{hg} = 6.82$
i	5.79	m	2	--
j	6.08	m	2	--
k	10.22	s	2	--
l	8.44	d	2	$^3J_{lm} = 9.15$
m	9.59	d	2	$^3J_{ml} = 9.15$
n	9.49	s	2	--
o	6.05	s	2	--
p	7.71	d	2	$^3J_{pq} = 8.48$
q	7.78	d	2	$^3J_{qp} = 8.48$
r	1.32	s	9	--
1	6.46	dd	4	$J_{\text{meta}} = 3.19; J_{\text{ortho}} = 6.06$
2	6.76	dd	4	$J_{\text{meta}} = 3.19; J_{\text{ortho}} = 6.06$
3	6.33	s	4	--
4-6	3.92-4.31	m	24	--

2.6.32 Synthesis of [2-10cBN24C8]⁴⁺

[2-2][OTf]₂ (0.125 g, 1.96×10^{-4} mol), BN24C8 (0.293 g, 5.87×10^{-4} mol) and 3,5-bis(methoxycarbonyl)benzyl bromide (0.225g, 7.83×10^{-4} mol) were dissolved in a two layer solution of CH₃NO₂/NaOTf_(aq) (20 mL, 3:1) and stirred for five days. The two layers were separated and the CH₃NO₂ layer washed twice with water, then subsequently dried with MgSO₄. The CH₃NO₂ solution was filtered and the solvent evaporated. The product was purified by column chromatography (SiO₂) using CH₃OH:2M NH₄Cl (aq):CH₃NO₂ (7:2:1) as the eluent. Like fractions were combined and the solvent evaporated. The residue was dissolved in CH₃NO₂ and H₂O and NaOTf added to anion exchange the rotaxane. The layers were separated and the organic layer dried with MgSO₄ and filtered. The CH₃NO₂ was evaporated yielding an orange solid ($R_f = 0.38$, 0.162 g, 45 %) ESI-MS: m/z [2-10cBN24C8 - OTf]⁺ calc. 775.2143, found 775.2113.

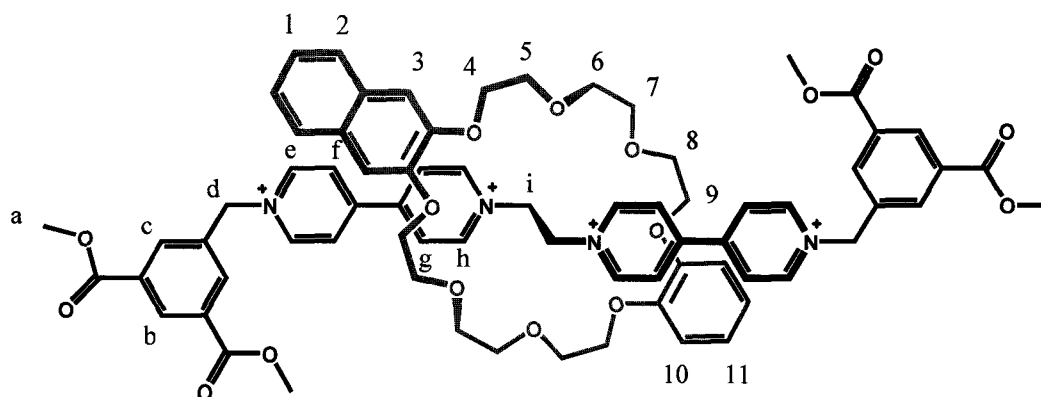


Table 2.36 – ^1H NMR of $[2\text{-}10\text{cBN}24\text{C}8][\text{OTf}]_4$ in CD_3CN . $\text{MW}_{\text{OTf}} = 1849.667$ g/mol

Proton	δ (ppm)	Multiplicity	# Protons	J (Hz)
a	3.97	s	12	--
b	8.68	s	2	--
c	8.41	s	4	--
d	5.89	s	4	--
e	8.80	d	4	$^3J_{\text{ef}} = 6.45$
f	7.97	d	4	$^3J_{\text{fe}} = 6.45$
g	8.24	d	4	$^3J_{\text{gh}} = 6.52$
h	9.33	d	4	$^3J_{\text{hg}} = 6.52$
i	5.64	s	4	--
1	6.96	dd	2	$J_{\text{meta}} = 3.58; J_{\text{ortho}} = 5.59$
2	7.35	dd	2	$J_{\text{meta}} = 3.58; J_{\text{ortho}} = 5.59$
3	7.00	s	2	--
4-9	4.01-4.20	m	24	--
10	6.42	dd	2	$J_{\text{meta}} = 3.58; J_{\text{ortho}} = 5.59$
11	6.64	dd	2	$J_{\text{meta}} = 3.58; J_{\text{ortho}} = 5.59$

CHAPTER 3

An Intramolecular Charge Transfer [2]Pseudorotaxane Switch

3.1 INTRODUCTION

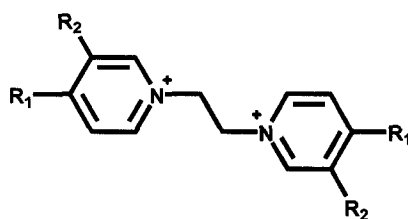
Control over the relative position and motion of components in interpenetrated or interlocked molecules can impart machine-like properties at the molecular level. Examples include threading and unthreading of [2]pseudorotaxanes,⁶²⁻⁶⁶ translation of the macrocycle in a [2]rotaxane molecular shuttle,^{46,67-71} rotation of the rings in a [2]catenane,⁷²⁻⁷⁵ or reorientation^{50, 76, 77} (flipping, pirouetting) of the cyclic ring in [2]rotaxanes.

As mentioned in Chapter 1, 1,2-bis(pyridinium)ethane cations have demonstrated their synthetic value as templates for the construction of interpenetrated and interlocked molecules. The interaction between a cationic 1,2-bis(pyridinium)ethane thread and a dibenzo-24-crown-8 ether (**DB24C8**) ring occurs by three sets of complementary interactions: (i) ion-dipole interactions between the N⁺-pyridinium and the oxygen atoms on the crown ether, (ii) a set of eight weak *CH*...O hydrogen bonds between the *ortho*-N⁺ hydrogen atoms and the oxygen atoms on the crown ether and (iii) π -stacking between the electron-rich catechol rings of the crown ether and the electron-poor pyridinium rings of the thread (Figure 1.20).

During a systematic study of [2]pseudorotaxane formation between 1,2-bis(pyridinium)ethane threads and 24-crown-8 ether rings, it was noted that the presence of an electron-donating NH₂ group at the 4-position of the pyridinium group dramatically

reduced the observed association constant.³⁸ This was attributed to a reduction in the acidity of the participating hydrogen bonding groups on the thread and a reduction in the charge at the pyridinium nitrogen due to contributions from an unfavourable resonance form. It was reasoned that it should be possible to fine-tune the strength of a [2]pseudorotaxane interaction and control the threading-unthreading process using these different resonance structures.

For this reason, the new thread molecule **3-3a**²⁺ (Scheme 3.1) was designed, which can be represented by two possible resonance forms having dramatically different structures and charge distributions (Figure 3.1).⁷⁸ This molecule consists of a chromophoric structure D- π -A- π -D having two terminal donor groups (*N,N*-dimethylamino) and an inner acceptor group (bis-pyridinium). In principle, this should give rise to an intramolecular charge transfer (ICT) observable in the electronic spectrum and it was reasoned that it should be possible to turn **OFF** the ICT by addition of a Lewis acid, such as BF₃ or H⁺.



Thread	R ₁	R ₂
3-3a	4-N(CH ₃) ₂ Ph-	H
3-3b	4-NH(CH ₃) ₂ ⁺ Ph-	H
3-5a	H	4-N(CH ₃) ₂ Ph-
3-5b	H	4-NH(CH ₃) ₂ ⁺ Ph-
3-6	Ph	H
3-7	H	Ph

Scheme 3.1 – Numbering scheme for compounds in Chapter 3.

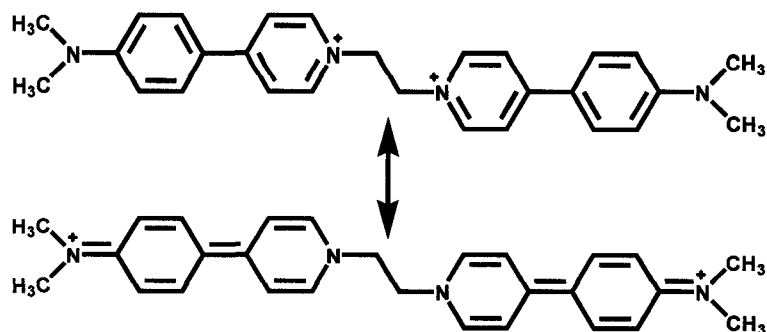


Figure 3.1 – Dicationic thread $3-3a^{2+}$ can be represented by two possible resonance forms

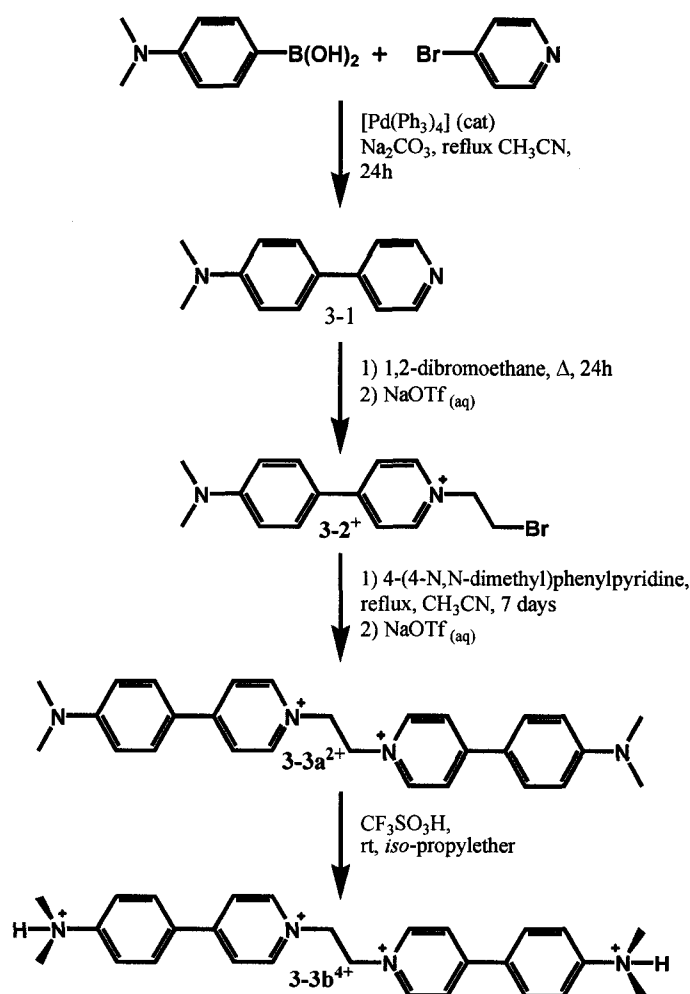
3.2 SYNTHESIS AND STRUCTURAL CHARACTERIZATION

3.2.1 Synthesis

The new thread $3-3a^{2+}$ was synthesized in three steps, the first being a Suzuki coupling between 4-*N,N*-dimethylaminophenylboronic acid and 4-bromopyridine hydrochloride. The resulting 4-(4'-*N,N*-dimethylaminophenyl)pyridine (**3-1**) was reacted with 1,2-dibromoethane to obtain the corresponding pyridiniummethyl bromide bromide salt which was directly converted to its triflate salt (**3-2**⁺). This was further reacted with an excess of **3-1** in CH₃CN to afford $3-3a^{2+}$ as the bromide salt which was subsequently anion exchanged to the triflate salt. Protonation of the thread $3-3a^{2+}$ was accomplished by dissolving the triflate salt in isopropyl ether and adding trifluoromethanesulfonic acid to the solution, resulting in precipitation of the thread as $3-3b^{4+}$ (Scheme 3.2).

The remaining threads in the series were synthesized in a similar manner, but without the formation of the pyridiniummethyl bromide intermediate. Instead, the corresponding pyridine was dissolved in CH₃CN with 1,2-dibromoethane, with the pyridine compound in excess. The isolated precipitates were the expected symmetrical

threads 1,2-bis[3-(4'-*N,N*-dimethylaminophenyl)pyridinium]ethane (**3-5a²⁺**), 1,2-bis(4-phenylpyridinium)ethane (**3-6²⁺**) and 1,2-bis(3-phenylpyridinium)ethane (**3-7²⁺**).



Scheme 3.2 – Synthesis of threads **3-3a²⁺** and **3-3b⁴⁺**.

3.2.2 X-ray Characterization

The X-ray crystal structures of **3-3a²⁺** and **3-3b⁴⁺** reveal significant differences in their solid-state structures (Figure 3.2). There is evidence that thread **3-3a²⁺** adopts a pseudo-quinoid form with, for example, reduced N1-C3 and C8-C9 distances (1.367(3), 1.466(4) Å, respectively) and a small dihedral angle between aromatic rings of 18.4°.

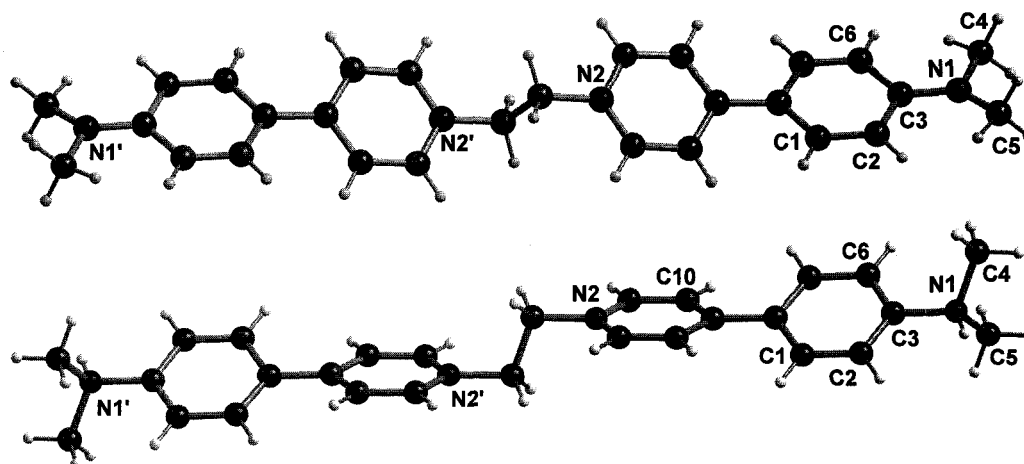


Figure 3.2 – X-ray structures of 3-3a²⁺ (top) and 3-3b⁴⁺ (bottom) showing the atom labeling scheme and bond distances.

supporting the delocalization of the positive charge. In contrast, the bonding parameters for 3-3b⁴⁺ are indicative of the more common bis(pyridinium)ethane form with longer N1-C3 and C8-C9 distances (1.483(5), 1.473(5) Å, respectively) and a more substantial dihedral angle of 55.4°.(Table 3.1)

Table 3.1 – Comparison of Bond Distances in 3-3a²⁺ and 3-3b⁴⁺.^a

Bond	Distances for 3-3a ²⁺ (Å)	Distances for 3-3b ⁴⁺ (Å)
N1-C3	1.367(3)	1.483(5)
C1-C2	1.376(4)	1.381(5)
C2-C3	1.415(4)	1.382(5)
C3-C6	1.406(4)	1.368(5)
C6-C7	1.374(4)	1.380(5)
C7-C8	1.403(4)	1.388(5)
C8-C9	1.466(4)	1.473(5)
C9-C10	1.401(4)	1.390(5)
C10-C11	1.365(4)	1.372(5)
C11-N2	1.348(3)	1.337(5)
N2-C12	1.349(3)	1.344(5)
C12-C13	1.365(4)	1.363(5)
C9-C13	1.410(4)	1.396(5)
N2-C14	1.471(3)	1.491(4)

^a The dihedral angle between the pyridine ring and the aniline ring is 18.4° for 3-3a²⁺ and 55.4° for 3-3b⁴⁺. Both molecules have a crystallographically imposed center of symmetry.

3.2.3 Molecular Orbital Analysis

For $3-3a^{2+}$, DFT(B3LYP) calculations localized the HOMO on the aniline ring and the LUMO on the pyridinium ring, with important contributions from the N atoms in each case (Figure 3.3).

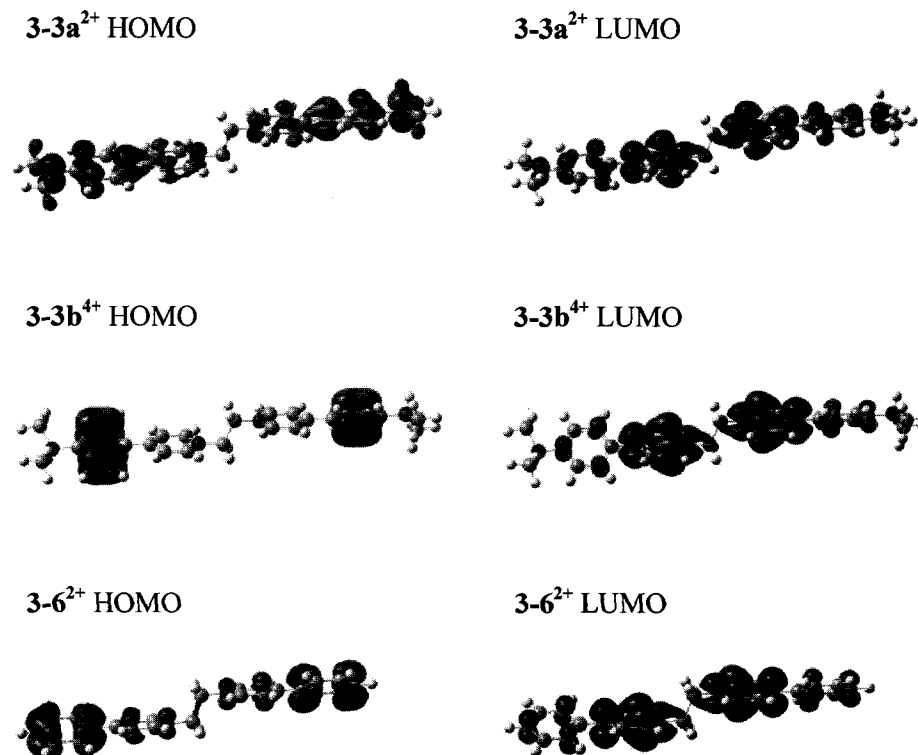


Figure 3.3 – HOMO/LUMO diagrams for $3-3a^{2+}$, $3-3b^{4+}$ and $3-6^{2+}$.

Figure 3.4 shows a comparison of the electron density distribution in $3-3a^{2+}$ and $3-3b^{4+}$ along with the unsubstituted thread 1,2-bis(4-phenylpyridinium)ethane, $3-6^{2+}$. It is clear that the protonated thread $3-3b^{4+}$ and the model compound, $3-6^{2+}$, have a similar electron distributions (dark blue colour) at the central recognition region, whereas $3-3a^{2+}$ is quite different (lighter blue), supporting the notion of different resonance forms for these threads.

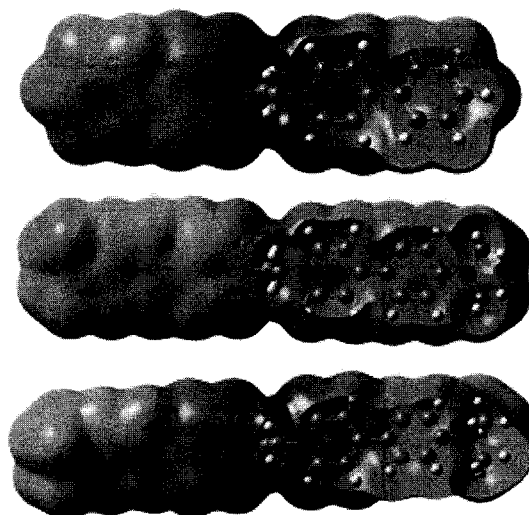


Figure 3.4 – DFT calculated (B3LYP) electron distributions for (top to bottom) the dication bis(4-phenylpyridinium)ethane $3-6^{2+}$, thread $3-3a^{2+}$, and protonated thread $3-3b^{4+}$.

3.3 RESULTS AND DISCUSSION OF THE PSEUDOROTAXANE STUDIES

Mixing one equivalent of the thread with one equivalent of **DB24C8** yields a [2]pseudorotaxane that undergoes slow exchange on the NMR time scale. The complexation process was studied in CD_3CN and the association constants (K_{assoc}) were determined using the single point method,⁷⁹ which involves using known concentrations of the components and the integral values of the ethylene bridge complexed and uncomplexed resonances on the thread. The new push-pull thread $3-3a^{2+}$ binds **DB24C8** in CD_3CN solution with a very small association constant ($34 M^{-1}$). This *OFF* scenario can be switched *ON* by the addition of two equivalents of acid to yield $3-3b^{4+}$, which can then act as a standard 1,2-bis(pyridinium)ethane thread for [2]pseudorotaxane formation. A substantial increase in the association constant was observed for $3-3b^{4+}$ (~ 5 fold) to a value ($156 M^{-1}$) that is comparable to that observed for $3-6^{2+}$ ($172 M^{-1}$), for which there is no substituent on the phenyl ring and no ICT. The association experiments for $3-3a^{2+}$ and

3-3b⁴⁺ with **DB24C8** were also run in CD₃NO₂ and resulted in slightly higher K_{assoc} values of 65 M⁻¹ and 251 M⁻¹, respectively. This maintains the approximate five fold increase in association. Other solvents were precluded due to poor solubility of the threads.

To further assess this system, an analogous series of thread molecules, **3-5a²⁺**, **3-5b⁴⁺** and **3-7²⁺** were synthesized with the same substituents but in the 3-position of the pyridinium ring. Although thread **3-5a²⁺** containing the *N,N*-dimethylaniline group has a lower association constant compared to **3-5b⁴⁺**, the effect is far less pronounced. This is a result of the absence of a suitable resonance structure that would allow the delocalization of the electron density from the electron rich ring (*N,N*-dimethylaniline) to the electron poor pyridinium. Therefore, the bis(pyridinium)ethane core is still maintained and complexation with the crown ether is possible. Table 3.2 summarizes the association constants for threads **3-3a²⁺** – **3-7²⁺** with **DB24C8**.

Table 3.2 – Association Constants, K_{assoc} and ΔG° values for **3-3a²⁺ – **3-7²⁺** with **DB24C8** in CD₃CN (2.0×10^{-3} M) at 298 K.**

Thread	K_{assoc} (M ⁻¹)	ΔG° (kJ mol ⁻¹)
3-3a²⁺	34	8.7
3-3b⁴⁺	156	12.5
3-6²⁺	172	12.8
3-5a²⁺	91	11.2
3-5b⁴⁺	116	11.8
3-7²⁺	125	12.0

The differences in association constants, the X-ray metrical parameters, and the DFT calculated electronic structures all support the idea that it is a major contribution from a pseudo-quinoid resonance form for thread **3-3a²⁺** that results in its anomalously poor ability to establish significant non-covalent interactions with the crown ether.

Moreover, protonation of **3-3a**²⁺ to give **3-3b**⁴⁺ restores the pyridinium character of the thread and significantly enhances its ability to interact non-covalently with **DB24C8** and form a [2]pseudorotaxane. This feature can then be used as a methodology to control threading and unthreading by turning *ON* and *OFF* the interaction.

As predicted, the D- π -A- π -D nature of the thread **3-3a**²⁺ provides a chromophore with two terminal donor groups and one inner acceptor group resulting in an ICT band with λ_{max} at 443 nm and a molar absorptivity of 25,945 L mol⁻¹ cm⁻¹ in CH₃CN. The resulting intense yellow-orange colouration of the naked thread can be completely eliminated upon the addition of H⁺ to give the thread **3-3b**⁴⁺ (Figure 3.5).

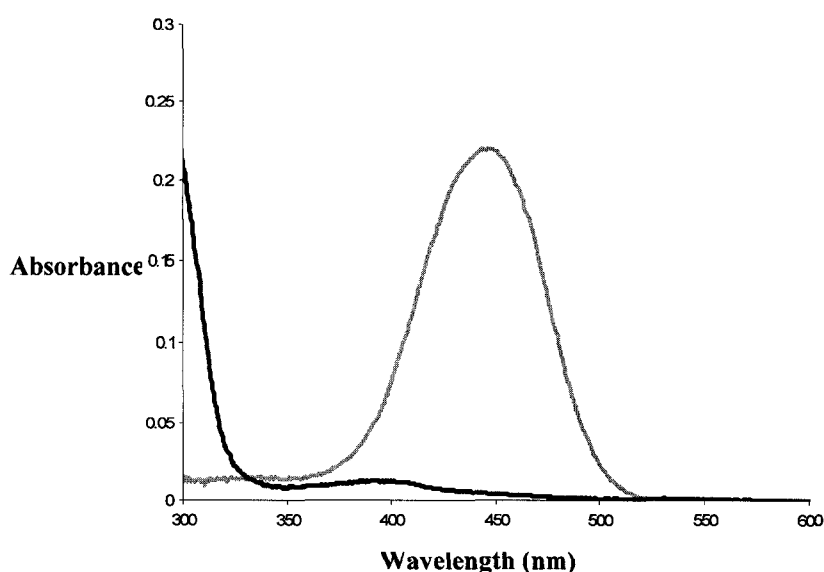


Figure 3.5 – UV-visible absorption spectra of a 1:1 mixture of **3-3a**²⁺ with **DB24C8** (yellow) and **3-3b**³⁺ with **DB24C8** (blue) and recorded in CD₃CN at a concentration of 1.0×10^{-5} M.

The colourless protonated thread **3-3b**⁴⁺ can then form a [2]pseudorotaxane with **DB24C8**, which gives rise to a very pale yellow colouration due to a charge-transfer

interaction between the electron-rich catechol rings of **DB24C8** and the electron-poor pyridinium rings of the thread.

3.4 SUMMARY AND CONCLUSIONS

In summary, the intramolecular charge transfer present in **3-3a**²⁺ reduces the ability of the bis(pyridinium)ethane unit to act as a recognition site for **DB24C8**. This is accomplished by decreasing the positive charge on the pyridinium nitrogen atom, reducing the acidity of the hydrogen atoms adjacent to the pyridinium N⁺, and increasing the electron density in the pyridinium rings. This induces a reduction of the association constant with **DB24C8** in CD₃CN compared to **3-3b**⁴⁺ and **3-6**²⁺, or **3-5a**²⁺, **3-5b**⁴⁺ and **3-7**²⁺, and is thus an effective *OFF* state for [2]pseudorotaxane formation.⁸⁰ When a Lewis acid such as H⁺ is added, protonation of the aniline nitrogen atom occurs and the resulting 1,2-bis(pyridinium)ethane thread penetrates the **DB24C8** cavity forming a [2]pseudorotaxane and converts it to the *ON* state. The linking of this mechanical action of [2]pseudorotaxane formation to a significant colour change can be described as a *NOT* logic gate (Table 3.3) since the threading of the two components to form the interpenetrated molecule is signaled by the loss of the bright orange colour. Cycling of the protonation and deprotonation of this system was successfully carried out using alternating equivalents of trifluoromethanesulfonic acid and triethylamine up to five times without any evidence of significant decomposition or loss of colour intensity.

Table 3.3 – Logic table for ICT pseudorotaxane system.

Input H^+	Output Abs ₄₄₃
0	1
1	0

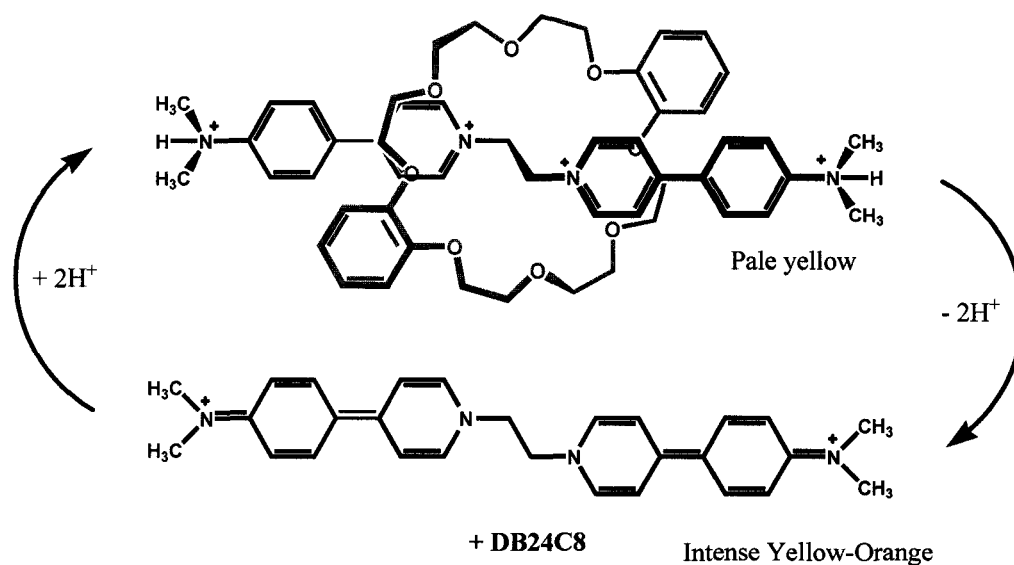


Figure 3.6 – Schematic representation of the threading and dethreading process initiated by alternating acid and base.

3.5 EXPERIMENTAL

3.5.1 General Comments

1,2-Bis(4-phenylpyridinium)ethane and 1,2-bis(3-phenylpyridinium)ethane were synthesized according to a literature procedure.³⁸ 4-(*N,N*-Dimethylamino)phenylboronic acid, 4-bromopyridine hydrochloride, 3-bromopyridine, sodium carbonate, tetrakis(triphenylphosphine)palladium(0), 1,2-dibromoethane and **DB24C8** were purchased from Aldrich and used as received. CD₃CN was dried according to a literature procedure.⁸¹ Conventional 2-D NMR experiments (¹H-¹H COSY and HETCOR) were used to help assign all peaks. UV-visible spectra were obtained using a Varian Cary 50 spectrometer. All calculations were performed using the Gaussian 03 suite of programs. Optimized gas-phase structures were obtained using the density functional theory (**DFT**) method B3LYP, a combination of Becke's three parameter hybrid exchange functional,^{82, 83} as implemented⁸⁴ in Gaussian 03, and the correlation functional of Lee, Yang and Parr,⁸⁵ in conjunction with the 6-31G(d,p) basis set. The HOMO and LUMO orbitals are shown at the 0.032 isodensity value.

3.5.2 Synthesis of 4-(4'-*N,N*-dimethylaminophenyl)pyridine (3-1)

This compound has been previously synthesized using alternative methods^{86, 87}, but was prepared using the following procedure. A 3-necked round bottom flask was charged with DMF (200 mL) and H₂O (100 mL). To this, 4-(*N,N*-dimethylamino)phenylboronic acid (2.00 g, 0.0121 mol), 4-bromopyridine hydrochloride (2.36 g, 0.0121 mol) and sodium carbonate (7.71 g, 0.0727 mol) were added and the solution degassed for one hour. Tetrakis(triphenylphosphine)palladium(0) was added and the solution degassed an additional 30 minutes. The reaction was refluxed for 24 h then cooled to room temperature and the solvents evaporated. H₂O was added to the resulting residue and the product was extracted into CH₂Cl₂ three times. The organic portions were combined, dried with MgSO₄, filtered and evaporated. **3-1** was obtained as a pale yellow solid (2.28 g, 0.0115 mol, 95%).

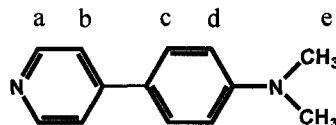


Table 3.4 – ¹H NMR of **3-1** in CD₃CN. MW = 198.264 g/mol

Proton	δ (ppm)	Multiplicity	# Protons	<i>J</i> (Hz)
a	8.50	d	2	³ <i>J</i> _{ab} = 6.14
b	7.54	d	2	³ <i>J</i> _{ba} = 6.14
c	7.64	d	2	³ <i>J</i> _{cd} = 8.88
d	6.83	d	2	³ <i>J</i> _{dc} = 8.88
e	2.99	s	6	--

3.5.3 Synthesis of [4-(4'-*N,N*-dimethylaminophenyl)pyridinium]ethylbromide (3-2)⁺

Compound **3-1** (0.750 g, 0.00378 mol) was dissolved in 1,2-dibromoethane (50mL) and refluxed for 24 h. The reaction was cooled to room temperature and the resulting precipitate was filtered using a Büchner funnel and washed with CH₂Cl₂. This afforded **3-2⁺** as yellow powder as the bromide salt (1.19 g, 0.00308 mol, 82 %) which was subsequently anion exchanged to the triflate salt. **ESI-MS**: *m/z* [**3-2** - OTf]⁺ calc. 339.9331, found 339.9341.

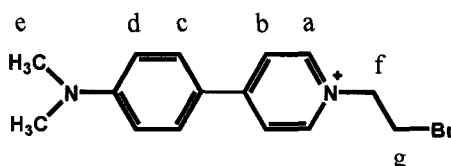


Table 3.5 – ¹H NMR of [3-2][Br] in D₂O. MW_{Br} = 386.125 g/mol

Proton	δ (ppm)	Multiplicity	# Protons	<i>J</i> (Hz)
a	8.44	d	2	³ <i>J</i> _{ab} = 6.92
b	8.02	d	2	³ <i>J</i> _{ba} = 6.92
c	7.81	d	2	³ <i>J</i> _{cd} = 9.01
d	6.85	d	2	³ <i>J</i> _{dc} = 9.01
e	2.96	s	6	--
f	4.74	t	2	³ <i>J</i> _{ef} = 5.69
g	3.85	t	2	³ <i>J</i> _{fe} = 5.69

Table 3.6 – ^1H NMR of [3-2][OTf] in CD_3CN . $\text{MW}_{\text{OTf}} = 455.290$ g/mol

Proton	δ (ppm)	Multiplicity	# Protons	J (Hz)
a	8.38	d	2	$^3J_{ab} = 7.10$
b	8.09	d	2	$^3J_{ba} = 7.10$
c	7.89	d	2	$^3J_{cd} = 9.14$
d	6.87	d	2	$^3J_{dc} = 9.14$
e	3.09	s	6	--
f	4.72	t	2	$^3J_{ef} = 5.92$
g	3.89	t	2	$^3J_{fe} = 5.92$

3.5.4 Synthesis of Compound 3-3a²⁺

[3-2][OTf] (0.850 g, 0.00187 mol) and 3-1 (0.740 g, 0.00373 mol) were dissolved in CH₃CN (50 mL) and refluxed for 7 days. The reaction was cooled to room temperature and the solvent evaporated. The residue was dissolved in CH₂Cl₂ and the resulting precipitate was filtered and washed with more CH₂Cl₂. This afforded a yellow powder 3-3a²⁺ as the bromide salt (0.718 g, 0.00123 mol, 66 %) which was subsequently anion exchanged to the triflate salt (0.811 g, 0.0112 mol, 91%) ESI-MS: *m/z* [3-3a - OTf]⁺ calc. 573.2142, found 573.2118.

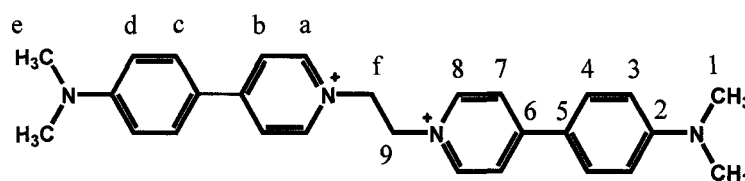
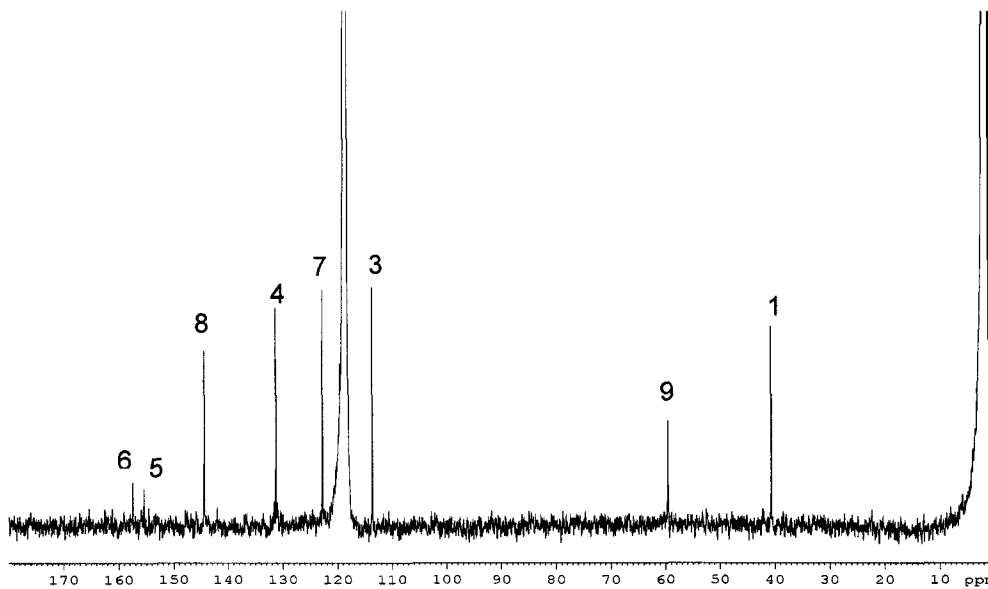


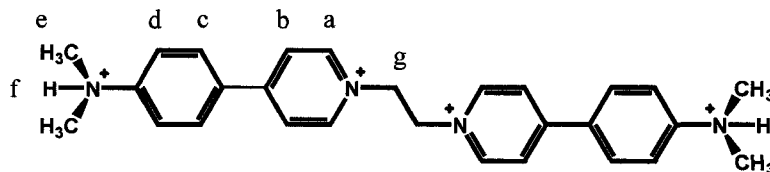
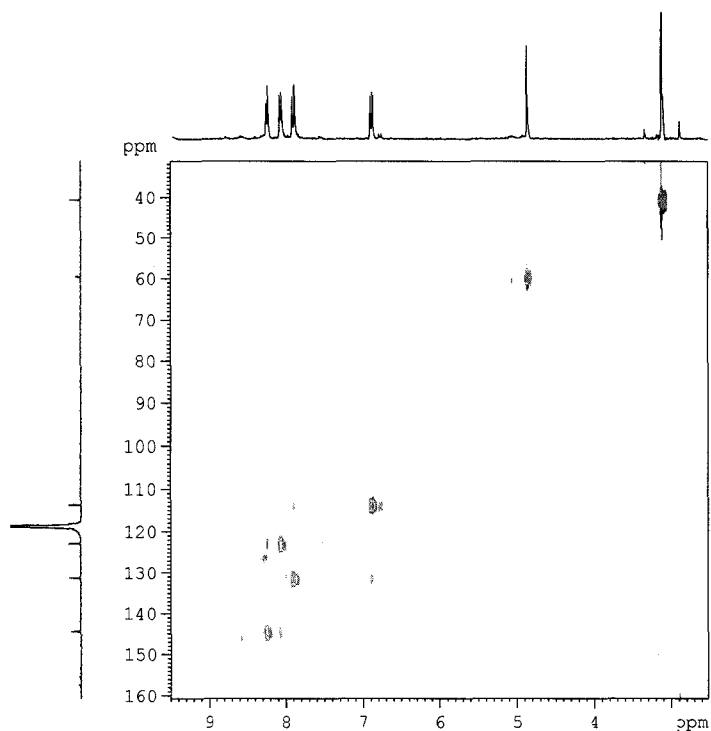
Table 3.7 – ¹H NMR of [3-3a][OTf]₂ in CD₃CN. MW_{OTf} = 722.719 g/mol

Proton	δ (ppm)	Multiplicity	# Protons	<i>J</i> (Hz)
a	8.29	d	4	³ <i>J</i> _{ab} = 7.02
b	8.05	d	4	³ <i>J</i> _{ba} = 7.02
c	7.88	d	4	³ <i>J</i> _{cd} = 9.08
d	6.87	d	4	³ <i>J</i> _{dc} = 9.08
e	3.10	s	12	--
f	4.88	s	4	--

Table 3.8 – ^{13}C NMR of [3-3a][OTf] $_2$ in CD_3CN .

Carbon	δ (ppm)	# Carbons
1	40.69	4
2	--	2
3	113.72	4
4	131.31	4
5	155.46	2
6	157.48	2
7	122.82	4
8	144.50	4
9	59.63	2

 ^{13}C spectrum of [3-3a][OTf] $_2$ 

HETCOR of [3-3a][OTf]₂Table 3.9 – ¹H NMR of [3-3b][OTf]₃ in CD₃CN. MW_{OTf} = 1022.873 g/mol

Proton	δ (ppm)	Multiplicity	# Protons	J (Hz)
a	8.74	d	4	$^3J_{ab} = 6.78$
b	8.35	d	4	$^3J_{ba} = 6.78$
c	7.84	d	4	$^3J_{cd} = 8.74$
d	8.12	d	4	$^3J_{dc} = 8.74$
e	3.31	d	12	$^3J_{ef} = 5.16$
f	9.45	br, s	2	--
g	5.14	s	4	--

3.5.5 Synthesis of Compound 3-4

A 3-necked round bottom flask was charged with DMF (200 mL) and THF (100 mL). To this 4-(*N,N*-dimethylaminophenyl)boronic acid (2.00 g, 0.0121 mol), 3-bromopyridine (1.92 g, 0.0121 mol) and sodium carbonate (7.71 g, 0.0727 mol) were added and the solution degassed for one hour. Tetrakis(triphenylphosphine)palladium(0) (0.700 g, 6.06×10^{-4} mol) was added and the solution degassed an additional 0.5 hour. The reaction was refluxed for 24 h then cooled to room temperature and the solvents evaporated. Water was added to the resulting residue and the product was extracted three times with CH_2Cl_2 . The organic portions were combined, dried with MgSO_4 , filtered and evaporated. Compound 3-4 was recrystallized from Et_2O and isolated as a beige solid. (2.14 g, 0.0108 mol, 89%).

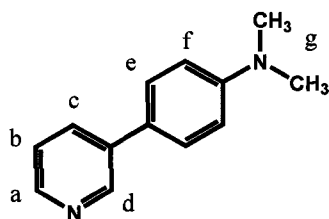


Table 3.10 – ^1H NMR of [3-4] in CD_3CN . MW = 198.264 g/mol

Proton	δ (ppm)	Multiplicity	# Protons	J (Hz)
a	8.43	d	1	$^3J_{ab} = 4.74$
b	7.34	dd	1	$^3J_{ba} = 4.74, ^3J_{bc} = 7.91$
c	7.90	d	1	$^3J_{cb} = 7.91$
d	8.79	s	1	--
e	7.54	d	2	$^3J_{ef} = 6.80$
f	6.85	d	2	$^3J_{fe} = 6.80$
g	2.97	s	6	--

3.5.6 Synthesis of Compound 3-5a²⁺

Compound 3-4 (1.00 g, 0.00504 mol) and 1,2-dibromoethane (0.190 g, 0.00101 mol) were dissolved in acetonitrile (50 mL) and refluxed for four days. The precipitate that formed was isolated by filtration. This afforded a pale yellow powder 3-5a⁺ as the bromide salt (0.512 g, 8.76×10^{-4} mol, 87%) which was subsequently anion exchanged to the triflate salt. (0.597 g, 8.26×10^{-4} mol, 94%) **ESI-MS**: m/z [3-5a - OTf]⁺ calc. 573.2142, found 573.2155.

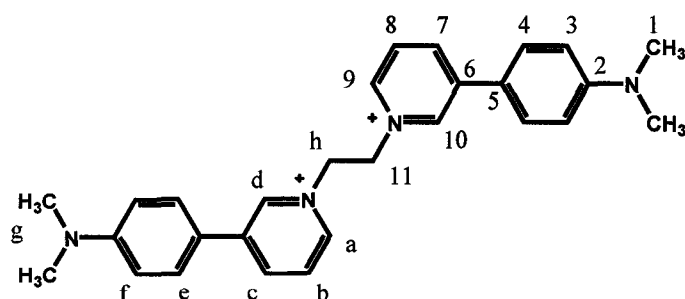
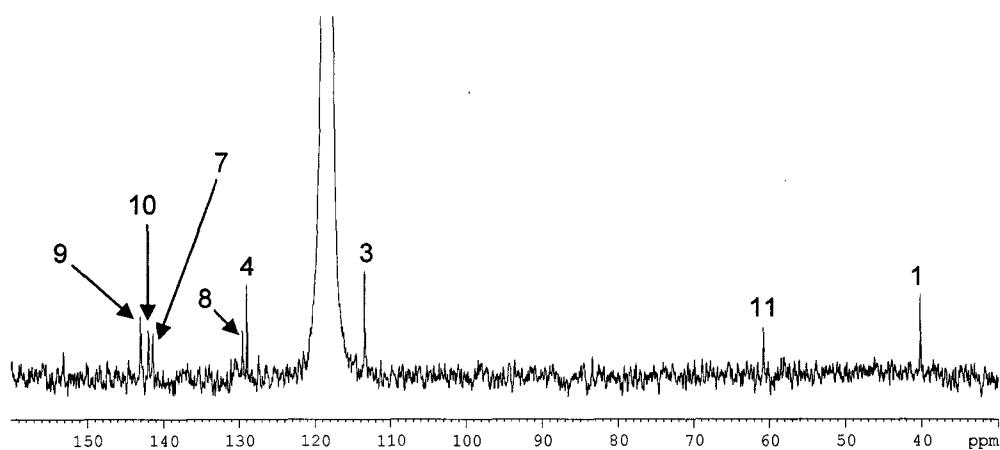


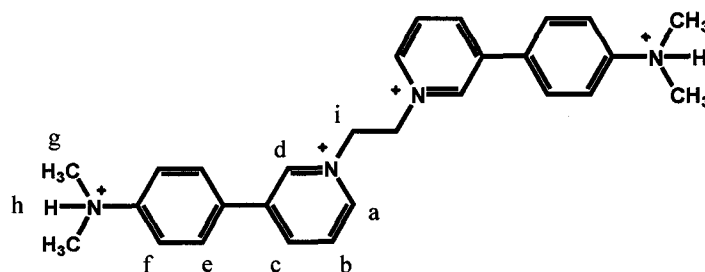
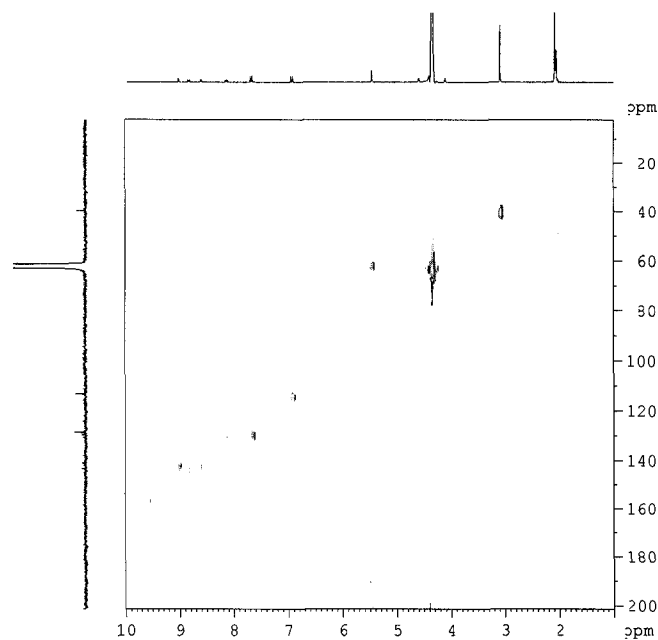
Table 3.11 – ¹H NMR of [3-5a][OTf]₂ in CD₃CN. MW_{OTf} = 722.719 g/mol

Proton	δ (ppm)	Multiplicity	# Protons	J (Hz)
a	8.70	d	2	³ J _{ab} = 8.00
b	7.97	dd	2	³ J _{ba} = 8.00, ³ J _{bc} = 6.08
c	8.33	d	2	³ J _{cb} = 6.08
d	8.84	s	2	--
e	7.60	d	4	³ J _{ef} = 9.02
f	6.88	d	4	³ J _{fe} = 9.02
g	3.04	s	12	--
h	5.09	s	4	--

Table 3.12 - ^{13}C NMR of [3-5a][OTf]₂ in CD₃CN.

Carbon	δ (ppm)	# Carbons
1	40.69	4
2	--	2
3	113.72	4
4	~129	4
5	--	2
6	--	2
7	~141.5	2
8	~129.5	2
9	~143	2
10	~142	2
11	~61	4

 ^{13}C spectrum of [3-5a][OTf]₂

HETCOR of [3-5a][OTf]₂Table 3.13 – ¹H NMR of [3-5b][OTf]₃ in CD₃CN. MW_{OTf} = 1022.873 g/mol

Proton	δ (ppm)	Multiplicity	# Protons	J (Hz)
a	8.85	d	2	$^3J_{ab} = 8.09$
b	8.20	dd	2	$^3J_{ba} = 8.09, ^3J_{bc} = 6.23$
c	8.83	d	2	$^3J_{cb} = 6.23$
d	9.24	s	2	--
e	7.86	d	4	$^3J_{ef} = 8.66$
f	8.02	d	4	$^3J_{fe} = 8.66$
g	3.32	s	12	--
h	9.89	s	2	--
i	5.29	s	4	--

CHAPTER 4

N-Benzylanilinium [2]Pseudorotaxanes

4.1 INTRODUCTION

A variety of [2]pseudorotaxanes have been reported that involve the interpenetration of dibenzo-24-crown-8 ether (**DB24C8**) by linear cationic molecules that act as a ring and a thread, respectively.⁸⁸ The first, extensively studied by Stoddart, uses secondary ammonium cations, such as *N,N*-dibenzylammonium, as the thread component.⁸⁹⁻⁹² A second, studied extensively by the Loeb group, uses 1,2-bis(pyridinium)ethane cationic compounds as the threads.^{37, 38} The dibenzylammonium cation binds **DB24C8** macrocycles by way of strong $NH\cdots O$ hydrogen bonds and $N^+\cdots O$ ion-dipole interactions, whereas the bis(pyridinium)ethane threads rely on a series of weaker $CH\cdots O$ hydrogen bonds, two sets of $N^+\cdots O$ ion-dipole interactions and significant π -stacking between electron poor pyridinium rings in the threads and electron rich catechol rings of the crown. Both of these systems display approximately the same range of association constants in CH_3CN at $25^\circ C$.^{38, 69, 93} In this chapter, a new type of thread is introduced; the *N*-benzylanilinium cation, which was designed to combine favourable features of these two systems into a hybrid binding motif.⁹⁴ The *N*-benzylanilinium system contains characteristics of both *N,N*-dibenzylammonium and bis(pyridinium)ethane threads (Figure 4.1). The new thread has a two atom bridge consisting of a $-CH_2NH_2^+$ unit between the two aromatic rings. This recognition site should provide (i) a positively charged group suitable for electrostatic ion-dipole

interactions with the crown ether oxygen atoms, (ii) two strongly acidic N–H protons for $NH\cdots O$ hydrogen bonding, (iii) two acidic benzyl CH protons for $CH\cdots O$ hydrogen bonding and (iv) electron-poor aromatic rings for π -stacking interactions with the catechol rings on the crown ether. Thus, the hybrid binding motif would be an excellent match, in size and shape, with the bis(pyridinium)ethane motif while providing the versatility of acid-base control reminiscent of the *N,N*-dibenzylammonium threads.

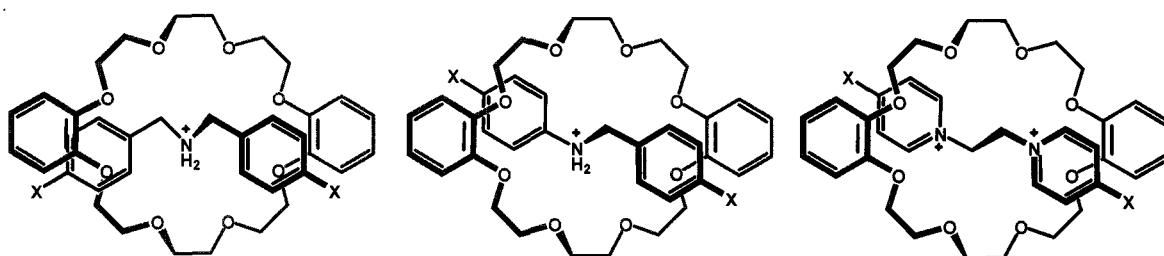


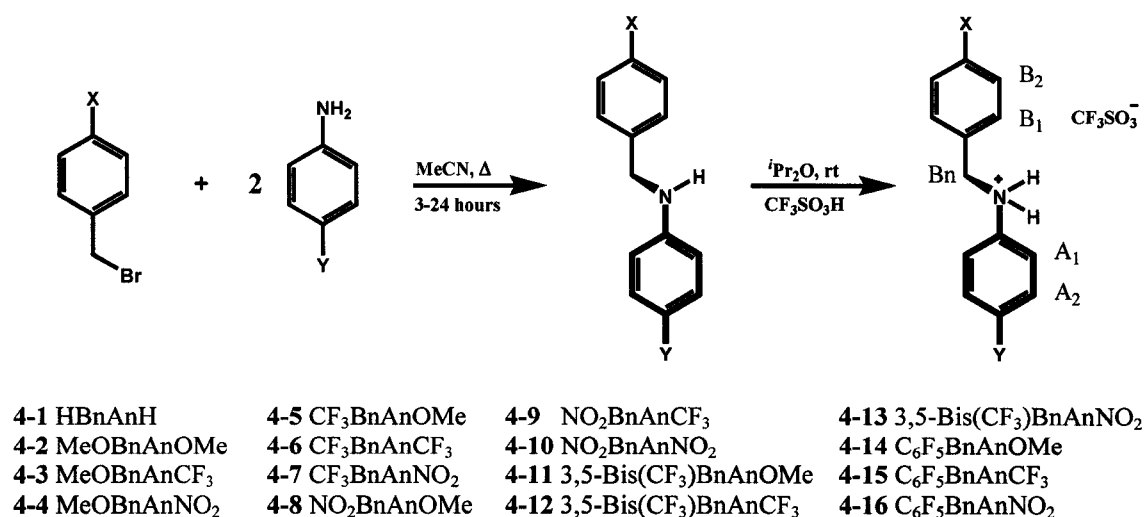
Figure 4.1 – *N,N*-dibenzylammonium (left), *N*-benzylanilinium (middle), bis(pyridinium)ethane (right) [2]pseudorotaxanes with DB24C8.

4.2 SYNTHESIS AND CHARACTERIZATION

4.2.1 - Synthesis

Various *N*-benzylanilinium threads were synthesized with different electron donating and withdrawing groups. Synthesis was easily carried out via a one-step alkylation with commercially available reagents. Two equivalents of the aniline and one equivalent of the benzyl bromide were required since one equivalent of the aniline is consumed as a base and helps to prevent the formation of tertiary amines.^{95, 96} Both reagents were dissolved in acetonitrile and the solution heated to reflux for 24 h. As the reaction was cooled to room temperature, the anilinium bromide precipitated from solution and was eliminated by vacuum filtration. The remaining solution containing the

product was concentrated and the residue purified by column chromatography on silica gel using 20% hexanes in chloroform as the eluent. Yields were moderate ranging from ~35% to 87%. The isolated *N*-benzylaniline threads were protonated by dissolving the solid in isopropyl ether and precipitating them from solution by dropwise addition of trifluoromethanesulfonic acid (Scheme 4.1). A family of 16 threads was synthesized to study the effect of electron withdrawing and donating substituents on the complexation abilities of the new recognition site with 24-membered crown ether rings. Each thread was characterized by ^1H NMR spectroscopy, two dimensional COSY experiments and high resolution ESI mass spectrometry, for which exact mass determinations were achieved. Throughout this chapter, a notation has been devised for the threads: XBnAnY, where X indicates the substituent(s) on the benzyl ring (not necessarily in the *para* position) and Y indicates the substituent on the aniline ring. **B**₂ and **B**₁ refer to the *meta* (or *para*) protons and **A**₁ and **A**₂ refer to the *ortho* and *meta* protons on the aniline ring. **Bn** represents the benzyl CH₂ protons.



Scheme 4.1 - Synthesis of benzylanilinium threads.

4.2.2 – X-ray Crystallography

Suitable single crystals of [4-5][OTf] were grown by slow evaporation of an acetonitrile solution. The X-ray structure (Figure 4.2) shows that in the solid state, the *N*-benzylanilinium cation adopts the anticipated *anti* conformation about the central C-N bond, which resembles the geometry observed for the analogous 1,2-bis(pyridinium)ethane cations.

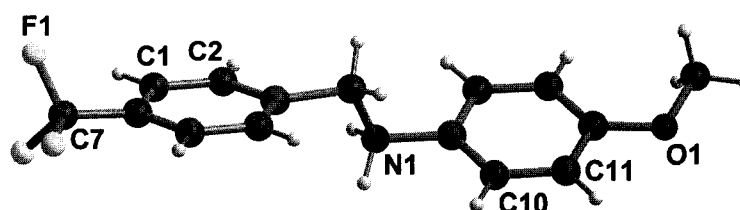


Figure 4.2 – Ball-and-stick representation of the X-ray structure of CF₃BnAnOMe [4-5·H]⁺ showing an *anti* conformation: dihedral angle = 171.8° (carbon = black, oxygen = red, nitrogen = blue, fluorine = yellow, hydrogen = white).

4.3 PSEUDOROTAXANE FORMATION

As a result of the enhanced acidity of these anilinium based threads, the protonated [HA]⁺ and non-protonated [A] species are in equilibrium in acetonitrile solution. Both species are involved in fast exchange on the NMR timescale and hence only a single averaged set of resonances is observed. The limiting chemical shifts and acidity constants (K_a) were obtained by titration experiments. In this method, each *N*-benzylaniline, 1.0 mL of 0.010 M solution, is titrated with increasing amounts of a 1.0 M solution of trifluoromethanesulfonic acid in CD₃CN until saturation is reached. Saturation is indicated by the benzyl CH₂ peak reaching its limiting downfield chemical shift (Figure 4.3).

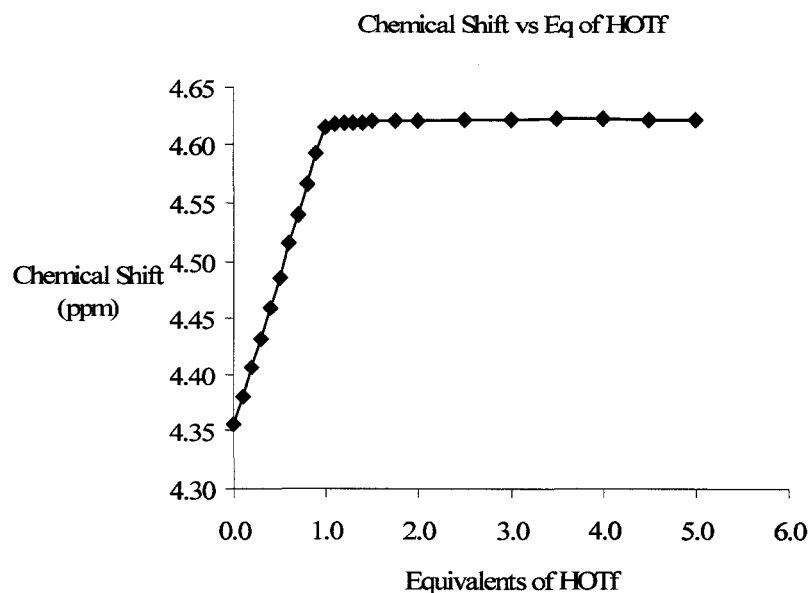


Figure 4.3 – Titration curve for $\text{CF}_3\text{BnAnOMe}$ (4-5).

Using the ^1H NMR spectra taken after each addition, the chemical shifts of the benzyl resonances were fit to a nonlinear least-squared model using WinEQNMR software⁹⁷ to obtain the acidity constant (K_a) of each thread (Table 4.1). Variation of the substituents on the aromatic rings of the threads allowed a comparison of the effects of EWG or EDG on the acidity and the ability to form [2]pseudorotaxanes. Results indicate that the substituent on the aniline ring has a greater effect on the acidity than that on the benzyl ring. This is intuitive since the substituent on the aniline ring can directly affect the stronger NH_2 hydrogen bond donors as well as the positive charge on the nitrogen atom. For instance, although the threads $\text{CF}_3\text{BnAnOMe}$ and MeOBnAnCF_3 both consist of the same groups, the former thread is less acidic ($K_a = 4.9 \times 10^{-5}$) than the latter ($K_a = 1.6 \times 10^{-3}$). Consideration of each series of threads, where the benzyl substituent is the same but the aniline substituent is varied from $-\text{OMe}$ to $-\text{CF}_3$ to $-\text{NO}_2$, shows that the acidity of the thread increases accordingly with the Hammett parameters⁹⁸ (-0.27, 0.54

and 0.78 respectively). The methoxy substituted threads are the least acidic, and the nitro substituted threads are the most acidic. There is a 1500-fold difference between acidity constants (K_a) of the most acidic thread ($C_6F_5BnAnNO_2$) and the least acidic thread ($MeOBnAnOMe$).

Table 4.1 - Summary of K_a 's of the N-benzylanilinium threads.

Thread	K_a	pKa
HBnAnH	8.3×10^{-3}	2.1
MeOBnAnOMe	4.7×10^{-5}	4.3
MeOBnAnCF ₃	1.6×10^{-3}	2.8
MeOBnAnNO ₂	8.6×10^{-3}	2.1
CF ₃ BnAnOMe	4.9×10^{-5}	4.3
CF ₃ BnAnCF ₃	2.0×10^{-3}	2.7
CF ₃ BnAnNO ₂	2.2×10^{-2}	1.6
3,5-BisCF ₃ BnAnOMe	3.9×10^{-4}	3.4
3,5-BisCF ₃ BnAnCF ₃	4.9×10^{-3}	2.3
3,5-BisCF ₃ BnAnNO ₂	3.8×10^{-3}	2.4
NO ₂ BnAnOMe	8.1×10^{-4}	3.1
NO ₂ BnAnCF ₃	6.1×10^{-3}	2.2
NO ₂ BnAnNO ₂	1.3×10^{-2}	1.9
C ₆ F ₅ BnAnOMe	6.6×10^{-4}	3.2
C ₆ F ₅ BnAnCF ₃	9.4×10^{-3}	2.0
C ₆ F ₅ BnAnNO ₂	6.2×10^{-2}	1.2

When equimolar solutions of a protonated thread and **DB24C8** are mixed together at 25°C in CD₃CN, equilibrium is rapidly attained and a new set of peaks, in addition to those assigned to the free components, is observed in the ¹H NMR spectrum (Figure 4.4). The chemical shifts of the new resonances are consistent with the formation of a [2]pseudorotaxane complex in solution [with a rate of association-dissociation that is slow compared to the NMR timescale. Chemical exchange between the free components and the [2]pseudorotaxane was also confirmed by EXSY NMR experiments (Figure 4.5).⁹⁹

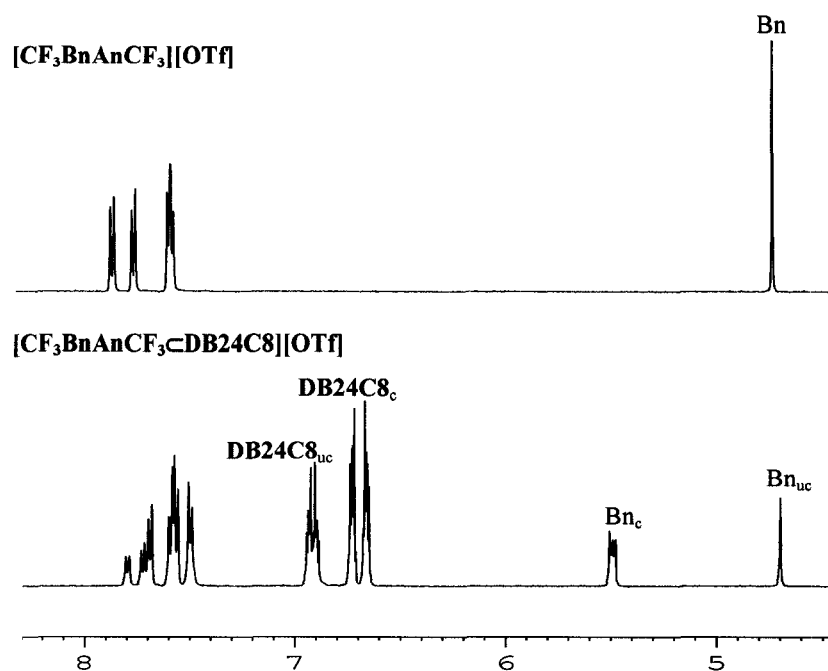


Figure 4.4 - ^1H NMR spectra of $[\text{CF}_3\text{BnAnCF}_3][\text{OTf}]$ (top) and $[\text{CF}_3\text{BnAnCF}_3\text{-DB24C8}][\text{OTf}]$ (bottom) in CD_3CN at 25°C ; “c” is for complexed and “uc” is for uncomplexed.

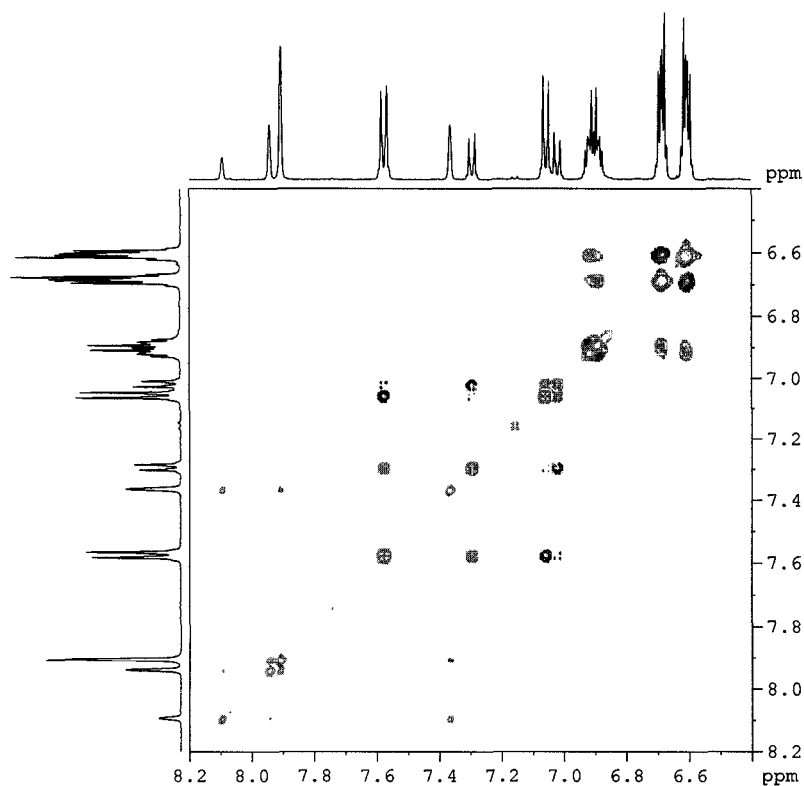


Figure 4.5 - EXSY NMR spectrum of $[3,5\text{-BisCF}_3\text{BnAnOMe-DB24C8}][\text{OTf}]$

Evidence for [2]pseudorotaxane formation was exhibited not only in solution, but in the “gas phase” (mass spectrometry) and solid state (single crystal X-ray crystallography, *vide infra*). It is important to note that **DB24C8** does not form a complex with an unprotonated thread.

In the case of the **24C8** complexes, the resonances due to NH_2 , CH_2 and *ortho* aromatic CH protons (**B₁** and **A₁**) were shifted downfield relative to the free thread, which is indicative of hydrogen bonding. Thus, in solution, a total of eight hydrogen bonds are responsible for maintaining the [2]pseudorotaxane structure (Table 4.2).

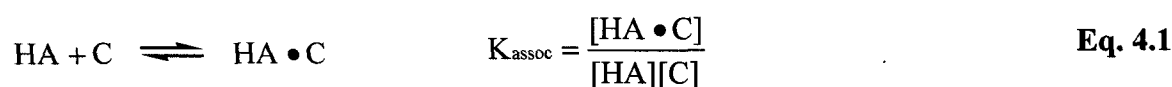
For the **DB24C8** adducts, the signals due to the NH_2 and CH_2 protons were shifted downfield. However, due to the lower basicity of the aryl ether oxygen atoms on the crown ether compared to **24C8**, there are not significant aromatic $CH\cdots O$ interactions with the *ortho* hydrogens (**B₁**) of the benzyl aromatic ring, regardless of the substituent on the thread. However, there is significant hydrogen bonding with the more acidic *ortho* protons (**A₁**) of the aniline aromatic ring which is reflected in the considerable downfield shift of these protons ($\Delta\delta$ ranging from 0.18 - 0.97 ppm). The resonances due to the hydrogen atoms in the *meta* or *para* positions (**B₂** and **A₂**) on the substituted rings are, in general, shifted upfield due to the shielding generated by the ring current of the catechol rings on the crown ether, indicating the presence of π -stacking interactions in a fashion similar to that observed in the bis(pyridinium)ethane [2]pseudorotaxanes (Table 4.2).

Table 4.2 - Summary of Changes in Chemical Shift ($\Delta\delta$, ppm) of the [2]Pseudorotaxanes Relative to the Free Threads.^a

Complex	B ₂	B ₁	Bn	A ₁	A ₂
24C8					
MeOBnAnOMe	-0.11	-0.29	-0.64	-0.51	-0.19
MeOBnAnCF ₃	-0.12	-0.30	-0.61	-0.58	-0.12
CF ₃ BnAnOMe	-0.10	-0.26	-0.59	-0.29	-0.12
CF ₃ BnAnCF ₃	-0.09	-0.26	-0.60	-0.51	-0.06
DB24C8					
MeOBnAnOMe	0.20	-0.08	-0.78	-0.37	0.14
MeOBnAnCF ₃	0.12	-0.14	-0.75	-0.18	0.33
MeOBnAnNO ₂	0.07	-0.17	-0.76	-0.25	0.35
CF ₃ BnAnOMe	0.33	0.03	-0.79	-0.24	0.14
CF ₃ BnAnCF ₃	0.22	-0.03	-0.79	-0.24	0.21
CF ₃ BnAnNO ₂	0.17	-0.06	-0.83	-0.40	0.21
NO ₂ BnAnOMe	0.37	0.06	-0.80	-0.28	0.06
NO ₂ BnAnCF ₃	0.26	-0.01	-0.86	-0.52	0.02
NO ₂ BnAnNO ₂	0.18	-0.05	-0.94	-0.97	-0.03
3,5-bisCF ₃ BnAnOMe	0.73	0.04	-0.74	-0.28	-0.04
3,5-bisCF ₃ BnAnCF ₃	0.62	0.01	-0.78	-0.31	-0.01
3,5-bisCF ₃ BnAnNO ₂	0.61	0.07	-0.76	-0.19	0.08
C ₆ F ₅ BnAnOMe			-0.91	-0.20	0.22
C ₆ F ₅ BnAnCF ₃			-1.09	-0.26	0.30
C ₆ F ₅ BnAnNO ₂			-1.15	-0.88	0.19

^a Negative : Downfield Shift; Positive: Upfield Shift.

Since the rate of threading/unthreading is slow on the NMR timescale, calculation of the concentrations of complexed and uncomplexed species is possible using the single-point method.⁷⁷ This method uses the known initial concentrations of crown ether and thread and the signal integrals of a complexed and uncomplexed NMR signal representing the same proton. The equation for K_{assoc} is:



However, due to the presence of simultaneous equilibria between protonated/nonprotonated and complexed/uncomplexed species, two correction factors needed to be introduced. Both correction factors involve the equilibrium concentration of protonated thread [HA]. The first factor corrects for the presence of unprotonated thread and the second accounts for inconsistencies in measuring the concentrations of thread and crown for the experiment.

$$[\text{HA}]_{\text{initial}} = C_o = [\text{HA} \cdot \text{C}] + [\text{HA}]_{\text{eq}} + [\text{A}]_{\text{eq}}$$

$$[\text{HA}]_{\text{eq}} = C_o - \chi_{[\text{HA} \cdot \text{C}]} C_o - \chi_{[\text{A}]} C_o = C_o(1 - \chi_{[\text{HA} \cdot \text{C}]} - \chi_{[\text{A}]}) \quad \text{Eq. 4.2}$$

$$\text{Complexed NMR Signal: } \chi_{[\text{HA} \cdot \text{C}]} = \frac{\int_{\text{complexed}}}{\int_{\text{complexed}} + \int_{\text{uncomplexed}}} \quad \text{Eq. 4.3}$$

$$\text{Uncomplexed NMR Signal: } \delta_{\text{obs}} = \chi_{[\text{A}]} \delta_{[\text{A}]} + \chi_{[\text{HA}]} \delta_{[\text{HA}]}$$

$$\chi_{[\text{HA}]} + \chi_{[\text{A}]} = 1$$

$$\delta_{\text{obs}} = \chi_{[\text{A}]} \delta_{[\text{A}]} + (1 - \chi_{[\text{A}]}) \delta_{[\text{HA}]}$$

$$\delta_{\text{obs}} = \chi_{[\text{A}]} \delta_{[\text{A}]} - \chi_{[\text{A}]} \delta_{[\text{HA}]} + \delta_{[\text{HA}]}$$

$$\delta_{\text{obs}} - \delta_{[\text{HA}]} = \chi_{[\text{A}]} (\delta_{[\text{A}]} - \delta_{[\text{HA}]})$$

$$\chi_{[\text{A}]} = \frac{\delta_{[\text{HA}]} - \delta_{\text{obs}}}{\delta_{[\text{HA}]} - \delta_{[\text{A}]}} \quad \text{Eq. 4.4}$$

$$\chi_{[\text{A}]} = \left(\frac{\int_{\text{uncomplexed}}}{\int_{\text{complexed}} + \int_{\text{uncomplexed}}} \right) \left(\frac{\delta_{[\text{HA}]} - \delta_{\text{obs}}}{\delta_{[\text{HA}]} - \delta_{[\text{A}]}} \right) \quad \text{Eq. 4.5}$$

$$[\text{HA}]_{\text{eq}} =$$

$$C_o \left[\left(1 - \frac{\int_{\text{complexed}}}{\int_{\text{complexed}} + \int_{\text{uncomplexed}}} - \frac{\int_{\text{uncomplexed}}}{\int_{\text{complexed}} + \int_{\text{uncomplexed}}} \left(\frac{\delta_{[\text{HA}]} - \delta_{\text{obs}}}{\delta_{[\text{HA}]} - \delta_{[\text{A}]}} \right) \right) \right] \quad \text{Eq. 4.6}$$

Scheme 4.2 – Derivation of Uncomplexed Protonated Thread [HA].

$$C_o = \frac{(\int \text{Benzyl uncomplexed} + \int \text{Benzyl complexed})/2}{(\int \text{Crown uncomplexed} + \int \text{Crown complexed})/\#\text{crown protons}^*} (0.01\text{M}) \quad \text{Eq. 4.7}$$

* DB24C8: # crown protons = 8; 24C8: # crown protons = 32.

Scheme 4.3 – Correction for actual initial concentration of protonated thread

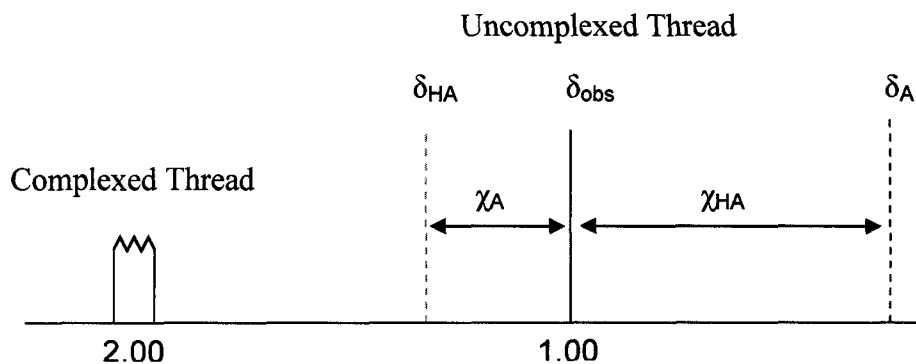


Figure 4.6 – Schematic of complexed and uncomplexed CH₂ peaks.

Equation 4.2 expresses the initial concentration of protonated thread C_o in terms of all the ways in which the thread can exist in the equilibrium: complexed with crown, uncomplexed protonated and uncomplexed unprotonated. **Equation 4.4** describes the actual correction factor for the presence of unprotonated thread, which is incapable of complexing with crown. Knowing that the unprotonated thread is incapable of complexation means that it must simply be subtracted from the equilibrium concentration of uncomplexed protonated thread. The amount of protonated and non-protonated thread is determined by comparing the position of the uncomplexed benzyl peak (δ_{obs}) from the NMR spectra of the K_{assoc} experiment, to the chemical shift limits of non-protonated thread ($\delta_{[\text{A}]}$) and completely protonated thread ($\delta_{[\text{HA}]}$) from the NMR spectra of the

titration experiments. This, in essence, gives the mole fraction of unprotonated uncomplexed thread relative to protonated thread. To get the absolute mole fraction of unprotonated thread, the value from **Equation 4.4** must be multiplied by the mole fraction of uncomplexed species.

The second correction, expressed in **Equation 4.7**, is used to account for inconsistencies between measured amounts of thread and crown. By taking the ratio of thread:crown from the spectrum of the actual NMR experiment, a more accurate value for the relative concentrations in solution is obtained. The crown, in all cases, was assigned the target concentration of 0.010 M. The measurements of the threads were deemed less reliable because the amounts were small (1-4 mg), the threads are hygroscopic and some were prone to deprotonation by atmospheric water. Determining the actual concentration of thread by comparison of ratios in the experiment provided a means for accounting for these discrepancies and allowed the determination of more accurate K_{assoc} values.

Table 4.3 – Summary of experimental (in red) and calculated (in black) Equilibrium Constants with DB24C8.

An Bn	H	OMe	CF₃	NO₂
H	100 (102)	—	—	—
OMe	—	113 (84)	190 (205)	472 (343)
CF₃	—	174 (187)	531 (522)	316 (336)
NO₂	—	541 (496)	800 (493)	1504 (228)
C₆F₅	—	168 (176)	662 (655)	689 (392)
3,5- bisCF₃	—	466 (447)	611 (659)	632 (557)

Table 4.4 Summary of experimental (in red) and calculated (in black) Equilibrium Constants with 24C8.

An Bn	OMe	CF ₃
OMe	631 (364)	1855 (1274)
CF ₃	1776 (1569)	1930 (1162)

The calculated values obtained for K_{assoc} with **DB24C8** and **24C8** were in the same ranges as those determined for both bis(pyridinium)ethane and *N,N*-dibenzylammonium with the same crowns.^{38, 100} The highest K_{assoc} with **DB24C8**, 1500 M^{-1} , was with the $\text{NO}_2\text{BnAnNO}_2$ thread **[4-10]⁺**, which is higher than the value of 1300 M^{-1} for 4,4'-dinitro-*N,N*-dibenzylammonium.⁹⁶ This, again, suggests that the π -stacking ability of **DB24C8** enhances complexation, likely due to a perfect parallel alignment between the crown ether in the 'S'-conformation and the thread in the *anti* conformation, which resembles the behaviour seen with the bis(pyridinium)ethane threads. However, in the case of **24C8**, the highest value of K_{assoc} was 1900 M^{-1} for **CF₃BnAnCF₃ [4-6]⁺** (Hammett $\sigma = 0.54$), which is much lower than $K_{\text{assoc}} = 4500 \text{ M}^{-1}$ for 4,4'-di(methoxycarbonyl)-*N,N*-dibenzylammonium (Hammett $\sigma = 0.44$).¹⁰¹ The lower Hammett parameter and higher K_{assoc} implies that the hydrogen bonding and ion-dipole in the dibenzylammonium threads is more significant than the benzylianilinium. However, the ¹H NMR shifts of the benzyl peaks for **MeOBnAnOMe [4-2]⁺** and **NO₂BnAnNO₂ [4-6]⁺**, 4.46 and 4.78 ppm respectively, compared to the 4,4'-dimethoxy-*N,N*-dibenzylammonium and 4,4'-dinitro-*N,N*-dibenzylammonium, 4.08 and 4.32 ppm respectively, suggesting the benzyl protons are more acidic.

Four general observations can be made regarding the calculated association constants: (1) Threads bearing electron withdrawing groups had higher association constants than those with electron donating groups, regardless of the crown ether used. This is expected on a purely electrostatic basis resulting in increased ion-dipole interactions and stronger $NH\cdots O$ hydrogen bonding. (2) Similar to the trend exhibited by dibenzylammonium threads¹⁰¹ and contrary to that observed for bis(pyridinium)ethane cations,³⁷ higher K_{assoc} were observed with **24C8** than with **DB24C8**. This can be attributed to the ability of aliphatic ether oxygen atoms to engage in more effective ion-dipole interactions and hydrogen bonding relative to the aromatic catechol oxygen atoms. (3) The EWG is more effective when placed on the anilinium ring than on the benzyl ring which is consistent with $NH\cdots O$ hydrogen bonding being a major contribution to the overall K_{assoc} . (4) There appears to be significant π -stacking involved in binding when **DB24C8** is the ring as indicated by upfield shifts for the *meta/para* protons **A₂** and **B₂**. The π -stacking is influenced equally by the inclusion of EWGs on either the benzyl or anilinium rings and is magnified considerably when both rings contain the same EWG (CF_3 or NO_2). This is reminiscent of the trends observed for bis(pyridinium)ethane threads with **DB24C8** and is probably a direct result of the observed *anti* conformation of the two atom bridge between the aromatic rings.

A closer look at the values in Table 4.3 reveals that these **24C8** complexes follow the expected trend. K_{assoc} increases from **MeOBnAnOMe [4-2]⁺**, **CF₃BnAnOMe [4-5]⁺**, **MeOBnAnCF₃ [4-3]⁺** to **CF₃BnAnCF₃ [4-6]⁺**. This follows the rationalization that EDG decrease the association while EWG increase the association. However, when both an EDG and an EWG are present, the group on the aniline ring has a larger effect on the complexation ability of the thread than the group that is on the benzyl ring.

In a fashion similar to that for the dibenzylammonium threads,^{102, 103} the addition of one equivalent of base (triethylamine) to solutions containing the [2]pseudorotaxanes caused dethreading of the macrocycle from the thread and shifted equilibrium toward the non-protonated species [A] which is incapable of complexation. The process can be reversed by the addition of one equivalent of acid resulting in the restoration of the [2]pseudorotaxane complex.

High resolution ESI mass spectrometry experiments confirmed the presence of the 1:1 complex in the gas phase and allowed for exact mass determinations (Table 4.5).

Table 4.5 – ESI-TOF calculated and found values for [2]pseudorotaxanes.

Thread	MW(Pseudorotaxane) Calculated (g/mol)	MW(Pseudorotaxane) Found (g/mol)
24C8 complexes		
MeOBnAnOMe	596.3435	596.3409
MeOBnAnCF ₃	634.3203	634.3215
CF ₃ BnAnOMe	634.3203	634.3210
CF ₃ BnAnCF ₃	672.2971	672.2984
DB24C8 complexes		
HBnAnH	632.3218	632.3247
MeOBnAnOMe	692.3435	692.3433
MeOBnAnCF ₃	730.3203	730.3175
MeOBnAnNO ₂	707.3174	707.3207
CF ₃ BnAnOMe	730.3203	730.3231
CF ₃ BnAnCF ₃	768.2971	768.2938
CF ₃ BnAnNO ₂	745.2943	745.2945
NO ₂ BnAnOMe	707.3174	707.3188
NO ₂ BnAnCF ₃	745.2943	745.2950
NO ₂ BnAnNO ₂	722.2920	722.2931
3,5-bisCF ₃ BnAnOMe	798.3071	798.3088
3,5-bisCF ₃ BnAnCF ₃	836.2840	836.2803
3,5-bisCF ₃ BnAnNO ₂	813.2816	813.2805
C ₆ F ₅ BnAnOMe	752.2853	752.2856
C ₆ F ₅ BnAnCF ₃	790.2621	790.2626
C ₆ F ₅ BnAnNO ₂	767.2598	767.2590

Solid state X-ray structures of $[\text{CF}_3\text{BnAnCF}_3\subset\text{DB24C8}][\text{OTf}]$, $[\text{HBnAnH}\subset\text{DB24C8}][\text{OTf}]$ and $[\text{MeOBnAnOMe}\subset\text{DB24C8}][\text{OTf}]$ also verified the [2]pseudorotaxane formation.

The structure of $[\text{CF}_3\text{BnAnCF}_3\subset\text{DB24C8}][\text{OTf}]$ (Figure 4.7) has the crown ether arranged in a “C”-shaped conformation around the anilinium ring. Four hydrogen bonds are formed between the $-\text{CH}_2\text{NH}_2^+$ unit of the thread $\text{CF}_3\text{BnAnCF}_3^+$ and **DB24C8**. The $\text{N}\cdots\text{O}$ distances vary from 2.78 Å (aliphatic oxygens) to 3.02 Å (aromatic oxygens) with $\text{NH}\cdots\text{O}$ angles of 170° and 147° , respectively. The $\text{C}\cdots\text{O}$ distances vary from 3.30 Å (aliphatic oxygens) to 3.23 Å (aromatic oxygens) with $\text{CH}\cdots\text{O}$ angles of 172° and 159° respectively. The other two aliphatic oxygen atoms are involved in ion-dipole interactions with N^+ and $\text{C}^{\delta+}$ at 2.97 Å and 2.92 Å and a torsion angle $\text{O}\cdots\text{N}-\text{C}\cdots\text{O}$ essentially linear at 179.8° . The distances between the centers of the aromatic rings on **DB24C8** to the center of the anilinium ring are 3.77 Å and 3.96 Å; these distances are in the upper range for π -stacking interactions.^{104, 105}

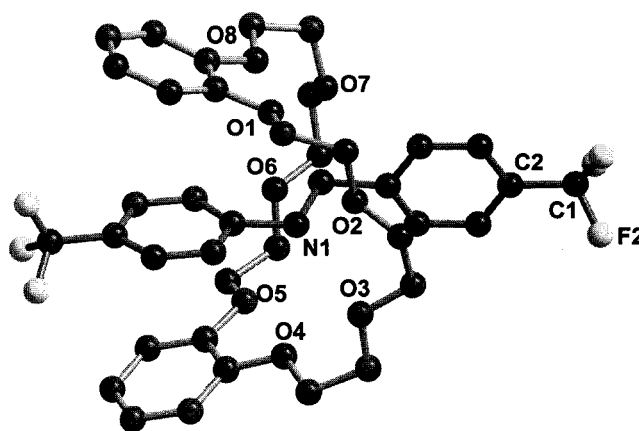


Figure 4.7 – Ball and Stick representation of the X-ray structure of $[\text{CF}_3\text{BnAnCF}_3\subset\text{DB24C8}]^+$ (carbon = black, oxygen = red, nitrogen = blue, fluorine = yellow).

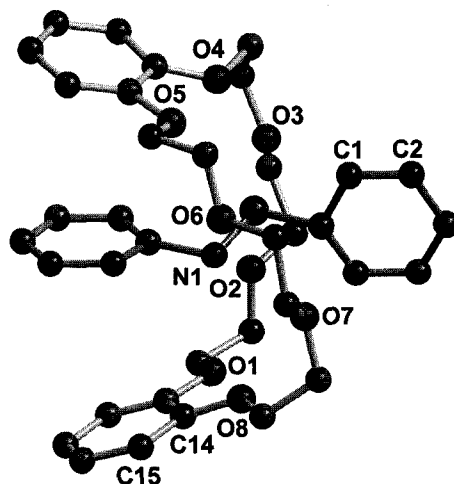


Figure 4.8 – Ball and Stick representation of the X-ray structure of $[\text{HBnAnH}\subset\text{DB24C8}]^+$ (carbon = black, oxygen = red, nitrogen = blue)

Similar to $[\text{CF}_3\text{BnAnCF}_3\subset\text{DB24C8}][\text{OTf}]$, the structure of $[\text{HBnAnH}\subset\text{DB24C8}][\text{OTf}]$ also has the crown ether arranged in a “C”-shaped conformation around the anilinium ring (Figure 4.8).

In contrast to $[\text{CF}_3\text{BnAnCF}_3\subset\text{DB24C8}][\text{OTf}]$, in the structure of $[\text{MeOBnAnOMe}\subset\text{DB24C8}][\text{OTf}]$ (Figure 4.9), **DB24C8** adopts the “S”-shaped conformation familiar in the structures of pseudorotaxanes formed with bis(pyridinium)ethane threads.^{41, 44, 45} The difference is that there are no face-to-face π -stacking interactions between aromatic rings. This is attributed to the fact that both sets of aromatic rings are electron-rich which is known to be unfavourable for stabilizing π -stacking.^{104, 105} As a consequence, the crown ether adopts an orientation which optimizes hydrogen-bonding and ion-dipole interactions. Thus, in a fashion similar to $[\text{CF}_3\text{BnAnCF}_3\subset\text{DB24C8}][\text{OTf}]$, four hydrogen bonds between the $-\text{CH}_2\text{NH}_2^+$ unit of the thread MeOBnAnOMe^+ and **DB24C8** are observed. The distances between N or C atoms and O atoms varies from 2.96 Å (aliphatic oxygens) to 3.25 Å (aromatic oxygens) with $\text{NH}\cdots\text{O}$ and $\text{CH}\cdots\text{O}$ angles of 172° and 157°, respectively. The other two aliphatic

oxygen atoms are involved in ion-dipole interactions with the N⁺ and C^{δ+} at 3.05 Å and a torsion angle O⋯N–C⋯O that is linear at 180°.

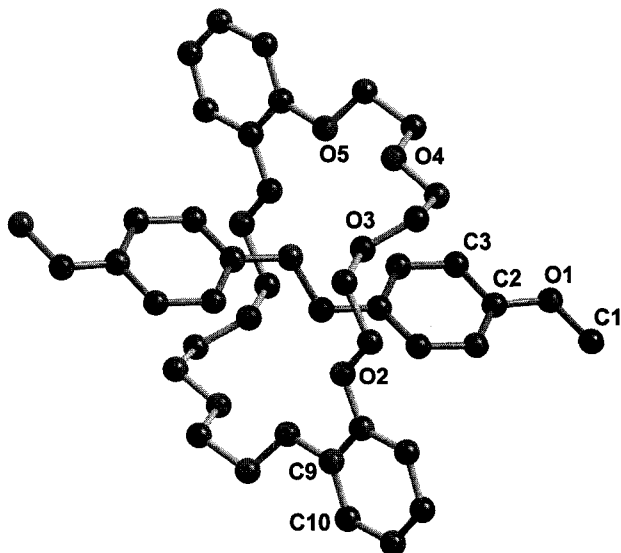


Figure 4.9 – Ball and Stick representation of the X-ray structure of [MeOBnAnOMe⊂DB24C8]⁺ (carbon = black, oxygen = red, nitrogen = blue).

4.4 SUMMARY AND CONCLUSIONS

In summary, it has been shown that the hybrid *N*-benzylanilinium cations can function as suitable threads for the formation of [2]pseudorotaxanes with 24-membered crown ethers. These pseudorotaxanes are pH-sensitive and the threading-unthreading process is controllable by the alternate addition of acid and base. The binding behaviour has characteristics of both dibenzylammonium and bis(pyridinium)ethane threads but probably is more similar to the ammonium ion threads. However, structurally, *N*-benzylanilinium threads are more similar to the bis(pyridinium)ethane threads. The next two chapters discuss the incorporation of this new recognition site into molecular shuttles and catenanes to complement the bis(pyridinium)ethane/24C8 motif and generate chemically controllable systems from these two structurally related thread components.

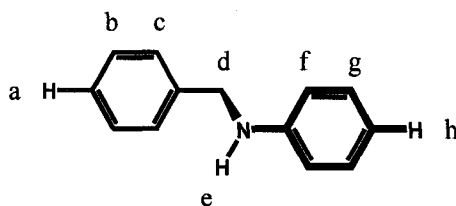
4.5 EXPERIMENTAL

4.5.1 General Comments

Sodium trifluoromethanesulfonate, trifluoromethanesulfonic acid, all aniline derivatives, benzylbromide derivatives and **DB24C8** were purchased from Aldrich and used as received.

4.5.2 Synthesis of Compound HBnAnH [4-1]

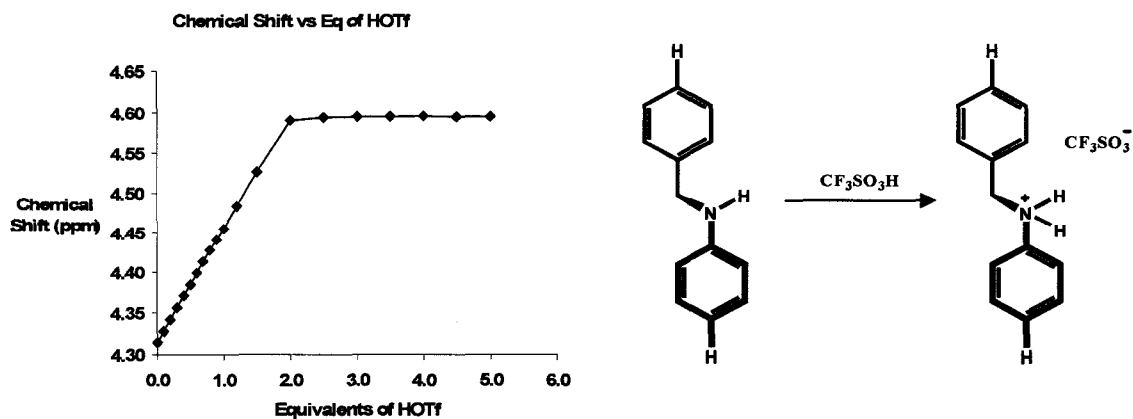
This compound can be purchased from Aldrich, but was synthesized using the following method. Aniline (1.00 g, 1.07×10^{-2} mol) and benzyl bromide (0.918 g, 5.37×10^{-3} mol) were dissolved in CH_3CN and refluxed for 3 hours. The reaction was cooled to room temperature and the solid anilinium bromide that precipitated was filtered and discarded. The filtrate containing the product was concentrated and the resulting residue dissolved in CHCl_3 and subjected to column chromatography (silica gel) using CHCl_3 :hexanes (4:1). ($R_f = 0.83$, 0.725 g, 73.7%) The pure isolated solid was dissolved in isopropyl ether (10 ml) and trifluoromethanesulfonic acid (1 equivalent) was added dropwise to yield the *N*-benzylanilinium as a white crystalline solid (1.13 g, 86%) . **ESI-MS**: m/z [4-1 - OTf]⁺ calc. 184.1121, found 184.1125.

Table 4.6 – ^1H NMR of [4-1] in CD_3CN . MW = 183.241 g/mol

Proton	δ (ppm)	Multiplicity	# Protons	J (Hz)
a	7.23	t	1	$^3J_{ab} = 7.39$
b	7.32	dd	2	$^3J_{ba} = 7.39, ^3J_{bc} = 7.46$
c	7.36	d	2	$^3J_{cb} = 7.46$
d	4.31	d	2	$^3J_{de} = 6.02$
e	4.92	br s	1	--
f	6.60	d	2	$^3J_{fg} = 7.27$
g	7.08	dd	2	$^3J_{gf} = 7.27, ^3J_{gh} = 7.31$
h	6.59	t	1	$^3J_{hg} = 7.31$

Table 4.7 – ^1H NMR of [4-1][OTf] in CD_3CN . MW_{OTf} = 333.317 g/mol

Proton	δ (ppm)	Multiplicity	# Protons	J (Hz)
a-c	7.36-7.52	m	1	--
d	4.60	s	2	--
e	9.05	br s	1	--
f-h	7.36-7.52	m	2	--

Titration of 4-1 monitoring chemical shift of H_d 

4.5.3 Synthesis of Compound MeOBnAnOMe [4-2]

This compound has been made before using different methods.¹⁰⁶⁻¹⁰⁸ 4-Methoxyaniline (1.00 g, 8.12×10^{-3} mol) and 4-methoxybenzyl chloride (0.636 g, 4.06×10^{-3} mol) were dissolved in CH₃CN and refluxed for 24 hours. The reaction was cooled to room temperature and the solid anilinium bromide that precipitated was filtered and discarded. The filtrate containing the product was concentrated and the resulting residue dissolved in CHCl₃ and subjected to column chromatography (silica gel) using CHCl₃:hexanes (4:1). ($R_f = 0.46$, 0.560 g, 57%) The pure isolated solid was dissolved in isopropyl ether (10 ml) and trifluoromethanesulfonic acid (1 equivalent) was added dropwise to yield the N-benzylanilinium as a white crystalline solid. ESI-MS: m/z [4-2 - OTf]⁺ calc. 244.1338, found 244.1320.

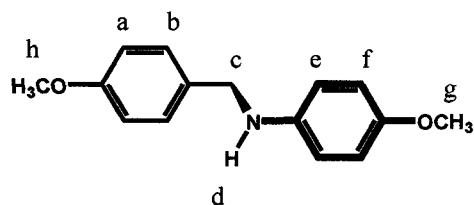
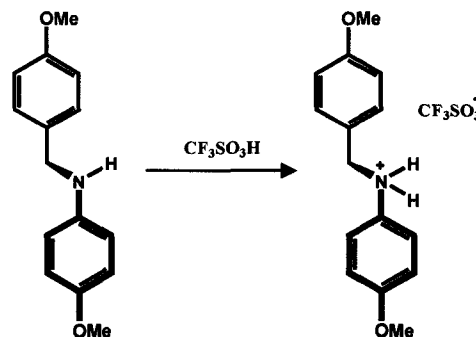
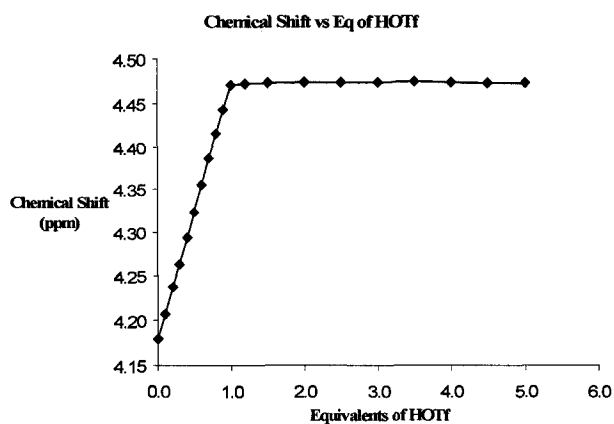


Table 4.8 – ¹H NMR of [4-2] in CD₃CN. MW = 243.291 g/mol

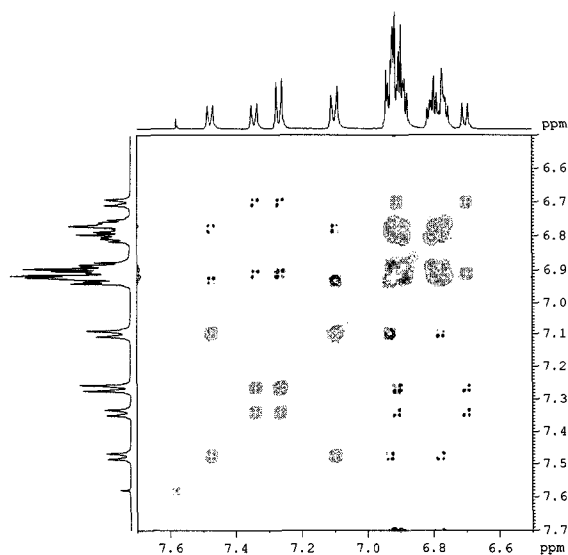
Proton	δ (ppm)	Multiplicity	# Protons	J (Hz)
a	7.27	d	2	$^3J_{ab} = 8.25$
b	6.87	d	2	$^3J_{ba} = 8.25$
c	4.17	s	2	--
d	4.49	br s	1	--
e	6.71	d	2	$^3J_{ef} = 6.78$
f	6.56	d	2	$^3J_{fe} = 6.78$
g	3.73	s	3	--
h	3.64	s	3	--

Table 4.9 – ^1H NMR of [4-2][OTf] in CD_3CN . $\text{MW}_{\text{OTf}} = 393.367$ g/mol

Proton	δ (ppm)	Multiplicity	# Protons	J (Hz)
a	6.92	d	2	$^3J_{ab} = 8.69$
b	7.27	d	2	$^3J_{ba} = 8.69$
c	4.46	s	2	--
d	8.65	br s	2	--
e	7.22	d	2	$^3J_{ef} = 9.05$
f	6.98	d	2	$^3J_{fe} = 9.05$
g	3.79	s	3	--
h	3.78	s	3	--

Titration of 4-2 monitoring chemical shift of H_c 

EXSY Spectrum of [4-2cDB24C8][OTf]



4.5.4 Synthesis of MeOBnAnCF₃ [4-3]

4-Trifluoromethylaniline (1.00 g, 6.21×10^{-3} mol) and 4-methoxybenzyl chloride (0.486 g, 3.10×10^{-3} mol) were dissolved in CH₃CN and refluxed for 24 hours. The reaction was cooled to room temperature and the solid anilinium bromide that precipitated was filtered and discarded. The filtrate containing the product was concentrated and the resulting residue dissolved in CHCl₃ and subjected to column chromatography (silica gel) using CHCl₃:hexanes (4:1). ($R_f = 0.81$, 0.600 g, 69%) The pure isolated solid was dissolved in isopropyl ether (10 ml) and trifluoromethanesulfonic acid (1 equivalent) was added dropwise to yield the *N*-benzylanilinium as a white crystalline solid. **ESI-MS:** m/z [4-3 - OTf]⁺ calc. 282.1106, found 282.1108.

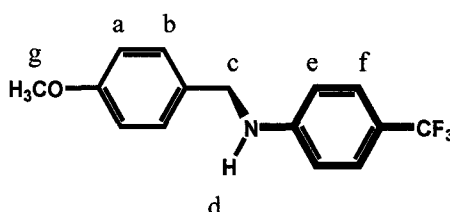
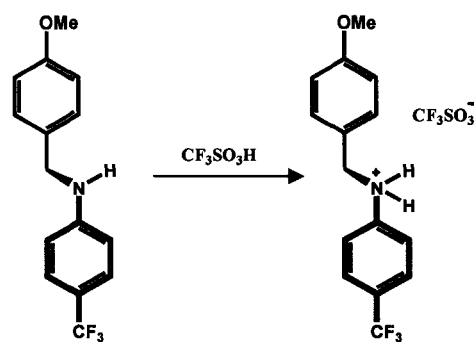
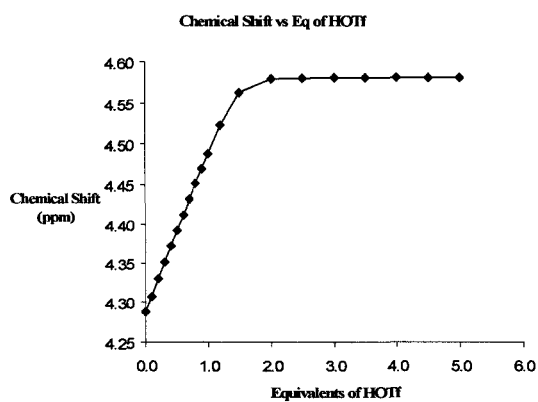
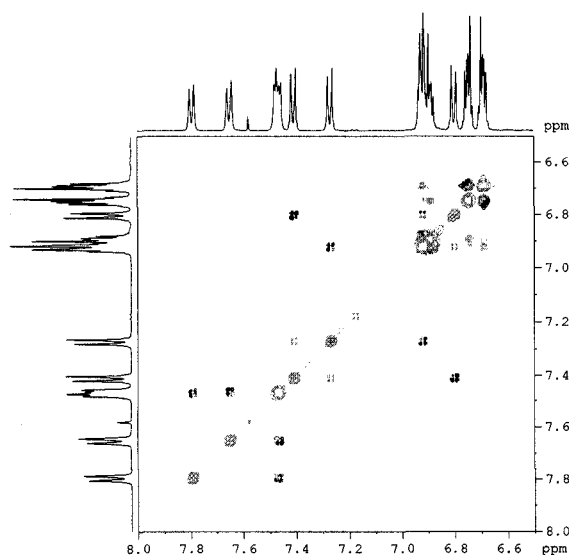


Table 4.10 – ¹H NMR of [4-3] in CD₃CN. MW = 281.264 g/mol

Proton	δ (ppm)	Multiplicity	# Protons	J (Hz)
a	6.88	d	2	$^3J_{ab} = 8.58$
b	7.27	d	2	$^3J_{ba} = 8.58$
c	4.28	d	2	$^3J_{cd} = 5.98$
d	5.42	br s	1	--
e	6.66	d	2	$^3J_{ef} = 8.62$
f	7.36	d	2	$^3J_{fe} = 8.62$
g	3.75	s	3	--

Table 4.11 – ^1H NMR of [4-3][OTf] in CD_3CN . $\text{MW}_{\text{OTf}} = 431.340$ g/mol

Proton	δ (ppm)	Multiplicity	# Protons	J (Hz)
a	6.92	d	2	$^3J_{ab} = 8.67$
b	7.28	d	2	$^3J_{ba} = 8.67$
c	4.58	s	2	--
d	9.20	br s	2	--
e	7.53	d	2	$^3J_{ef} = 8.50$
f	7.82	d	2	$^3J_{fe} = 8.50$
g	3.79	s	3	--

Titration of 4-3 monitoring chemical shift of H_c EXSY Spectrum of [4-3 \subset DB24C8][OTf]

4.5.5 Synthesis of MeOBnAnNO₂ [4-4]

4-Nitroaniline (2.00 g, 1.45×10^{-2} mol) and 4-methoxybenzyl chloride (1.13 g, 7.24×10^{-3} mol) were dissolved in CH₃CN and refluxed for 24 hours. The reaction was cooled to room temperature and the solid anilinium bromide that precipitated was filtered and discarded. The filtrate containing the product was concentrated and the resulting residue dissolved in CHCl₃ and subjected to column chromatography (silica gel) using CHCl₃:hexanes (4:1). (*R_f* = 0.50, 0.150 g, 8.0%) The pure isolated solid was dissolved in isopropyl ether (10 ml) and trifluoromethanesulfonic acid (1 equivalent) was added dropwise to yield the *N*-benzylanilinium as a yellow crystalline solid. ESI-MS: *m/z* [4-4 - OTf]⁺ calc. 259.1077, found 259.1085.

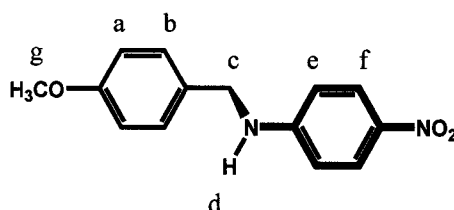


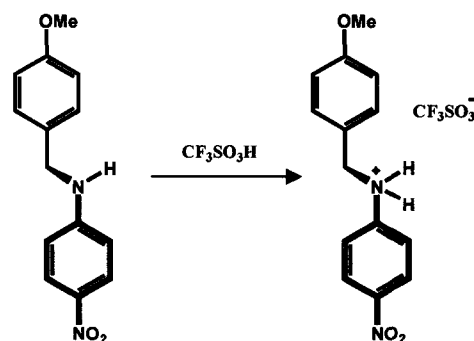
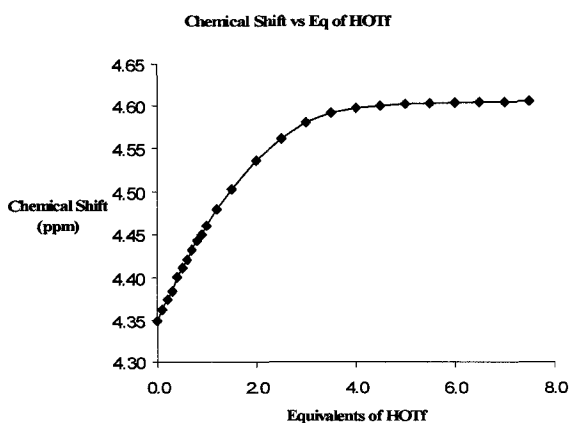
Table 4.12 – ¹H NMR of [4-4] in CD₃CN. MW = 258.266 g/mol

Proton	δ (ppm)	Multiplicity	# Protons	<i>J</i> (Hz)
a	6.89	d	2	³ <i>J</i> _{ab} = 8.62
b	7.27	d	2	³ <i>J</i> _{ba} = 8.62
c	4.34	s	2	³ <i>J</i> _{cd} = 5.91
d	6.03	s	1	--
e	6.62	d	2	³ <i>J</i> _{ef} = 9.24
f	7.99	d	2	³ <i>J</i> _{fe} = 9.24
g	3.76	s	3	--

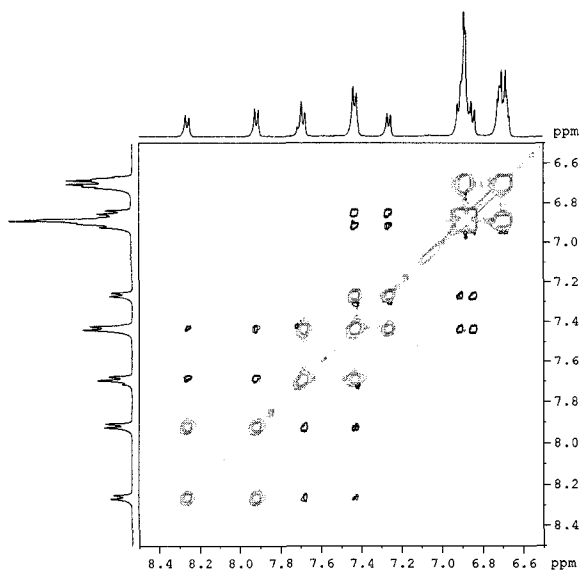
Table 4.13 – ¹H NMR of [4-4][OTf] in CD₃CN. MW_{OTf} = 408.342 g/mol

Proton	δ (ppm)	Multiplicity	# Protons	J (Hz)
a	6.92	d	2	³ J _{ab} = 8.70
b	7.27	d	2	³ J _{ba} = 8.70
c	4.61	s	2	--
d	--	--	2	--
e	7.57	d	2	³ J _{ef} = 9.02
f	8.30	d	2	³ J _{fe} = 9.02
g	3.79	s	3	--

Titration of 4-4 monitoring chemical shift of H_c

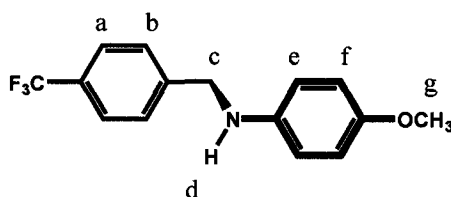


EXSY Spectrum of [4-4_cDB24C8][OTf]



4.5.6 Synthesis of CF₃BnAnOMe [4-5]

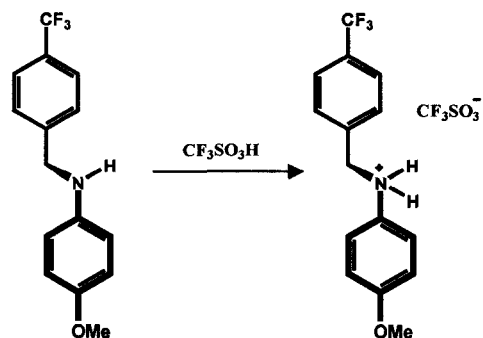
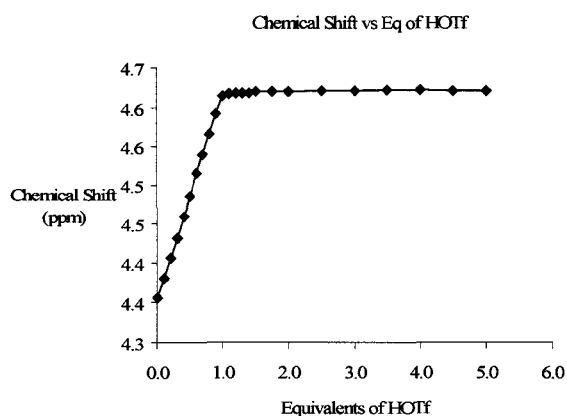
4-Methoxyaniline (1.00 g, 8.12×10^{-3} mol) and 4-trifluoromethylbenzyl bromide (0.971 g, 4.06×10^{-3} mol) were dissolved in CH₃CN and refluxed for 3 hours. The reaction was cooled to room temperature and the solid anilinium bromide that precipitated was filtered and discarded. The filtrate containing the product was concentrated and the resulting residue dissolved in CHCl₃ and subjected to column chromatography (silica gel) using CHCl₃:hexanes (4:1). ($R_f = 0.69$, 0.804 g, 55%) The pure isolated solid was dissolved in isopropyl ether (10 ml) and trifluoromethanesulfonic acid (1 equivalent) was added dropwise to yield the N-benzylanilinium as a white crystalline solid. **ESI-MS**: m/z [4-5 - OTf]⁺ calc. 282.1106, found 282.1103.

Table 4.14 – ¹H NMR of [4-5] in CD₃CN. MW = 281.264 g/mol

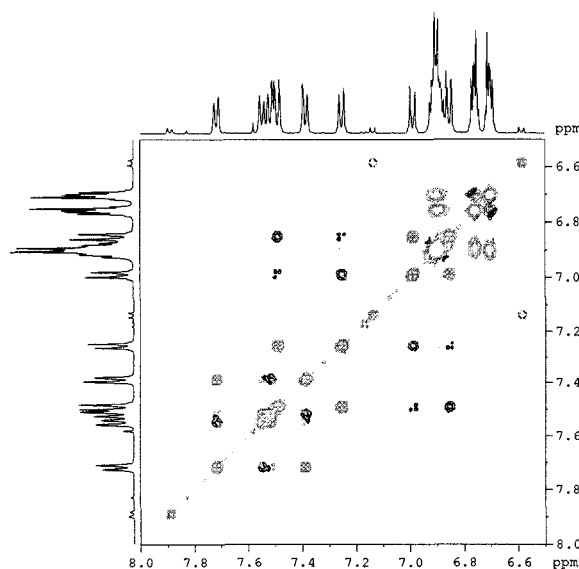
Proton	δ (ppm)	Multiplicity	# Protons	J (Hz)
a	7.63	d	2	$^3J_{ab} = 8.14$
b	7.53	d	2	$^3J_{ba} = 8.14$
c	4.35	s	2	--
d	4.75	s	1	--
e	6.71	d	2	$^3J_{ef} = 8.91$
f	6.54	d	2	$^3J_{fe} = 8.91$
g	3.65	s	3	--

Table 4.15 – ^1H NMR of [4-5][OTf] in CD_3CN . $\text{MW}_{\text{OTf}} = 431.340$ g/mol

Proton	δ (ppm)	Multiplicity	# Protons	J (Hz)
a	7.72	d	2	$^3J_{ab} = 8.14$
b	7.56	d	2	$^3J_{ba} = 8.14$
c	4.62	t	2	$^3J_{cd} = 5.64$
d	9.03	br s	2	--
e	7.31	d	2	$^3J_{ef} = 9.03$
f	7.01	d	2	$^3J_{fe} = 9.03$
g	3.81	s	3	--

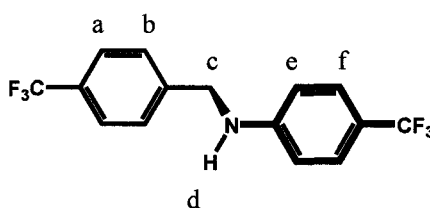
Titration of 4-5 monitoring chemical shift of H_c 

EXSY Spectrum [4-5cDB24C8][OTf]



4.5.7 Synthesis of CF₃BnAnCF₃ [4-6]

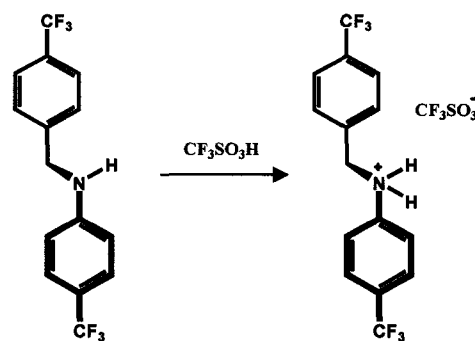
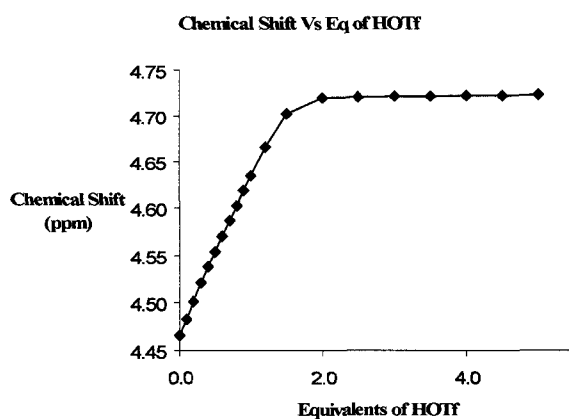
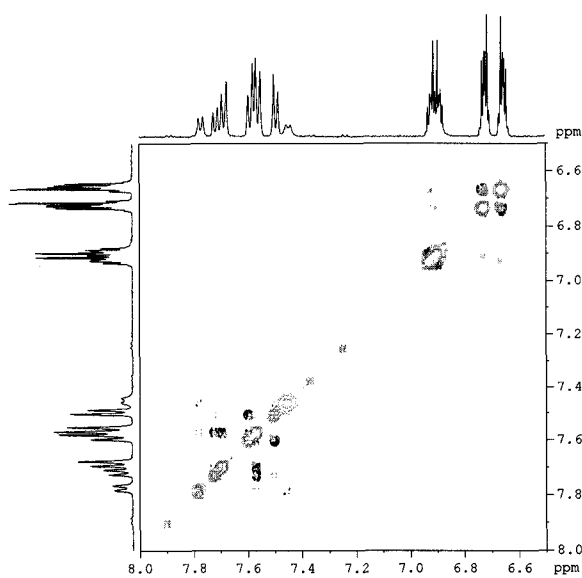
4-Trifluoromethylaniline (1.00 g, 6.21×10^{-3} mol) and 4-trifluoromethylbenzyl bromide (0.742 g, 3.10×10^{-3} mol) were dissolved in CH₃CN and refluxed for 24 hours. The reaction was cooled to room temperature and the solid anilinium bromide that precipitated was filtered and discarded. The filtrate containing the product was concentrated and the resulting residue dissolved in CHCl₃ and subjected to column chromatography (silica gel) using CHCl₃:hexanes (4:1). ($R_f = 0.83$, 0.340g, 34.4%) The pure isolated solid was dissolved in isopropyl ether (10 ml) and trifluoromethanesulfonic acid (1 equivalent) was added dropwise to yield the *N*-benzylanilinium as a white crystalline solid. ESI-MS: m/z [4-6 - OTf]⁺ calc. 320.0874, found 320.0884.

Table 4.16 – ¹H NMR of [4-6] in CD₃CN. MW = 319.237 g/mol

Proton	δ (ppm)	Multiplicity	# Protons	J (Hz)
a	7.65	d	2	$^3J_{ab} = 8.07$
b	7.53	d	2	$^3J_{ba} = 8.07$
c	4.47	d	2	$^3J_{cd} = 6.16$
d	5.59	br s	1	--
e	6.67	d	2	$^3J_{ef} = 8.58$
f	7.38	d	2	$^3J_{fe} = 8.58$

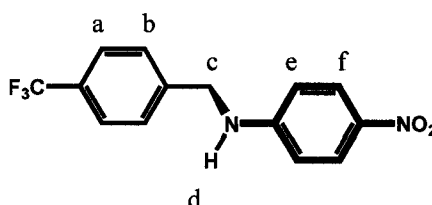
Table 4.17 – ^1H NMR of [4-6][OTf] in CD_3CN . $\text{MW}_{\text{OTf}} = 469.313$ g/mol

Proton	δ (ppm)	Multiplicity	# Protons	J (Hz)
a	7.72	d	2	$^3J_{ab} = 9.06$
b	7.58	d	2	$^3J_{ba} = 9.06$
c	4.73	s	2	--
d	9.48	br s	2	--
e	7.60	d	2	$^3J_{ef} = 8.60$
f	7.84	d	2	$^3J_{fe} = 8.60$

Titration of 4-6 monitoring chemical shift of H_c EXSY Spectrum of [4-6 c DB24C8][OTf]

4.5.8 Synthesis of CF₃BnAnNO₂ [4-7]

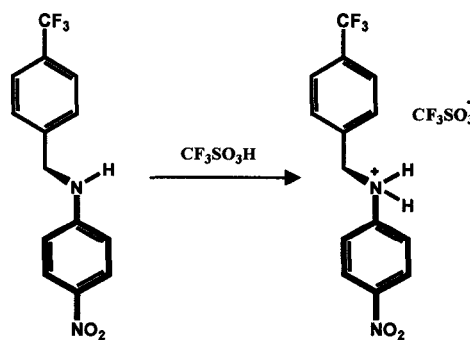
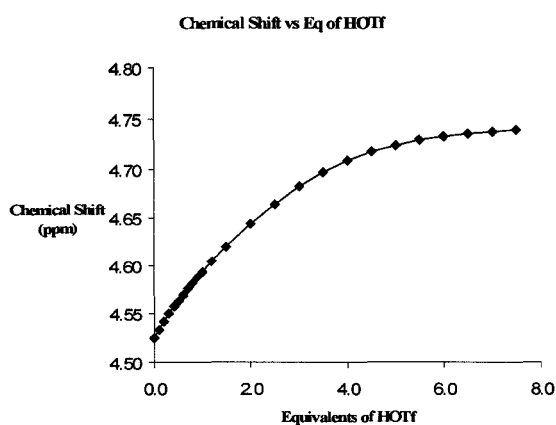
4-Nitroaniline (2.00 g, 1.45×10^{-2} mol) and 4-trifluorobenzyl chloride (1.72 g, 7.24×10^{-3} mol) were dissolved in CH₃CN and refluxed for 24 hours. The reaction was cooled to room temperature and the solid anilinium bromide that precipitated was filtered and discarded. The filtrate containing the product was concentrated and the resulting residue dissolved in CHCl₃ and subjected to column chromatography (silica gel) using CHCl₃:hexanes (4:1). ($R_f = 0.53$, 1.05 g, 49%) The pure isolated solid was dissolved in isopropyl ether (10 ml) and trifluoromethanesulfonic acid (1 equivalent) was added dropwise to yield the *N*-benzylanilinium as a yellow crystalline solid. ESI-MS: m/z [4-7 - OTf]⁺ calc. 297.0845, found 297.0854.

Table 4.18 – ¹H NMR of [4-7] in CD₃CN. MW = 296.239 g/mol

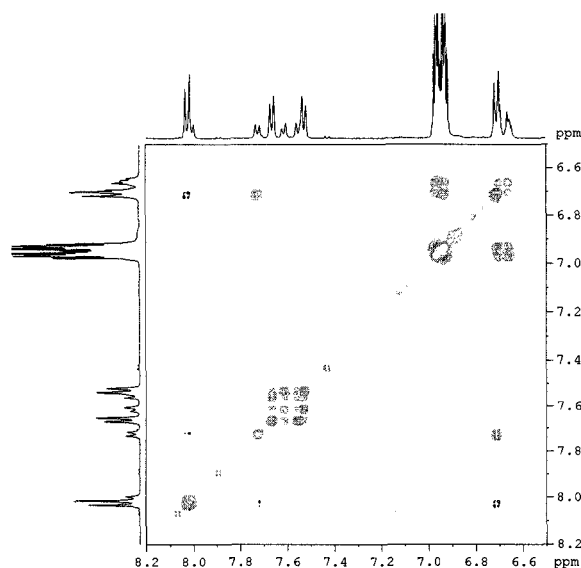
Proton	δ (ppm)	Multiplicity	# Protons	J (Hz)
a	7.66	d	2	$^3J_{ab} = 8.04$
b	7.53	d	2	$^3J_{ba} = 8.04$
c	4.52	d	2	$^3J_{cd} = 6.18$
d	6.18	br s	1	--
e	6.63	d	2	$^3J_{ef} = 9.17$
f	8.00	d	2	$^3J_{fe} = 9.17$

Table 4.19 – ^1H NMR of [4-7][OTf] in CD_3CN . $\text{MW}_{\text{OTf}} = 446.315$ g/mol

Proton	δ (ppm)	Multiplicity	# Protons	J (Hz)
a	7.72	d	2	$^3J_{ab} = 8.14$
b	7.57	d	2	$^3J_{ba} = 8.14$
c	4.74	s	2	--
d	9.17	br s	2	--
e	7.60	d	2	$^3J_{ef} = 8.98$
f	8.31	d	2	$^3J_{fe} = 8.98$

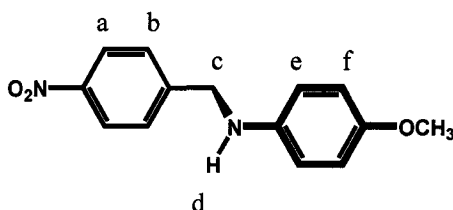
Titration of 4-7 monitoring chemical shift of H_c 

EXSY Spectrum of [4-7cDB24C8][OTf]



4.5.9 Synthesis of NO₂BnAnOMe [4-8]

4-Methoxyaniline (1.14 g, 9.26×10^{-3} mol) and 4-nitrobenzyl bromide (1.00 g, 4.63×10^{-3} mol) were dissolved in CH₃CN and refluxed for 24 hours. The reaction was cooled to room temperature and the solid anilinium bromide that precipitated was filtered and discarded. The filtrate containing the product was concentrated and the resulting residue dissolved in CHCl₃ and subjected to column chromatography (silica gel) using CHCl₃:hexanes (4:1). ($R_f = 0.50$, 0.915 g, 56%) The pure isolated solid was dissolved in isopropyl ether (10 ml) and trifluoromethanesulfonic acid (1 equivalent) was added dropwise to yield the N-benzylanilinium as a yellow crystalline solid. ESI-MS: m/z [4-8 - OTf]⁺ calc. 259.1077, found 259.1082.

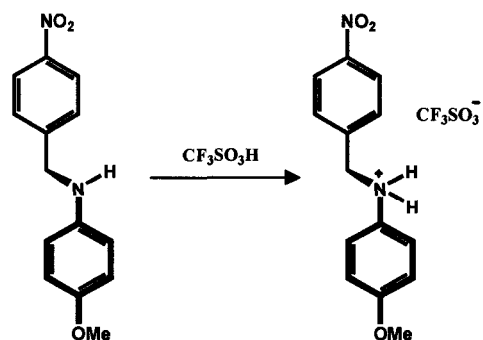
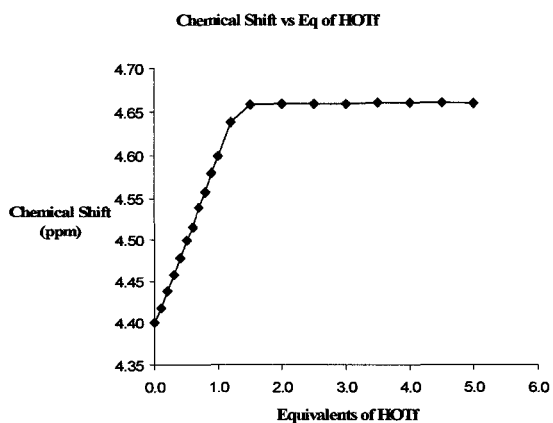
Table 4.20 – ¹H NMR of [4-8] in CD₃CN. MW = 258.266 g/mol

Proton	δ (ppm)	Multiplicity	# Protons	J (Hz)
a	8.15	d	2	$^3J_{ab} = 8.57$
b	7.57	d	2	$^3J_{ba} = 8.57$
c	4.40	s	2	--
d	--	br s	1	--
e	6.71	d	2	$^3J_{ef} = 8.87$
f	6.54	d	2	$^3J_{fe} = 8.87$
g	3.66	s	3	--

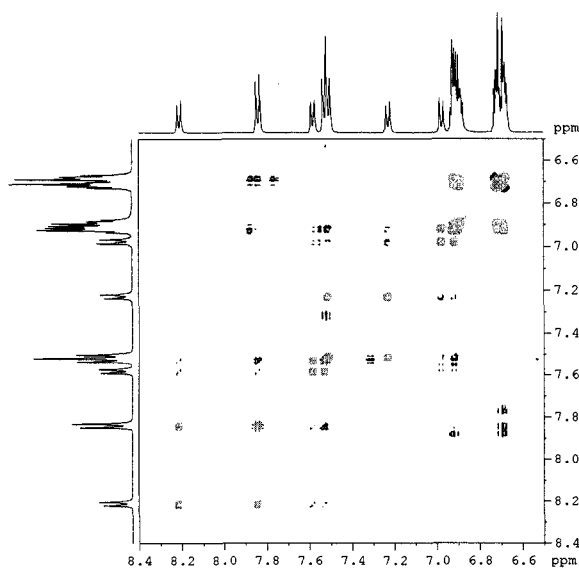
Table 4.21 – ¹H NMR of [4-8][OTf] in CD₃CN. MW_{OTf} = 408.342 g/mol

Proton	δ (ppm)	Multiplicity	# Protons	<i>J</i> (Hz)
a	8.21	d	2	³ <i>J</i> _{ab} = 8.72
b	7.60	d	2	³ <i>J</i> _{ba} = 8.72
c	4.66	s	2	--
d	9.10	s	2	--
e	7.30	d	2	³ <i>J</i> _{ef} = 9.04
f	7.00	d	2	³ <i>J</i> _{fe} = 9.04
g	3.81	s	3	--

Titration of 4-8 monitoring chemical shift of H_c

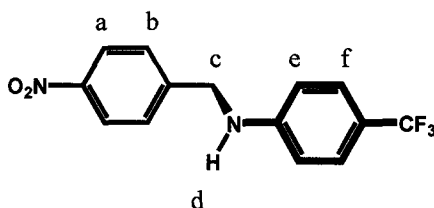


EXSY Spectrum of [4-8_cDB24C8][OTf]



4.5.10 Synthesis of NO₂BnAnCF₃ [4-9]

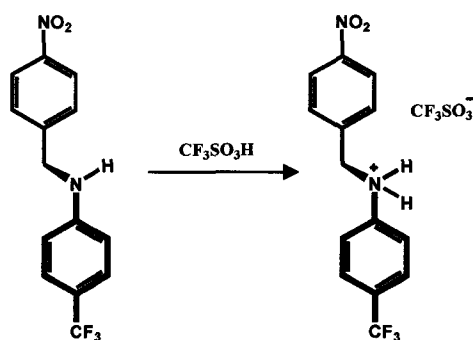
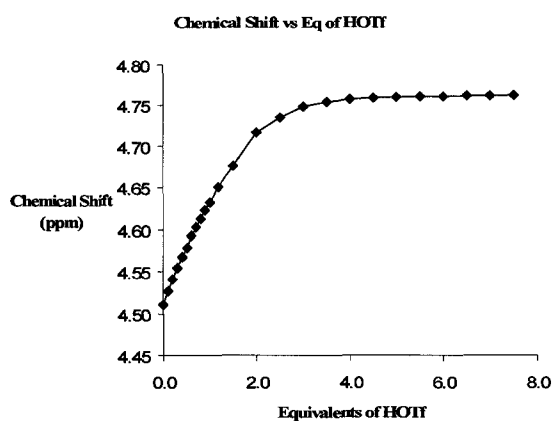
4-Trifluoromethylaniline (2.00 g, 1.24×10^{-2} mol) and 4-nitrobenzyl bromide (1.34 g, 6.21×10^{-3} mol) were dissolved in CH₃CN and refluxed for 24 hours. The reaction was cooled to room temperature and the solid anilinium bromide that precipitated was filtered and discarded. The filtrate containing the product was concentrated and the resulting residue dissolved in CHCl₃ and subjected to column chromatography (silica gel) using CHCl₃:hexanes (4:1). ($R_f = 0.69$, 0.600 g, 33%) The pure isolated solid was dissolved in isopropyl ether (10 ml) and trifluoromethanesulfonic acid (1 equivalent) was added dropwise to yield the *N*-benzylanilinium as a white crystalline solid. **ESI-MS:** m/z [4-9 - OTf]⁺ calc. 297.0845, found 297.0835.

Table 4.22 – ¹H NMR of [4-9] in CD₃CN. MW = 296.239 g/mol

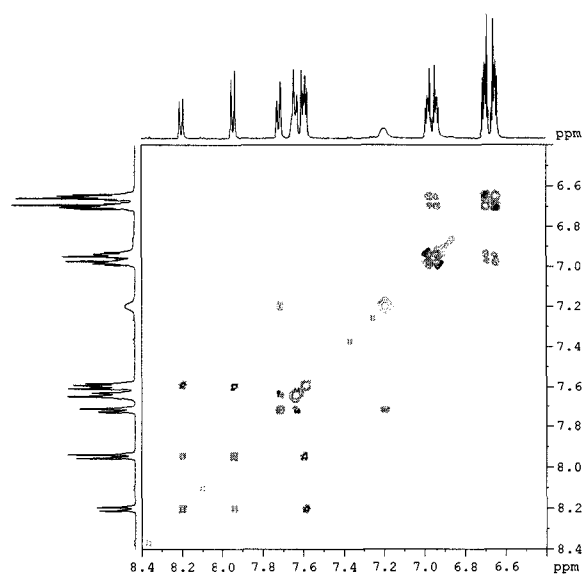
Proton	δ (ppm)	Multiplicity	# Protons	J (Hz)
a	8.17	d	2	$^3J_{ab} = 8.68$
b	7.56	d	2	$^3J_{ba} = 8.68$
c	4.51	d	2	$^3J_{cd} = 6.27$
d	5.66	br s	1	--
e	6.66	d	2	$^3J_{ef} = 8.63$
f	7.37	d	2	$^3J_{fe} = 8.63$

Table 4.23 – ^1H NMR of [4-9][OTf] in CD_3CN . $\text{MW}_{\text{OTf}} = 446.315$ g/mol

Proton	δ (ppm)	Multiplicity	# Protons	J (Hz)
a	8.23	d	2	$^3J_{ab} = 8.80$
b	7.62	d	2	$^3J_{ba} = 8.80$
c	4.76	s	2	--
d	--	--	2	--
e	7.61	d	2	$^3J_{ef} = 8.84$
f	7.85	d	2	$^3J_{fe} = 8.84$

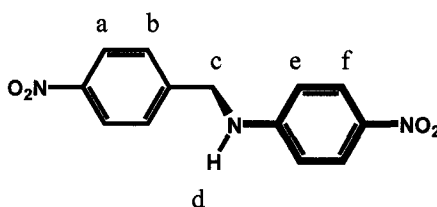
Titration of 4-9 monitoring chemical shift of H_c 

EXSY Spectrum of [4-9cDB24C8][OTf]



4.5.11 Synthesis of NO₂BnAnNO₂ [4-10]

4-Nitroaniline (1.00 g, 7.24×10^{-3} mol) and 4-nitrobenzyl bromide (0.782 g, 3.62×10^{-3} mol) were dissolved in CH₃CN and refluxed for 24 hours. The reaction was cooled to room temperature and the solid anilinium bromide that precipitated was filtered and discarded. The filtrate containing the product was concentrated and the resulting residue dissolved in CHCl₃ and subjected to column chromatography (silica gel) using CHCl₃:hexanes (4:1). ($R_f = 0.27$, 0.360 g, 36%) The pure isolated solid was dissolved in isopropyl ether (10 ml) and trifluoromethanesulfonic acid (1 equivalent) was added dropwise to yield the *N*-benzylanilinium as a yellow crystalline solid. ESI-MS: m/z [4-10 - OTf]⁺ calc. 274.0822, found 274.0829.

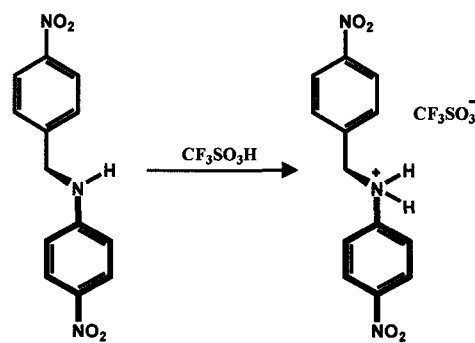
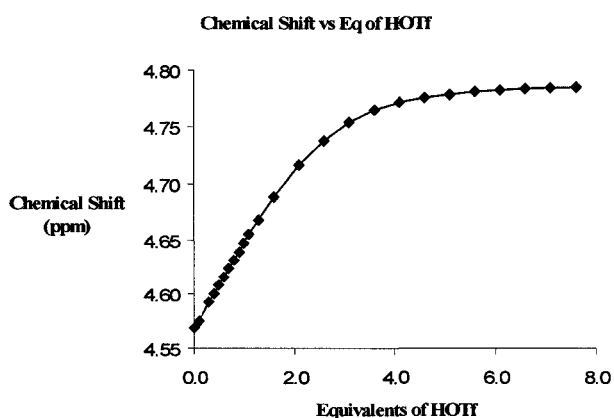
Table 4.24 – ¹H NMR of [4-10] in CD₃CN. MW = 273.241 g/mol

Proton	δ (ppm)	Multiplicity	# Protons	J (Hz)
a	8.18	d	2	$^3J_{ab} = 8.91$
b	7.56	d	2	$^3J_{ba} = 8.91$
c	4.57	s	2	--
d	6.21	br s	1	--
e	6.63	d	2	$^3J_{ef} = 9.27$
f	8.00	d	2	$^3J_{fe} = 9.27$

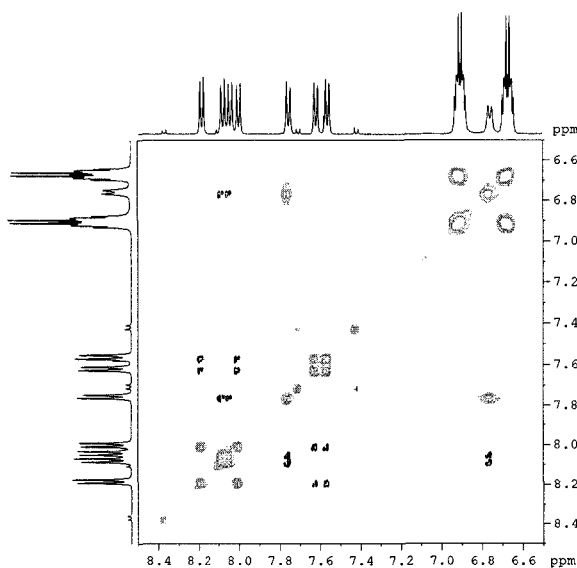
Table 4.25 – ¹H NMR of [4-10][OTf] in CD₃CN. MW_{OTf} = 423.317 g/mol

Proton	δ (ppm)	Multiplicity	# Protons	J (Hz)
a	8.32	d	2	³ J _{ab} = 8.74
b	7.63	d	2	³ J _{ba} = 8.74
c	4.78	s	2	--
d	9.50	br s	2	--
e	7.61	d	2	³ J _{ef} = 8.22
f	8.22	d	2	³ J _{fe} = 8.22

Titration of 4-10 monitoring chemical shift of H_c

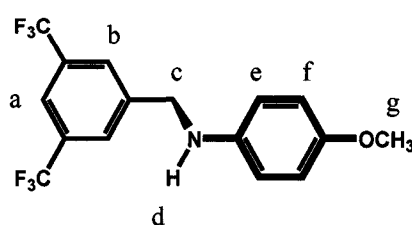


EXSY Spectrum of [4-10<DB24C8][OTf]



4.5.12 Synthesis of 3,5-BisCF₃BnAnOMe [4-11]

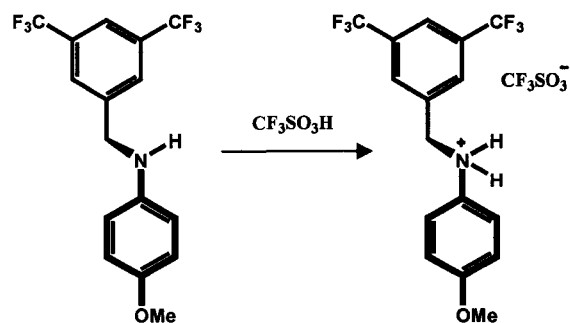
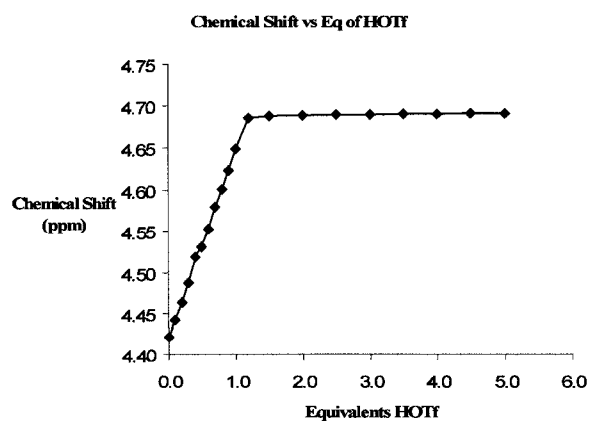
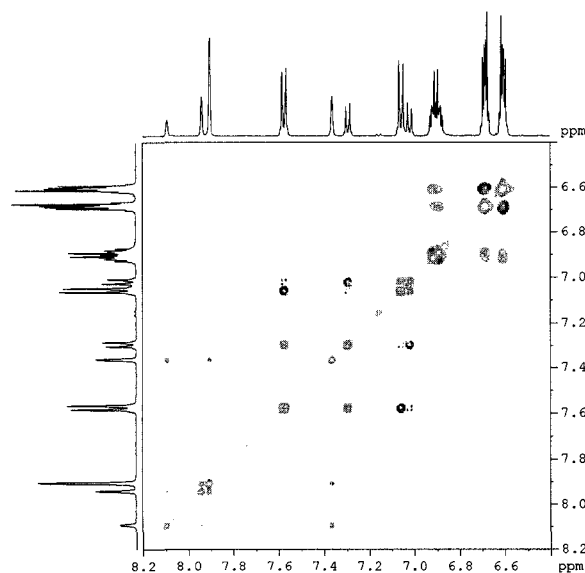
4-Methoxyaniline (2.00 g, 1.62×10^{-2} mol) and 3,5-dimethylbenzyl bromide (2.49 g, 8.12×10^{-3} mol) were dissolved in CH₃CN and refluxed for 24 hours. The reaction was cooled to room temperature and the solid anilinium bromide that precipitated was filtered and discarded. The filtrate containing the product was concentrated and the resulting residue dissolved in CHCl₃ and subjected to column chromatography (silica gel) using CHCl₃:hexanes (4:1). ($R_f = 0.76$, 1.41 g, 50%) The pure isolated solid was dissolved in isopropyl ether (10 ml) and trifluoromethanesulfonic acid (1 equivalent) was added dropwise to yield the *N*-benzylanilinium as a white crystalline solid. ESI-MS: m/z [4-11 - OTf]⁺ calc. 350.0971, found 350.0971.

Table 4.26 – ¹H NMR of [4-11] in CD₃CN. MW = 349.262 g/mol

Proton	δ (ppm)	Multiplicity	# Protons	J (Hz)
a	7.86	s	1	--
b	7.94	s	2	--
c	4.42	s	2	--
d	4.79	br s	1	--
e	6.72	d	2	$^3J_{ef} = 8.91$
f	6.55	d	2	$^3J_{fe} = 8.91$
g	3.66	s	3	--

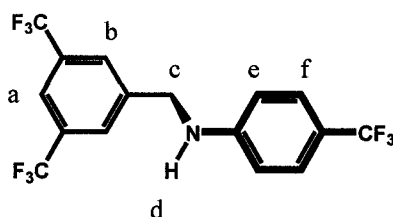
Table 4.27 – ^1H NMR of [4-11][OTf] in CD_3CN . $\text{MW}_{\text{OTf}} = 499.311$ g/mol

Proton	δ (ppm)	Multiplicity	# Protons	J (Hz)
a	8.09	s	1	--
b	7.95	s	2	--
c	4.69	br s	2	--
d	9.09	br s	2	--
e	7.31	d	2	$^3J_{\text{ef}} = 8.98$
f	7.03	d	2	$^3J_{\text{fe}} = 8.98$
g	3.81	s	3	--

Titration of 4-11 monitoring chemical shift of H_c EXSY Spectrum of [4-11 \subset DB24C8][OTf]

4.5.13 Synthesis of 3,5-BisCF₃BnAnCF₃ [4-12]

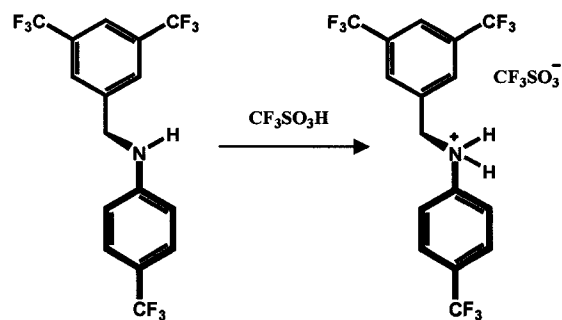
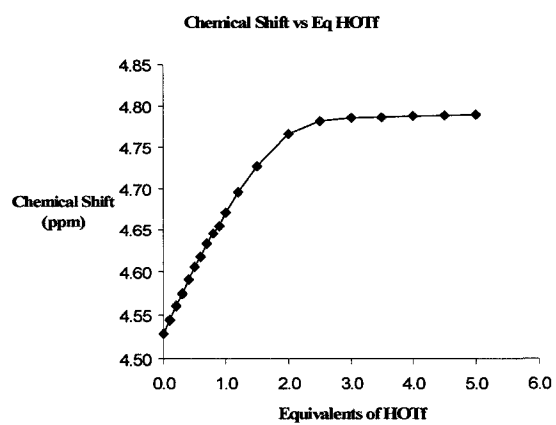
4-Trifluoromethylaniline (2.00 g, 1.24×10^{-2} mol) and 3,5-dimethylbenzyl bromide (1.91 g, 6.21×10^{-3} mol) were dissolved in CH₃CN and refluxed for 24 hours. The reaction was cooled to room temperature and the solid anilinium bromide that precipitated was filtered and discarded. The filtrate containing the product was concentrated and the resulting residue dissolved in CHCl₃ and subjected to column chromatography (silica gel) using CHCl₃:hexanes (4:1) ($R_f = 0.83$, 1.46 g, 61%). The pure isolated solid was dissolved in isopropyl ether (10 ml) and trifluoromethanesulfonic acid (1 equivalent) was added dropwise to yield the *N*-benzylanilinium as a white crystalline solid. ESI-MS: m/z [4-12 - OTf]⁺ calc. 388.0742, found 388.0743.

Table 4.28 – ¹H NMR of [4-12] in CD₃CN. MW = 387.235 g/mol

Proton	δ (ppm)	Multiplicity	# Protons	J (Hz)
a	7.89	s	1	--
b	7.93	s	2	--
c	4.52	d	2	--
d	6.65	br s	1	--
e	6.68	d	2	$^3J_{ef} = 8.49$
f	7.39	d	2	$^3J_{fe} = 8.49$

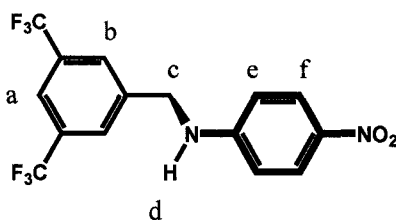
Table 4.29 – ^1H NMR of [4-12][OTf] in CD_3CN . $\text{MW}_{\text{OTf}} = 537.261$ g/mol

Proton	δ (ppm)	Multiplicity	# Protons	J (Hz)
a	8.10	s	1	--
b	7.96	s	2	--
c	4.78	s	2	--
d	--	--	2	--
e	7.58	d	2	$^3J_{\text{ef}} = 8.36$
f	7.85	d	2	$^3J_{\text{fe}} = 8.36$

Titration of 4-12 monitoring chemical shift of H_c 

4.5.14 Synthesis of 3,5-BisCF₃BnAnNO₂ [4-13]

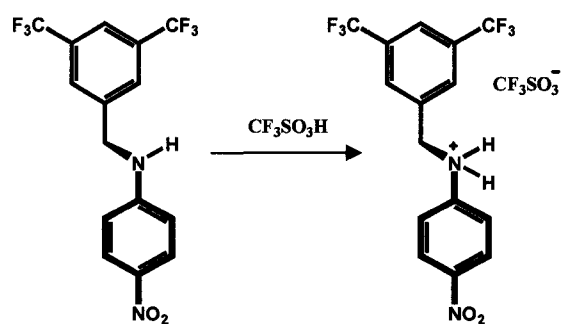
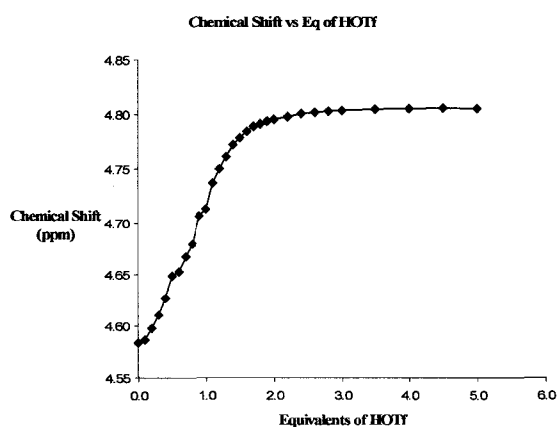
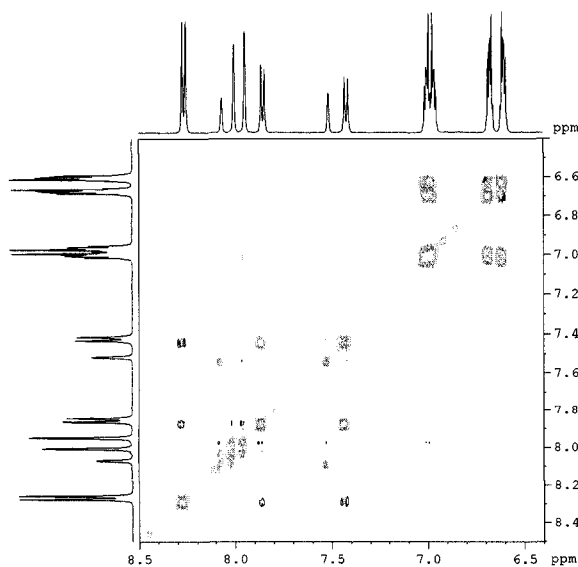
4-Nitroaniline (0.900 g, 6.51×10^{-3} mol) and 3,5-dimethylbenzyl bromide (1.00 g, 3.26×10^{-3} mol) were dissolved in CH₃CN and refluxed for 48 hours. The reaction was cooled to room temperature. The product precipitated as a yellow solid and was collected by vacuum filtration (0.518 g, 44%). The pure isolated solid was dissolved in isopropyl ether (10 ml) and trifluoromethanesulfonic acid (1 equivalent) was added dropwise to yield the *N*-benzylanilinium as a pale yellow crystalline solid. ESI-MS: m/z [4-13 - OTf]⁺ calc. 365.0719, found 365.0735.

Table 4.30 – ¹H NMR of [4-13] in CD₃CN. MW = 364.243 g/mol

Proton	δ (ppm)	Multiplicity	# Protons	J (Hz)
a	7.91	s	1	--
b	7.93	s	2	--
c	4.59	d	2	$^3J_{cd} = 6.20$
d	6.15	br s	1	--
e	6.65	d	2	$^3J_{ef} = 8.21$
f	8.02	d	2	$^3J_{fe} = 8.21$

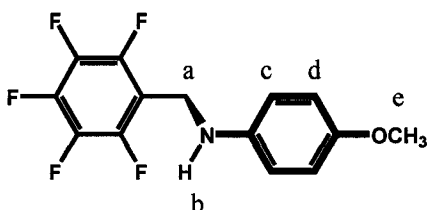
Table 4.31 – ^1H NMR of [4-13][OTf] in CD_3CN . $\text{MW}_{\text{OTf}} = 514.313$ g/mol

Proton	δ (ppm)	Multiplicity	# Protons	J (Hz)
a	8.12	s	1	--
b	8.02	s	2	--
c	4.81	s	2	--
d	--	--	2	--
e	7.67	d	2	$^3J_{ef} = 9.03$
f	8.35	d	2	$^3J_{fe} = 9.03$

Titration of 4-13 monitoring chemical shift of H_c EXSY Spectrum of [4-13 c DB24C8][OTf]

4.5.15 Synthesis of C₆F₅BnAnOMe [4-14]

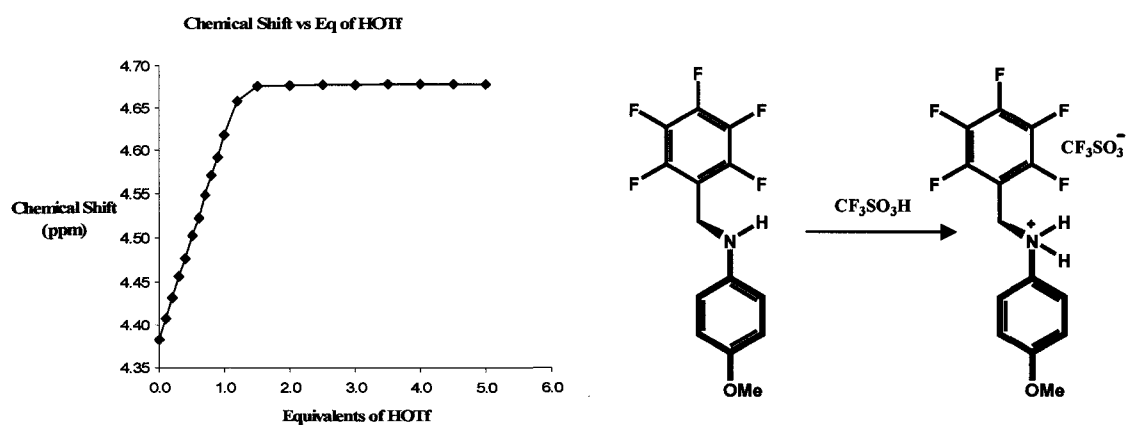
4-Methoxyaniline (0.944 g, 7.66×10^{-3} mol) and pentafluorobenzyl bromide (1.00 g, 3.83×10^{-3} mol) were dissolved in CH₃CN and refluxed for 24 hours. The reaction was cooled to room temperature and the solid anilinium bromide that precipitated was filtered and discarded. The filtrate containing the product was concentrated and the resulting residue dissolved in CHCl₃ and subjected to column chromatography (silica gel) using CHCl₃:hexanes (4:1). ($R_f = 0.67$, 1.01 g, 86%) The pure isolated solid was dissolved in isopropyl ether (10 ml) and trifluoromethanesulfonic acid (1 equivalent) was added dropwise to yield the *N*-benzylanilinium as a white crystalline solid. **ESI-MS: m/z [4-14 - OTf]⁺ calc. 304.0756, found 304.0767.**

Table 4.32 – ¹H NMR of [4-14] in CD₃CN. MW = 303.221 g/mol

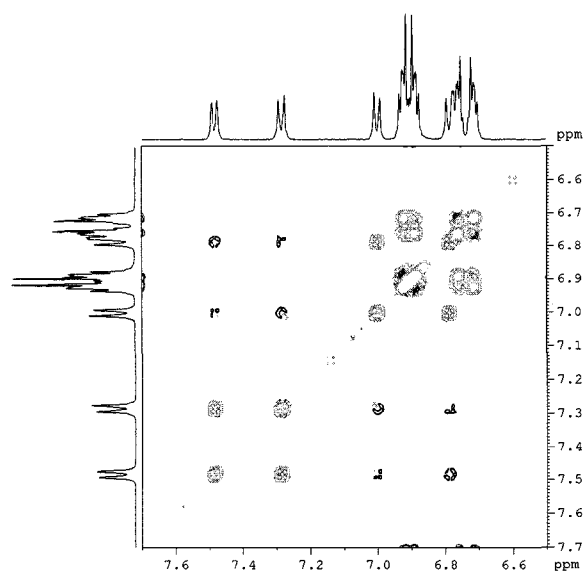
Proton	δ (ppm)	Multiplicity	# Protons	J (Hz)
a	4.41	s	2	--
b	4.41	s	1	--
c	6.77	d	2	$^3J_{cd} = 9.07$
d	6.67	d	2	$^3J_{dc} = 9.07$
e	3.70	s	3	--

Table 4.33 – ^1H NMR of [4-14][OTf] in CD_3CN . $\text{MW}_{\text{OTf}} = 453.297$ g/mol

Proton	δ (ppm)	Multiplicity	# Protons	J (Hz)
a	4.70	s	2	--
b	9.21	s	2	--
c	7.34	d	2	$^3J_{\text{cd}} = 9.00$
d	7.04	d	2	$^3J_{\text{dc}} = 9.00$
e	3.84	s	3	--

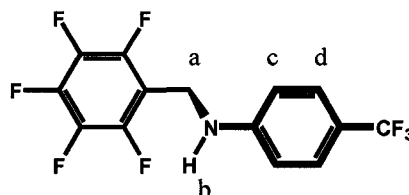
Titration of 4-14 monitoring chemical shift of H_a 

EXSY Spectrum of [4-14cDB24C8][OTf]



4.5.16 Synthesis of C₆F₅BnAnCF₃ [4-15]

4-Trifluoromethylaniline (1.00 g, 6.21 × 10⁻³ mol) and pentafluorobenzyl bromide (0.810 g, 3.10 × 10⁻³ mol) were dissolved in CH₃CN and refluxed for 24 hours. The reaction was cooled to room temperature and the solid anilinium bromide that precipitated was filtered and discarded. The filtrate containing the product was concentrated and the resulting residue dissolved in CHCl₃ and subjected to column chromatography (silica gel) using CHCl₃:hexanes (4:1). (R_f = 0.83, 0.864 g, 41%) The pure isolated solid was dissolved in isopropyl ether (10 ml) and trifluoromethanesulfonic acid (1 equivalent) was added dropwise to yield the *N*-benzylanilinium as a white crystalline solid. **ESI-MS**: *m/z* [4-15 - OTf]⁺ calc. 342.0524, found 342.0532.

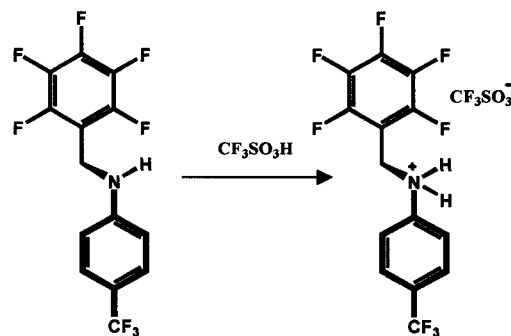
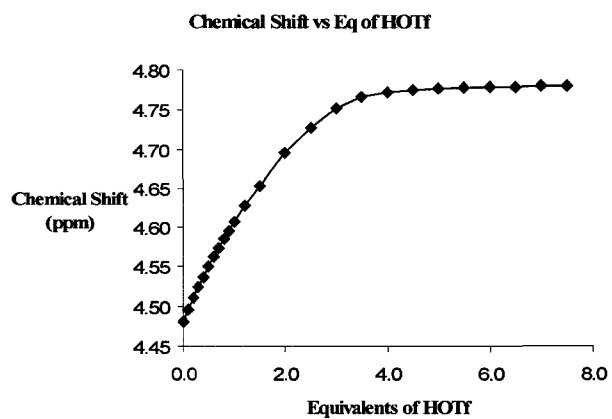
Table 4.34 – ¹H NMR of [4-15] in CD₃CN. MW = 341.194 g/mol

Proton	δ (ppm)	Multiplicity	# Protons	<i>J</i> (Hz)
a	4.48	d	2	³ <i>J</i> _{ab} = 6.43
b	5.37	br s	1	--
c	6.75	d	2	³ <i>J</i> _{cd} = 8.66
d	7.42	d	2	³ <i>J</i> _{dc} = 8.66

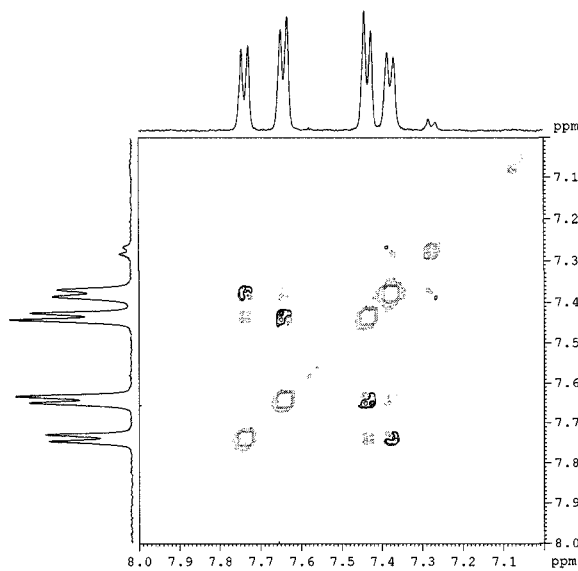
Table 4.35 – ¹H NMR of [4-15][OTf] in CD₃CN. MW_{OTf} = 491.270 g/mol

Proton	δ (ppm)	Multiplicity	# Protons	<i>J</i> (Hz)
a	4.78	s	2	--
b	--	--	2	--
c	7.61	d	2	³ <i>J</i> _{cd} = 8.53
d	7.85	d	2	³ <i>J</i> _{dc} = 8.53

Titration of 4-15 monitoring chemical shift of H_a

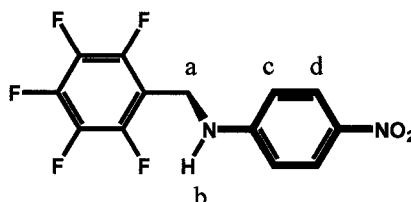


EXSY Spectrum of [4-15<DB24C8][OTf]



4.5.17 Synthesis of C₆F₅BnAnNO₂ [4-16]

4-Nitroaniline (2.00 g, 1.45×10^{-2} mol) and 4-pentafluorobenzyl bromide (1.89 g, 7.24×10^{-3} mol) were dissolved in CH₃CN and refluxed for 24 hours. The reaction was cooled to room temperature and the solid anilinium bromide that precipitated was filtered and discarded. The filtrate containing the product was concentrated and the resulting residue dissolved in CHCl₃ and subjected to column chromatography (silica gel) using CHCl₃:hexanes (4:1). (*R_f* = 0.57, 0.937g, 41%) The pure isolated solid was dissolved in isopropyl ether (10 ml) and trifluoromethanesulfonic acid (1 equivalent) was added dropwise to yield the *N*-benzylanilinium as a pale yellow crystalline solid. ESI-MS: *m/z* [4-16 - OTf]⁺ calc. 319.0500, found 319.0494.

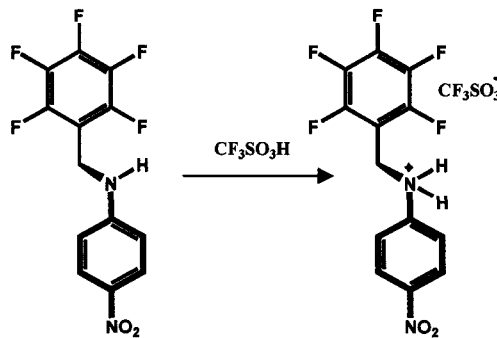
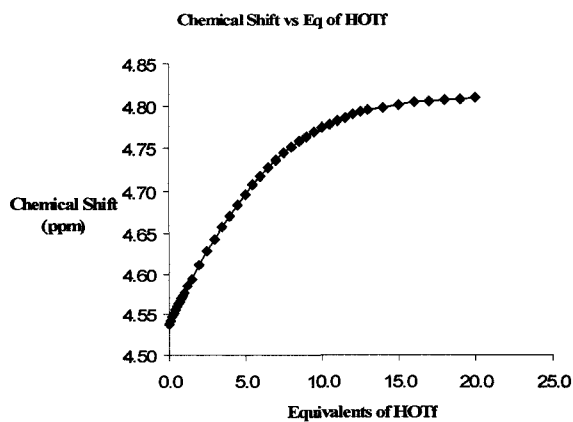
Table 4.36 – ¹H NMR of [4-16] in CD₃CN. MW_{OTf} = 318.196 g/mol

Proton	δ (ppm)	Multiplicity	# Protons	<i>J</i> (Hz)
a	4.53	d	2	³ <i>J</i> _{ab} = 6.22
b	5.97	br s	1	--
c	6.70	d	2	³ <i>J</i> _{cd} = 9.22
d	8.04	d	2	³ <i>J</i> _{dc} = 9.22

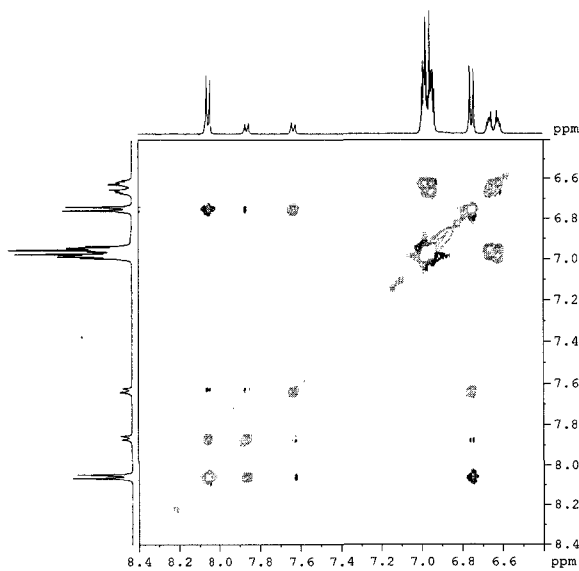
Table 4.37 – ¹H NMR of [4-16][OTf] in CD₃CN. MW_{OTf} = 468.272 g/mol

Proton	δ (ppm)	Multiplicity	# Protons	<i>J</i> (Hz)
a	4.81	s	2	--
b	--	--	2	--
c	7.67	d	2	³ <i>J</i> _{cd} = 8.95
d	8.33	d	2	³ <i>J</i> _{dc} = 8.95

Titration of 4-16 monitoring chemical shift of H_a



EXSY Spectrum of [4-16 \subset DB24C8][OTf]



CHAPTER 5

[2]Rotaxane Molecular Shuttles

5.1 INTRODUCTION

In a [2]rotaxane molecular shuttle, there are two recognition sites on the thread for the ring to occupy. As a result, there exists the possibility of two translational isomers. The bis(dipyridinium)ethane/**24C8** motif has been incorporated into molecular shuttles, where both recognition sites were bis(pyridinium)ethane based.^{46, 48} The first description of a shuttle using this motif was degenerate, consisting of two identical 1,2-bis(4,4'-dipyridinium)ethane sites capped with *t*-butylbenzyl stoppers (one blue and one green) and **DB24C8** as the macrocycle (Figure 5.1). At room temperature, the ¹H NMR spectrum showed that the crown ether was shuttling between the two sites as there was only one set of proton resonances. VT ¹H NMR spectroscopy determined coalescence to occur at 20°C and the rate of exchange between the two equally populated states was calculated to be 320 s⁻¹ with a $\Delta G^\ddagger = 57.5$ kJ/mol. A similar, but non-degenerate, shuttle was studied where one of the *t*-butylbenzyl capped dipyridinium ends was substituted with *t*-butylpyridine (Figure 5.2). In this shuttle, coalescence occurred at 0°C with an exchange rate of 222 s⁻¹ and $\Delta G^\ddagger = 54.3$ kJ/mol. Integration of the peaks in the limiting spectrum allowed for the determination of the isomer ratios which was found to be 2:1, with the 1,2-bis(4,4'-dipyridinium)ethane site (blue site) being favoured over the 1-(4,4'-dipyridinium)-2-(*t*-butylpyridinium)ethane site (green site). Although a population

difference was introduced by making the two recognition sites different, there is no control mechanism incorporated into the design of the shuttle.

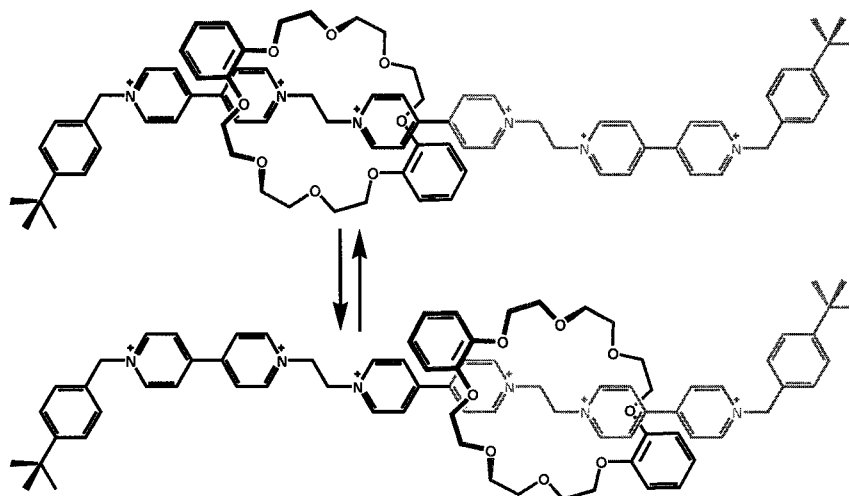


Figure 5.1 – Degenerate [2]rotaxane molecular shuttle.

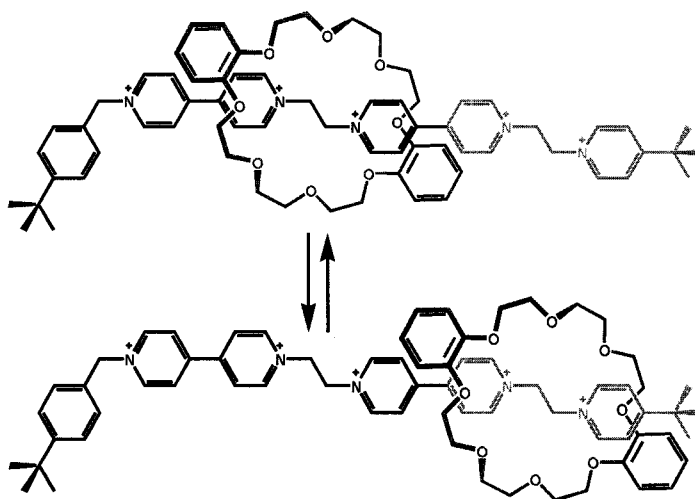


Figure 5.2 – Non-degenerate [2]rotaxane molecular shuttle.

In Chapter 4, the benzylianium recognition site was presented as a hybrid between the well-established dibenzylammonium and bis(pyridinium)ethane binding motifs (Figure 4.1). The benzylianium combined the strong hydrogen bonding capabilities and acid/base control of the dibenzylammonium with the structural properties

and enhanced π -stacking properties of bis(pyridinium)ethane. In Chapter 3, it was discussed how electronic control over the complexation and decomplexation of the [2]pseudorotaxane system was accompanied by a colour change due to the *ON/OFF* switching of an intramolecular charge transfer. It seemed reasonable to incorporate both properties into a [2]rotaxane molecular shuttle. The proposed system consists of two recognition sites, one a bis(pyridinium)ethane, the other a benzylianium, **DB24C8** as the macrocyclic ring, as well as a chromophoric unit, 4-pyridiniumaniline. Acid/base will be used as a means of chemically controlling the position of the ring.

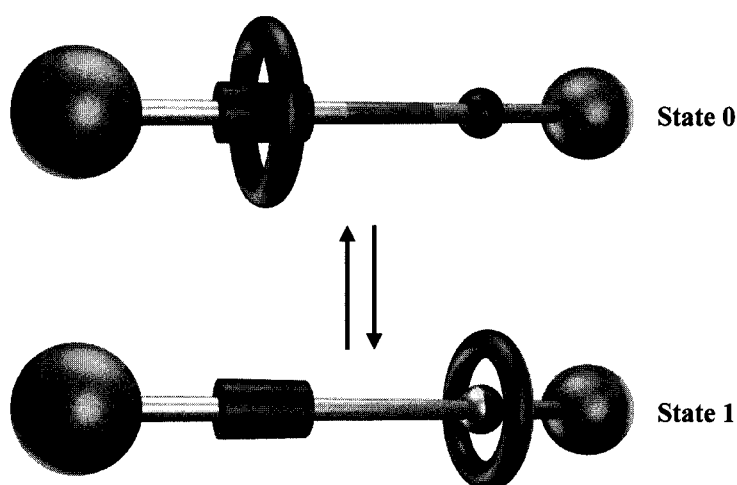


Figure 5.3 – Illustration of proposed [2]rotaxane molecular shuttle.

5.2 SYNTHESIS AND STRUCTURAL CHARACTERIZATION

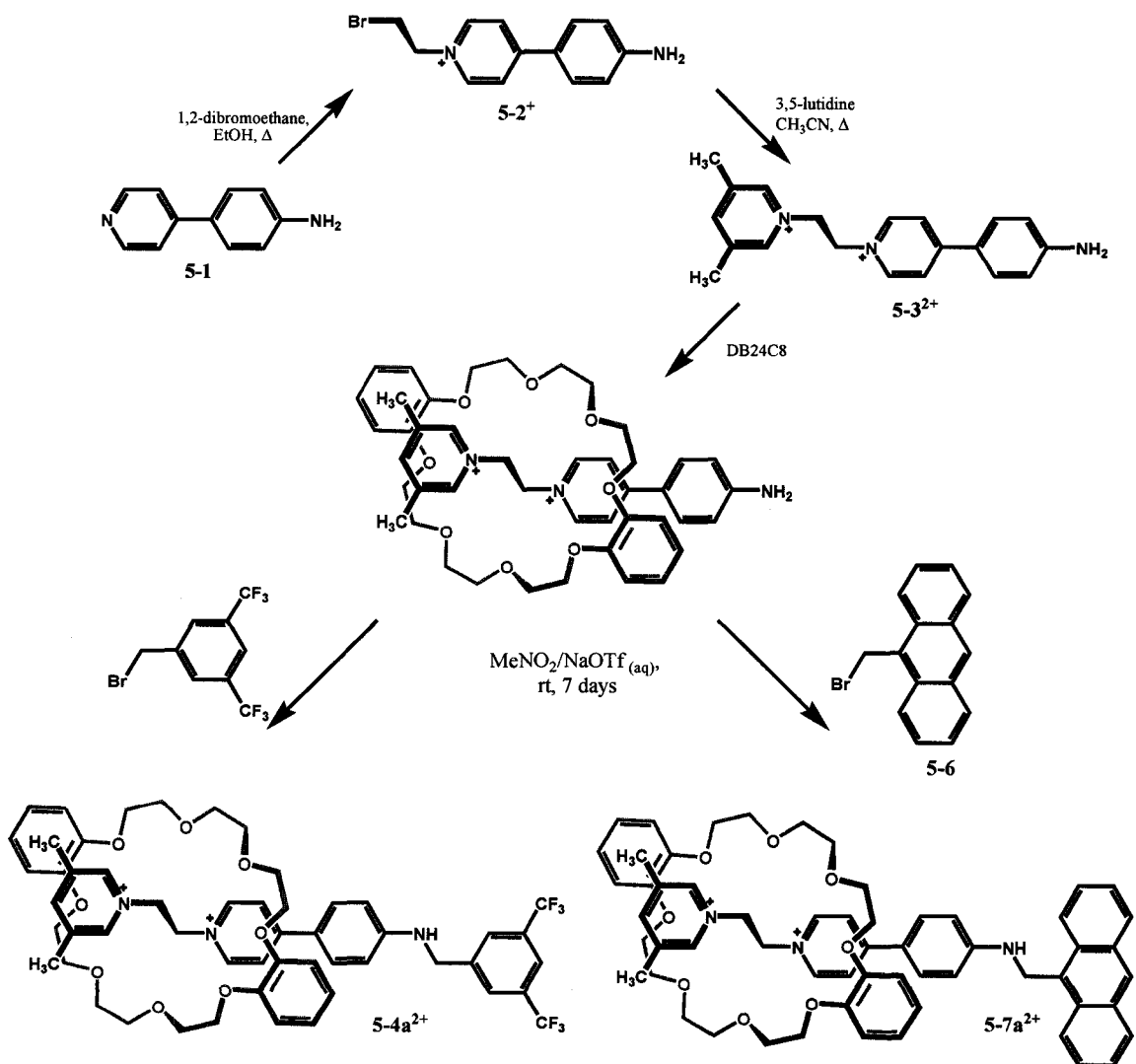
5.2.1 Synthesis

The bis(pyridinium)ethane site was constructed first. Beginning with a Suzuki coupling reaction, 4-pyridylaniline (**5-1**) was synthesized and then subsequently reacted with 1,2-dibromoethane to make **5-2⁺**. Further reaction with 3,5-lutidine, which also

conveniently acts as a stopper, gave **5-3²⁺**. Once the bis(pyridinium)ethane site was intact, it was combined with five equivalents of **DB24C8** and half an equivalent of one of various benzyl bromide compounds to give the [2]rotaxane molecular shuttle (Scheme 5.1). As mentioned in Chapter 4, one equivalent of the aniline is consumed as a base as the other equivalent forms the benzylianium site. The excess crown is added to favour [2]pseudorotaxane formation. Since only one recognition site is intact when the pseudorotaxane is formed and the second recognition site is not established until the rotaxane is capped, only the [2]rotaxane is synthesized. This is synthetically important because separation of [2]rotaxane and [3]rotaxane is not required as it was in the examples mentioned at the beginning of this chapter.^{46, 48} The [3]rotaxane, although it may give pertinent information, is not a viable switch as both recognition sites are occupied.

Part of the synthetic attractiveness of this system lies in the ability to incorporate different properties into the shuttle simply by changing the benzyl bromide stoppering group. 3,5-Bis(trifluoromethyl)benzyl bromide and 9-bromomethylantracene (**5-6**) are used as stoppering groups to prepare **5-4a²⁺** and **5-7a²⁺**, respectively. Furthermore, an intramolecular charge transfer between the electron rich aniline nitrogen and the positively charged pyridinium nitrogen generates an intense yellow colour. Many features have been incorporated into the design of this molecular system. These features and the different ways of monitoring the mechanical shuttling movements will be examined.

Throughout this chapter, compound numbers followed by an “a” signify non-protonated species whereas those followed by a “b” signify the protonated species.



Scheme 5.1 – Synthetic scheme for the synthesis of the [2]rotaxane molecular shuttles **5-4a²⁺** and **5-7a²⁺**.

5.2.2 ¹H NMR Spectroscopy

Figure 5.4 shows the ¹H NMR spectra of capped thread **5-5a²⁺** and [2]rotaxane **5-4a²⁺** in CD₃CN illustrating typical bis(pyridinium)ethane interactions with **DB24C8**. The ethylene protons **d** and **e** as well as the *ortho* pyridinium protons **c** and **f** shift downfield since they are involved in hydrogen bonding with the crown ether. The proton resonances **b**, **g** and **h** shift upfield due to π -stacking interactions caused by the ring currents of the aromatic rings on the crown ether. Interestingly, the protons on the

benzylaniline side of the thread **i**, **k**, **l** and **m** do not shift at all. This indicates that the crown is only situated on the bis(pyridinium)ethane site, which is as expected since unprotonated benzylaniline is incapable of complexing with **DB24C8**.

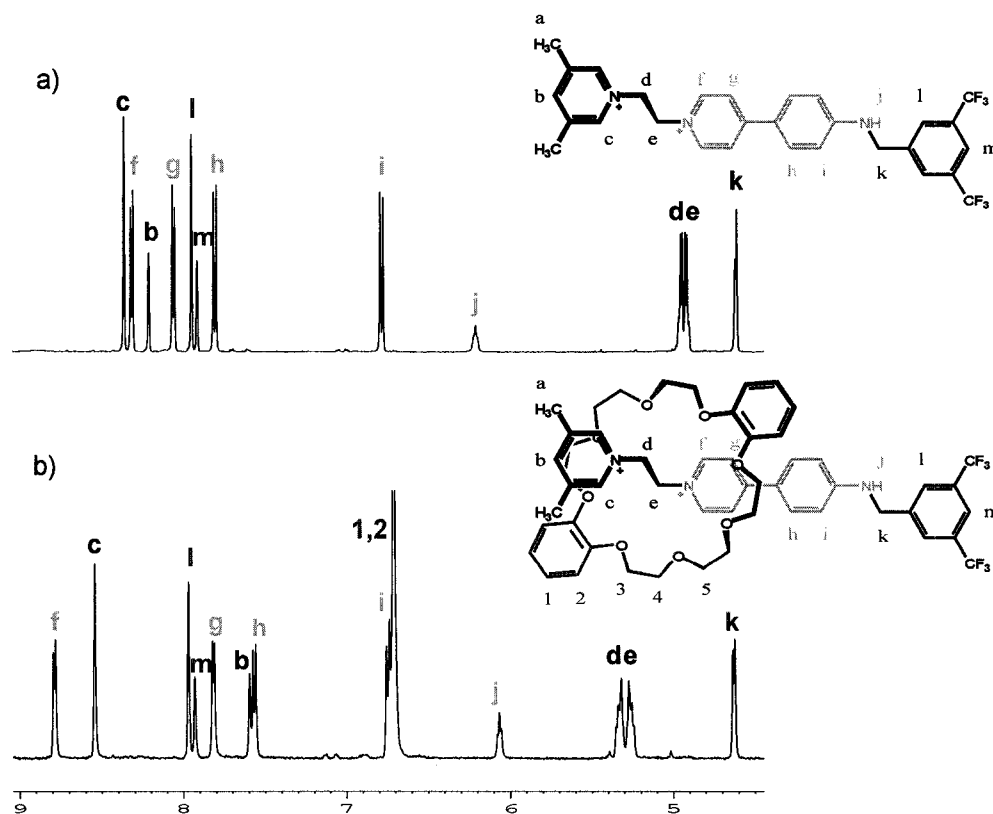


Figure 5.4 – Partial ^1H NMR spectra of a) capped thread **5-5a** $^{2+}$ and b) [2]rotaxane **5-4a** $^{2+}$ in CD_3CN at 500 MHz.

5.2.3 X-ray Crystallography

Single crystals of **[5-4a][OTf] $_2$** were grown by slow evaporation of an acetonitrile solution. Figure 5.5 illustrates the structure and shows the crown located at the bis(dipyridinium)ethane site, in a “C”-shaped conformation instead of the typical “S”-shaped conformation seen for most other crystal structures with this binding motif.^{37-46, 49}

However, this is similar to what was observed in the **[CF $_3$ BnAnCF $_3$ cDB24C8][OTf]**

structure in the previous chapter (Figure 4.7); the crown ether was in a “C” conformation over the anilinium ring of the thread. In that compound, the conformation was attributed to enhanced π -stacking with the more electron poor anilinium ring in an arrangement that supported stronger hydrogen bonding. Here, the intramolecular charge transfer from the aniline nitrogen to the pyridinium nitrogen results in reduction of the positive charge at the pyridinium nitrogen and an increase in the electron density of the aromatic ring which repels the electron rich catechol rings of the crown ether.^{100, 101} Consequently, the crown ether aromatic rings interact in a π -stacking manner with the lutidinium ring despite the presence of the methyl groups which could sterically encumber this conformation. The π -stacking distances as measured from centroid to centroid of the aromatic rings are 3.82 and 3.75 Å which are in the upper limits of distance for which π -stacking interactions are plausible. The dihedral angle C12-C13-C15-C16 is 11.1° which lends some credence to the proposed intramolecular charge transfer reasoning. Both bis(pyridinium)ethane and benzylanilinium recognition sites are in the *anti* conformation.

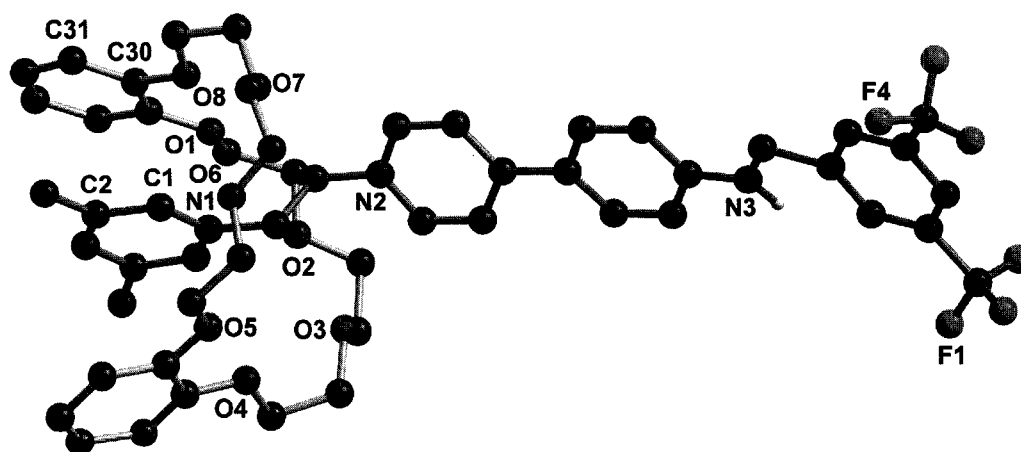
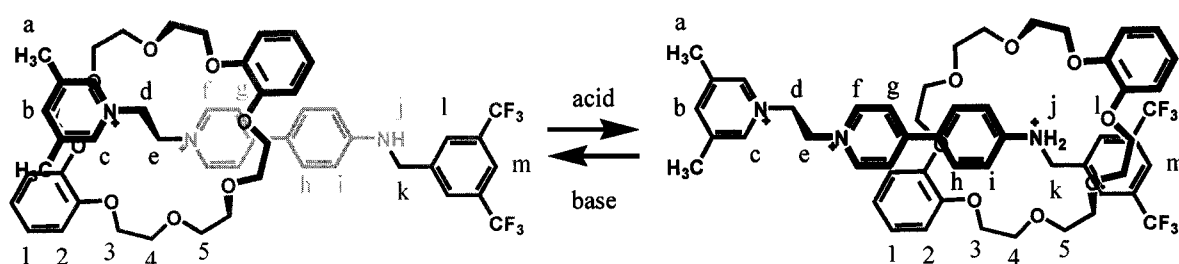


Figure 5.5 – X-ray crystal structure of [5-4a][OTf]₂ rotaxane; black = carbon, blue = nitrogen, red = oxygen, fluorine = green. Hydrogen atoms and triflate anions have been omitted for clarity.

5.3 ACID/BASE SHUTTLING PART I

5.3.1 ^1H NMR Spectroscopy

The colour scheme depicted in Scheme 5.2 divides the molecular shuttle into three sections. The blue is the bis(dipyridinium)ethane site, the green is the benzylianium site and the yellow/black is the 4-pyridiniumaniline chromophore unit that links the two sites together. As previously mentioned, when the benzylianium site is not protonated, **DB24C8** exclusively occupies the bis(pyridinium)ethane site (Scheme 5.2, left). However, once the thread is protonated, the crown has two viable sites with which it can interact. The ^1H NMR spectra in CD_3CN of the unprotonated (top) and protonated (bottom) molecular shuttles are shown in Figure 5.6. The spectrum of the protonated species (**5-4b $^{3+}$**) reveals that, at room temperature, the crown is shuttling between the two sites. Comparing the integration of peaks representing the benzyl CH_2 protons, **k**, when **DB24C8** is present at the benzylianium site (**k**) and when it is at the bis(pyridinium)ethane site (**k'**) reveals that **DB24C8** prefers the protonated benzylianium site in a ratio of 3:1.



Scheme 5.2 – Labeling scheme for [2]rotaxane molecular shuttle acid/base switch **5-4a $^{2+}$** and **5-4b $^{3+}$** .

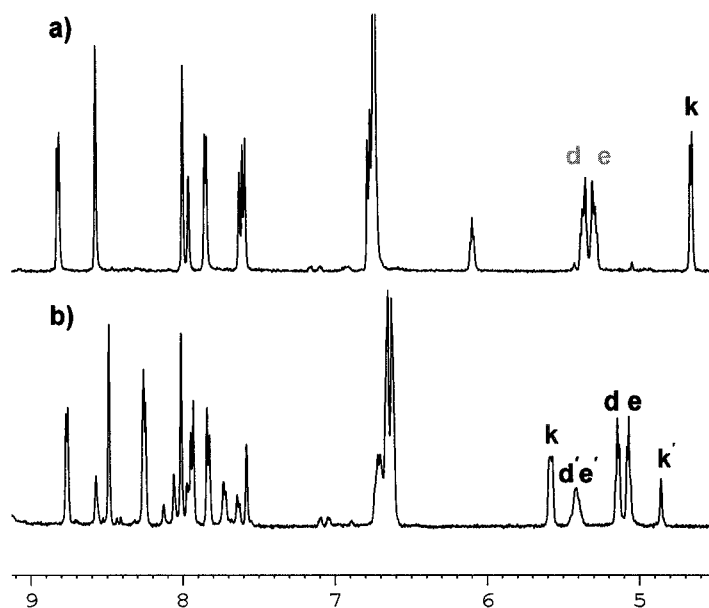


Figure 5.6 – ^1H NMR spectra of a) $5\text{-}4\text{a}^{2+}$ and b) $5\text{-}4\text{b}^{3+}$ in CD_3CN at 500 MHz and 30°C .

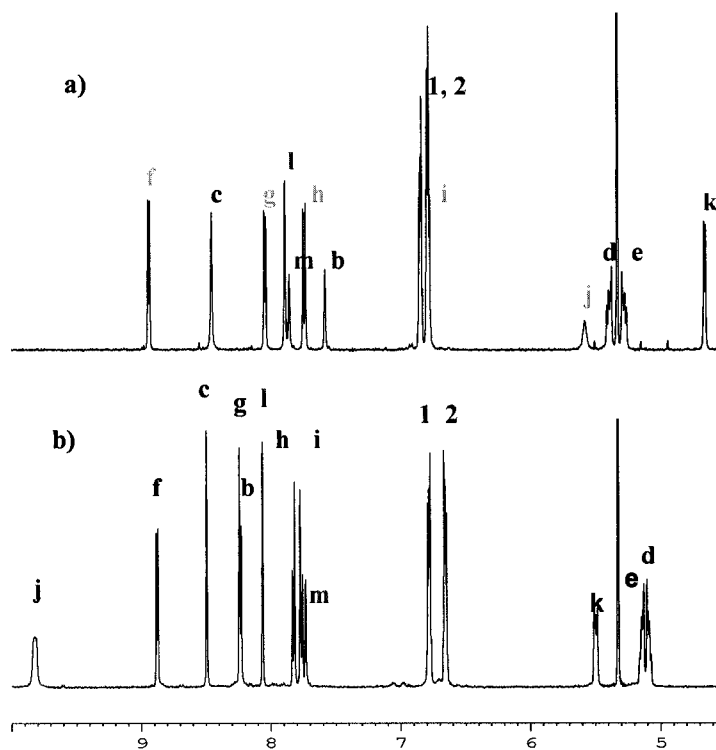


Figure 5.7 – ^1H NMR spectra of a) $5\text{-}4\text{a}^{2+}$ and b) $5\text{-}4\text{b}^{3+}$ in CD_2Cl_2 at 500 MHz and 30°C .

Figure 5.7 shows the ^1H NMR spectra in CD_2Cl_2 of unprotonated (top) and protonated (bottom) molecular shuttles. In the unprotonated spectrum, again, only one set of peaks is present indicating that the crown ether resides only on the bis(pyridinium)ethane site. In contrast to the CD_3CN scenario, the spectrum of the protonated shuttle in CD_2Cl_2 only has one set of peaks. In order to determine which site the crown is at, the chemical shifts in the CD_2Cl_2 ^1H NMR spectrum of protonated shuttle (**5-4b**³⁺) must be compared to the chemical shifts of the protonated capped thread (**5-5b**³⁺). Table 5.1 gives a tabulated comparison of these shifts. It shows that protons **f**, **c**, **b**, **d** and **e**, those located at the bis(pyridinium)ethane site, do not shift at all between the two spectra. This indicates that these protons are not interacting directly with the crown ether. Conversely, protons associated with the benzylianium site, **i**, **j**, **k** and **l** shift downfield whereas **h** and **m** shift upfield. The downfield shift is a result of hydrogen bonding interactions with the crown ether oxygen atoms and the upfield shift is due to π -stacking interactions between the electron rich crown aromatic rings and the electron poor aromatic rings of the thread. To summarize, the ^1H NMR spectra in CD_2Cl_2 of unprotonated and protonated molecular shuttles **5-4a**²⁺ and **5-4b**³⁺ give direct evidence that when the thread is unprotonated the crown resides only at the bis(pyridinium)ethane site and when the thread is protonated the crown resides only at the benzylianium site. This implies that in CD_2Cl_2 , molecular shuttle **5-4** demonstrates authentic bistability.

Addition of base returns the shuttle to its original state. The shuttle can be cycled by repeated addition of acid and base without significant degradation of the compound. This was confirmed by both ^1H NMR and UV-visible spectroscopic analysis.

Table 5.1 – Comparison of ^1H NMR Chemical Shifts in CD_2Cl_2 .

Proton	5-5a ²⁺	5-4a ²⁺	$\Delta\delta$	5-5b ³⁺	5-4b ³⁺	$\Delta\delta$
b	8.10	7.58	0.52	8.23	8.24	-0.01
c	9.21	8.45	0.76	8.47	8.49	-0.02
d	5.19	5.39	-0.20	5.10	5.09	0.01
e	5.14	5.27	-0.13	5.15	5.14	0.01
f	9.22	8.94	0.29	8.86	8.88	-0.02
g	8.07	8.04	0.04	8.32	8.23	0.08
h	7.79	7.74	0.05	8.02	7.83	0.19
i	6.80	6.78	0.02	7.66	7.77	-0.10
j	--	5.58	--	9.21	9.63	-0.42
k	4.64	4.66	-0.01	4.82	5.50	-0.68
l	7.86	7.89	-0.02	7.88	8.06	-0.18
m	7.86	7.85	0.01	8.05	7.73	0.32

5.3.2 ^{19}F NMR Spectroscopy

The incorporation of trifluoromethyl groups on the benzyl stopper on the benzylianium side of the thread offers the potential to use ^{19}F NMR spectroscopy as another method of monitoring the switching of the crown ether between recognition sites. Since fluorine atoms have nine electrons, in contrast to one electron for a hydrogen atom, fluorine has a higher sensitivity to its local environment than hydrogen. As a result, the chemical shift range of fluorine is much larger than for hydrogen. In fact, fluorine's range spans from about -300 ppm to 400 ppm.^{109, 110} Chemical shifts are reported with respect to CFCl_3 as the reference.

It has been established that in CD_2Cl_2 , the molecular shuttle shows complete bias for the crown to sit at a particular site depending on whether the thread is protonated or not. Based on this knowledge, the ^{19}F NMR spectra of the capped thread (**5-5**) and [2]rotaxane (**5-4**), both protonated and unprotonated, were run in CD_2Cl_2 . Not surprisingly, the chemical shift of the $-\text{CF}_3$ resonances of the unprotonated capped thread

and unprotonated [2]rotaxane were almost identical, -63.60 ppm and -63.54 ppm, respectively. As previously stated, the crown ether is stationed at the bis(pyridinium)ethane site when the thread is not protonated, thus the immediate chemical environment of the trifluoromethyl groups in the capped thread and in the [2]rotaxane are the same. Protonation of the capped thread results in an upfield shift of the CF_3 peak (-64.28 ppm) compared to the unprotonated capped thread (-63.60 ppm). Since the crown ether shuttles to the benzylianium site when the thread is protonated, there should be a difference in the chemical shift of the fluorine atoms between the protonated capped thread and the protonated [2]rotaxane. Indeed, the fluorine shift for protonated [2]rotaxane is located downfield at -63.34 ppm compared to the protonated capped thread resonance at -64.28 ppm. However, the overall chemical shift difference between unprotonated [2]rotaxane (-63.54 ppm) and protonated [2]rotaxane (-63.34 ppm) is 0.20 ppm which is insignificant considering that the chemical shift range for fluorine is over 700 ppm! Although the chemical shift is slightly sensitive to both the protonation of the thread and the presence of the crown ether, the effects seem to cancel each other out resulting in a less dramatic chemical shift difference when compared to the chemical shift of the unprotonated rotaxane (Figure 5.8).

Table 5.2 – Summary of ^{19}F chemical shifts for capped thread (5-5) and rotaxane (5-4)

Compound	^{19}F Chemical Shift
5-5a ²⁺	-63.60
5-5b ³⁺	-64.28
5-4a ²⁺	-63.54
5-4b ³⁺	-63.34

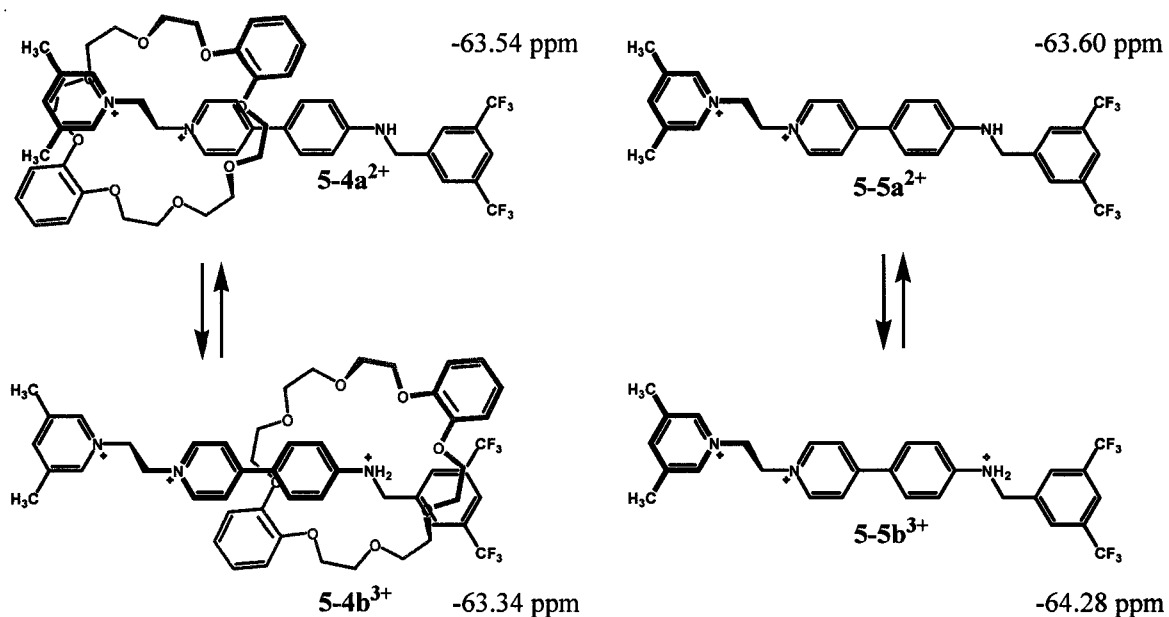


Figure 5.8 – Illustration showing relationship between structure and ^{19}F chemical shift.

5.3.3 UV-Visible Spectroscopy

Due to the strategic positioning of the 4-pyridiniumaniline chromophore unit, the movement of the crown from one site to the other upon protonation/deprotonation of the thread is accompanied by a dramatic colour change. As a consequence of the ICT between the aniline nitrogen and the pyridinium nitrogen when the thread is not protonated, the [2]rotaxane is an intense yellow colour. Upon protonation of the aniline nitrogen, which triggers the crown to move to the benzylianium site, the ICT is eliminated and the intense colour disappears.

Table 5.3 summarizes the data obtained from the UV-visible spectroscopy experiments. The molar absorptivities (ϵ) for **5-5a²⁺** in CH_2Cl_2 and CH_3CN were calculated to be 39,681 and 35,811 $\text{L cm}^{-1} \text{mol}^{-1}$, respectively, with the λ_{max} in both cases centered at ~ 415 nm. These values are comparable to those found for similar compounds.¹¹¹

The UV-visible spectrum of the [2]rotaxane **5-4a²⁺** in CH₂Cl₂ shows the ICT absorption band at $\lambda_{\text{max}} = 410$ nm. (Figure 5.9) Addition of acid gives **5-4b³⁺** with elimination of the ICT, hence the ICT absorption band disappears. Similarly, the UV-visible spectrum of **5-4a²⁺** in CH₃CN has λ_{max} centered at 407 nm (Figure 5.10). Again, when the rotaxane is protonated to give **5-4b³⁺**, the ICT band is eliminated. A weak charge transfer band, the result of interaction between the electron rich catechol rings of the crown ether and the electron poor pyridinium rings in the thread, should be present in the case where the ¹H NMR shows a 3:1 population ratio (*i.e.* in CH₃CN), however, the solutions are too dilute to see this interaction. The molar absorptivities of the chromophore in the rotaxanes in CH₂Cl₂ and CH₃CN are 28,224 and 25,342 L cm⁻¹ mol⁻¹, respectively. Both values are slightly lower than the chromophore in the capped thread, thus the crown has a hypochromic effect on the chromophore. The solvent does not appear to have any effect on the wavelength of maximum absorption, although it does seem to affect the absorption coefficient. In both the capped thread and the rotaxane, the absorption coefficients are slightly lower in the more polar solvent, CH₃CN.

Table 5.3 – Summary of UV-vis data for **5-5a²⁺ capped thread and **5-4a²⁺** rotaxane**

Compound	λ_{max}	Absorbance	ϵ (L cm ⁻¹ mol ⁻¹)
5-5a²⁺ CH ₂ Cl ₂	415	0.397	39,681
5-5a²⁺ CH ₃ CN	416	0.358	35,811
5-4a²⁺ CH ₂ Cl ₂	410	0.282	28,224
5-4a²⁺ CH ₃ CN	407	0.253	25,342

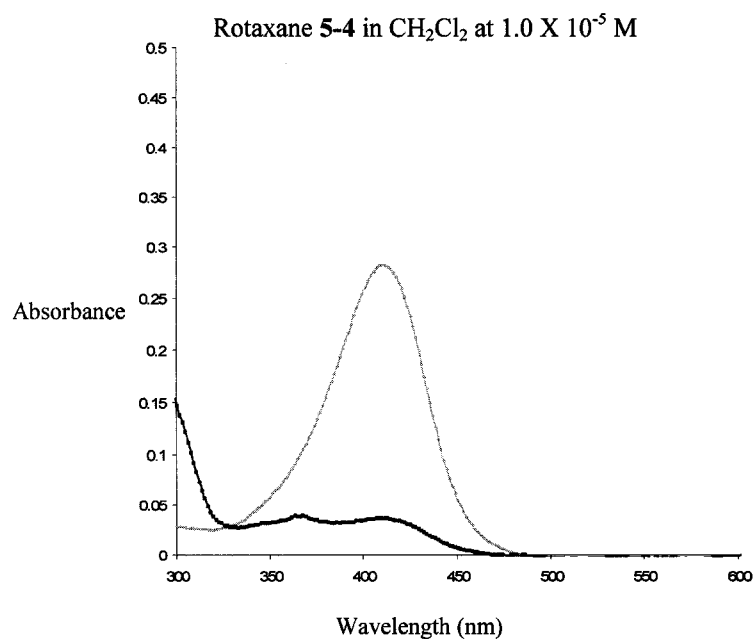


Figure 5.9 – UV-visible spectra of 5-4a²⁺ (yellow) and 5-4b³⁺ (black) [2]rotaxanes in CH₂Cl₂.

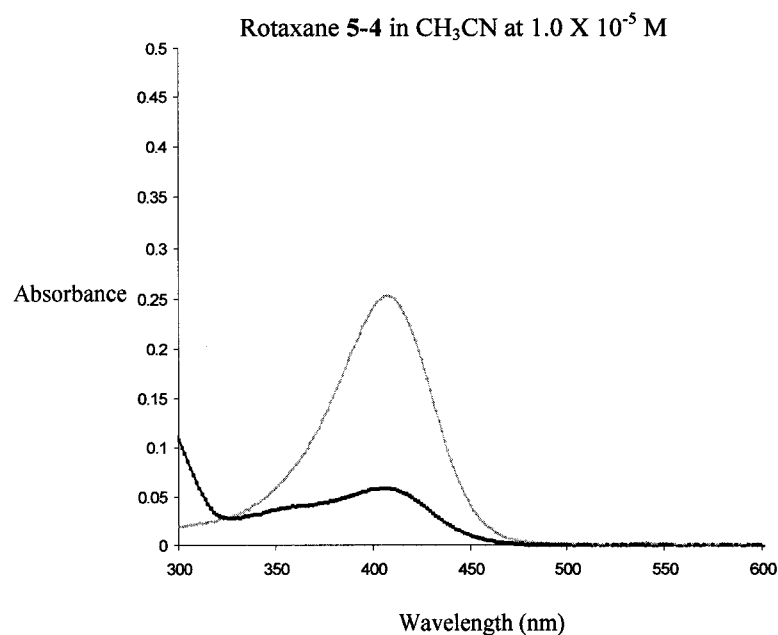


Figure 5.10– UV-visible spectra of 5-4a²⁺ (yellow) and 5-4b³⁺ (black) [2]rotaxanes in CH₃CN.

5.4 ACID/BASE SHUTTLING PART II

At this point, it has been discussed how the [2]rotaxane system with the aforementioned components demonstrates true bistability and how the position of the crown with respect to the thread can be monitored. ^1H NMR, ^{19}F NMR and UV-visible spectroscopies all provide a manner in which to determine at which site the crown is located. Apart from these analytical techniques, the switching is also observable to the naked eye because of the drastic change in colour between protonated and unprotonated states. It has been established that in a non-polar solvent, CH_2Cl_2 , the crown resides exclusively at the bis(pyridinium)ethane site when the rotaxane is not protonated and when the rotaxane is protonated, the crown sits exclusively at the benzylianium site.

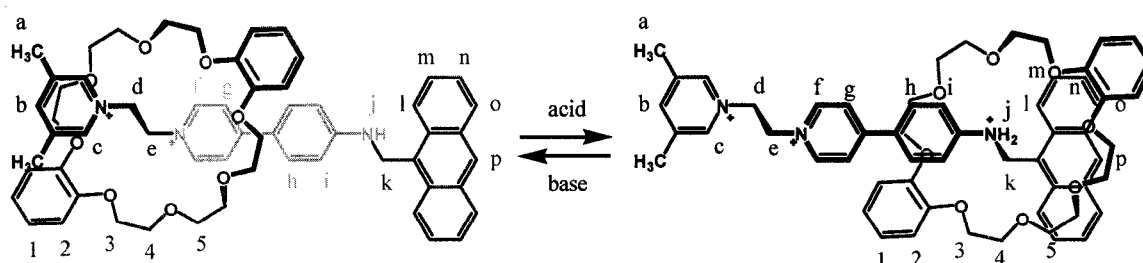
Part of the attractiveness of this system is that different properties can be incorporated fairly easily. It was of interest to further demonstrate this versatility by exchanging the 3,5-bis(trifluoromethyl)benzyl group for an anthracenyl group. The synthesis is exactly the same except 9-bromomethylantracene (**5-6**) is used as the bulky group in the last step which forms the rotaxane (Scheme 5.1). Anthracene introduces the ability to monitor the shuttling behaviour by fluorescence spectroscopy.

5.4.1 ^1H NMR Spectroscopy

Scheme 5.3 shows the labeling system for the [2]rotaxanes **5-7a**²⁺ and **5-7b**³⁺. The ^1H NMR spectra for the unprotonated and protonated rotaxanes in CD_3CN are shown in Figure 5.10. The features of these ^1H NMR spectra are similar to those outlined for rotaxane **5-4**. The unprotonated species **5-7a**²⁺ has only one set of peaks representing the co-conformation with the crown at the bis(pyridinium)ethane site. Similar to **5-4**, the addition of acid to a solution of **5-7a**²⁺ in CD_3CN , produces two sets of peaks with a ratio

of 9:1 for the crown at the benzylanilinium site over the bis(pyridinium)ethane site. Rotaxane **5-7** appears to be almost completely bistable even in acetonitrile. Protonation of the rotaxane results in downfield shifts of protons **j**, **k**, and **i** due to protonation of the aniline nitrogen and hydrogen bonding interactions with the crown ether. Protons **c**, **d**, **e** and **f** shift upfield since they are no longer involved in hydrogen bonding whereas **b** shifts downfield since it is no longer involved in π -stacking.

The spectra of **5-7a²⁺** and **5-7b³⁺** in CD₂Cl₂ show only one set of peaks. Again, this implies that the shuttle is completely bistable.



Scheme 5.3 – Labeling scheme for molecular shuttles **5-7a²⁺** and **5-7b³⁺**.

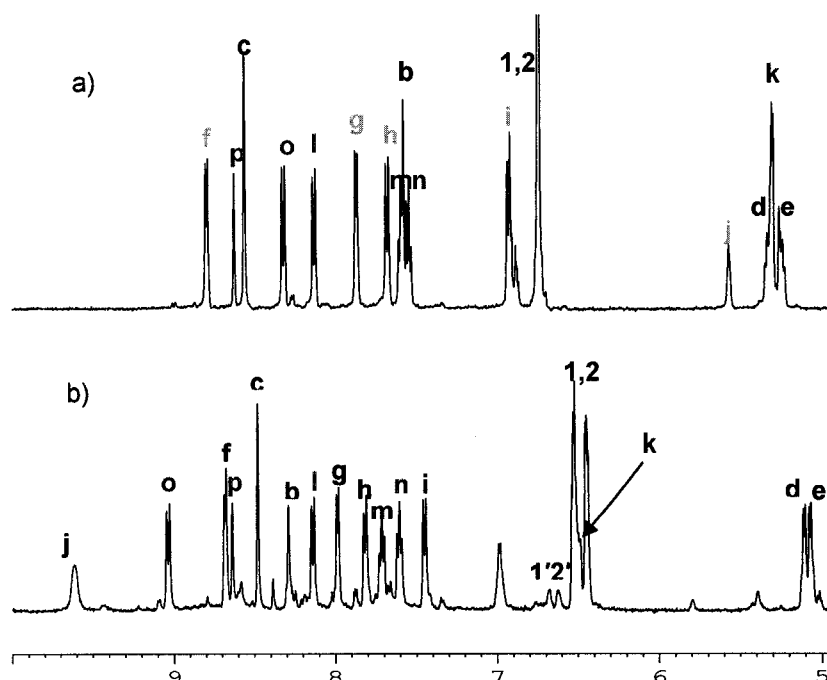


Figure 5.11 ¹H NMR spectrum of a) **5-7a²⁺** and b) **5-7b³⁺** in CD₃CN at 500 MHz and 30°C.

5.4.2 UV-Visible Spectroscopy

Table 5.4 summarizes the data and Figures 5.12 and 5.13 show the UV-visible spectra for rotaxanes **5-7a**²⁺ and **5-7b**³⁺ in CH₂Cl₂ and CH₃CN, respectively. The UV-visible spectra of **5-7a**²⁺/**5-7b**³⁺ show the same trends as the previous shuttle. The unprotonated species has a large absorption band centered on ~420 nm with large molar absorptivity values of 24,440 and 25,443 L cm⁻¹mol⁻¹ in CH₂Cl₂ and CH₃CN, respectively. Upon protonation of the thread, the ICT is eliminated. Without the ICT absorption band, three absorption maxima at 389 nm, 368 nm and 348 nm become apparent. These peaks are the absorption bands of the anthracene fragment which are masked by the ICT absorption band in the spectrum of the unprotonated species.

Table 5.4 – Summary of UV-visible data for 5-7a²⁺

Compound	λ_{\max} (nm)	Absorbance	Molar Absoptivity (L cm ⁻¹ mol ⁻¹)
5-7a ²⁺ (CH ₂ Cl ₂)	424	0.244	24440
5-7a ²⁺ (CH ₃ CN)	418	0.254	25443

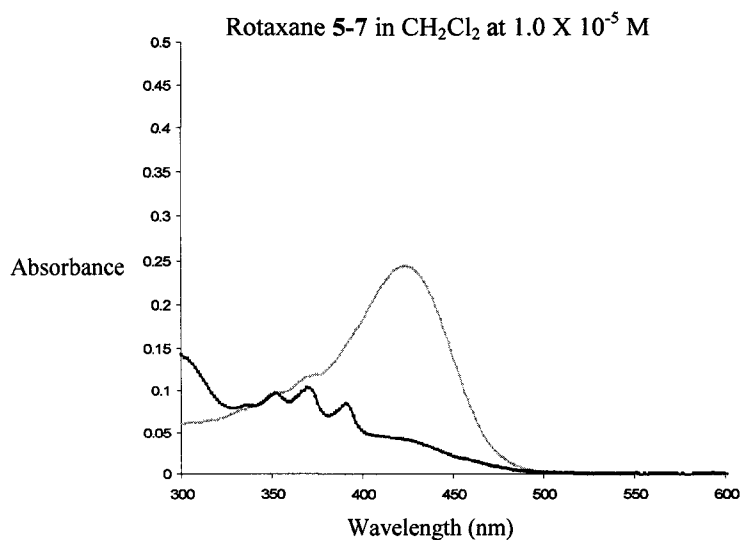


Figure 5.12 – UV-visible spectrum of 5-7a²⁺ (yellow) and **5-7b**³⁺ (black) OTf in CH₂Cl₂.

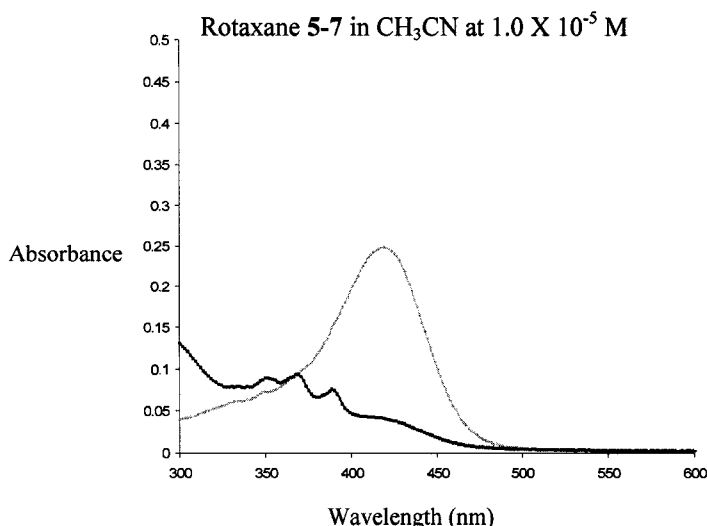


Figure 5.13 – UV-visible spectrum of **5-7a²⁺** (yellow) and **5-7b³⁺** (black) OTf in CH₃CN.

5.4.3 Fluorescence Spectroscopy

The property that makes rotaxane **5-7** different from **5-4** is the fluorescence of the anthracene fragment. From the absorption spectrum, it is known that anthracene has an absorption maximum at ~250 nm. Figures 5.14 and 5.15 depict the emission spectra of **5-7a²⁺** and **5-7b³⁺** in CH₃CN and CH₂Cl₂, respectively. Note that each spectrum has a sharp peak at 500 nm which is an artifact of the instrument used to record the data and occurs at double the excitation wavelength (250 nm). Excitation of **5-7a²⁺** results in a spectrum with stunted emission due to reductive quenching of fluorescence by the lone pair of electrons of the aniline nitrogen.⁹⁰ Protonation eliminates the quenching by the lone pair resulting in enhanced fluorescence as seen in the spectrum of **5-7b³⁺**.

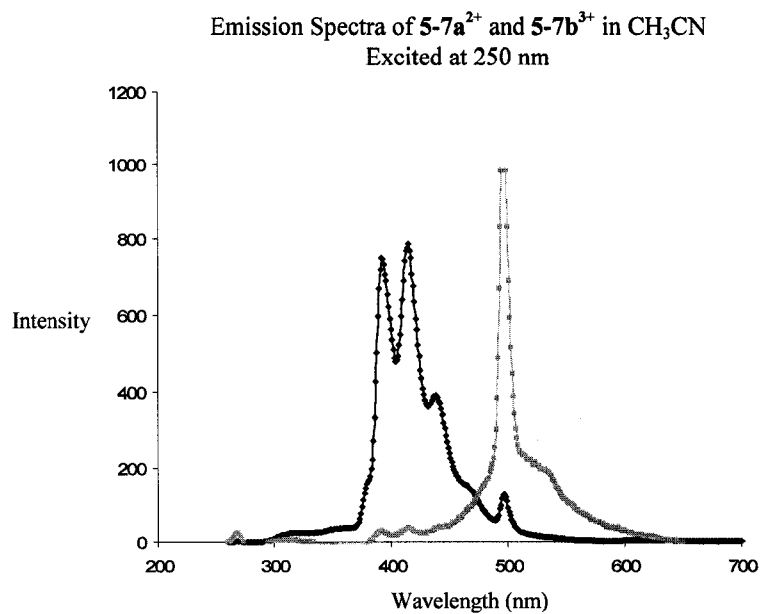


Figure 5.14 – Fluorescence emission spectra of 5-7a²⁺ (yellow) and 5-7b³⁺ (black) in CH₃CN at 1.0×10^{-5} M.

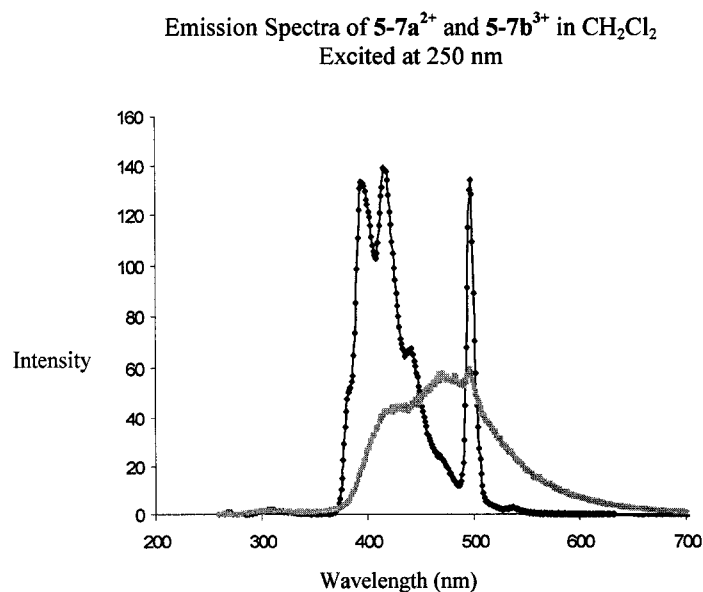


Figure 5.15 – Fluorescence emission spectra of 5-7a²⁺ (yellow) and 5-7b³⁺ (black) in CH₂Cl₂ at 1.0×10^{-5} M.

5.5 SUMMARY AND CONCLUSIONS

A molecular shuttle system consisting of bis(pyridinium)ethane and benzylanilinium recognition sites with **DB24C8** as the mobile fragment has been described. Also incorporated into the thread portion of the rotaxane are a chromophore unit, 4-pyridiniumaniline, as well as, bulky stoppers that possessed spectroscopic handles that can be exploited in order to monitor the position of the crown on the thread. Aside from ^1H NMR spectroscopy, the chromophore permitted monitoring by UV-visible spectroscopy; the 3,5-bis(trifluoromethyl)benzyl stopper permitted monitoring by ^{19}F NMR spectroscopy and the 9-methylantracenyl stopper by fluorescence spectroscopy. Analysis by these methods showed that when the rotaxane is not protonated, the crown resides exclusively at the bis(pyridinium)ethane recognition site, regardless of the solvent. This is a result of only one of the two sites being viable for interaction with the crown ether. In contrast, protonation converts the benzylanilinium into an attractive recognition site, which introduces competition between recognition sites. In CH_3CN , the crown prefers the benzylanilinium site in a 3:1 ratio for **5-4** and 9:1 for **5-7**. In CH_2Cl_2 , the crown resides exclusively at the benzylanilinium site. This means that in the non-polar solvent, this rotaxane system demonstrates complete bistability. Subsequent chapters will further demonstrate the versatility of this system as it is modified to be incorporated into [2]catenanes as well as to potentially form self-assembled monolayers and extended networks.

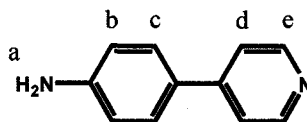
5.6 EXPERIMENTAL

5.6.1 General Comments

4-(4,4,5,5-Tetramethyl-1,3,2-dioxaborolan-2-yl)aniline, 4-bromopyridine hydrochloride, sodium carbonate, 9-methanolanthracene and phosphorus tribromide were purchased from Aldrich and used as received. Fluorescence-emission data were collected on a Cary Eclipse Fluorescence Spectrophotometer. Emission spectra were recorded using EM Science OmniSolv[®] High Purity Solvents.

5.6.2 Synthesis of Compound 5-1

This compound was synthesized according to a literature procedure.¹¹² 4-(4,4,5,5-Tetramethyl-1,3,2-dioxaborolan-2-yl)aniline (5.00 g, 2.28×10^{-2} mol), 4-bromopyridine hydrochloride (4.44 g, 2.28×10^{-2} mol) and sodium carbonate (12.10 g, 1.14×10^{-1} mol) were dissolved in DMF (200 mL) and H₂O (100 mL) and degassed with nitrogen for 2 hours. Tetrakis(triphenylphosphine)palladium(0) (1.32 g, 1.14×10^{-4} mol) was added and the solution degassed for an additional hour. The reaction was refluxed for 24 hours and subsequently cooled to room temperature. The DMF and H₂O were removed by rotary evaporation. The resulting residue was dissolved in CH₂Cl₂ (100 mL) and washed with H₂O (3 × 100 mL). The CH₂Cl₂ was dried with MgSO₄, filtered and concentrated. **5-1** precipitated from CH₂Cl₂ as a pure pale yellow powder. (1.15 g, 80%)

Table 5.5 – ^1H NMR of 5-1 in CDCl_3 . MW = 170.205 g/mol

Proton	δ (ppm)	Multiplicity	# Protons	J (Hz)
a	3.88	br s	2	--
b	6.76	d	2	$^3J_{bc} = 8.42$
c	7.49	d	2	$^3J_{cb} = 8.42$
d	7.44	d	2	$^3J_{de} = 6.08$
e	8.57	d	2	$^3J_{ed} = 6.08$

Table 5.6 – ^1H NMR of 5-1 in CD_3CN .

Proton	δ (ppm)	Multiplicity	# Protons	J (Hz)
a	4.43	br s	2	--
b	6.73	d	2	$^3J_{bc} = 8.43$
c	7.52	d	2	$^3J_{cb} = 8.43$
d	7.50	d	2	$^3J_{de} = 5.76$
e	8.50	d	2	$^3J_{ed} = 5.76$

5.6.3 Synthesis of Compound 5-2⁺

Compound 5-1 (1.00 g, 5.88×10^{-3} mol) was refluxed in 1,2-dibromoethane (40 mL) and ethanol (20 mL) for 6 hours. The precipitate that formed was collected by vacuum filtration, was stirred in CH_2Cl_2 and filtered affording a yellow solid as the bromide salt. (0.921 g, 44 %) The bromide salt was anion exchanged to the triflate salt by dissolving the solid in H_2O , warming the solution and adding NaOTf. The solution was cooled and the yellow crystals were collected by vacuum filtration. (1.05 g, 96 %)

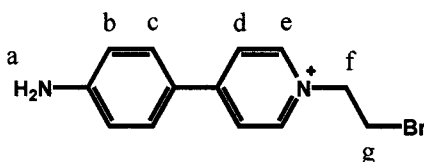


Table 5.7 – ¹H NMR of [5-2][Br] in D₂O. MW_{Br-} = 358.073 g/mol

Proton	δ (ppm)	Multiplicity	# Protons	<i>J</i> (Hz)
a	--	--	2	--
b	6.81	d	2	³ <i>J</i> _{bc} = 8.69
c	7.71	d	2	³ <i>J</i> _{cb} = 8.69
d	8.03	d	2	³ <i>J</i> _{de} = 6.86
e	8.50	d	2	³ <i>J</i> _{ed} = 6.86
f	4.76	t	2	³ <i>J</i> _{fg} = 5.70
g	3.83	t	2	³ <i>J</i> _{gf} = 5.70

Table 5.8 – ¹H NMR of [5-2][OTf] in CD₃CN. MW_{OTf-} = 427.233 g/mol

Proton	δ (ppm)	Multiplicity	# Protons	<i>J</i> (Hz)
a	5.12	br s	2	--
b	6.79	d	2	³ <i>J</i> _{bc} = 8.71
c	7.78	d	2	³ <i>J</i> _{cb} = 8.71
d	8.08	d	2	³ <i>J</i> _{de} = 6.89
e	8.42	d	2	³ <i>J</i> _{ed} = 6.89
f	4.74	t	2	³ <i>J</i> _{fg} = 5.88
g	3.89	t	2	³ <i>J</i> _{gf} = 5.88

5.6.4 Synthesis of Compound 5-3

[5-2][OTf] (0.635 g, 1.49×10^{-3} mol) and 3,5-lutidine (0.239 g, 2.23×10^{-3} mol) were dissolved in acetonitrile (25 mL) and refluxed for 24 hours. The precipitate that formed was isolated by vacuum filtration and washed with CH_2Cl_2 . This yielded the product as a yellow solid as the bromide salt. (0.150 g, 21 %) The bromide salt was anion exchanged to the triflate salt by dissolving the solid in H_2O , warming the solution and adding NaOTf. The solution was cooled and the yellow crystals collected by vacuum filtration.

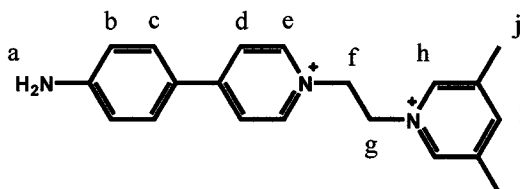


Table 5.9 – ^1H NMR of [5-3][Br]₂ in D₂O. MW_{Br-} = 465.022 g/mol

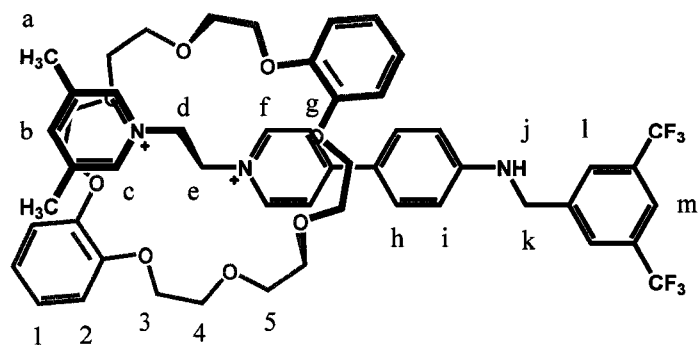
Proton	δ (ppm)	Multiplicity	# Protons	J (Hz)
a	--	--	2	--
b	6.80	d	2	$^3J_{bc} = 8.76$
c	7.71	d	2	$^3J_{cb} = 8.76$
d	8.01	d	2	$^3J_{de} = 7.02$
e	8.27	d	2	$^3J_{ed} = 7.02$
f	5.04	t	2	$^3J_{fg} = 5.72$
g	4.98	t	2	$^3J_{gf} = 5.72$
h	8.31	s	2	--
i	8.18	s	1	--
j	2.30	s	6	--

Table 5.10 – ^1H NMR of [5-3][OTf]₂ in CD₃CN. MW_{OTf} = 603.540 g/mol

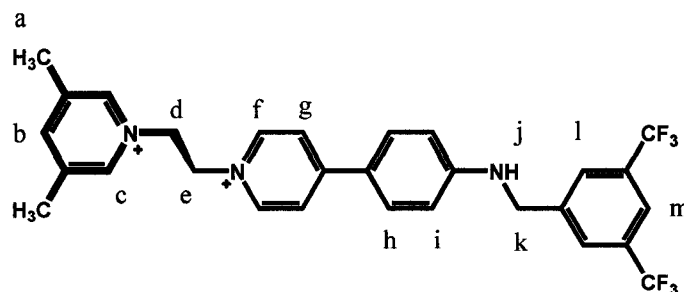
Proton	δ (ppm)	Multiplicity	# Protons	J (Hz)
a	5.18	br s	2	--
b	6.80	d	2	$^3J_{bc} = 8.80$
c	7.79	d	2	$^3J_{cb} = 8.80$
d	8.06	d	2	$^3J_{de} = 7.12$
e	8.30	d	2	$^3J_{ed} = 7.12$
f	4.96	m	2	--
g	4.90	m	2	--
h	8.36	s	2	--
i	8.22	s	1	--
j	2.45	s	6	--

5.6.5 Synthesis of Compound 5-4²⁺ and 5-5²⁺

[5-3][Br] (0.200 g, 4.30×10^{-4} mol), **DB24C8** (0.964 g, 2.14×10^{-3} mol) and 3,5-bis(trifluoromethyl)benzyl bromide (0.0660 g, 2.15×10^{-4} mol) were dissolved in a two layer CH₃NO₂ (10 mL) and H₂O (5 mL) solution to which NaOTf (0.150 g, 8.60×10^{-4} mol) was added and stirred at room temperature for 7 days. The CH₃NO₂ layer was separated from the H₂O layer, washed several times with water and dried with MgSO₄. The CH₃NO₂ was evaporated and the residue washed several times with toluene to eliminate excess 3,5-bis(trifluoromethyl)benzyl bromide and **DB24C8**. The rotaxane was further purified by column chromatography on silica gel using 7:2:1 MeOH: 2M NH₄Cl: MeNO₂ as the eluent. The isolated solid was dissolved in CH₃NO₂ and NaOTf added. The resulting solid was then washed with water numerous times. The product was isolated as a yellow solid. ($R_f=0.82$, 0.0700 g, 25.5 %) **ESI-MS**: m/z [5-4a - OTf]⁺ calc. 1128.3721, found 1128.3763. The capped thread was also isolated from the column. It was dissolved in CH₃NO₂ and NaOTf added. The resulting solid was then washed with water numerous times and the product was isolated as a yellow solid. ($R_f = 0.64$, 0.0200 g, 7%) **ESI-MS**: m/z [5-5a - OTf]⁺ calc. 680.1624, found 680.1634.

Table 5.11 – ^1H NMR of [5-4][OTf] $_2$ in CD_3CN . $\text{MW}_{\text{OTf}} = 1278.180$ g/mol

Proton	δ (ppm)	Multiplicity	# Protons	J (Hz)
a	2.15	s	6	--
b	7.59	s	1	--
c	8.55	s	2	--
d	5.33	m	2	--
e	5.26	m	2	--
f	8.80	d	2	$^3J_{fg} = 7.01$
g	7.84	d	2	$^3J_{gf} = 7.01$
h	7.58	d	2	$^3J_{hi} = 8.72$
i	6.71	d	2	$^3J_{ih} = 8.72$
j	6.13	t	1	$^3J_{jk} = 6.13$
k	4.63	d	2	$^3J_{kj} = 6.13$
l	7.97	s	2	--
m	7.93	s	1	--
1-2	6.71	m	8	--
3-5	3.85-4.03	m	24	--

Table 5.12 – ^1H NMR of [5-5][OTf]₂ in CD₃CN. MW_{OTf} = 829.673 g/mol

Proton	δ (ppm)	Multiplicity	# Protons	J (Hz)
a	2.44	s	6	--
b	8.21	s	1	--
c	8.37	s	2	--
d	4.95	t	2	$^3J_{de} = 5.46$
e	4.91	t	2	$^3J_{ed} = 5.46$
f	8.32	d	2	$^3J_{fg} = 7.04$
g	8.06	d	2	$^3J_{gf} = 7.04$
h	7.81	d	2	$^3J_{hi} = 8.86$
i	6.78	d	2	$^3J_{ih} = 8.86$
j	6.21	br s	1	--
k	4.62	d	2	$^3J_{kj} = 5.21$
l	7.95	s	2	--
m	7.92	s	1	--

Table 5.13 -- ^1H NMR of [5-5][OTf]₃ in CD₃CN. MW_{OTf} = 829.673 g/mol

Proton	δ (ppm)	Multiplicity	# Protons	J (Hz)
a	2.46	s	6	--
b	8.24	s	1	--
c	8.38	s	2	--
d	5.01	t	2	$^3J_{\text{de}} = 6.37$
e	5.10	t	2	$^3J_{\text{ed}} = 6.37$
f	8.67	d	2	$^3J_{\text{fg}} = 6.85$
g	8.30	d	2	$^3J_{\text{gf}} = 6.85$
h	8.05	d	2	$^3J_{\text{hi}} = 8.66$
i	7.68	d	2	$^3J_{\text{ih}} = 8.66$
j	9.51	br s	2	--
k	4.83	s	2	--
l	8.02	s	2	--
m	8.10	s	1	--

5.6.6 Synthesis of Compound 5-6

This compound was synthesized according to a literature procedure.¹¹³⁻¹¹⁵ 9-Methanolanthracene (2.00 g, 0.00960 mol) was dissolved in dry THF in a 3-necked flask, under nitrogen and at 0°C. Phosphorus tribromide (1.95 g, 0.677 mL, 0.0072 mol) was added dropwise using a glass syringe needle. The reaction was stirred at 0°C for 2 hours. The solvent was evaporated using a rotary evaporator and the resulting residue recrystallized from CHCl₃. This yielded 9-bromomethylantracene (**5-6**) as a yellow crystalline solid. (0.861 g, 33 %)

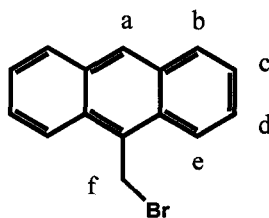


Table 5.14 – ¹H NMR of [**5-6**] in CD₃CN. MW = 271.152 g/mol

Proton	δ (ppm)	Multiplicity	# Protons	J (Hz)
a	8.61	s	1	--
b	8.11	d	2	³ J _{bc} = 8.00
c	7.55	dd	2	³ J _{cb} = 8.00, ³ J _{cd} = 7.14
d	7.68	ddd	2	³ J _{dc} = 7.14, ³ J _{de} = 8.87 ⁴ J _{db} = 1.12
e	8.37	d	2	³ J _{ed} = 8.87
f	5.66	s	2	--

5.6.7 Synthesis of Compound 5-7

[5-3][Br] (0.240 g, 5.16×10^{-4} mol), **DB24C8** (1.16 g, 2.58×10^{-3} mol) and compound **5-6** (0.0700 g, 2.58×10^{-4} mol) were dissolved in a two layer CH_3NO_2 (10 mL) and H_2O (5 mL) solution to which NaOTf (0.300 g, 1.74×10^{-3} mol) was added and stirred at room temperature for 7 days. The CH_3NO_2 layer was separated from the water layer, washed several times with water and dried with MgSO_4 . The nitromethane was evaporated and the residue washed several times with toluene to remove excess 9-bromomethylantracene (**5-6**) and **DB24C8**. The rotaxane was further purified by column chromatography on silica gel using 7:2:1 CH_3OH : 2M NH_4Cl : CH_3NO_2 as the eluent. The isolated solid was dissolved in CH_3NO_2 and NaOTf added. The resulting solid was then washed with water numerous times and the product was isolated as a yellow solid. ($R_f = 0.81$, 0.0850 g, 26%) **ESI-MS**: m/z [**5-7a** - OTf] $^+$ calc. 1092.4286, found 1092.4282.

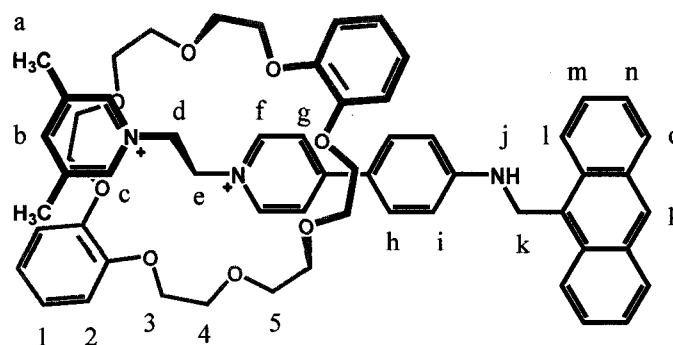


Table 5.15 – ^1H NMR of [5-7][OTf] $_2$ in CD_3CN . $\text{MW}_{\text{OTf}} = 1242.301$ g/mol

Proton	δ (ppm)	Multiplicity	# Protons	J (Hz)
a	2.16	s	6	--
b	7.59	s	1	--
c	8.57	s	2	--
d	5.36	m	2	--
e	5.28	m	2	--
f	8.80	d	2	$^3J_{fg} = 6.94$
g	7.88	d	2	$^3J_{gf} = 6.94$
h	7.69	d	2	$^3J_{hi} = 8.64$
i	6.95	d	2	$^3J_{ih} = 8.64$
j	5.59	t	1	$^3J_{jk} = 4.07$
k	5.33	br s	2	$^3J_{kj} = 4.07$
l	8.14	d	2	$^3J_{lm} = 8.51$
m	7.61	ddd	2	$^3J_{ml} = 8.51$, $^3J_{mn} = 6.97$, $^4J_{mo} = 1.09$
n	7.56	dd	2	$^3J_{no} = 8.01$, $^3J_{nm} = 6.97$
o	8.33	d	2	$^3J_{on} = 8.01$
p	8.63	s	1	--
1-2	6.76	br s	8	--
3-5	3.79-4.06	m	24	--

CHAPTER 6

[2]Catenane Circumrotational Shuttle

6.1 INTRODUCTION

Previously in the Loeb group, a [3]catenane was synthesized with **DB24C8** macrocyclic rings, 1,2-bis(4,4'-dipyridinium)ethane recognition threads and terphenyl units as the linking spacer groups. It was determined that the presence of the crown ether templated the formation of the [3]catenane by forming a host-guest adduct between the [3]catenane and an external crown ether.⁴⁵

In Chapter 4, the structural similarities between the bis(pyridinium)ethane and benzylanilinium recognition motif were established in terms of their similarities in size and shape and the *anti* conformation at the two atom bridge between the aromatic rings. Thus, knowing that the benzylanilinium recognition site is similar in dimension to the bis(pyridinium)ethane, it seemed reasonable that both recognition sites could be incorporated into a new catenane in a similar fashion to the original [3]catenane described above. Although the previous [3]catenane was synthesized using a one-step, self-assembly procedure, a catenane with different recognition sites would require a stepwise approach. In addition, the goal herein was to synthesize a [2]catenane capable of performing as a molecular switch (Figure 6.1). It would function in a similar manner to and show properties comparable to the [2]rotaxane molecular shuttles described in Chapter 5. This would be an example of a circumrotational molecular machine, for which there are very few known examples.³⁴

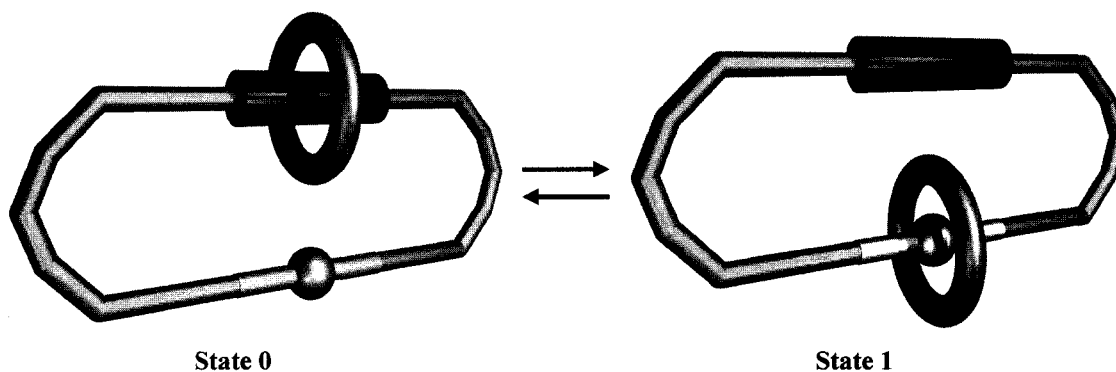


Figure 6.1 – Illustration of a [2]catenane molecular switch.

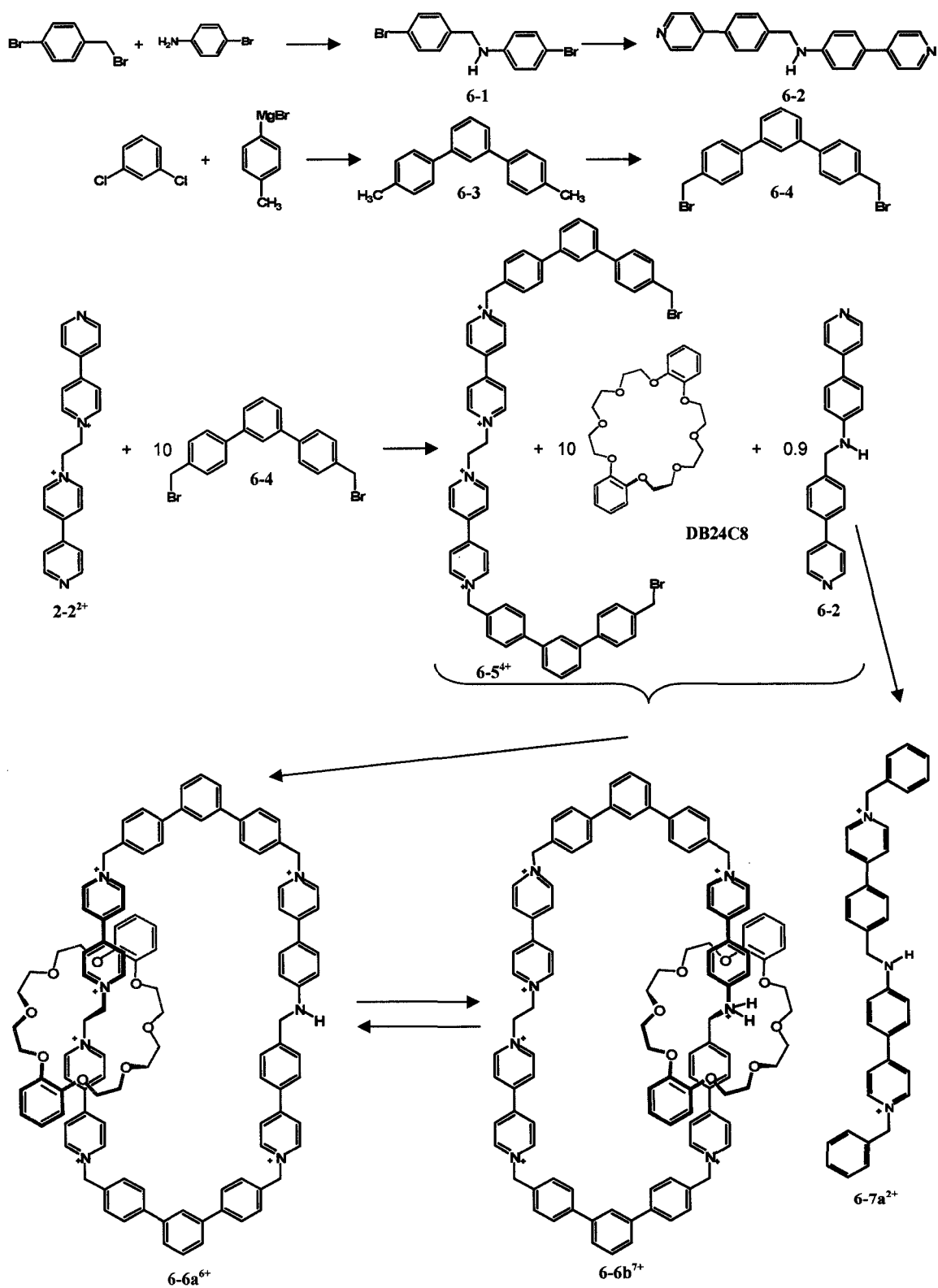
6.2 SYNTHESIS AND STRUCTURAL CHARACTERIZATION

6.2.1 Synthesis

Synthesis of the [2]catenane requires eight steps overall: two to make the terphenyl linker (6-4), two for the benzylianium site (6-2), two for the bis(dipyridinium)ethane site (2-2²⁺) and two for the actual assembly of the catenane (6-6a⁶⁺). The complete synthesis is outlined in Scheme 6.1. The synthesis of bis(dipyridinium)ethane (2-2²⁺) was described in Chapter 2. To insert the benzylianium site into the catenane, it must be substituted at the 4-position of the benzyl and anilinium aromatic rings with pyridyl substituents so that it has a structure similar to that of the bis(4,4'-dipyridinium)ethane site. The lengths of these two components from terminal nitrogen to terminal nitrogen, as measured from model structures constructed and minimized using the MM2 method (CACHe version 6.1.12), are 18.11 Å for the bis(dipyridinium)ethane thread (2-2²⁺) and 18.09 Å for the benzylianium thread (6-2). Thus, in size and shape the proposed new benzylianium thread should be a good fit for the catenane.

The first step in forming the benzylianium site was an S_N2 reaction between 4-bromobenzylbromide and 4-bromoaniline. Next, the isolated product **6-1** was reacted under Suzuki coupling conditions with two equivalents of 4-pyridylboronic acid to give **6-2**. The 4, 4''-bis(bromomethyl)-1,1',3',1''-terphenyl linker (**6-4**) was synthesized stepwise by a lithiation of 1,3-dichlorobenzene, followed by reaction with *p*-tolylmagnesium bromide to give 4,4''-dimethyl-1,1'3',1''-terphenyl (**6-3**). The dimethylterphenyl **6-3** was then brominated using *N*-bromosuccinimide and benzoyl peroxide in CCl₄ to give **6-4**.

Once these components were synthesized, the catenane was assembled in two subsequent steps. First **[2-2][OTf]₂** was reacted with ten equivalents of the bis(bromomethyl)terphenyl linker **6-4** in CH₃CN to afford **6-5⁴⁺** in 69% yield. A large excess of the linker was used to ensure that both pyridyl ends of the thread were alkylated. The next step involved [2]pseudorotaxane formation between **[6-5][OTf]₄** and **DB24C8** followed by ring closure using the second thread **6-2**. The reaction was performed under dilute conditions to favour ring formation so that the pyridyl ends of one **6-2** molecule react only with the two ends of a single **[6-5][OTf]₄⊂DB24C8**. For this reason ten equivalents of crown ether are used to drive the equilibrium to favour pseudorotaxane formation despite the dilute conditions. To isolate the [2]catenane, the CH₃CN reaction solvent was evaporated and the residue suspended in toluene to dissolve the excess crown ether. The residue that did not dissolve was filtered using vacuum filtration and the isolated solid subjected to column chromatography on silica gel using a 5:3:2 mixture of CH₃OH: 2M NH₄Cl_(aq): CH₃NO₂ as the eluent. Fractions containing the product (R_f = 0.66) were combined and anion exchanged to the triflate salt.

Scheme 6.1 – Synthesis of [2]catenane 6-6⁶⁺.

6.2.2 ^1H NMR Spectroscopy

Assignments for protons in catenane **6-6a**⁶⁺ follow the numbering scheme outlined in Figure 6.2. Figure 6.3 shows the partial ^1H NMR spectrum of **6-6a**⁶⁺ in CD₃CN. The resonances are assigned based on ^1H - ^1H COSY NMR spectroscopy as well as comparison to ^1H NMR and COSY spectra of individual components **6-2** and **6-5**⁴⁺ and model compound **6-7**²⁺. Comparison of proton shifts **n - y** of **6-6a**⁶⁺ with **6-5**⁴⁺ shows typical **DB24C8** interactions with the bis(pyridinium)ethane site. The ethylene protons **s** and **t** shift downfield from 5.30 ppm (**6-5**⁴⁺) to 5.56 ppm (**6-6a**⁶⁺) due to hydrogen bonding interactions with the crown ether. Similar downfield shifts due to hydrogen bonding occur for **u** and **r**, the *ortho* inner pyridinium protons, from 9.04 ppm (**6-5**⁴⁺) to 9.31 ppm (**6-6a**⁶⁺). Aromatic π -stacking interactions induce upfield shifts for protons **p**, **q**, **v** and **w** from \sim 8.48 ppm (**6-5**⁴⁺) to \sim 8.20 ppm (**6-6a**⁶⁺). Protons **o**, **x**, **n** and **y** do not shift because the crown ether does not extend far enough to interact with these protons. In contrast, the chemical shifts for protons **a - d** and **I - L** on the benzylianium thread portion of **6-6a**⁶⁺ do not shift significantly when compared to model compound **6-7**²⁺. This implies that in the unprotonated state, in an identical fashion to the molecular shuttles described in Chapter 5, the crown ether resides exclusively on the bis(pyridinium)ethane site of the catenane in CD₃CN. Table 6.1 summarizes the chemical shift differences between the [2]catenane **6-6a**⁶⁺ and model compounds **6-5**⁴⁺ and **6-7**²⁺.

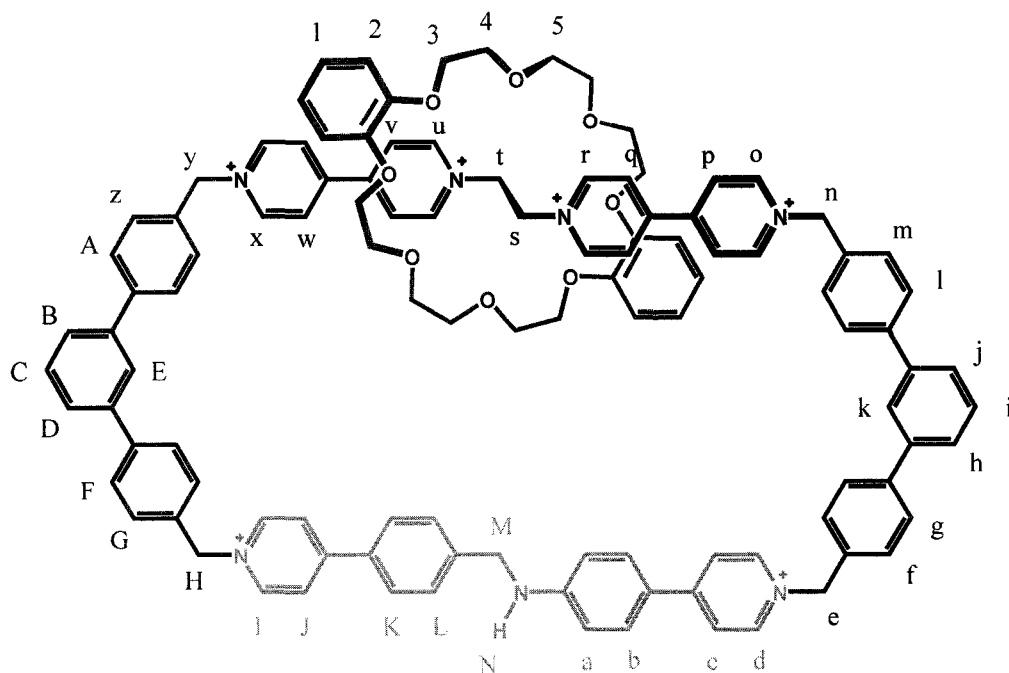


Figure 6.2 – Proton assignments for 6-6a⁶⁺.

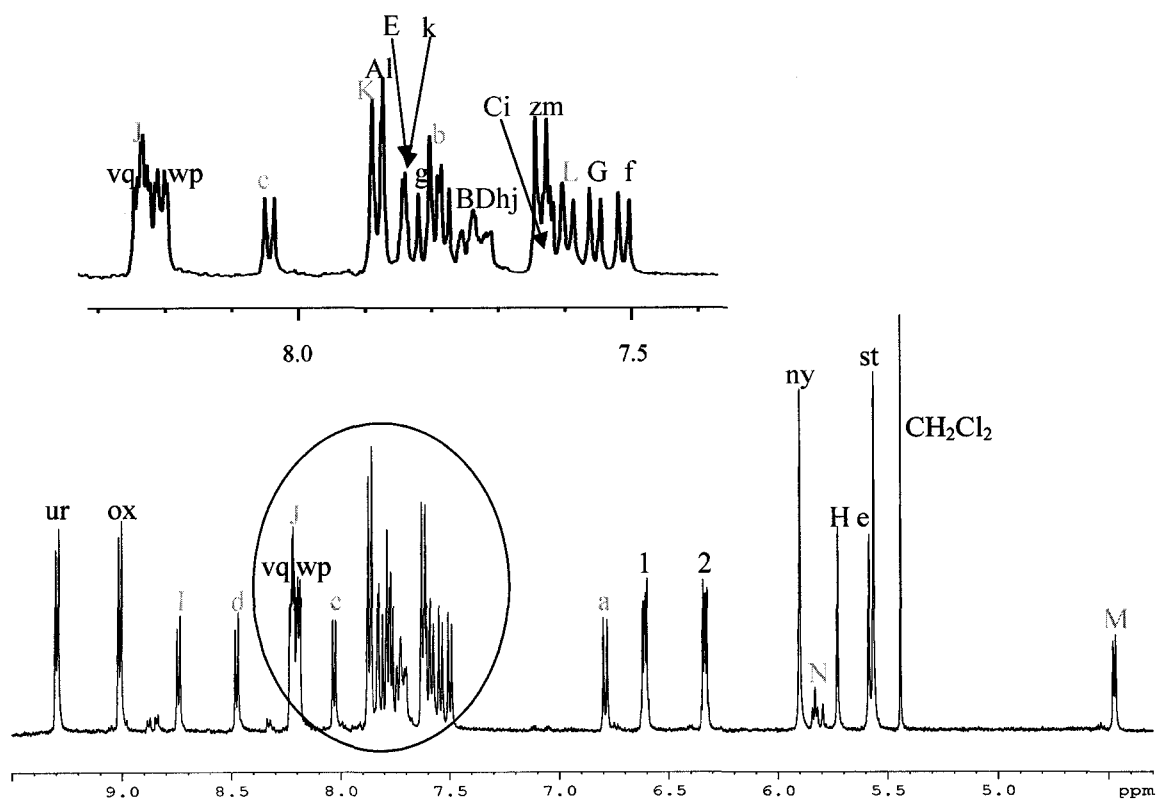


Figure 6.3 – ¹H NMR spectrum of 6-6a⁶⁺ in CD₃CN.

Table 6.1 – Summary of chemical shift comparisons between 6-6a⁶⁺ and model compounds 6-5⁴⁺ and 6-7²⁺

Proton(s)	δ 6-5 ⁴⁺ (ppm)	δ 6-6a ⁶⁺ (ppm)
ny	5.90	5.90
ox	9.05	9.03
pw	8.47	8.19
qv	8.50	8.22
ru	9.04	9.31
st	5.30	5.56
Proton(s)	δ 6-7 ²⁺ (ppm)	δ 6-6a ⁶⁺ (ppm)
H	5.70	5.74
I	8.72	8.76
J	8.23	8.22
K	7.89	7.87
L	7.60	7.58
M	4.57	4.48
N	6.11	5.87
a	6.78	6.79
b	7.77	7.78
c	8.03	8.04
d	8.45	8.49
e	5.54	5.59

6.2.3 Mass Spectrometry

The molecular weight of [6-6a][OTf]₆ is 2533.4409 g/mol and its exact mass is 2531.4990 g/mol. A sample of [6-6a][OTf]₆ was analyzed in a solution of 1:1 methanol:acetonitrile and the spectra for the 2+, 3+, 4+ and 5+ molecular ions are shown in Figure 6.4. Sufficient resolution for each of the charged molecular ions allowed for exact mass measurements for these ions to within 5 ppm of calculated exact masses, confirming that [6-6a][OTf]₆ was isolated. Table 6.2 summarizes these values. The spectra show the typical splitting patterns for multiply charged species. Figure 6.4a shows the m/z peak split into two peaks within one mass unit for the 2+ species, Figure 6.4b the

m/z peak is split into three peaks for the 3+ species, Figure 6.4c shows it split into four peaks for the 4+ species and Figure 6.4d shows it split into five peaks for the 5+ species.

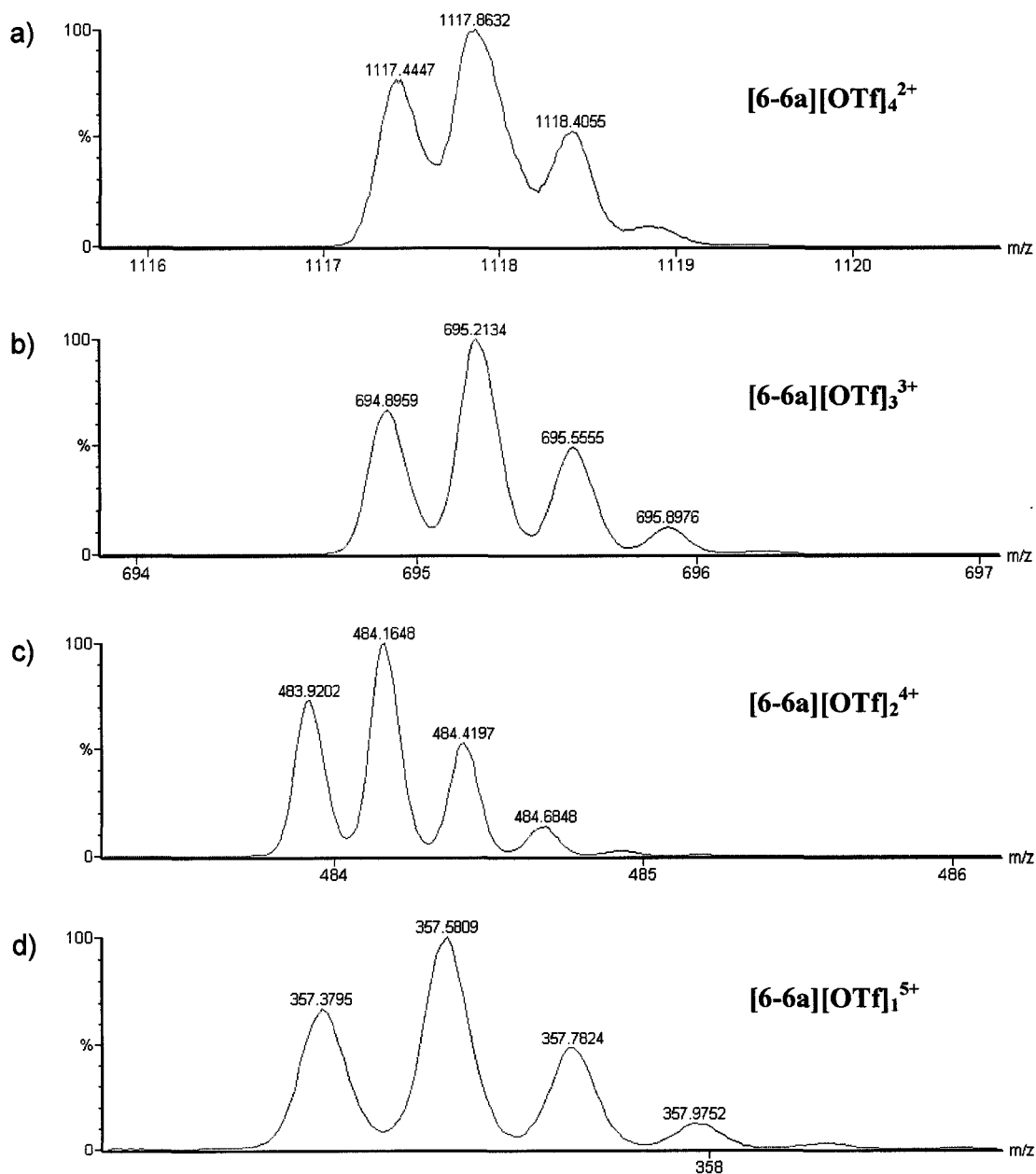


Figure 6.4 – ESI-Mass spectra of experimental data for a) 6-6a²⁺, b) 6-6a³⁺, c) 6-6a⁴⁺, d) 6-6a⁵⁺.

Table 6.2 – Calculated and found exact masses for compound [6-6a][OTf]₆.

Molecular Ion	Calculated m/z (g/mol)	Experimental m/z (g/mol)	Δ (ppm)
6-6a ²⁺	1116.7969	1116.7972	0.3
6-6a ³⁺	694.8804	694.8835	4.5
6-6a ⁴⁺	483.9222	483.9246	5.0
6-6a ⁵⁺	357.3472	357.3465	2.0

6.3 ACID/BASE SHUTTLING

6.3.1 ¹H NMR Spectroscopy

Figure 6.5 illustrates the ¹H NMR spectra of non-protonated 6-6a⁶⁺ and protonated 6-6b⁷⁺ in CD₃CN at room temperature. Earlier analysis of 6-6a⁶⁺ indicated that DB24C8 resides exclusively at the bis(pyridinium)ethane site. Addition of one equivalent of trifluoromethanesulfonic acid to a solution of the [2]catenane, protonates the aniline nitrogen producing a second viable recognition site for the crown ether. The molecular shuttles discussed in the previous chapter demonstrated incomplete bias of recognition sites when they are dissolved in CD₃CN, but bistability in CD₂Cl₂. The catenane is insoluble in CH₂Cl₂ precluding studies from being carried out in this solvent. Integration of the crown ether aromatic protons of 2 and 2', where the "prime" indicates complexation between DB24C8 and the benzylianium site, indicates that there is a 5:1 complexation ratio of DB24C8 with the bis(pyridinium)ethane site over the benzylianium site. These results are contrary to those of the molecular shuttles where the protonated benzylianium site was preferred in ratios of 3:1 (5-4b³⁺) and 9:1 (5-7b³⁺).

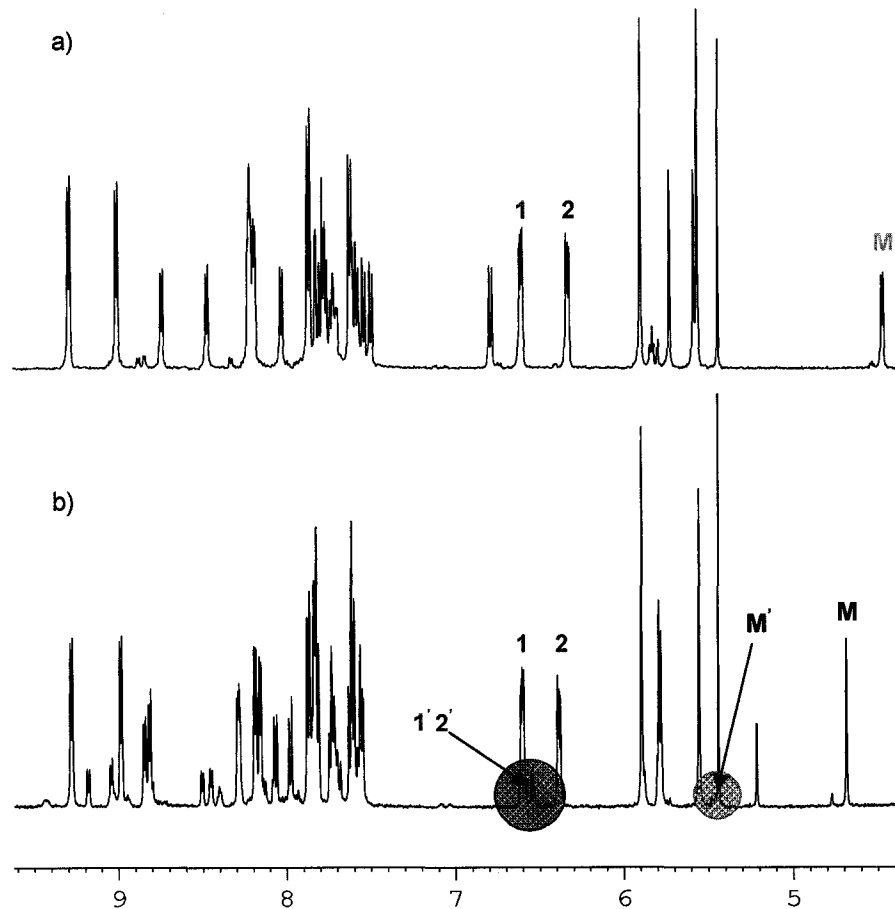


Figure 6.5 – ^1H NMR spectra of a) non-protonated ($6\text{-}6\text{a}^{6+}$) and b) protonated ($6\text{-}6\text{b}^{7+}$) in CD_3CN at room temperature.

6.3.2 [2]Pseudorotaxane Model Compound Study

To understand why the ratio of **DB24C8** complexation with benzylianium site:bis(pyridinium)ethane site is inverted compared to the [2]rotaxane molecular shuttles discussed in the Chapter 5, model compounds $6\text{-}7\text{a}^{2+}$ and $6\text{-}7\text{b}^{3+}$ were studied. It is noteworthy that unprotonated $6\text{-}7\text{a}^{2+}$ and **DB24C8** do not form a pseudorotaxane in CD_3CN (Figure 6.6). Since the unprotonated $6\text{-}7\text{a}^{2+}$ cannot form a pseudorotaxane complex with **DB24C8**, even though it is a $2+$ charged species, this implies that during catenane synthesis the reacting species, **6-2**, which is neutral, cannot form a

pseudorotaxane either. This has important implications for synthesis, as it ensures that the [3]catenane will not be formed.

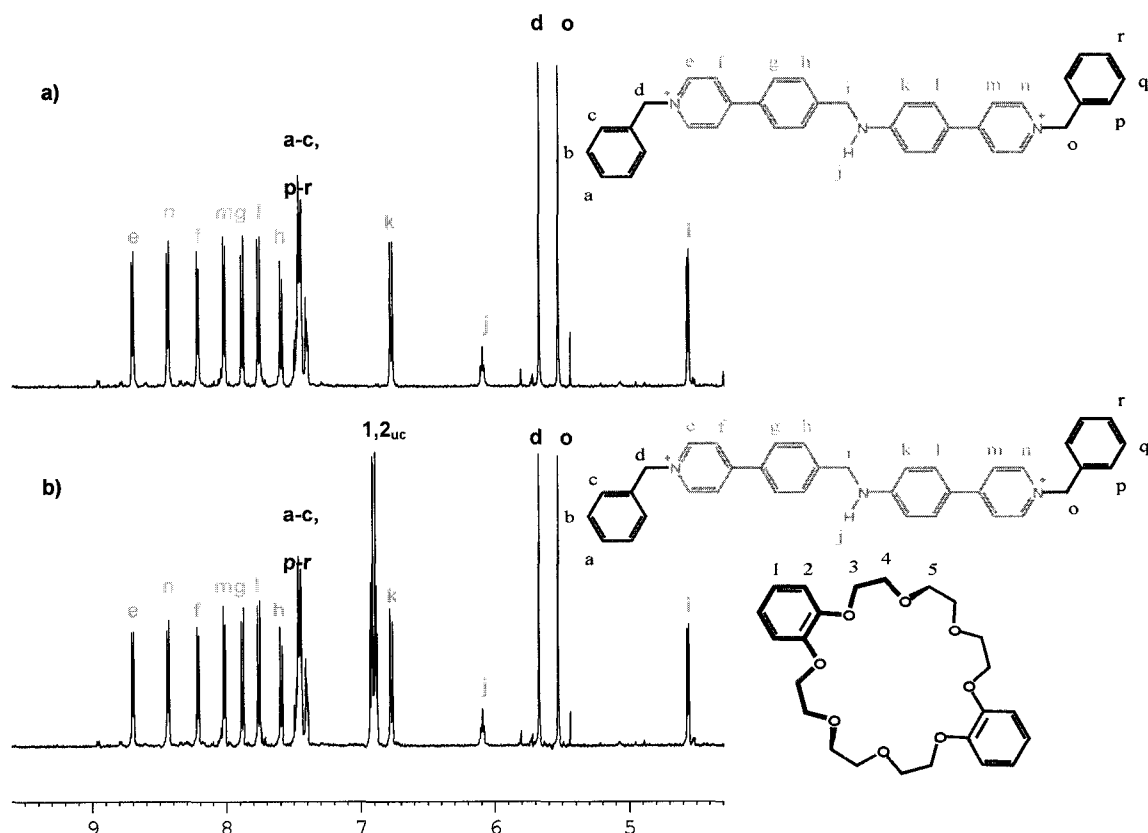


Figure 6.6 – ^1H NMR spectra in CD_3CN of a) unprotonated model compound **6-7a**²⁺ and b) a mixture of unprotonated model compound **6-7a**²⁺ and **DB24C8**.

Protonation of the model compound **6-7a**²⁺ with trifluoromethansulfonic acid generates **6-7b**³⁺. The ^1H NMR spectrum of a 1:1 solution in CD_3CN of **6-7b**³⁺ and **DB24C8** (Figure 6.7b), exhibits three sets of peaks: one for pseudorotaxane one for uncomplexed thread and one for uncomplexed crown ether. Integration of the benzyl CH_2 protons, i_{uc} and i_c , gives a 3:2 ratio of uncomplexed to complexed. The K_{assoc} for the interaction of protonated **6-7b**³⁺ with **DB24C8**, determined by the single point method, is $\sim 600 \text{ M}^{-1}$. In comparison, the association constant for benzylated

bis(dipyridinium)ethane, the model compound for the other site, is $\sim 1000 \text{ M}^{-1}$.³⁸ Since the association of **DB24C8** with the bis(pyridinium)ethane site model compound is stronger (1000 M^{-1}) than association of **DB24C8** with the benzylanilinium site model compound **6-7b**³⁺ (600 M^{-1}), it makes sense that the complexation ratio in the [2]catenane favours **DB24C8** with the bis(pyridinium)ethane site over the benzylanilinium site.

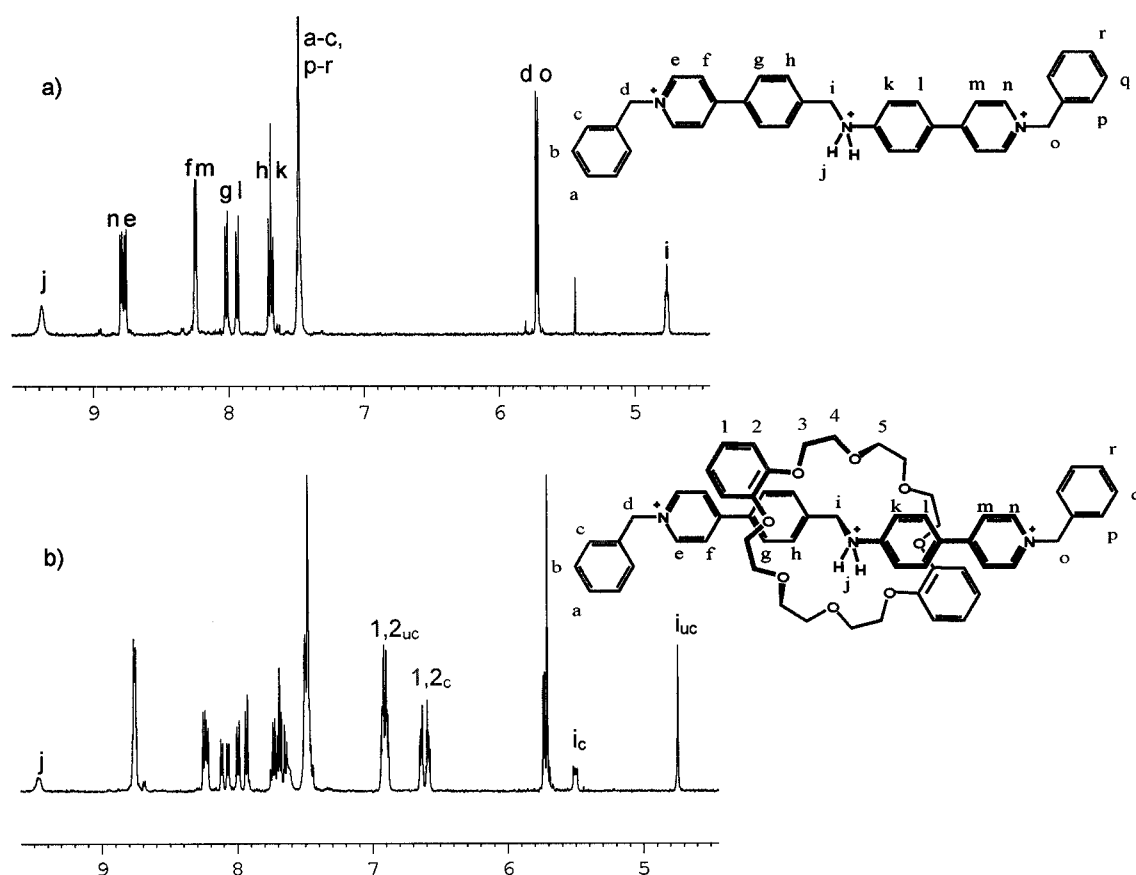


Figure 6.7 – ^1H NMR spectra in CD_3CN at $2.0 \times 10^{-3} \text{ M}$ of a) protonated model compound **6-7b**³⁺ and b) a mixture of protonated model compound **6-7b**³⁺ and **DB24C8**.

6.3.3 UV-Visible Spectroscopy

The UV-visible spectra of **6-6a**⁶⁺ and **6-6b**⁷⁺, shown in Figure 6.8, were obtained using $2.0 \times 10^{-5} \text{ M}$ solutions in CH_3CN . The molar absorptivity (ϵ) of **6-6a**⁶⁺ was

calculated to be $22,680 \text{ L mol}^{-1} \text{ cm}^{-1}$ with λ_{max} at 412 nm. As previously noted with the [2]rotaxane molecular shuttles, the large absorption is due to the intramolecular charge transfer between the aniline nitrogen and pyridinium nitrogen on the benzylianium recognition site. Protonation of the aniline nitrogen removes the ICT, eliminating the absorption band centered at 412 nm. Although the crown ether is not switched completely between the two sites upon protonation/deprotonation, the colour and absorption still indicate the position of the crown. When the catenane solution absorbs strongly (deep yellow/orange solution), the crown resides on the bis(pyridinium)ethane site and when the catenane does not absorb in the UV-visible region (colourless solution), the crown ether is shuttling back and forth between the two sites.

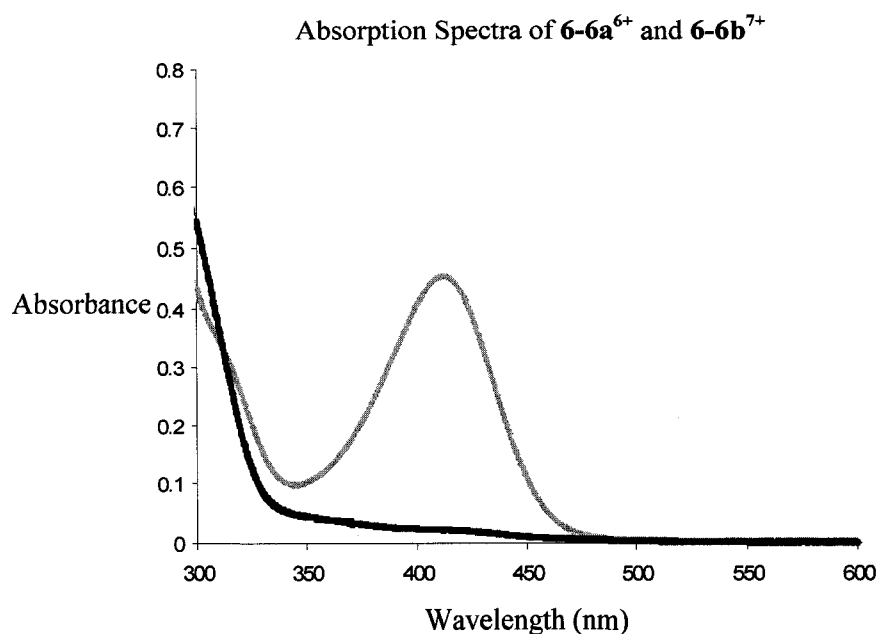


Figure 6.8 – UV-visible spectra of $2.0 \times 10^{-5} \text{ M}$ CH_3CN solutions of non-protonated **6-6a⁶⁺** (yellow) and protonated **6-6b⁷⁺** (black).

6.4 SUMMARY AND CONCLUSIONS

In this chapter, a two station circumrotational [2]catenane has been described and analyzed. The system consists of two different recognition sites, a bis(pyridinium)ethane site and a benzylanilinium site, for the **DB24C8** macrocycle to occupy. Addition of acid activates the benzylanilinium site allowing the ring to shuttle between the two recognition sites. It was found that **DB24C8** prefers the bis(pyridinium)ethane site over the protonated benzylanilinium site in a ratio of 5:1. A comparison of binding associations between **DB24C8** and model compounds for the two recognition sites verify that the ring has a stronger affinity for the bis(pyridinium)ethane recognition site. To improve this system, increasing the solubility of the catenane in non-polar solvents such as CH_2Cl_2 , may enhance the hydrogen bonding interactions between the benzylanilinium site and **DB24C8**. Furthermore, modifying the system so that the ring can only move in one direction, clockwise or counterclockwise, would also be of interest.

6.5 EXPERIMENTAL

6.5.1 General Comments

4-Bromobenzyl bromide, 4-bromoaniline, 4-pyridylboronic acid, 1,3-dichlorobenzene, *p*-tolylmagnesium bromide, *n*-butyllithium and *N*-bromosuccinimide were purchased from Aldrich and used as received. Benzoyl peroxide was purchased from Acros and used as received.

6.5.2 Synthesis of Compound 6-1

4-bromobenzyl bromide (5.0 g, 0.0200 mol) and 4-bromoaniline (6.88 g, 0.0400 mol) were dissolved in CH₃CN (50 mL) and heated to reflux for 30 minutes. The resulting precipitate was filtered and discarded. The solvent was removed and the resulting solid was purified by column chromatography (SiO₂, dry column) using a 1:1 CHCl₃:hexanes mixture as the eluent. Like fractions were combined and evaporated to yield **6-1** as a white powder. (*R*_f = 0.58, 6.21 g, 91%).

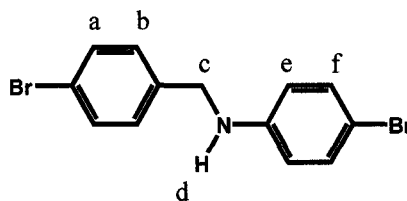
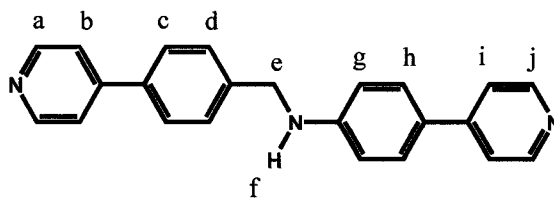


Table 6.3 – ¹H NMR of **6-1** in CD₃CN. MW = 341.0411 g/mol

Proton	δ (ppm)	Multiplicity	# Protons	<i>J</i> (Hz)
a	7.47	d	2	³ <i>J</i> _{ab} = 8.37
b	7.27	d	2	³ <i>J</i> _{ba} = 8.37
c	4.26	d	2	³ <i>J</i> _{cd} = 6.07
d	5.09	br s	1	--
e	6.51	d	2	³ <i>J</i> _{ef} = 8.84
f	7.19	d	2	³ <i>J</i> _{fe} = 8.84

6.5.3 Synthesis of Compound 6-2

DMF (250 mL) and H₂O (100 mL) were added to a 500 ml round bottom Schlenk flask and degassed with nitrogen for 2 hours. To this, **6-2** (1.11 g, 0.00325 mol), 4-pyridyl boronic acid (1.00 g, 0.00814 mol) and Na₂CO₃ (2.07 g, 0.195 mol) were added and the solution degassed for an additional hour. [Pd(PPh₃)₄] (0.188 g, 1.63 × 10⁻⁴ mol) was added and the solution degassed for an additional half an hour. The reaction was refluxed for 5 days and the progress monitored using ¹H NMR spectroscopy. After 5 days, the reaction was cooled to room temperature and the solvents were evaporated. The residue was dissolved in CH₂Cl₂ and washed with H₂O. The CH₂Cl₂ layer was dried with MgSO₄, filtered and concentrated. The product precipitated as a pale yellow powder which was collected by filtration. The filtrate was evaporated and the residue was subjected to column chromatography (SiO₂, 1% MeOH in CHCl₃ as the eluent.) More product was isolated (R_f = 0.13). The product was recrystallized from acetone. (0.800 g, 73%)

Table 6.4 – ^1H NMR of 6-2 in CD_3CN . MW = 337.417g/mol

Proton	δ (ppm)	Multiplicity	# Protons	J (Hz)
a	8.60	d	2	$^3J_{ab} = 6.08$
b	7.59	d	2	$^3J_{ba} = 6.08$
c	8.48	d	2	$^3J_{cd} = 6.16$
d	7.49	d	2	$^3J_{dc} = 6.16$
e	4.46	d	2	$^3J_{ef} = 6.20$
f	5.41	br t	1	$^3J_{fe} = 6.20$
g	6.73	d	2	$^3J_{gh} = 8.70$
h	7.54	d	2	$^3J_{hg} = 8.70$
i	7.51	d	2	$^3J_{ij} = 8.18$
j	7.71	d	2	$^3J_{ji} = 8.18$

6.5.4 Synthesis of Compound 6-3

This compound was prepared according to a modified literature procedure.¹¹⁶ 1,3-Dichlorobenzene (14.7 g, 11.4 mL, 0.100 mol) was dissolved in dry THF (250 mL) in a 3-necked round bottom flask under N₂ atmosphere and equipped with a low temperature thermometer. The solution was cooled to -70°C using a hexane/liquid nitrogen low temperature bath. To this, *n*-butyllithium (2.5 M, 40.0 mL, 0.100 mol) was added dropwise over 30 minutes using a syringe. This was stirred at -70°C for two hours at which time a white slurry solution was formed. To this slurry, *p*-tolylmagnesium bromide (39.1 g, 1.0 M, 0.200 L, 0.200 mol) was added dropwise while keeping the reaction at -70°C. Once all of the Grignard reagent was added, the solution was warmed to room temperature and stirred for an additional 48 hours. The reaction was quenched with dilute HCl_(aq) and the product extracted with diethyl ether. The combined organic portions were washed twice with H₂O. The product was recrystallized from isopropanol as a white crystalline solid (18.1 g, 77%).

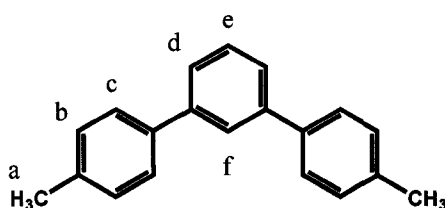


Table 6.5 – ¹H NMR of 6-3 in CD₃CN. MW = 258.357 g/mol

Proton	δ (ppm)	Multiplicity	# Protons	J (Hz)
a	2.38	s	6	--
b	7.29	d	4	³ J _{bc} = 8.05
c	7.61	d	4	³ J _{cb} = 8.05
d	7.58	d	2	³ J _{de} = 7.30
e	7.50	t	1	³ J _{ed} = 7.30
f	7.84	s	1	--

6.5.5 Synthesis of Compound 6-4

This compound was synthesized according to a modified literature procedure.¹¹⁶ **6-3** (5.00 g, 0.0194 mol), *N*-bromosuccinimide (7.58 g, 0.0426 mol) and benzoyl peroxide (0.047 g, 1.94×10^{-4} mol) were dissolved in CCl_4 (150 mL). The reaction was heated to reflux for 72 hours. The precipitate that formed was filtered off and discarded. The CCl_4 filtrate was washed with H_2O three times and then dried with MgSO_4 . The CCl_4 was evaporated and the resulting solid recrystallized from ethanol. The isolated solid was purified by column chromatography (SiO_2 gel) using 9:1 hexanes: CHCl_3 as the eluent. Like fractions were combined and evaporated to yield **6-4** as a white crystalline solid. (3.25 g, 40%, $R_f = 0.30$)

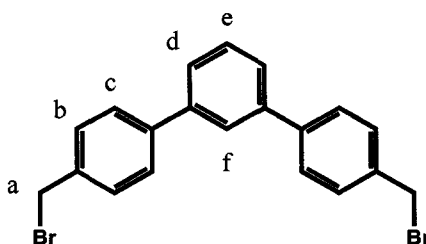
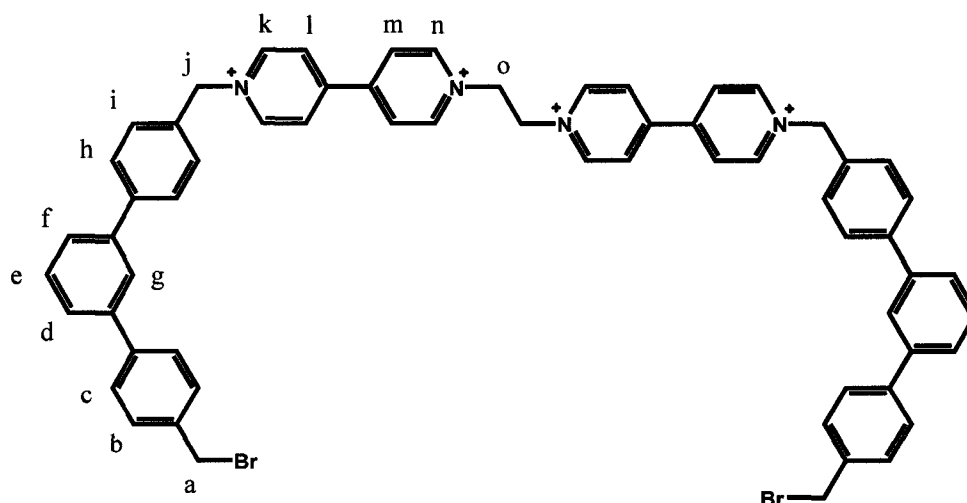


Table 6.6 – ^1H NMR of **6-4** in CD_3CN . MW = 416.149 g/mol

Proton	δ (ppm)	Multiplicity	# Protons	J (Hz)
a	4.66	s	4	--
b	7.54	d	4	$^3J_{bc} = 8.16$
c	7.72	d	4	$^3J_{cb} = 8.16$
d	7.65	d	2	$^3J_{de} = 7.70$
e	7.56	t	1	$^3J_{ed} = 7.70$
f	7.91	s	1	--

6.5.6 Synthesis of Compound 6-5⁴⁺

[2-2][OTf]₂ (0.400 g, 6.26×10^{-4} mol) and **6-4** (2.61 g, 6.26×10^{-3} mol) were dissolved in CH₃CN (75 mL) and stirred at room temperature for seven days. The precipitate was filtered, collected and stirred in CH₂Cl₂ for 20 minutes and filtered to eliminate excess **6-4**. The precipitate was anion exchanged to the triflate salt in a two layer CH₃NO₂/NaOTf_(aq) solution. The layers were separated and the CH₃NO₂ layer washed with H₂O and then dried using MgSO₄. The CH₃NO₂ was evaporated and **6-5⁴⁺** was isolated as a pale yellow solid. (0.700 g, 69%). **ESI-MS:** *m/z* [**6-5** - OTf]⁺ calc. 1457.1119, found 1457.1144.

Table 6.7 – ^1H NMR of [6-5][OTf]₄ in CD₃CN. MW_{OTf} = 1609.188 g/mol

Proton	δ (ppm)	Multiplicity	# Protons	J (Hz)
a	4.66	s	4	--
b	7.54	d	4	$^3J_{bc} = 8.18$
c	7.71	d	4	$^3J_{cb} = 8.18$
d	7.68	d	2	$^3J_{de} = 7.86$
e	7.57	t	2	$^3J_{ed} = 7.86, ^3J_{ef} = 8.05$
f	7.67	d	2	$^3J_{fe} = 8.05$
g	7.91	s	2	--
h	7.86	d	4	$^3J_{hi} = 8.23$
i	7.62	d	4	$^3J_{ih} = 8.23$
j	5.89	s	4	--
k	9.05	d	4	$^3J_{kl} = 6.90$
l	8.47	d	4	$^3J_{lk} = 6.90$
m	8.50	d	4	$^3J_{mn} = 6.86$
n	9.04	d	4	$^3J_{nm} = 6.86$
o	5.30	s	4	--

6.5.7 Synthesis of Compound **6-6a**⁶⁺

[**6-5**][OTf]₄ (0.155 g, 9.63×10^{-5} mol) and **DB24C8** (0.432 g, 9.63×10^{-4} mol) were dissolved in a two phase CH₃NO₂/H₂O mixture and stirred at room temperature for 30 minutes to allow pseudorotaxane formation. **6-2** (0.0330 g, 9.63×10^{-5} mol) was then added along with NaOTf (0.0330 g, 1.93×10^{-4} mol) and the reaction stirred at room temperature for 21 days. The water layer was separated, and the CH₃NO₂ evaporated. The resulting residue was washed three times with CH₂Cl₂ to remove excess **DB24C8**. The precipitate from CH₂Cl₂ was filtered using vacuum filtration and subjected to column chromatography on silica gel using a 5:3:2 mixture of CH₃OH: 2M NH₄Cl: CH₃NO₂ as the eluent. Fractions containing the product were combined and the solvents evaporated. The residue was dissolved in a two layer CH₃NO₂/NaOTf_(aq) solution to anion exchange the catenane to the triflate salt. The H₂O layer was eliminated and the CH₃NO₂ layer was washed several times with H₂O to extract the NH₄Cl salts. The layers were separated and the CH₃NO₂ layer was dried using MgSO₄. The CH₃NO₂ was evaporated to yield **6-6a**⁶⁺ as a yellow-orange solid. (*R*_f = 0.66, 0.030 g, 12%). **ESI-MS**: *m/z* [**6-6a** - 2OTf]²⁺ calc. 1116.7969, found 1116.7969.

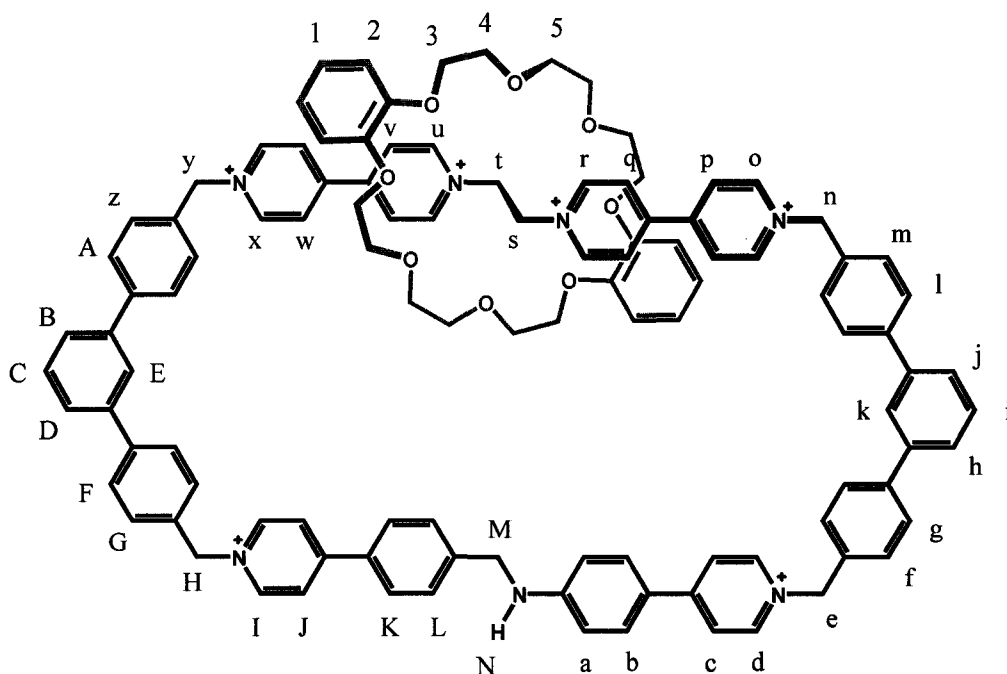


Table 6.8 – ^1H NMR of $[6-6][\text{OTf}]_6$ in CD_3CN . $\text{MW}_{\text{OTf}} = 2533.441$ g/mol

Proton	δ (ppm)	Multiplicity	# Protons	J (Hz)
a	6.79	d	2	$^3J_{ab} = 8.74$
b	7.78	d	2	$^3J_{ba} = 8.74$
c	8.04	d	2	$^3J_{cd} = 6.91$
d	8.49	d	2	$^3J_{dc} = 6.91$
e	5.59	s	2	--
f	7.51	d	2	$^3J_{fg} = 8.36$
g	7.80	d	2	$^3J_{gf} = 8.36$
h	7.70-7.74	d	1	--
i	7.62	dd	1	--
j	7.70-7.74	d	1	--
k	7.83	s	1	--
l	7.87	d	2	$^3J_{lm} = 8.23$
m	7.64	d	2	$^3J_{ml} = 8.23$
n	5.90	s	2	--
o	9.03	d	2	$^3J_{op} = 6.75$
p	8.19	d	2	$^3J_{po} = 6.75$
q	8.22	d	2	$^3J_{qr} = 6.72$
r	9.31	d	2	$^3J_{rq} = 6.72$

s	5.56	s	2	--
t	5.56	s	2	--
u	9.31	d	2	${}^3J_{uv} = 6.72$
v	8.22	d	2	${}^3J_{vu} = 6.72$
w	8.19	d	2	${}^3J_{wx} = 6.75$
x	9.03	d	2	${}^3J_{xw} = 6.75$
y	5.90	s	2	--
z	7.64	d	2	${}^3J_{zA} = 8.23$
A	7.87	d	2	${}^3J_{Az} = 8.23$
B	7.70-7.74	d	1	--
C	7.62	dd	1	--
D	7.70-7.74	d	1	--
E	7.83	s	1	--
F	7.77	d	2	${}^3J_{FG} = 8.61$
G	7.55	d	2	${}^3J_{GF} = 8.61$
H	5.74	s	2	--
I	8.76	d	2	${}^3J_{IJ} = 6.79$
J	8.22	d	2	${}^3J_{JI} = 6.79$
K	7.87	d	2	${}^3J_{KL} = 8.22$
L	7.58	d	2	${}^3J_{LK} = 8.22$
M	4.48	d	2	${}^3J_{MN} = 5.57$
N	5.87	t	1	${}^3J_{NM} = 5.57$
1	6.62	m	4	${}^3J_{ortho} = 5.83, {}^3J_{meta} = 3.58,$
2	6.33	m	4	${}^3J_{ortho} = 5.83, {}^3J_{meta} = 3.58,$
3-5	3.99-4.04	m	24	--

6.5.8 Synthesis of Compound 6-7a²⁺

6-2 (0.050 g, 1.48×10^{-4} mol) and benzyl bromide (0.101 g, 0.070 mL, 5.93×10^{-4} mol) were dissolved in CH₃CN (25 mL) and stirred at room temperature for three days. The precipitate was collected by filtration and washed with CH₂Cl₂. The product was anion exchanged to the triflate salt by dissolving the precipitate in H₂O and adding NaOTf. **6-7a²⁺** was isolated by vacuum filtration as a yellow solid. (0.045 g, 37 %) ESI-MS: m/z [**6-7a** - OTf]⁺ calc. 668.2189, found 668.2204.

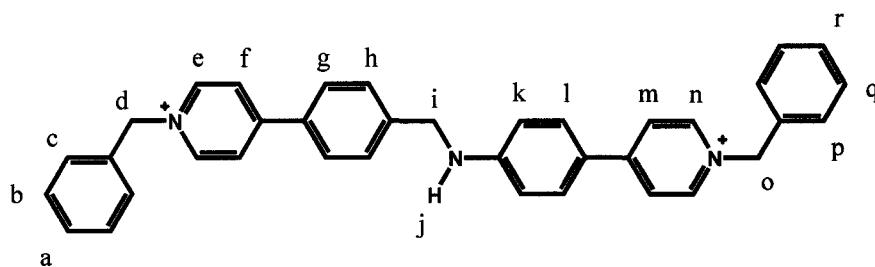


Table 6.9 – ¹H NMR of [6-7][OTf] in CD₃CN. MW_{OTf} = 817.816 g/mol

Proton	δ (ppm)	Multiplicity	# Protons	J (Hz)
a-c	7.40-7.49	m	5	--
d	5.70	s	2	--
e	8.72	d	2	³ $J_{ef} = 6.82$
f	8.23	d	2	³ $J_{fe} = 6.82$
g	7.89	d	2	³ $J_{gh} = 8.28$
h	7.60	d	2	³ $J_{hg} = 8.28$
i	4.57	d	2	³ $J_{ij} = 6.11$
j	6.11	t	1	³ $J_{ji} = 6.11$
k	6.78	d	2	³ $J_{kl} = 8.82$
l	7.77	d	2	³ $J_{lk} = 8.82$
m	8.03	d	2	³ $J_{mn} = 7.12$
n	8.45	d	2	³ $J_{nm} = 7.12$
o	5.54	s	2	--
p-r	7.40-7.49	m	5	--

CHAPTER 7

Towards [2]Rotaxane Functional Materials

7.1 INTRODUCTION

For the most part, the molecular motions of interlocked chemical systems that have been presented in this thesis have been investigated in solution, where molecules are dispersed randomly. In order for molecular motors and machines to be coupled to the macroscopic world, they must be organized so that they can perform in a cooperative manner. It has been suggested that this could be accomplished by organizing the molecules 1) at an interface, 2) on surfaces, 3) within membranes or 4) in crystalline lattices. Whatever the scenario, it is important that the interlocked components maintain their dynamic movement. To date, most endeavors are only in the initial stages and scientists are just beginning to understand their true capabilities and potential.

7.2 FUTURE DIRECTIONS OF STUDY

7.2.1 Surface Studies

Self-assembled monolayers (SAMs) consist of a single layer of molecules adsorbed onto a surface. The most widely studied systems are thiolate compounds adsorbed onto gold substrates. SAMs are particularly attractive because of their ease of preparation from a dilute solution of the adsorbate onto a clean metal surface.¹¹⁷ The surface properties of SAMs are defined by the molecular structure of the monolayer. One particular interfacial property that is relatively easy to study is the wetting behaviour of

the surface. Using a contact angle goniometer, the advancing and receding contact angles of water (or some other liquid) with the surface are measured. When water is the testing liquid, a large contact angle, usually between 70 and 90°, indicates a hydrophobic surface; a small contact angle, usually between 10 and 30°, indicates a hydrophilic surface.

Although there are few studies of [2]rotaxanes on surfaces, there is evidence of mechanical shuttling in condensed monolayers.^{118, 119} Figure 7.1 describes an approach to controlling the wettability of a surface using bistable rotaxanes as SAMs. The molecular shuttles depicted possess two recognition sites, represented by the blue sphere and the yellow oval, which the macrocycle can occupy. The macrocycle can be modified by the addition of functional groups, denoted by the bright green lobes. The exposed portion of the shuttle is represented by a green box. Each of these features can be adapted to affect the properties of the surface. The main focus of this system is to show that the switching of the macrocycle from one site to the other has a direct effect on the wettability of the surface. For instance, if the exposed capping group on the rotaxane is a perfluorinated fragment, this would impose extreme hydrophobic properties on the surface. If the macrocycle is substituted with hydroxyl groups and is located at the blue sphere, hence is 'buried' in the monolayer, the hydrophobic properties of the capping group would prevail. External perturbation of the shuttle, changing the yellow oval to a black oval, would cause the macrocycle to shift to the oval site, hence exposing the hydroxyl groups, thereby making the surface hydrophilic. Contact angle measurements could be used to verify the change in hydrophobicity and hydrophilicity.

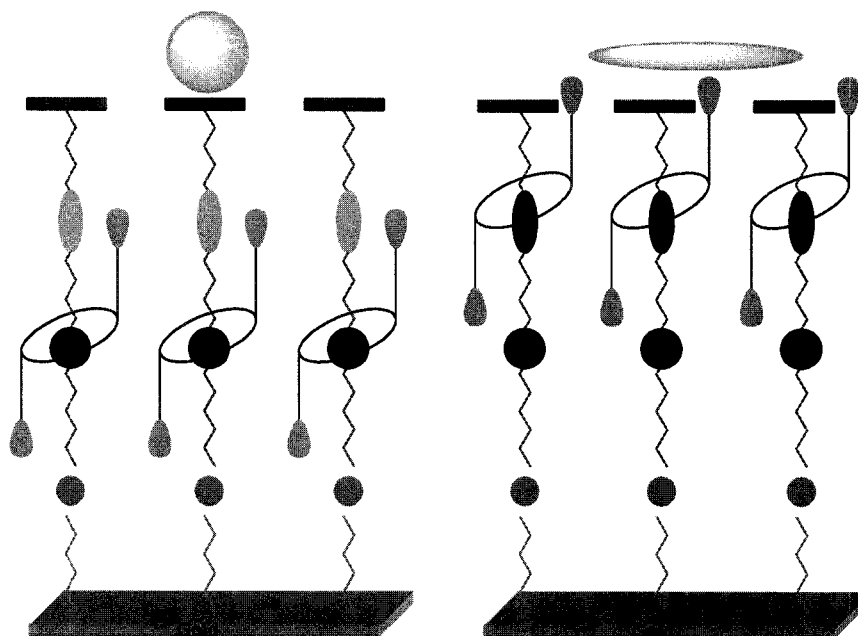


Figure 7.1 – Controlling the wettability of a surface using SAMs of rotaxanes

7.2.2 MORF's

Metal organic *rotaxane* frameworks (MORFs) are a subclass of metal organic frameworks (MOFs), a term coined by Yaghi.¹²⁰ MOFs are a class of porous materials consisting of a scaffold composed of organic linkers between metal atoms. The voids that are created within the scaffold have been shown to have useful storage capabilities for gases, such as methane and hydrogen, due to the extremely large surface area of the pores. MORFs are similar to MOFs with the exceptional difference being that the organic linkers are rotaxanes instead of just simple organic compounds. Only two well defined MORF systems are known: diaminoalkane/cucurbituril polyrotaxanes by K. Kim¹²¹ and 1,2-bis(4,4'-dipyridyl)ethane/DB24C8 polyrotaxanes from the Loeb group.⁴⁹ The Loeb motif has been used to generate 1-, 2- and 3-dimensional frameworks using a variety of metals ranging from transition metals such as Cu(II), Co(II), Cd(II) and Ni(II), to lanthanide metals, such as Eu(III), Sm(III) and Yb(III). One advantage to using rotaxanes

as the organic linkers is the potential for fine-tuning that may be achieved by simple supramolecular modification. In other words, the properties of the MORF may be modified simply by exchanging the wheel component used in the self-assembly process. This is reminiscent of the approach described above for changing the properties of a surface through controllable switching of self-assembled monolayers.

7.3 PROGRESS MADE TO THIS END

7.3.1 Surface Studies

The cartoons in Figure 7.2 are schematic representations of the compound **7-7a²⁺**. The blue sphere represents the bis(pyridinium)ethane site, the yellow oval is the benzylianium site, the green box represents the capping group that is exposed at the surface, the red circle is the crown ether, the bright green lobes on the red circle represent groups that could be incorporated onto the aromatic rings of the crown ether, the grey sphere represents the metal atom used to combine the rotaxane with the surface linker, which is represented by the orange chain. Once again, the versatility of this rotaxane system is demonstrated. The rotaxane that has been synthesized has an anthracene capping group, however, any benzyl bromide should, in theory, be easily exchanged for the anthracene which could directly affect the surface properties of the SAM. Furthermore, any crown ether can be used that may impose different properties to the system under study. CAChe simulations of model compounds suggest that a chain of three atoms off the four position of the benzo aromatic ring of the crown ether should be sufficient to surpass the capping group and be exposed at the surface.

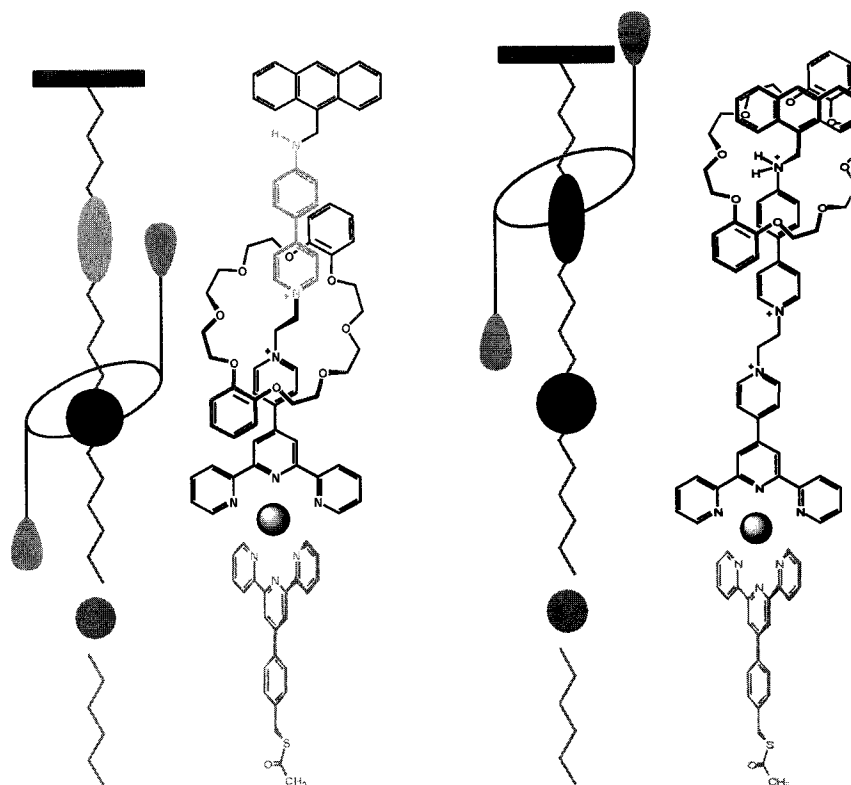


Figure 7.2 – Cartoon schematic of rotaxanes 7-7a²⁺ and 7-7b³⁺.

4'-Aryl-2,2',6',2''-terpyridines have been incorporated into the thread to act as a stopper and to provide a means of attaching the rotaxane to a surface linker. This design allows for any rotaxane synthesized with a terpyridine stopper to be incorporated into a monolayer, while using the same surface linker. Keeping the surface linker constant removes any ambiguity concerning the integrity of the monolayer/gold interface.

The surface linker, 4'-acetylthiobenzyl-2,2',6',2''-terpyridine (7-5) is considered a protected thiol. There is evidence that a thioacetate is capable of forming self-assembled monolayers on gold surfaces.¹²² There is also contrasting evidence that it is not capable.¹²³

There are two methods by which self-assembled monolayers of rotaxane 7-7²⁺ on a gold surface may be formed. The first would be to build the SAMs in a layer by layer

approach.^{124, 125} In this method, compound 7-5 would be adsorbed onto a gold substrate (Figure 7.3a), followed by addition of a metal whose coordination sphere would be filled by loosely coordinated solvent molecules (Figure 7.3b). Last would be the addition of rotaxane 7-7²⁺ which would replace the labile solvent molecules and coordinate to the metal (Figure 7.3c).

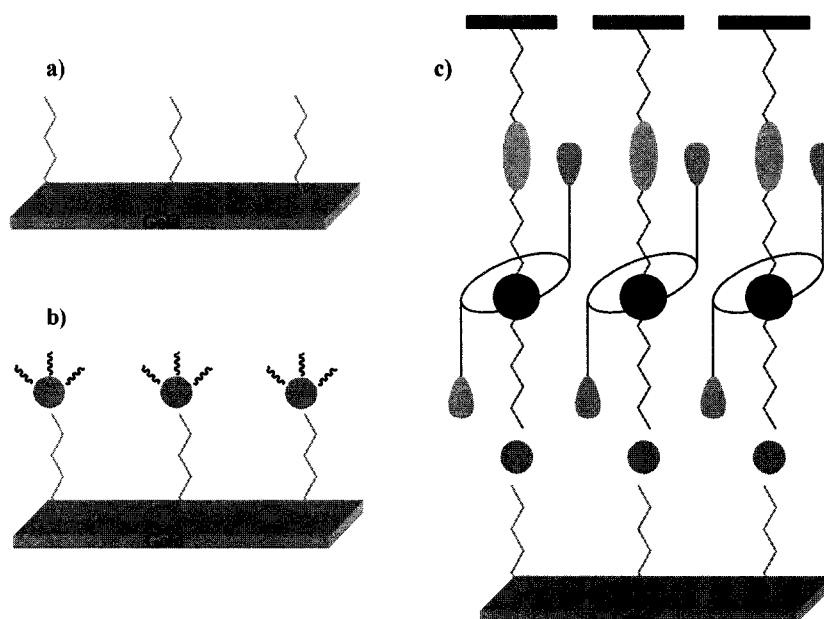


Figure 7.3 – Layer by layer approach to monolayer formation.

The second method would involve first coordinating the surface linker and the rotaxane to a metal, then making a monolayer of the intact molecular assembly.

Thickness, composition and structure are the three basic properties that characterize SAMs. Each property can be probed using different techniques: thickness by ellipsometry and X-ray photoelectron spectroscopy (XPS), composition by XPS and reflection absorption infrared spectroscopy (RAIRS), structure by RAIRS, contact angle goniometry, XPS, ellipsometry, AFM and SEM. Both methods for forming SAMS

outlined above would first be tested using model compound **7-2** (Scheme 7.1). Several different methods for analyzing and characterizing the monolayers would be used, including RAIRS and contact angle measurements. Compound **7-2** makes an ideal model compound because it should provide a signature strong IR stretch vibration band for the carbonyl and it should give low contact angles with H₂O as the testing liquid drop. The surface linker **7-5** would lose its thioacetate carbonyl stretch vibration or its S-H stretch vibration, thus the absence of a strong band at 1690 cm⁻¹ or 2550 cm⁻¹ would be used as an indication of monolayer formation. Addition of a metal might be identified by a change in contact angle, or a strong UV-visible absorption band from metal-to-ligand charge transfer. Presence of **7-2** would be indicated by a strong IR absorption band at ~1700 cm⁻¹ for the carbonyl stretch vibration.

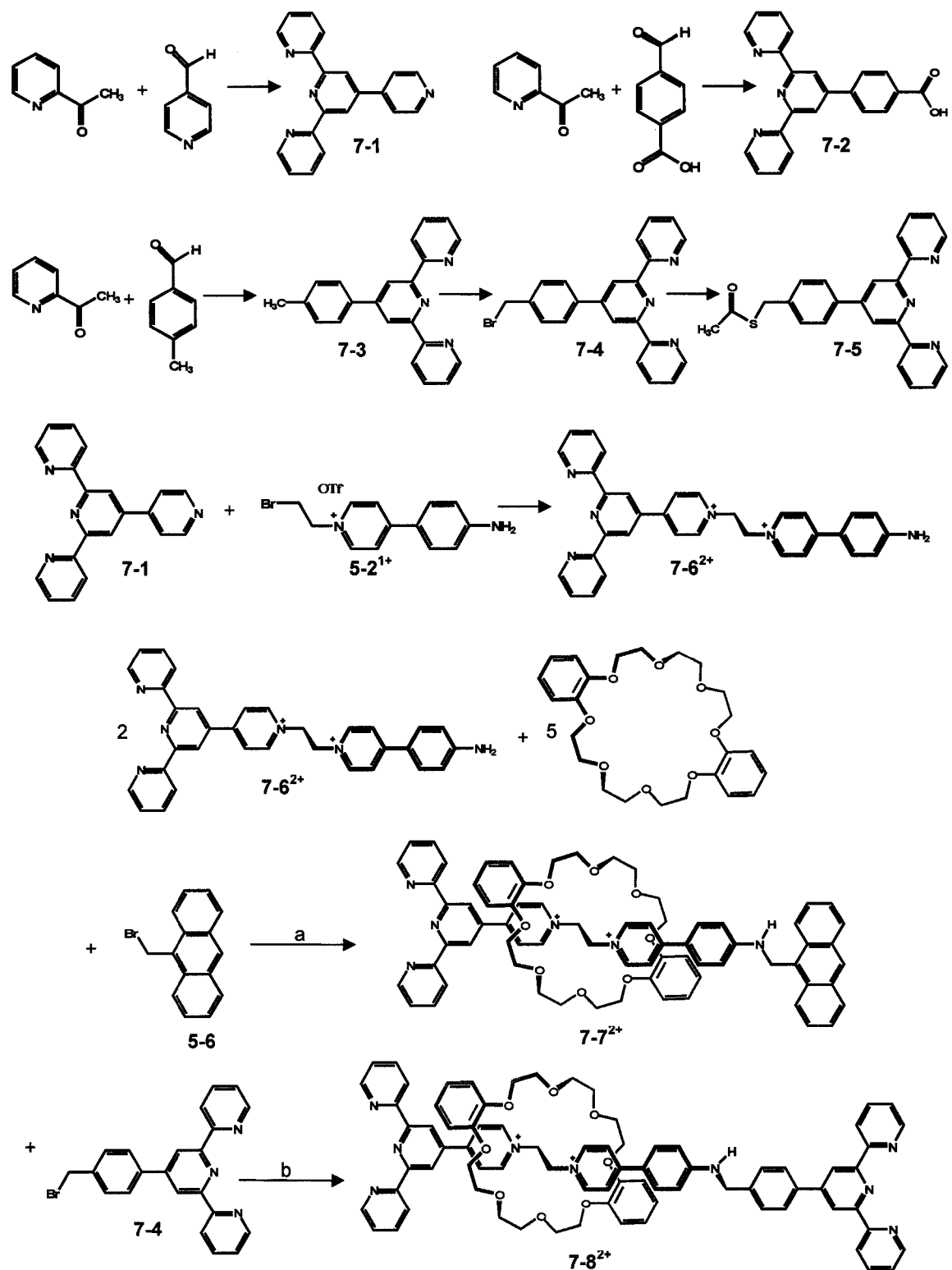
7.3.2 MORFs

One of the major challenges for this chemistry is to construct solid state materials that contain mechanically switchable components. Using the [2]rotaxane molecular shuttles, such as **7-8²⁺**, for constructing MORFs would incorporate such a switch. The prospect of the shuttling motion would provide an extra impact to these materials. Another feature that makes this system different from the MORFs reported thus far, is that the organic linker is a permanently interlocked [2]rotaxane. Unlike the scenario where the organic linkers are initially [2]pseudorotaxanes, having intact [2]rotaxanes means that the conditions required for chelation to a metal center should not interfere with the integrity of the mechanical linkage.

7.4 SYNTHESIS AND STRUCTURAL CHARACTERIZATION

7.4.1 Synthesis

Synthesis and isolation of [2]rotaxane molecular shuttles **7-7²⁺** and **7-8²⁺** were performed in much the same way as the [2]rotaxanes described in Chapter 5. Scheme 7.1 outlines the synthetic methodology. The rotaxanes described in this chapter are 4'-aryl-2,2',6',2''-terpyridine based. 4'-Substituted 2,2',6',2''-terpyridines were synthesized using a Kröhnke condensation between 2-acetyl pyridine and the corresponding aldehyde in the presence of a base, followed by addition of ammonium acetate.¹²⁶⁻¹²⁸ This methodology was used to generate compounds **7-1** – **7-3**. Compound **7-3** was used in a subsequent reaction to synthesize the corresponding benzyl bromide (**7-4**) by reaction with NBS in the presence of benzoyl peroxide. Compound **7-5** was obtained by a simple substitution reaction of **7-4** with potassium thioacetate. The pre-thread (**7-6²⁺**) was produced by reacting **7-1** with [**5-2**][OTf] in refluxing propionitrile. Assembling of the [2]rotaxanes **7-7²⁺** and **7-8²⁺** was accomplished by reaction of **7-6²⁺** with excess **DB24C8**, to form the corresponding [2]pseudorotaxane, followed by addition of either **5-6** or **7-4** as the capping reagent. Preparative TLC was used to isolate the rotaxanes using 5:3:2 CH₃OH:2M NH₄Cl:CH₃NO₂ as the eluent.

**Scheme 7.1 – Synthetic scheme for [2]rotaxanes molecular shuttles.**

7.4.2 ^1H NMR Spectroscopy

Both rotaxanes were characterized by ^1H NMR spectroscopy and 2-D ^1H - ^1H COSY spectroscopy experiments. Figures 7.4 and 7.5 describe the labeling of the protons and show the ^1H NMR spectra for rotaxanes $7\text{-}2^{2+}$ and $7\text{-}8^{2+}$, respectively. Capped threads are not available, but the proton shifts can be compared to the pre-thread $7\text{-}6^{2+}$ and the respective cap compounds **5-6** and **7-4**. The rotaxanes show similar trends to those observed for the rotaxanes described in Chapter 5 and the catenane in Chapter 6. The ethylene protons, **h** and **i**, as well as the *ortho* pyridinium protons, **g** and **j**, shift downfield as a result of hydrogen bonding interactions between these protons and the oxygen atoms of the crown ether. Protons **f** and **k** shift upfield due to π -stacking interactions. The chemical shifts corresponding to the protons on the cap fragment in the rotaxanes do not change significantly compared to the shifts of the same protons in the free cap compounds.

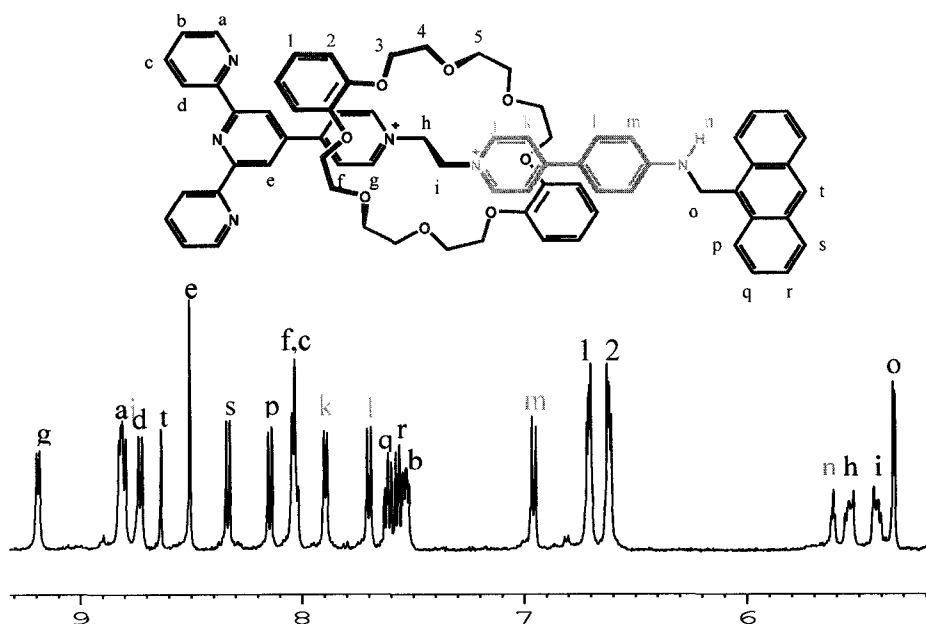


Figure 7.4 – ^1H NMR spectrum of $7\text{-}7^{2+}$ in CD_3CN at 500 MHz and 30°C .

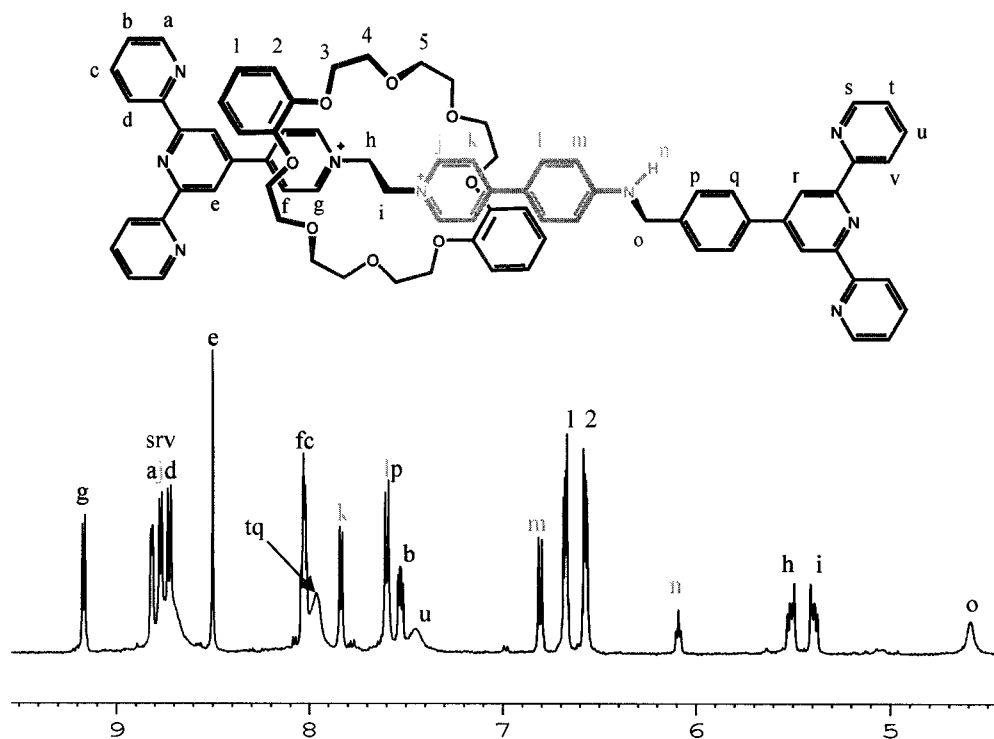


Figure 7.5 – ^1H NMR spectrum of $7\text{-}8^{2+}$ in CD_3CN at 500 MHz and 30°C .

7.4.3 Infrared Spectroscopy

The IR spectra of compounds **7-2** and **7-5** were recorded since the solution IR spectra will be compared to the surface RAIRS spectra of the monolayers. The IR spectrum of **7-2** (Figure 7.6) shows a typical strong carbonyl stretch vibration band from the carboxylic acid at 1705 cm^{-1} . Similarly, the IR spectrum of **7-5** (Figure 7.7) has a strong carbonyl stretch vibration band from the thioacetate at 1681 cm^{-1} .

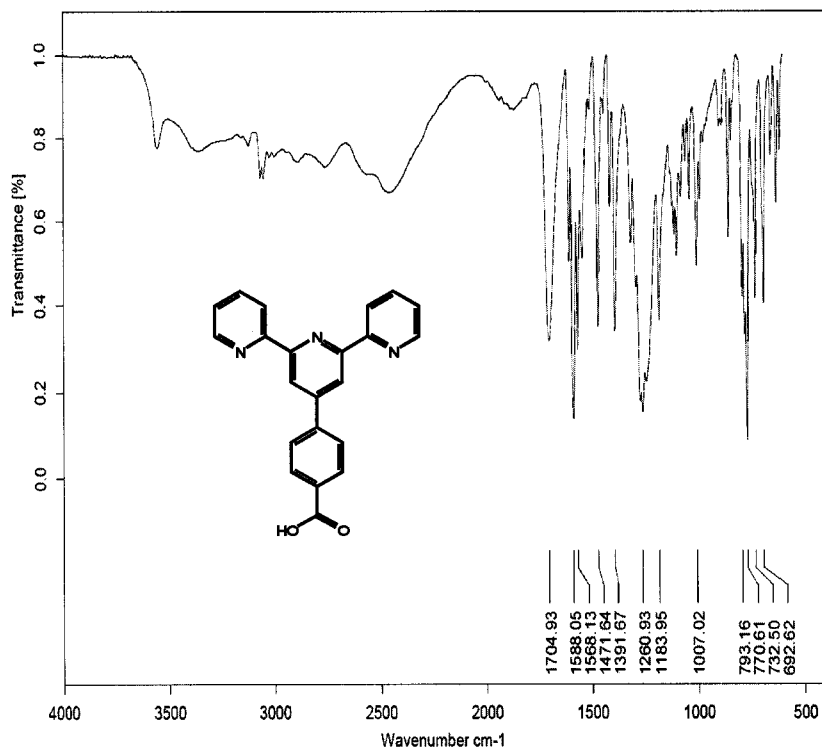


Figure 7.6 – IR spectrum of 7-2.

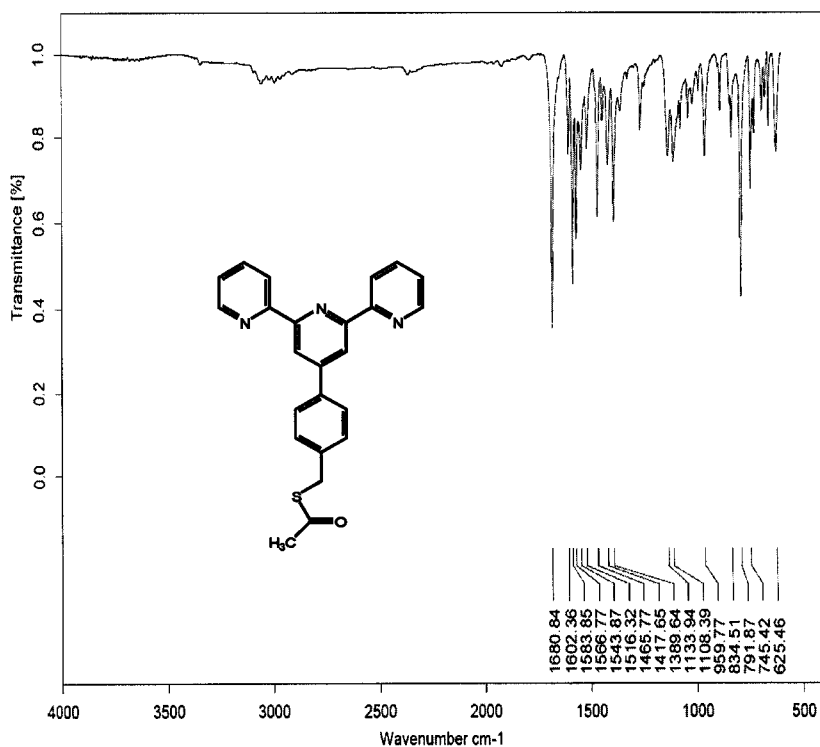


Figure 7.7 – IR spectrum of 7-5.

7.5 SUMMARY AND CONCLUSIONS

Two different experimental approaches to the synthesis of functional materials have been described. Both methodologies make use of simple modifications of pre-existing systems to change the properties of the materials. However, many issues need to be addressed and studied.

For the surface chemistry, one might ask: does the position of the benzylianium site make a difference? Will the benzylianium site be easily protonated and deprotonated by a simple rinsing of the surface with acid or base solutions? Can the position of the bis(pyridinium)ethane and benzylianium sites be exchanged and the switching of the crown ether still occur? How dense can the monolayers be without affecting the movement of the macrocycle between sites? Can the rotaxane assemblies be diluted with another adsorbate and still influence the properties of the surface? Will the position of the shuttle be able to affect the properties of the surface?

For the solid state MORFs-based materials there are still some fundamental questions that need to be answered. How can the number of counterions be reduced? How can the stability of the solid be increased so that a MORF can be evacuated and activated without decomposition of the crystalline lattice? How can interpenetration of networks be avoided? How can the porosity of the material be maximized to allow for “freedom” of motion? How can the motion be monitored and controlled without the need for diffusion of a chemical reactant into and out of the porous material?

It is possible that the answers to these and other important questions could lead to the future development of molecular motors and machines relevant to our macroscopic world.

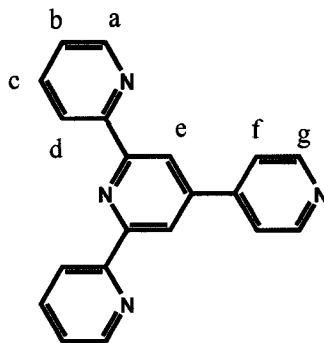
7.6 EXPERIMENTAL

7.6.1 General Comments

4-Pyridinecarboxaldehyde, 4-carboxybenzaldehyde, 4-tolualdehyde, 2-acetylpyridine and ammonium acetate were purchased from Aldrich and used as received. IR spectra were recorded on a Bruker -Equinox – Infrared Microscopy and Mapping instrument.

7.6.2 Synthesis of 7-1

4-Pyridinecarboxaldehyde (12.4 g, 10.9 mL, 0.103 mol) was dissolved in ethanol (40 mL) and cooled to 0°C. To this was added 2-acetylpyridine (25.0 g, 23.2 mL, 0.207 mol) dissolved in ethanol (20 mL) and 40% aqueous solution of NaOH (30 mL). The mixture was stirred at -10°C for an additional hour then allowed to warm to room temperature and stirred overnight. Ammonium acetate (40.0 g, 0.516 mol) was added directly to the reaction mixture and refluxed for 24 hours. The reaction was cooled to room temperature and placed in the freezer for 24 hours. The precipitate that formed was filtered and recrystallized from CH₃CN. (3.15 g, 10 %)

Table 7.1 – ^1H NMR of 7-1 in CD_3CN . MW = 310.352 g/mol

Proton	δ (ppm)	Multiplicity	# Protons	J (Hz)
a	8.74	d	2	$^3J_{ab} = 4.78$
b	7.46	ddd	2	$^3J_{ba} = 4.78, ^3J_{bc} = 7.66,$ $^4J_{bd} = 0.98$
c	7.98	ddd	2	$^3J_{cd} = 7.88, ^3J_{cb} = 7.66,$ $^4J_{ca} = 1.78$
d	8.71	d	2	$^3J_{dc} = 7.88$
e	8.79	s	2	--
f	7.83	d	2	$^3J_{ortho} = 6.10, ^4J_{meta} = 1.64$
g	8.76	d	2	$^3J_{ortho} = 6.10, ^4J_{meta} = 1.64$

7.6.3 Synthesis of 7-2

4-Carboxybenzaldehyde (15.5 g, 0.103 mol) was dissolved in methanol (40 mL) and cooled to 0°C. To this was added 2-acetylpyridine (25.0 g, 23.2 mL, 0.207 mol) dissolved in methanol (20 mL) and 40% aqueous solution of NaOH (30 mL). The mixture was stirred at -10°C for an additional hour then allowed to warm to room temperature and stirred overnight. Ammonium acetate (40.0 g, 0.516 mol) was added directly to the reaction mixture and refluxed for 24 hours. The reaction was cooled to room temperature and the solution was acidified with 1.0 M HCl_(aq) to pH = 6. The precipitate that formed was filtered and the residue dissolved in hot MeOH. The hot MeOH solution was filtered and the precipitate collected was identified as the desired product (0.470 g, 1.29 %).

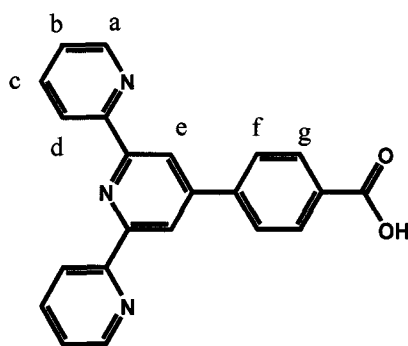


Table 7.2 – ¹H NMR of 7-2 in DMSO-d₆. MW = 353.374 g/mol

Proton	δ (ppm)	Multiplicity	# Protons	J (Hz)
a	8.75	d	2	³ J _{ab} = 5.53
b	7.52	ddd	2	³ J _{ba} = 5.53, ³ J _{bc} = 6.93,
c	8.03	ddd	2	³ J _{cd} = 7.46, ³ J _{cb} = 6.93,
d	8.67	d	2	⁴ J _{ca} = 1.62
e	8.75	s	2	³ J _{dc} = 7.46
f	8.04	d	2	--
g	8.12	d	2	³ J _{fg} = 8.24
				³ J _{gf} = 8.24

7.6.4 Synthesis of 7-3

4-Tolualdehyde (12.6 g, 12.4 mL, 0.105 mol) was dissolved in methanol (40 mL) and cooled to 0°C. To this was added 2-acetylpyridine (25.4 g, 23.5 mL, 0.209 mol) dissolved in methanol (20 mL) and 40% aqueous solution of NaOH (30 mL). The mixture was stirred at -10°C for an additional hour then allowed to warm to room temperature and stirred overnight. CH₃CO₂NH₄ (40.0 g, 0.516 mol) was added to the reaction mixture which was then refluxed for 24 hours. The reaction was cooled to room temperature and the methanol evaporated. The product was extracted with CHCl₃, then the CHCl₃ was dried with MgSO₄, filtered and evaporated. The residue was recrystallized from CH₃CN to yield 7-3 as an off-white powder (11.26 g, 33 %).

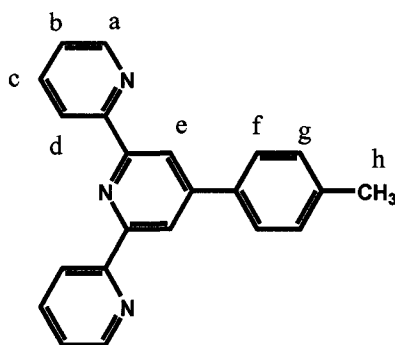
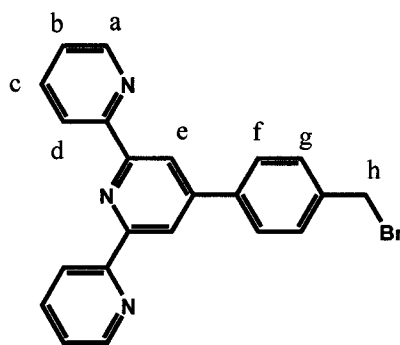


Table 7.3 – ¹H NMR of 7-3 in CD₃CN. MW = 323.390 g/mol

Proton	δ (ppm)	Multiplicity	# Protons	J (Hz)
a	8.73	d	2	³ J _{ab} = 5.75
b	7.44	ddd	2	³ J _{ba} = 5.75, ³ J _{bc} = 7.52, ⁴ J _{bd} = 0.79
c	7.96	ddd	2	³ J _{cd} = 7.82, ³ J _{cb} = 7.52, ⁴ J _{ca} = 1.67
d	8.68	d	2	³ J _{dc} = 7.82
e	8.73	s	2	--
f	7.81	d	2	³ J _{fg} = 8.07
g	7.40	d	2	³ J _{gf} = 8.07
h	2.43	s	3	--

7.6.5 Synthesis of 7-4

Compound 7-3 (3.23 g, 0.0100 mol) was dissolved in CCl_4 (200 mL). To this solution was added *N*-bromosuccinimide (2.14 g, 0.0120 mol) and benzoyl peroxide (0.0242 g, 1.00×10^{-4} mol) and the reaction solution refluxed for five hours, then cooled to room temperature and stirred overnight. The reaction was filtered to remove succinimide and then the CCl_4 organic layer was washed with $\text{NaHCO}_3(\text{aq})$ (2×100 mL) then H_2O (2×100 mL), dried with MgSO_4 , filtered and then evaporated on a rotary evaporator to give



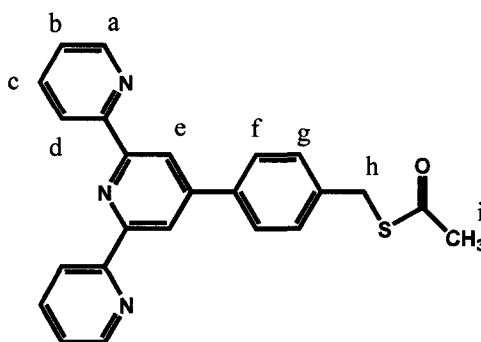
an off-white powder (1.39 g, 35 %).

Table 7.4 – ^1H NMR of 7-4 in CD_3CN . MW = 402.287 g/mol

Proton	δ (ppm)	Multiplicity	# Protons	J (Hz)
a	8.73	d	2	$^3J_{ab} = 4.96$
b	7.45	dd	2	$^3J_{ba} = 4.96, ^3J_{bc} = 7.41$
c	7.97	ddd	2	$^3J_{cb} = 7.41, ^3J_{cd} = 7.81, ^4J_{ca} = 1.62$
d	8.69	d	2	$^3J_{dc} = 7.81$
e	8.75	s	2	--
f	7.90	d	2	$^3J_{fg} = 8.20$
g	7.63	d	2	$^3J_{gf} = 8.20$
h	4.69	s	2	--

7.6.6 Synthesis of 7-5

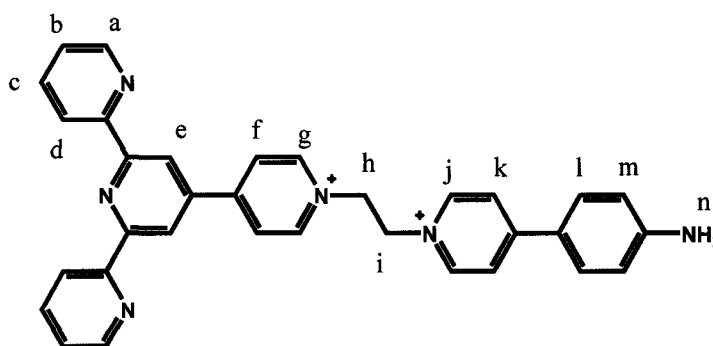
7-4 (1.00 g, 2.47×10^{-3} mol) and potassium thioacetate (0.400 g, 3.50×10^{-3} mol) were dissolved in acetone (75 mL) and refluxed for six hours. The reaction was cooled to room temperature and the solvent evaporated. The residue was dissolved in CH_2Cl_2 and washed with H_2O (3×50 mL). The CH_2Cl_2 layer was dried using MgSO_4 , filtered and evaporated to yield a pale brown powder. (0.893 g, 90%)

Table 7.5 – ^1H NMR of 7-5 in CD_3CN . MW = 397.492 g/mol

Proton	δ (ppm)	Multiplicity	# Protons	J (Hz)
a	8.72	d	2	$^3J_{ab} = 5.34$
b	7.44	ddd	2	$^3J_{ba} = 5.34, ^3J_{bc} = 7.58, ^3J_{bd} = 0.91$
c	7.96	ddd	2	$^3J_{cd} = 7.88, ^3J_{cb} = 7.58, ^4J_{ca} = 1.72$
d	8.68	d	2	$^3J_{dc} = 7.88$
e	8.73	s	2	--
f	7.85	d	2	$^3J_{fg} = 8.21$
g	7.50	d	2	$^3J_{gf} = 8.21$
h	4.20	s	2	--
i	2.36	s	3	--

7.6.7 Synthesis of 7-6²⁺

Compound 7-1 (1.96 g, 0.00632 mol) and [5-2][OTf] were dissolved in propionitrile and refluxed for 7 days. The precipitate that formed was filtered while the solution was still hot. This yielded [7-6][Br]₂ as a pale yellow solid. (0.520 g, 37 %) The product was anion exchanged by dissolving the bromide salt in H₂O and adding NaOTf. [7-6][OTf]₂ precipitated and was collected by vacuum filtration. (0.597 g, 95%)

Table 7.6 – ¹H NMR of [7-6][Br]₂ in D₂O. MW_{Br-} = 668.424 g/mol

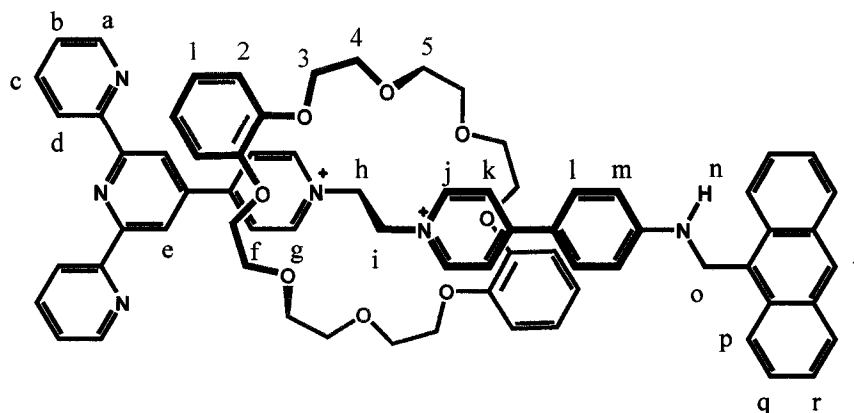
Proton	δ (ppm)	Multiplicity	# Protons	J (Hz)
a	8.67	d	2	³ J _{ab} = 4.82
b	7.82	dd	2	³ J _{ba} = 4.82, ³ J _{bc} = 7.46
c	8.06	ddd	2	³ J _{cb} = 7.46, ³ J _{cd} = 7.83, ⁴ J _{ca} = 1.42
d	8.40	d	2	³ J _{dc} = 7.83
e	8.58	s	2	--
f	8.57	d	2	³ J _{fg} = 6.68
g	8.98	d	2	³ J _{gf} = 6.68
h	5.36	t	2	³ J _{hi} = 5.99
i	5.20	t	2	³ J _{ih} = 5.99
j	8.50	d	2	³ J _{jk} = 6.92
k	8.15	d	2	³ J _{kj} = 6.92
l	7.82	d	2	³ J _{lm} = 8.54
m	6.88	d	2	³ J _{ml} = 8.54
n	--	--	2	--

Table 7.7 – ^1H NMR of [7-6][OTf]₂ in CD₃CN. MW_{OTf} = 806.754 g/mol

Proton	δ (ppm)	Multiplicity	# Protons	J (Hz)
a	8.75	d	2	$^3J_{ab} = 6.47$
b	7.51	dd	2	$^3J_{ba} = 6.47, ^3J_{bc} = 7.06$
c	7.97	dd	2	$^3J_{cb} = 7.06, ^3J_{cd} = 7.38,$
d	8.74	d	2	$^3J_{dc} = 7.38$
e	8.89	s	2	--
f	8.52	d	2	$^3J_{fg} = 5.89$
g	8.75	d	2	$^3J_{gf} = 5.89$
h	5.13	t	2	$^3J_{hi} = 6.13$
i	4.97	t	2	$^3J_{ih} = 6.13$
j	8.31	d	2	$^3J_{jk} = 7.03$
k	8.08	d	2	$^3J_{kj} = 7.03$
l	7.81	d	2	$^3J_{lm} = 8.78$
m	6.81	d	2	$^3J_{ml} = 8.78$
n	5.19	br s	2	--

7.6.8 Synthesis of 7-7²⁺

Compound [7-6][Br]₂ (0.300 g, 4.49×10^{-4} mol), **DB24C8** (1.01 g, 2.24×10^{-3} mol) and **5-6** (0.0610 g, 2.24×10^{-4} mol) were dissolved in a two phase mixture of CH₃NO₂ and H₂O. To this, two equivalents of NaOTf (0.150 g, 8.72×10^{-4} mol) were added and the reaction mixture stirred at room temperature for seven days. The CH₃NO₂ layer was separated from the H₂O layer, washed with H₂O (2 × 5 mL), dried with MgSO₄ and evaporated. The residue was dissolved in CH₂Cl₂ and the precipitate filtered. The precipitate was adsorbed onto a preparative TLC sheet and developed using 5:3:2 CH₃OH:2M NH₄Cl: CH₃NO₂ as the eluent. The product was isolated from the band with $R_f = 0.82$ (0.110 g, 34%). **ESI-MS**: m/z [7-7 - OTf]⁺ calc. 1295.4770, found 1295.4808.

Table 7.8 – ^1H NMR of [7-7][OTf] $_2$ in CD_3CN . $\text{MW}_{\text{OTf}} = 1445.500$ g/mol

Proton	δ (ppm)	Multiplicity	# Protons	J (Hz)
a	8.82	d	2	$^3J_{ab} = 5.95$
b	7.53	dd	2	$^3J_{ba} = 5.95, ^3J_{bc} = 6.55$
c	8.03	dd	2	$^3J_{cb} = 6.55, ^3J_{cd} = 7.20,$
d	8.73	d	2	$^3J_{dc} = 7.20$
e	8.51	s	2	--
f	8.04	d	2	$^3J_{fg} = 6.50$
g	9.19	d	2	$^3J_{gf} = 6.50$
h	5.54	m	2	--
i	5.42	m	2	--
j	8.80	d	2	$^3J_{jk} = 6.88$
k	7.90	d	2	$^3J_{kj} = 6.88$
l	7.70	d	2	$^3J_{lm} = 8.70$
m	6.96	d	2	$^3J_{ml} = 8.70$
n	5.62	t	1	$^3J_{no} = 4.20$
o	5.35	d	2	$^3J_{on} = 4.20$
p	8.15	d	2	$^3J_{pq} = 8.85$
q	7.61	dd	2	$^3J_{qp} = 8.85$
r	7.57	dd	2	$^3J_{rs} = 8.29$
s	8.33	d	2	$^3J_{sr} = 8.29$
t	8.64	s	1	--
1	6.71	m	4	--
2	6.62	m	4	--
3-5	3.96-4.13	m	24	--

7.6.9 Synthesis of 7-8²⁺

Compound [7-6][OTf]₂ (0.241 g, 2.99 × 10⁻⁴ mol), DB24C8 (1.34 g, 2.99 × 10⁻³ mol) and 7-5 (0.120 g, 2.99 × 10⁻⁴ mol) were dissolved in a two phase mixture of CH₃NO₂ and H₂O. To this, two equivalents of NaOTf (0.103 g, 5.98 × 10⁻⁴ mol) were added and the reaction mixture stirred at room temperature for seven days. The CH₃NO₂ layer was separated from the H₂O layer, washed with H₂O (2 × 5 mL), dried with MgSO₄ and evaporated. The residue was dissolved in CH₂Cl₂ and the precipitate filtered. The precipitate was adsorbed onto a preparative TLC sheet and developed using 5:3:2 CH₃OH:2M NH₄Cl: CH₃NO₂ as the eluent. The product was isolated from the band with R_f = 0.78 (0.0800 g, 17%). **ESI-MS:** *m/z* [7-8 - OTf]⁺ calc. 1426.5253, found 1426.5309.

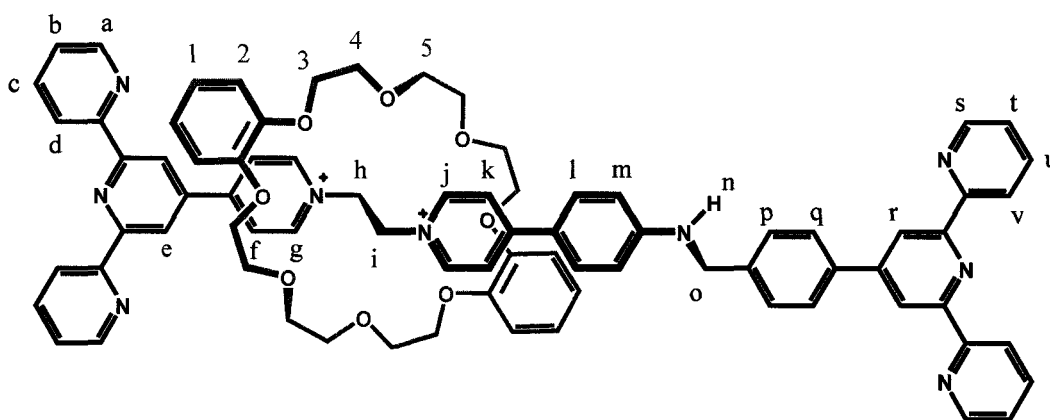


Table 7.9 – ^1H NMR of [7-8][OTf]₂ in CD₃CN. MW_{OTf} = 1576.635 g/mol

Proton	δ (ppm)	Multiplicity	# Protons	J (Hz)
a	8.81	d	2	$^3J_{ab} = 4.74$
b	7.53	dd	2	$^3J_{ba} = 4.74, ^3J_{bc} = 7.40$
c	8.03	dd	2	$^3J_{cb} = 7.40, ^3J_{cd} = 7.77,$ $^4J_{ca} = 1.66$
d	8.72	d	2	$^3J_{dc} = 7.77$
e	8.50	s	2	--
f	8.03	d	2	$^3J_{fg} = 6.64$
g	9.17	d	2	$^3J_{gf} = 6.64$
h	5.51	m	2	--
i	5.39	m	2	--
j	8.77	d	2	$^3J_{jk} = 6.88$
k	7.83	d	2	$^3J_{kj} = 6.88$
l	7.60	d	2	$^3J_{lm} = 8.74$
m	6.81	d	2	$^3J_{ml} = 8.74$
n	6.09	t	1	$^3J_{no} = 6.08$
o	4.59	br s	2	$^3J_{on} = 6.08$
p	7.60	d	2	$^3J_{pq} = 8.73$
q	~7.96	br d	2	$^3J_{qp} = 8.73$
r	~8.73	br s	2	--
s	~8.73	br d	2	--
t	~7.96	br dd	2	--
u	7.45	br dd	2	--
v	~8.73	br d	2	--
1	6.67	m	4	--
2	6.57	m	4	--
3-5	3.92-4.12	m	24	--

REFERENCES

1. *The American Heritage® Dictionary of the English Language*. Fourth ed.; Houghton Mifflin Company: Boston, **2000**.
2. Balzani, V., Venturi, M., Credi, A., *Molecular Devices and Machines: A Journey into the Nanoworld*. Wiley-VCH: Weinheim, **2003**.
3. J. Iwamura, K. M., Stereochemical consequences of dynamic gearing. *Accounts of Chemical Research* **1988**, 21, (4), 175-182.
4. Stevens, A. M.; Richards, C. J., A metallocene molecular gear. *Tetrahedron Letters* **1997**, 38, (44), 7805-7808.
5. Bedard, T. C.; Moore, J. S., Design and synthesis of molecular turnstiles. *Journal of the American Chemical Society* **1995**, 117, (43), 10662-71.
6. Kelly, T. R.; Bowyer, M. C.; Bhaskar, K. V.; Bebbington, D.; Garcia, A.; Lang, F.; Kim, M. H.; Jette, M. P., A Molecular Brake. *Journal of the American Chemical Society* **1994**, 116, (8), 3657-8.
7. Harrington, L. E.; Cahill, L. S.; McGlinchey, M. J., Toward an Organometallic Molecular Brake with a Metal Foot Pedal: Synthesis, Dynamic Behavior, and X-ray Crystal Structure of [(9-Indenyl)tritycene]chromium Tricarbonyl. *Organometallics* **2004**, 23, (12), 2884-2891.
8. Kelly, T. R., Progress toward a Rationally Designed Molecular Motor. *Accounts of Chemical Research* **2001**, 34, (6), 514-522.
9. Dominguez, Z.; Dang, H.; Strouse, M. J.; Garcia-Garibay, M. A., Molecular "Compasses" and "Gyroscopes". I. Expedient Synthesis and Solid State Dynamics of an Open Rotor with a Bis(triarylmethyl) Frame. *Journal of the American Chemical Society* **2002**, 124, (11), 2398-2399.
10. Godinez, C. E.; Zepeda, G.; Garcia-Garibay, M. A., Molecular Compasses and Gyroscopes. II. Synthesis and Characterization of Molecular Rotors with Axially Substituted Bis[2-(9-triptycyl)ethynyl]arenes. *Journal of the American Chemical Society* **2002**, 124, (17), 4701-4707.
11. Dominguez, Z.; Dang, H.; Strouse, M. J.; Garcia-Garibay, M. A., Molecular "Compasses" and "Gyroscopes." III. Dynamics of a Phenylene Rotor and Clathrated Benzene in a Slipping-Gear Crystal Lattice. *Journal of the American Chemical Society* **2002**, 124, (26), 7719-7727.

12. Godinez, C. E.; Zepeda, G.; Mortko, C. J.; Dang, H.; Garcia-Garibay, M. A., Molecular Crystals with Moving Parts: Synthesis, Characterization, and Crystal Packing of Molecular Gyroscopes with Methyl-Substituted Triptycyl Frames. *Journal of Organic Chemistry* **2004**, 69, (5), 1652-1662.
13. Garcia-Garibay, M. A., Crystalline molecular machines: Encoding supramolecular dynamics into molecular structure. *Proceedings of the National Academy of Sciences of the United States of America* **2005**, 102, (31), 10771-10776.
14. Kovbasyuk, L.; Kramer, R., Allosteric supramolecular receptors and catalysts. *Chemical Reviews* **2004**, 104, (6), 3161-87.
15. Rebek, J., Jr., Binding forces, equilibria and rates: new models for enzymic catalysis. *Accounts of Chemical Research* **1984**, 17, (7), 258-64.
16. Al-Sayah, M. H.; Branda, N. R., Metal ions as allosteric inhibitors in hydrogen-bonding receptors. *Angewandte Chemie, International Edition* **2000**, 39, (5), 945-947.
17. Petitjean, A.; Khoury, R. G.; Kyritsakas, N.; Lehn, J.-M., Dynamic Devices. Shape Switching and Substrate Binding in Ion-Controlled Nanomechanical Molecular Tweezers. *Journal of the American Chemical Society* **2004**, 126, (21), 6637-6647.
18. Gokel, G. W., Hydraphiles: design, synthesis and analysis of a family of synthetic, cation-conducting channels. *Chemical Communications (Cambridge)* **2000**, (1), 1-9.
19. Gokel, G. W.; Mukhopadhyay, A., Synthetic models of cation-conducting channels. *Chemical Society Reviews* **2001**, 30, (5), 274-286.
20. Gokel, G. W.; Leevy, W. M.; Weber, M. E., Crown Ethers: Sensors for Ions and Molecular Scaffolds for Materials and Biological Models. *Chemical Reviews (Washington, DC, United States)* **2004**, 104, (5), 2723-2750.
21. Feringa, B. L., In Control of Motion: From Molecular Switches to Molecular Motors. *Accounts of Chemical Research* **2001**, 34, (6), 504-513.
22. Koumura, N.; Geertsema, E. M.; van Gelder, M. B.; Meetsma, A.; Feringa, B. L., Second Generation Light-Driven Molecular Motors. Unidirectional Rotation Controlled by a Single Stereogenic Center with Near-Perfect Photoequilibria and Acceleration of the Speed of Rotation by Structural Modification. *Journal of the American Chemical Society* **2002**, 124, (18), 5037-5051.
23. Pijper, D.; van Delden, R. A.; Meetsma, A.; Feringa, B. L., Acceleration of a Nanomotor: Electronic Control of the Rotary Speed of a Light-Driven Molecular Rotor. *Journal of the American Chemical Society* **2005**, 127, (50), 17612-17613.

24. Ishow, E.; Credi, A.; Balzani, V.; Spadola, F.; Mandolini, L., A molecular-level plug/socket system: electronic energy transfer from a binaphthyl unit incorporated into a crown ether to an anthracenyl unit linked to an ammonium ion. *Chemistry--A European Journal* **1999**, *5*, (3), 984-989.
25. Jeon, W. S.; Ziganshina, A. Y.; Lee, J. W.; Ko, Y. H.; Kang, J.-K.; Lee, C.; Kim, K., A [2]pseudorotaxane-based molecular machine: reversible formation of a molecular loop driven by electrochemical and photochemical stimuli. *Angewandte Chemie, International Edition* **2003**, *42*, (34), 4097-4100.
26. Raymo, F. M.; Stoddart, J. F., Interlocked macromolecules. *Chemical Reviews (Washington, D. C.)* **1999**, *99*, (7), 1643-1663.
27. Raymo, F. M.; Houk, K. N.; Stoddart, J. F., The Mechanism of the Slippage Approach to Rotaxanes. Origin of the "All-or-Nothing" Substituent Effect. *Journal of the American Chemical Society* **1998**, *120*, (36), 9318-9322.
28. Elizarov, A. M.; Chang, T.; Chiu, S.-H.; Stoddart, J. F., Self-Assembly of Dendrimers by Slippage. *Organic Letters* **2002**, *4*, (21), 3565-3568.
29. Horn, M.; Ihringer, J.; Glink, P. T.; Stoddart, J. F., Kinetic versus thermodynamic control during the formation of [2]rotaxanes by a dynamic template-directed clipping process. *Chemistry--A European Journal* **2003**, *9*, (17), 4046-4054.
30. Jimenez, M. C.; Dietrich-Buchecker, C.; Sauvage, J.-P., Towards synthetic molecular muscles: contraction and stretching of a linear rotaxane dimer. *Angewandte Chemie, International Edition* **2000**, *39*, (18), 3284-3287.
31. Vale, R. D.; Milligan, R. A., The way things move: Looking under the hood of molecular motor proteins. *Science (Washington, D. C.)* **2000**, *288*, (5463), 88-95.
32. Prasanna de Silva, A.; McClenaghan, N. D., Molecular-scale logic gates. *Chemistry--A European Journal* **2004**, *10*, (3), 574-586.
33. Qu, D.-H.; Wang, Q.-C.; Tian, H., A half adder based on a photochemically driven [2]rotaxane. *Angewandte Chemie, International Edition* **2005**, *44*, (33), 5296-5299.
34. Hernandez, J. V.; Kay, E. R.; Leigh, D. A., A reversible synthetic rotary molecular motor. *Science (Washington, DC, United States)* **2004**, *306*, (5701), 1532-1537.
35. Liu, Y.; Flood, A. H.; Bonvallet, P. A.; Vignon, S. A.; Northrop, B. H.; Tseng, H.-R.; Jeppesen, J. O.; Huang, T. J.; Brough, B.; Baller, M.; Magonov, S.; Solares, S. D.; Goddard, W. A.; Ho, C.-M.; Stoddart, J. F., Linear Artificial Molecular Muscles. *Journal of the American Chemical Society* **2005**, *127*, (27), 9745-9759.

36. Allwood, B. L.; Spencer, N.; Shahriari-Zavareh, H.; Stoddart, J. F.; Williams, D. J., Complexation of paraquat by a bisparaphenylene-34-crown-10 derivative. *Journal of the Chemical Society, Chemical Communications* **1987**, (14), 1064-6.
37. Loeb, S. J.; Wisner, J. A., A new motif for the self-assembly of [2]pseudorotaxanes; 1,2-bis(pyridinium)ethane axles and [24]crown-8 ether wheels. *Angewandte Chemie, International Edition* **1998**, 37, (20), 2838-2840.
38. Loeb, S. J.; Tiburcio, J.; Vella, S. J.; Wisner, J. A., A versatile template for the formation of [2]pseudorotaxanes. 1,2-Bis(pyridinium)ethane axles and 24-crown-8 ether wheels. *Organic & Biomolecular Chemistry* **2006**, 4, (4), 667-680.
39. Tiburcio, J.; Davidson, G. J. E.; Loeb, S. J., Pseudo-polyrotaxanes based on a protonated version of the 1,2-bis(4,4'-bipyridinium)ethane-24-crown-8 ether motif. *Chemical Communications (Cambridge, United Kingdom)* **2002**, (12), 1282-1283.
40. Loeb, S. J.; Wisner, J. A., 1,2-Bis(4,4'-dipyridinium)ethane: a versatile dication for the formation of [2]rotaxanes with dibenzo-24-crown-8 ether. *Chemical Communications (Cambridge)* **1998**, (24), 2757-2758.
41. Davidson, G. J. E.; Loeb, S. J.; Parekh, N. A.; Wisner, J. A., Zwitterionic [2]rotaxanes utilising anionic transition metal stoppers. *Journal of the Chemical Society, Dalton Transactions* **2001**, (21), 3135-3136.
42. Davidson, G. J. E.; Loeb, S. J., Iron(II) complexes utilising terpyridine containing [2]rotaxanes as ligands. *Dalton Transactions* **2003**, (22), 4319-4323.
43. Davidson, G. J. E.; Loeb, S. J.; Passaniti, P.; Silvi, S.; Credi, A., Wire-type ruthenium(II) complexes with terpyridine-containing [2]rotaxanes as ligands: synthesis, characterization, and photophysical properties. *Chemistry--A European Journal* **2006**, 12, (12), 3233-3242.
44. Loeb, S. J.; Wisner, J. A., [3]Rotaxanes employing multiple 1,2-bis(pyridinium)ethane binding sites and dibenzo-24-crown-8 ethers. *Chemical Communications (Cambridge)* **2000**, (10), 845-846.
45. Hubbard, A. L.; Davidson, G. J. E.; Patel, R. H.; Wisner, J. A.; Loeb, S. J., Host-guest interactions template: the synthesis of a [3]catenane. *Chemical Communications (Cambridge, United Kingdom)* **2004**, (2), 138-139.
46. Loeb, S. J.; Wisner, J. A., [2]Rotaxane molecular shuttles employing 1,2-bis(pyridinium)ethane binding sites and dibenzo-24-crown-8 ethers. *Chemical Communications (Cambridge)* **2000**, (19), 1939-1940.
47. Loeb, S. J.; Tramontozzi, D. A., Branched [n]rotaxanes (n = 2-4) from multiple dibenzo-24-crown-8 ether wheels and 1,2-bis(4,4'-dipyridinium)ethane axles. *Organic & Biomolecular Chemistry* **2005**, 3, (8), 1393-1401.

48. Tramontozzi, D. A. Dendrimeric and Polymeric Rotaxanes Incorporating the *Loeb* Recognition Motif. Windsor, Windsor, **2005**.
49. Loeb, S. J., Metal-organic rotaxane frameworks; MORFs. *Chemical Communications (Cambridge, United Kingdom)* **2005**, (12), 1511-1518.
50. Loeb, S. J.; Tiburcio, J.; Vella, S. J., A mechanical "flip-switch". Interconversion between co-conformations of a [2]rotaxane with a single recognition site. *Chemical Communications (Cambridge, United Kingdom)* **2006**, (15), 1598-1600.
51. Pedersen, C. J., Cyclic polyethers and their complexes with metal salts. *Journal of the American Chemical Society* **1967**, 89, (10), 2495-6.
52. Reinhoudt, D. N.; De Jong, F.; Tomassen, H. P. M., Metal fluorides as base for the "templated" synthesis of crown ethers. *Tetrahedron Letters* **1979**, (22), 2067-70.
53. Leon, J. W.; Kawa, M.; Frechet, J. M. J., Isophthalate Ester-Terminated Dendrimers: Versatile Nanoscopic Building Blocks with Readily Modifiable Surface Functionalities. *Journal of the American Chemical Society* **1996**, 118, (37), 8847-8859.
54. Sotiriou-Leventis, C.; Mao, Z., A facile synthesis of 2,7-diazapyrene. *Journal of Heterocyclic Chemistry* **2000**, 37, (6), 1665-1667.
55. Hunter, C. A., Quantifying intermolecular interactions: Guidelines for the molecular recognition toolbox. *Angewandte Chemie, International Edition* **2004**, 43, (40), 5310-5324.
56. Breault, G. A.; Hunter, C. A.; Mayers, P. C., Influence of Solvents on Aromatic Interactions in Metal Tris-Bipyridine Complexes. *Journal of the American Chemical Society* **1998**, 120, (14), 3402-3410.
57. Lane, A. S.; Leigh, D. A.; Murphy, A., Peptide-Based Molecular Shuttles. *Journal of the American Chemical Society* **1997**, 119, (45), 11092-11093.
58. Da Ros, T.; Guldi, D. M.; Morales, A. F.; Leigh, D. A.; Prato, M.; Turco, R., Hydrogen Bond-Assembled Fullerene Molecular Shuttle. *Organic Letters* **2003**, 5, (5), 689-691.
59. Leigh, D. A.; Morales, M. A. F.; Perez, E. M.; Wong, J. K. Y.; Saiz, C. G.; Slawin, A. M. Z.; Carmichael, A. J.; Haddleton, D. M.; Brouwer, A. M.; Buma, W. J.; Wurlpel, G. W. H.; Leon, S.; Zerbetto, F., Patterning through controlled submolecular motion: Rotaxane-based switches and logic gates that function in solution and polymer films. *Angewandte Chemie, International Edition* **2005**, 44, (20), 3062-3067.
60. Gordon, A. J., Ford, R. A., *The Chemist's Companion*. Wiley: New York, **1972**.

61. Kosower, E. M., The effect of solvent on spectra. I. A new empirical measure of solvent polarity-Z-values. *Journal of the American Chemical Society* **1958**, *80*, 3253-60.
62. Clemente-Leon, M.; Credi, A.; Martinez-Diaz, M.-V.; Mingotaud, C.; Stoddart, J. F., Towards organization of molecular machines at interfaces: Langmuir films and Langmuir-Blodgett multilayers of an acid-base switchable rotaxane. *Advanced Materials (Weinheim, Germany)* **2006**, *18*, (10), 1291-1296.
63. Credi, A.; Balzani, V.; Langford, S. J.; Stoddart, J. F., Logic Operations at the Molecular Level. An XOR Gate Based on a Molecular Machine. *Journal of the American Chemical Society* **1997**, *119*, (11), 2679-2681.
64. Montalti, M., A supramolecular assembly controlled by anions: threading and unthreading of a pseudorotaxane. *Chemical Communications (Cambridge)* **1998**, (14), 1461-1462.
65. Sambrook, M. R.; Beer, P. D.; Wisner, J. A.; Paul, R. L.; Cowley, A. R.; Szemes, F.; Drew, M. G. B., Anion-Templated Assembly of Pseudorotaxanes: Importance of Anion Template, Strength of Ion-Pair Thread Association, and Macrocyclic Ring Size. *Journal of the American Chemical Society* **2005**, *127*, (7), 2292-2302.
66. Kim, K.; Jeon, W. S.; Kang, J.-K.; Lee, J. W.; Jon, S. Y.; Kim, T.; Kim, K., A pseudorotaxane on gold: Formation of self-assembled monolayers, reversible dethreading and rethreading of the ring, and ion-gating behavior. *Angewandte Chemie, International Edition* **2003**, *42*, (20), 2293-2296.
67. Leigh, D. A.; Perez, E. M., Shuttling through reversible covalent chemistry. *Chemical Communications (Cambridge, United Kingdom)* **2004**, (20), 2262-2263.
68. Badjic, J. D.; Balzani, V.; Credi, A.; Silvi, S.; Stoddart, J. F., A Molecular Elevator. *Science (Washington, DC, United States)* **2004**, *303*, (5665), 1845-1849.
69. Keaveney, C. M.; Leigh, D. A., Shuttling through anion recognition. *Angewandte Chemie, International Edition* **2004**, *43*, (10), 1222-1224.
70. Balzani, V.; Credi, A.; Raymo, F. M.; Stoddart, J. F., Artificial molecular machines. *Angewandte Chemie, International Edition* **2000**, *39*, (19), 3348-3391.
71. Ashton, P. R.; Ballardini, R.; Balzani, V.; Baxter, I.; Credi, A.; Fyfe, M. C. T.; Gandolfi, M. T.; Gomez-Lopez, M.; Martinez-Diaz, M. V.; Piersanti, A.; Spencer, N.; Stoddart, J. F.; Venturi, M.; White, A. J. P.; Williams, D. J., Acid-Base Controllable Molecular Shuttles. *Journal of the American Chemical Society* **1998**, *120*, (46), 11932-11942.
72. Leigh, D. A.; Wong, J. K. Y.; Dehez, F.; Zerbetto, F., Unidirectional rotation in a mechanically interlocked molecular rotor. *Nature (London, United Kingdom)* **2003**, *424*, (6945), 174-179.

73. Ceccarelli, M.; Mercuri, F.; Passerone, D.; Parrinello, M., The Microscopic Switching Mechanism of a [2]Catenane. *Journal of Physical Chemistry B* **2005**, 109, (36), 17094-17099.
74. Stoddart, J. F.; Williams, D. J.; Amabilino, D. B.; Anelli, P.-L.; Ashton, P. R.; Brown, G. R.; Cordova, E.; Godinez, L. A.; Hayes, W.; et al., Molecular Meccano. 3. Constitutional and Translational Isomerism in [2]Catenanes and [n]Pseudorotaxanes. *Journal of the American Chemical Society* **1995**, 117, (45), 11142-70.
75. Liu, Y.; Bonvallet, P. A.; Vignon, S. A.; Khan, S. I.; Stoddart, J. F., Donor-acceptor pretzelanes and a cyclic bis[2]catenane homologue. *Angewandte Chemie, International Edition* **2005**, 44, (20), 3050-3055.
76. Poleschak, I.; Kern, J.-M.; Sauvage, J.-P., A copper-complexed rotaxane in motion: pirouetting of the ring on the millisecond timescale. *Chemical Communications (Cambridge, United Kingdom)* **2004**, (4), 474-476.
77. Sauvage, J.-P., Transition metal-complexed catenanes and rotaxanes as molecular machine prototypes. *Chemical Communications (Cambridge, United Kingdom)* **2005**, (12), 1507-1510.
78. Vella, S. J.; Tiburcio, J.; Gault, J. W.; Loeb, S. J., Push-Pull [2]Pseudorotaxanes. Electronic Control of Threading by Switching ON/OFF an Intramolecular Charge Transfer. *Organic Letters* **2006**, 8, (16), 3421-3424.
79. Stauffer, D. A.; Barrans, R. E., Jr.; Dougherty, D. A., Concerning the thermodynamics of molecular recognition in aqueous and organic media. Evidence for significant heat capacity effects. *Journal of Organic Chemistry* **1990**, 55, (9), 2762-7.
80. Das, S.; Nag, A.; Goswami, D.; Bharadwaj, P. K., Zinc(II)- and Copper(I)-Mediated Large Two-Photon Absorption Cross Sections in a Bis-cinnamaldiminato Schiff Base. *Journal of the American Chemical Society* **2006**, 128, (2), 402-403.
81. Armarego, W. L. F., Chai, C. L. L., *Purification of Laboratory Chemicals*. Fifth ed.; Butterworth Heinemann: New York, **2004**.
82. Becke, A. D., Density-functional thermochemistry. III. The role of exact exchange. *Journal of Chemical Physics* **1993**, 98, (7), 5648-52.
83. Becke, A. D., A new mixing of Hartree-Fock and local-density-functional theories. *Journal of Chemical Physics* **1993**, 98, (2), 1372-7.
84. Stephens, P. J.; Devlin, F. J.; Chabalowski, C. F.; Frisch, M. J., Ab Initio Calculation of Vibrational Absorption and Circular Dichroism Spectra Using Density Functional Force Fields. *Journal of Physical Chemistry* **1994**, 98, (45), 11623-7.

85. Lee, C.; Yang, W.; Parr, R. G., Development of the Colle-Salvetti correlation-energy formula into a functional of the electron density. *Physical Review B: Condensed Matter and Materials Physics* **1988**, 37, (2), 785-9.
86. McEwen, W. E.; Terss, R. H.; Elliott, I. W., Formation of aldehydes from partially hydrogenated N-acyl-pyridine, -quinoline and -isoquinoline derivatives. *Journal of the American Chemical Society* **1952**, 74, 3605-9.
87. Belen'kii, L. I.; Poddubnyi, I. S.; Luiksaar, S. I.; Krayushkin, M. M., Some reactions of pyridinium salts derived from trichloromethylarenes with N- and C-nucleophiles. *Chemistry of Heterocyclic Compounds (New York, NY, United States)(Translation of Khimiya Geterotsiklicheskikh Soedinenii)* **2000**, 36, (10), 1172-1176.
88. Raymo, F. M., Stoddart, J. F. In, *Molecular Catenanes, Rotaxanes and Knots*. Wiley-VCH: Weinheim, **1999**.
89. Ashton, P. R.; Campbell, P. J.; Chrystal, E. J. T.; Glinke, P. T.; Menzer, S.; Philp, D.; Spencer, N.; Stoddart, J. F.; Tasker, P. A.; Williams, D. J., Dialkylammonium ion/crown ether complexes: the forerunners of a new family of interlocked molecules. *Angewandte Chemie, International Edition in English* **1995**, 34, (17), 1865-9.
90. Ashton, P. R.; Chrystal, E. J. T.; Glink, P. T.; Menzer, S.; Schiavo, C.; Spencer, N.; Stoddart, J. F.; Tasker, P. A.; White, A. J. P.; Williams, D. J., Molecular meccano. 6. Pseudorotaxanes formed between secondary dialkylammonium salts and crown ethers. *Chemistry--A European Journal* **1996**, 2, (6), 709-728.
91. Glink, P. T.; Schiavo, C.; Stoddart, J. F.; Williams, D. J., The genesis of a new range of interlocked molecules. *Chemical Communications (Cambridge)* **1996**, (13), 1483-1490.
92. Cantrill, S. J.; Pease, A. R.; Stoddart, J. F., A molecular meccano kit. *Dalton* **2000**, (21), 3715-3734.
93. Elizarov, A. M.; Chiu, S.-H.; Stoddart, J. F., An Acid-Base Switchable [2]Rotaxane. *Journal of Organic Chemistry* **2002**, 67, (26), 9175-9181.
94. Loeb, S. J.; Tiburcio, J.; Vella, S. J., [2]Pseudorotaxane Formation with N-Benzylanilinium Axles and 24-Crown-8 Ether Wheels. *Organic Letters* **2005**, 7, (22), 4923-4926.
95. Onaka, M.; Umezono, A.; Kawai, M.; Izumi, Y., N-Alkylation of aniline derivatives by use of potassium cation-exchanged Y-type zeolite. *Journal of the Chemical Society, Chemical Communications* **1985**, (17), 1202-3.

96. Hayat, S.; Atta ur, R.; Iqbal Choudhary, M.; Khan, K. M.; Schumann, W.; Bayer, E., N-Alkylation of anilines, carboxamides and several nitrogen heterocycles using CsF-Celite/alkyl halides/CH₃CN combination. *Tetrahedron* **2001**, *57*, (50), 9951-9957.
97. Hynes, M. J., EQNMR: a computer program for the calculation of stability constants from nuclear magnetic resonance chemical shift data. *Journal of the Chemical Society, Dalton Transactions: Inorganic Chemistry (1972-1999)* **1993**, (2), 311-12.
98. Hansch, C.; Leo, A.; Taft, R. W., A survey of Hammett substituent constants and resonance and field parameters. *Chemical Reviews (Washington, DC, United States)* **1991**, *91*, (2), 165-95.
99. Perrin, C. L.; Dwyer, T. J., Application of two-dimensional NMR to kinetics of chemical exchange. *Chemical Reviews (Washington, DC, United States)* **1990**, *90*, (6), 935-67.
100. Ashton, P. R.; Fyfe, M. C. T.; Hickingbottom, S. K.; Fraser Stoddart, J.; White, A. J. P.; Williams, D. J., Hammett correlations beyond the molecule. *Journal of the Chemical Society, Perkin Transactions 2: Physical Organic Chemistry* **1998**, (10), 2117-2128.
101. Ashton, P. R.; Bartsch, R. A.; Cantrill, S. J.; Hanes, R. E., Jr.; Hickingbottom, S. K.; Lowe, J. N.; Preece, J. A.; Stoddart, J. F.; Talanov, V. S.; Wang, Z.-H., Secondary dibenzylammonium ion binding by [24]crown-8 and [25]crown-8 macrocycles. *Tetrahedron Letters* **1999**, *40*, (19), 3661-3664.
102. Montalti, M.; Ballardini, R.; Prodi, L.; Balzani, V., Electronic energy transfer in adducts of aromatic crown ethers with protonated 9-methylaminomethylanthracene. *Chemical Communications (Cambridge)* **1996**, (17), 2011-2012.
103. Ashton, P. R.; Ballardini, R.; Balzani, V.; Gomez-Lopez, M.; Lawrence, S. E.; Martinez-Diaz, M. V.; Montalti, M.; Piersanti, A.; Prodi, L.; Stoddart, J. F.; Williams, D. J., Hydrogen-Bonded Complexes of Aromatic Crown Ethers with (9-Anthracenyl)ammonium Derivatives. Supramolecular Photochemistry and Photophysics. pH-Controllable Supramolecular Switching. *Journal of the American Chemical Society* **1997**, *119*, (44), 10641-10651.
104. Hunter, C. A.; Sanders, J. K. M., The nature of p-p interactions. *Journal of the American Chemical Society* **1990**, *112*, (14), 5525-34.
105. Hunter, C. A.; Lawson, K. R.; Perkins, J.; Urch, C. J., Aromatic interactions. *Journal of the Chemical Society, Perkin Transactions 2* **2001**, (5), 651-669.
106. Apodaca, R.; Xiao, W., Direct Reductive Amination of Aldehydes and Ketones Using Phenylsilane: Catalysis by Dibutyltin Dichloride. *Organic Letters* **2001**, *3*, (11), 1745-1748.

107. Sprinzak, Y., Reduction and Benzylolation by Means of Benzyl Alcohol. II. N-Benzylolation. The Preparation of Secondary Aromatic Benzylamines. *Journal of the American Chemical Society* **1956**, 78, (13), 3207-3208.
108. Pratt, E. F.; McGovern, T. P., Oxidation by Solids. III. Benzalanilines from N-Benzylanilines and Related Oxidations by Manganese Dioxide. *Journal of Organic Chemistry* **1964**, 29, (6), 1540-1543.
109. Fields, R., Nuclear magnetic resonance. *Journal of Fluorine Chemistry* **1986**, 33, (1-4), 287-92.
110. Harris, R. K.; Jackson, P., High-resolution fluorine-19 magnetic resonance of solids. *Chemical Reviews (Washington, DC, United States)* **1991**, 91, (7), 1427-40.
111. Coe, B. J.; Harris, J. A.; Brunschwig, B. S.; Garin, J.; Orduna, J.; Coles, S. J.; Hursthouse, M. B., Contrasting Linear and Quadratic Nonlinear Optical Behavior of Dipolar Pyridinium Chromophores with 4-(Dimethylamino)phenyl or Ruthenium(II) Ammine Electron Donor Groups. *Journal of the American Chemical Society* **2004**, 126, (33), 10418-10427.
112. Lamothe, M.; Pauwels, P. J.; Belliard, K.; Schambel, P.; Halazy, S., Differentiation between partial agonists and neutral 5-HT_{1B} antagonists by chemical modulation of 3-[3-(N,N-dimethylamino)propyl]-4-hydroxy- N-[4-(pyridin-4-yl)phenyl]benzamide (GR-55562). *J Med Chem FIELD Full Journal Title: Journal of medicinal chemistry* **1997**, 40, (22), 3542-50.
113. Stack, D. E.; Hill, A. L.; Diffendaffer, C. B.; Burns, N. M., Synthesis of a New Fluorescent Probe Specific for Catechols. *Organic Letters* **2002**, 4, (25), 4487-4490.
114. Langhals, H.; Saulich, S., Bichromophoric Perylene Derivatives: Energy Transfer from Non-Fluorescent Chromophores. *Chemistry A European Journal* **2002**, 8, (24), 5630-5643.
115. Lan, P.; Berta, D.; Porco, J. A.; South, M. S.; Parlow, J. J., Polymer-Assisted Solution-Phase (PASP) Suzuki Couplings Employing an Anthracene-Tagged Palladium Catalyst. *Journal of Organic Chemistry* **2003**, 68, (25), 9678-9686.
116. Hart, H.; Rajakumar, P., 2'-Substituted Meta-Terphenyls as Building Blocks for Cyclophanes with Intra-Annular Functionality. *Tetrahedron* **1995**, 51, (5), 1313-1336.
117. Ulman, A., Formation and Structure of Self-Assembled Monolayers. *Chemical Reviews (Washington, D. C.)* **1996**, 96, (4), 1533-1554.
118. Tseng, H.-R.; Wu, D.; Fang, N. X.; Zhang, X.; Stoddart, J. F., The metastability of an electrochemically controlled nanoscale machine on gold surfaces. *ChemPhysChem* **2004**, 5, (1), 111-116.

119. Noergaard, K.; Laursen, B. W.; Nygaard, S.; Kjaer, K.; Tseng, H.-R.; Flood, A. H.; Stoddart, J. F.; Bjoernholm, T., Structural evidence of mechanical shuttling in condensed monolayers of bistable rotaxane molecules. *Angewandte Chemie, International Edition* **2005**, *44*, (43), 7035-7039.
120. Rowsell, J. L. C.; Yaghi, O. M., Metal-organic frameworks: a new class of porous materials. *Microporous and Mesoporous Materials* **2004**, *73*, (1-2), 3-14.
121. Kim, K., Mechanically interlocked molecules incorporating cucurbituril and their supramolecular assemblies. *Chemical Society Reviews* **2002**, *31*, (2), 96-107.
122. Tour, J. M.; Jones, L., II; Pearson, D. L.; Lamba, J. J. S.; Burgin, T. P.; Whitesides, G. M.; Allara, D. L.; Parikh, A. N.; Atre, S., Self-Assembled Monolayers and Multilayers of Conjugated Thiols, α,ω -Dithiols, and Thioacetyl-Containing Adsorbates. Understanding Attachments between Potential Molecular Wires and Gold Surfaces. *Journal of the American Chemical Society* **1995**, *117*, (37), 9529-34.
123. Niklewski, A.; Azzam, W.; Strunskus, T.; Fischer, R. A.; Woell, C., Fabrication of Self-Assembled Monolayers Exhibiting a Thiol-Terminated Surface. *Langmuir* **2004**, *20*, (20), 8620-8624.
124. Lin, C.; Kagan, C. R., Layer-By-Layer Growth of Metal-Metal Bonded Supramolecular Thin Films and Its Use in the Fabrication of Lateral Nanoscale Devices. *Journal of the American Chemical Society* **2003**, *125*, (2), 336-337.
125. Ansell, M. A.; Cogan, E. B.; Page, C. J., Coordinate Covalent Cobalt-Diisocyanide Multilayer Thin Films Grown One Molecular Layer at a Time. *Langmuir* **2000**, *16*, (3), 1172-1179.
126. Duprez, V.; Krebs, F. C., New carboxy-functionalized terpyridines as precursors for zwitterionic ruthenium complexes for polymer-based solar cells. *Tetrahedron Letters* **2006**, *47*, (22), 3785-3789.
127. Vaduvescu, S.; Potvin, P. G., Linear multinuclear RuII photosensitizers. *European Journal of Inorganic Chemistry* **2004**, (8), 1763-1769.
128. Wang, J.; Hanan, G. S., A facile route to sterically hindered and non-hindered 4'-aryl-2,2':6',2''-terpyridines. *Synlett* **2005**, (8), 1251-1254.

VITA AUCTORIS

Name: Sarah Vella

Date of Birth: March 5th, 1977

Place of Birth: Windsor, Ontario, Canada

Citizenship: Canadian

Education:

Ph. D. Chemistry (2006)
University of Windsor,
Windsor, Ontario

B. Sc. Honours Biochemistry (2000)
University of Windsor,
Windsor, Ontario

Professional Work History:

Research Assistant
University of Windsor, Windsor, Ontario, Canada
May 1999-December 2006

Graduate Assistant
University of Windsor, Windsor, Ontario, Canada
September 1999-December 2005

Research Chemist - Organic Synthesis and Materials Division
IBM T.J. Watson Center, Yorktown Heights, New York, USA
September 2002-December 2002

Research Chemist - Organic Synthesis and Materials Division
IBM T.J. Watson Center, Yorktown Heights, New York, USA
June 2001-August 2001

Research Chemist - Organic Synthesis and Materials Division
IBM T.J. Watson Center, Yorktown Heights, New York, USA
June 2000-September 2000

Scholarships and Awards:

Name of Award	Amount	Type of Award	Year Held
OGSST	\$15000	Provincial	May 2005-April 2006
Tuition Scholarship	\$5500	Institutional	May 2004-April 2005
NSERC PGS-B	\$21000/year	National	September 2002-August 2004
NSERC PGS-A	\$17500/year	National	September 2000-August 2002
Tuition Scholarship	\$5500	Institutional	May 2003-April 2004
Tuition Scholarship	\$5500	Institutional	May 2002-April 2003
Organic Division Poster Prize	\$250	National	June 2002
Tuition Scholarship	\$5500	Institutional	May 2001-April 2002
Tuition Scholarship	\$5500	Institutional	May 2000-April 2001
Governor General's Award in Chemistry/Biochemistry	N/A	National/Institutional	2000
NSERC Undergraduate Research Award	\$3600	National	May 1999 - August 1999
University of Windsor Entrance Scholarship	\$8000	Institutional	September 1996 - April 2000
Chrysler Scholarship	\$4000	National	September 1996 - April 2000
Governor General's Award for Secondary School	N/A	National/Institutional	1996

Publications:

S. J. Vella, J. Tiburcio, J. W. Gauld, S. J. Loeb. "Push-Pull [2]pseudorotaxanes. Electronic control of threading by switching on/off an intramolecular charge transfer." *Organic Letters*, **2006**, 8, 3421-3424.

S. J. Loeb, J. Tiburcio, S. J. Vella. "A mechanical 'flip-switch'. Interconversion between co-conformations of a [2]rotaxane with a single recognition site.", *Chemical Communications*, **2006**, 15, 1598-1600.

S. J. Loeb, J. Tiburcio, S. J. Vella, J. A. Wisner. "A versatile template for the formation of [2]pseudorotaxanes. 1,2-Bis(pyridinium)ethane axles and 24-crown-8 ether wheels", *Organic & Biomolecular Chemistry*, **2006**, 4, 667-680.

S. J. Vella, S. J. Loeb, J. Tiburcio. "[2]Pseudorotaxane Formation with *N*-Benzylanilinium Axles and 24-Crown-8 Ether Wheels". *Organic Letters*, **2005**, 7, 4923-4926.

S. J. Vella, T. Breen Carmichael, A. Afzali, "Selective Electroless Metal Deposition Using Microcontact Printing of Phosphine-Phosphonic Acid Inks" *Langmuir*, **2004**, 20, 5593-5598.

S. J. Vella, T. L. Breen, A. Afzali, "Selective electroless metallization using microcontact printing of functionalized copolymers" *Polymeric Materials Science and Engineering*, **2002**, 87, 412-413.

Patents:

T. L. Breen, A. Afzali, S. J. Vella, M. M. Khojasteh, "Materials and Methods for Immobilization of Catalysts on Surfaces and for Selective Electroless Metallization" U.S. Pat. No: 2003132121, **2003**.

Conference Presentations:

S. J. Vella, S. J. Loeb. "Acid-Base Driven Molecular Shuttles: From Rotaxanes to Catenanes". *89th Canadian Chemical Conference and Exhibition*, Halifax, Nova Scotia, Canada, **2006**. (Ph.D. Work- poster presentation)

S. J. Vella, S. J. Loeb, J. Tiburcio. "Bistable [2]Rotaxanes Performing As Linear Molecular Motors". *RSC MC7 Conference*, Edinburgh, Scotland, United Kingdom, **2005**. (Ph.D. Work- oral poster presentation)

S. J. Vella, S. J. Loeb. "Rotaxane Molecular Shuttles Displaying Logic Gate Functionality". *88th Canadian Chemical Conference and Exhibition*, Saskatoon, Saskatchewan, Canada, **2005**. (Ph.D. Work- oral presentation)

S. J. Vella, S. J. Loeb, "A New Binding Motif for the Construction of Interlocked Molecules" *86th Canadian Chemical Conference and Exhibition*, Ottawa, Ontario, Canada, **2003**. (Ph.D. Work- oral poster presentation)

S. J. Vella, S. J. Loeb, "Towards Surface Bound Molecular Shuttles" *85th Canadian Chemical Conference and Exhibition*, Vancouver, British Columbia, Canada, **2002**. (Organic Division Poster Prize- \$250) (Ph.D. Work- oral poster presentation)

T. L. Breen, S. J. Vella, A. Afzali "Selective Electroless Metallization Using Microcontact Printing of Functionalized Copolymers" *Materials Research Society 2001 Fall Meeting*, Boston, Massachusetts, USA, **2001**. (Ph.D. Work- oral poster presentation)

S. J. Vella, S. J. Loeb "A [2]Rotaxane Molecular "Flip-Switch" *84th Canadian Chemical Conference and Exhibition*, Montreal, Quebec, Canada, **2001**. (Ph.D. Work- oral poster presentation)

S. J. Vella, T. L. Breen "From Solution to Surfaces: A Study of [2]Rotaxanes". *IBM Advancement of Science Summer Research Poster Session*. Yorktown Heights, New York, USA, **2001**. (Ph.D. Work- oral poster presentation)

S.J. Vella, S. J. Loeb "Flipping [2]Rotaxanes: A New Type of Mechanical Molecular Switch". *83rd Canadian Chemical Conference and Exhibition*, Calgary, Alberta, Canada, **2000**. (Ph.D. Work- oral poster presentation)

S.J. Vella, T.L. Breen "Microcontact Printing & Electroless Deposition: A Method for Plating a Pattern". *IBM Advancement of Science Summer Research Poster Session*. Yorktown Heights, New York, USA, **2000**. (Ph.D. Work- oral poster presentation)

S.J. Vella, S.J. Loeb "Flipping [2]Rotaxanes. A New Type of Mechanical Molecular Switch". *23rd Southwestern Ontario Undergraduate Chemistry Conference*, St. Catherine's, Ontario, Canada, **2000**. (Undergraduate Work- oral presentation)